ALUATION OF SELF-BORING PRESSUREMETER
STS IN BOSTON BLUE CLAY

September 1980
Interim Report

Prepared for
FEDERAL HIGHWAY ADMINISTRATION
Offices of Research & Development
Materials Division
Washington, D.C. 20590

FOREWORD

This report presents the results of MIT's research related to self-boring pressuremeter tests performed in Boston Blue Clay. The research included 20 tests with the French PAFSOR and 14 tests with the English Camkometer. Data were obtained for evaluation of in situ horizontal stress, limit pressure, and undrained stress-strain-strength parameters. The in situ derived parameters were compared with those derived through laboratory testing and with theoretical values.

Results of the study indicate that the PAFSOR horizontal pressure was generally much less than theoretical values or those obtained by other methods. However, specific reasons for the poor correlation have not been identified although it is suspected that operating procedures had a significant influence on test results.

A second report is being prepared by the Politecnico di Torino, in cooperation with MIT, that presents and evaluates self-boring pressuremeter test data obtained at other sites with varying clay types and stress history.

Copies of the report are being distributed by the Materials Division, Office of Research, to other researchers, and to appropriate members of the FCP Project 5B team.

Charles F. Scheffey
Director, Office of Research

NOTICE

Technical Report Documentation Page

1. Report No. FHWA/RD-80/052	2. Government Accession No.	3. Recipient's Catalog No.

4. Title and Subtitle	5. Report Date September 1980
EVALUATION OF SELF-BORING PRESSUREMETER TESTS IN BOSTON BLUE CLAY	6. Performing Organization Code

7. Author(s) C.C. Ladd, J.T. Germaine, M.M. Baligh and S.M. Lacasse	8. Performing Organization Report No. R79-4

9. Performing Organization Name and Address Constructed Facilities Division Department of Civil Engineering Massachusetts Institute of Technology Cambridge, Massachusetts 02139	10. Work Unit No. (TRAIS) FCP 35B2-501
	11. Contract or Grant No. DOT-FH-11-9264

12. Sponsoring Agency Name and Address U.S. Department of Transportation Federal Highway Administration Washington, D.C. 20590	13. Type of Report and Period Covered Interim Report May 1977-February 1979
	14. Sponsoring Agency Code M/0632

DEPARTMENT OF
TRANSPORTATION

APR 6 1981

LIBRARY

16. Abstract

The research performed "undrained" self-boring pressuremeter tests (SBPT) at two sites in a deep marine clay deposit of moderate sensitivity (Boston Blue clay) having a decreasing overconsolidation ratio with depth. The program involved 20 tests with the French PAFSOR and 14 tests with the English CAMKOMETER devices.

The initial pressure (P_O) recorded after self-boring was generally much less than the insitu total horizontal stress (σ_{ho}), perhaps mainly due to improper installation techniques. However, the Marsland-Randolph graphical iteration method yielded quite reasonable estimates of σ_{ho}, especially in the upper "stiff" clay, and this technique should be further evaluated via SBPT programs in other clay deposits.

Values of undrained shear strength (c_u) obtained from elastic-plastic and various derived methods of analysis were very sensitive to the input data, often showed considerable scatter and generally exceeded the in situ c_u appropriate for bearing capacity and stability analyses. In particular, derived peak strengths in the deep "soft" clay were too high by a factor of two or more. However, most of the tests did give reasonable estimates of undrained shear modulus.

17. Key Words Pressuremeter, in situ stress, undrained strength, undrained modulus, clays, in situ testing, site exploration	18. Distribution Statement This document is available to the public through the National Technical Information Service, Springfield, Virginia 22151

19. Security Classif. (of this report) Unclassified	20. Security Classif. (of this page) Unclassified	21. No. of Pages 239	22. Price

Form DOT F 1700.7 (8-72)   Reproduction of completed page authorized

PREFACE

TABLE OF CONTENTS

iii

TABLE OF CONTENTS (contiuned)

v

LIST OF TABLES

vi

LIST OF TABLES(continued)

LIST OF FIGURES

xi

LIST OF FIGURES (continued)

LIST OF SYMBOLS

a_o	Almansi strain
CIUC	Isotropically consolidated-undrained triaxial compression test
CK_oU	K_o consolidated-undrained shear test
CK_oUC	K_o consolidated-undrained triaxial compression test
CK_oUDSS	K_o consolidated-undrained direct simple shear test
CK_oUE	K_o consolidated-undrained triaxial extension test
CK_oUPSC	K_o consolidated-undrained plane strain compression test
CK_oUPSE	K_o consolidated-undrained plane strain extension test
CRSC	Constant rate of strain consolidation test
c_u	Undrained shear strength
$c_u(Ave)$	Average c_u for combination of failure modes
$c_u(FV)$	Undrained shear strength from field vane test
$c_u(Peak)$	Maximum undrained shear stress from pressuremeter test
$c_u(Ult)$	Undrained shear stress from pressuremeter test after large strains are imposed
$c_u(V)$	Undrained shear strength in vertical compression
DCT	Dutch cone test
DSS	Direct simple shear test
E_u	Undrained Young's modulus
FV	Field vane test
G	Shear modulus
g_o	Green strain
K	Coefficient of earth pressure $= \sigma'_h/\sigma'_v$

K_o	Coefficient of earth pressure at rest
MPT	Menard pressuremeter test
N_c	Cone factor
N_p	Theoretical strength factor for pressuremeter test
OCR	Overconsolidation ratio
P	Corrected membrane pressure
P_f	Pressure corresponding to initial yielding
P_l	Limit pressure
P_o	Pressure corresponding to corrected start of pressuremeter test
P_o'	Stabilized initial membrane pressure minus in situ equilibrium pore pressure
PAF	Autoforeur probe
PAFSOR	Same as PAF-1972
PSC	Plane strain compression test
PSE	Plane strain extension test
q	Maximum shear stress $= 0.5(\sigma_1 - \sigma_3)$
q_c	Cone penetration resistance
q_f	Maximum shear stress at failure $= 0.5(\sigma_1 - \sigma_3)_f$
r	Circular cylindrical coordinate
r_o	Initial r coordinate of a cavity
SBPT	Self-boring pressuremeter test
S_t	Sensitivity $= c_u(\text{undisturbed})/c_u(\text{remolded})$
t	Time
u	Pore water pressure

u_o	Initial pore water pressure
UC	Unconfined compression test
UUC	Unconsolidated-undrained compression test
V	Volume of measurement cell
V_c	Initial volume of measurement cell
V_o	Volume corresponding to corrected start of pressuremeter test
γ	Shear strain
Δ	Prefix indicating increment in parameter
$\Delta\dot{V}$	Rate of volume injection into membrane
$\dot{\varepsilon}$	Strain rate
ε_o	Cauchy strain = $\Delta r/r_o$
ε_{of}	Cauchy strain at maximum shear stress
ν	Poisson's ratio
σ_h	Total horizontal stress
σ_{ho}	Total in situ horizontal stress
σ'_{ho}	Effective in situ horizontal stress
σ_r	Total radial stress = major principal stress in cavity expansion
σ_v	Total vertical stress
σ'_v	Effective vertical stress
σ'_{vc}	Effective vertical consolidation stress
σ'_{vm}	Vertical maximum past pressure
σ_{vo}	Total in situ vertical stress
σ'_{vo}	Effective in situ vertical stress
σ_θ	Total circumferential stress = minor principal stress in cavity expansion

τ	Shear stress
τ_{ff}	Shear stress on failure plane at failure
ϕ'	Effective angle of internal friction

1. INTRODUCTION

1.1 BACKGROUND

In situ testing has a long history in geotechnical
engineering, plate load tests having been incorporated into
building codes even prior to modern soil mechanics. The
standard penetration test and earlier forms of the Dutch
cone test, both in use before 1930, represented the main
methods for early subsurface exploration. These eventually
led to widely used design procedures based on empirical
correlations, while development of the field vane test in
Sweeden during the 1940's enabled the first "simple" measure-
ment of the in situ undrained shear strength of saturated
clays. During the past 10 or so years, in situ testing has
benefited from greatly expanded interest and research, both
regarding reevaluation of existing methods and development
of new, more sophisticated testing techniques. The stimu-
lus for this expanded effort has resulted from:

1) a growing disenchantment with the reliability of
   simple laboratory tests and concern over the costs
   of more elaborate testing programs.
2) the necessity for reassessing the more empirically
   oriented in situ tests in light of recent advances
   in the understanding of soil behavior.
3) attempts to measure certain in situ properties,
   such as modulus and lateral stress, not readily
   evaluated by laboratory tests.
4) increased interest in economical testing methods
   that better define spacial variations in properties.

While many in the profession often consider laboratory
and in situ testing as competing approaches, and some even
view the latter as the ultimate solution to evaluation of

1

parameters in design practice, the writers do not hold this opinion. Rather these approaches should be considered as complementary, for each has interrelated strengths and weaknesses as discussed by Ladd et al. (1977) and summarized below.

Laboratory tests usually have well defined, directly controllable boundary conditions and generally use devices designed to produce uniformity of stresses and strains within the test specimens. Flexibility in loading and drainage conditions, exact knowledge of the soil type tested, and easy interpretation of the test results to yield well defined soil properties all represent definite advantages. But the laboratory approach requires that samples of the in situ soil be obtained, which can be expensive and also lead to major problems due to sample disturbance. On the other hand, since in situ tests are performed within the soil deposit, they offer the potential for both cost savings and reduction in disturbance in the soil, although these may not always be achieved in practice, and they are generally better suited to investigate spacial variations in soil properties. But in situ tests usually have more complex boundary conditions than exist in laboratory devices, major variations in stresses and strains (and perhaps variable drainage conditions) often occurring within the soil mass affected by the test. Such factors greatly complicate interpretation of test data and hence most in situ tests require empirical correlations in order to obtain soil parameters for design purposes.

Amongst recent developments in in situ testing capabilities, none represent a more exciting prospect than the self-boring pressuremeter test (SBPT). Though based on the same measurement concepts as the Menard pressuremeter, this device has a cutting head such that the cylindrical

2

probe can be inserted into the ground with far less distur-
bance than caused by predrilling a hole. The SBPT thus
has the potential for measuring in situ horizontal stress.
An analytical solution was also developed that allows the
complete undrained stress-strain curve to be derived from
data obtained during undrained expansion of a vertical
cylindrical cavity in a saturated clay. The SBPT therefore
has the theoretical capability of making in situ measure-
ments of lateral stress and undrained strength-deformation
properties of cohesive soils in greater detail and more
accurately than heretofore possible. This is an exciting
prospect that can benefit many areas of foundation engineer-
ing, especially regarding underground construction such as
tunnels.

Serious questions exist, however, as to whether the
full potential of the SBPT can be readily achieved in
practice. For example, the precise installation technique
may not only affect the measured in situ lateral stress,
but also the values of strength and modulus derived
from data obtained during subsequent expansion of the
cylindrical probe. Other factors, such as variations in
the rate of strain imposed within the soil mass, can further
complicate interpretation of the stress-strain data. The
SBPT also requires a very high level of technical expertise
and is costly compared to other in situ procedures. The
geotechnical engineering profession therefore needs to
evaluate and assess the capabilities and limitations of
the test before utilizing it in design practice.

The Federal Highway Administration (FHWA) fortunately
included the above evaluation task amongst its research
objectives. Part of this program consists of performing
self-boring pressuremeter tests in soil deposits wherein
parameters derived from SBPT data can be compared to

3

results established via laboratory tests, other types of in situ tests and/or full scale field testing. Since Boston Blue clay is ideally suited for this purpose, for it constitutes one of the most highly tested and best known clay deposits in the world, the FHWA selected it as a test site. Also, the Massachusetts Institute of Technology (MIT) had already performed tests in Boston Blue clay with the "English" version of the SBPT. These data were supplemented by further testing using the "French" device in cooperation with the California Department of Transportation (CALDOT), which had the equipment on loan from the French Highways Administration for evaluation in several other soil deposits.

1.2 OBJECTIVES OF RESEARCH AND SCOPE OF WORK

The research objectives were: (1) to evaluate operational procedures for in situ testing with the French self-boring pressuremter device; (2) to evaluate the soil parameters measured with the SBPT and determine their applicability to geotechnical engineering problems; and (3) to present and evaluate methods of analysis for deriving soil parameters from SBPT data. To accomplish these objectives, work by MIT included the following tasks:

Task A

(1) Make arrangements with a drilling contractor (CON-TEC, INC of Concord, NH) to modify its equipment as needed to perform tests with the French device, called the PAFSOR, based on requirements provided by CALDOT personnel.

(2) Arrange for access to the Boston Blue clay test site in Saugus, Massachusetts located adjacent to the I-95 embankment fill that had previously been used by MIT for extensive in situ and laboratory testing and

4

evaluation of embankment performance.

TASK B

(1) Develop and conduct a program of PAFSOR tests at two
    locations (one being adjacent to prior testing with
    the English device called the CAMKOMETER) in coopera-
    tion with CALDOT personnel who were already familiar
    with operation of the PAFSOR equipment and test proce-
    dures.

(2) Perform additional in situ and laboratory tests as
    required to provide further information regarding soil
    properties at the exact location of the SBPT program.

TASK C

(1) Analyze the PAFSOR and CAMKOMETER data to derive
    stress-strain-strength relationships and measurements
    of in situ lateral stress and correlate these results
    with values previously determined for Boston Blue clay.
    The analyses would utilize and evaluate various
    theories and curve fitting procedures developed to
    derive such relationships and assess the sensitivity
    of the measurements to testing procedures and site
    conditions.

The PAFSOR test program, conducted during May and June
of 1977, yielded values of in situ horizontal stress signi-
ficantly less than predicted from laboratory results and
the contract was subsequently modified to include further
investigation of in situ lateral stress. MIT designed and
had constructed three earth pressure cells with varying
tip geometries for insertion at the bottom of a predrilled
hole. Measurements of lateral stress were then made with
each cell over a period of several weeks to months at three
different depths within the Boston Blue clay deposit. MIT
also obtained undisturbed samples at each location of the

5

PAFSOR tests for subsequent laboratory strength and consolidation tests performed by both MIT and CALDOT.

During the course of the research, MIT had several informal discussions with Professor Michele Jamiolkowski of the Politecnico di Torino in Italy regarding their extensive experience with PAFSOR and CAMKOMETER tests in a variety of soil types. This eventually led to another contract modification wherein Politecnico di Torino agreed to present detailed results from five case studies (four in Italy and one in Iran) as a cooperative effort with MIT.

Finally, the FHWA plans to purchase the latest SBPT equipment in order to continue its program of evaluating this type of in situ testing.

1.3 ORGANIZATION OF REPORTS

This report is restricted to the results of MIT's research related to self-boring pressuremeter tests performed in Boston Blue clay. Chpater 2 summarizes background information on the SBPT, while Chapter 3 gives an overview of the test program and general site conditions and presents details concerning "reference" values of in situ stress and undrained stress-strain-strength properties for the Boston Blue clay. General results from the SBPT program are contained in Chapter 4. The next three chapters, which form the main body of the report, present a detailed evaluation of data obtained from the SBPT, namely in situ horizontal stress, limit pressure, and undrained stress-strain-strength parameters. These chapters discuss the effects of testing variables and evaluate different methods used to derive soil parameters.

Politecnico di Torino, in cooperation with MIT, will prepare a second report that presents and evaluates

6

self-boring pressuremeter test data obtained at other sites with varying clay types and stress history. The nature and scope of any additional reports have not yet been decided, this depending for example on whether or not MIT becomes engaged in further field testing and developmental work.

2. THE SELF-BORING PRESSUREMETER TEST*

2.1 HISTORICAL BACKGROUND

The concept of the pressuremeter test was first pro-
posed by F. Kogler of Germany in 1933 and subsequently devel-
oped by Menard (1956) while working on his Master's degree
at the University of Illinois. As shown in Figure 2-1,
the Menard pressuremeter test (MPT) consists of a cylindri-
cal probe (diameter ≈ 6 cm) connected to a pressure loading
and volume measurement system. The 20 cm long measurement
cell, located between two 10 cm long guard cells, is
lowered into a predrilled borehole and the test performed
by monitoring the volume of water injected into the central
cell as a result of pressure increments applied at one min-
ute intervals. Typical data obtained from this procedure
are illustrated in Figure 2-2, the corrected pressure (P)
being the applied pressure adjusted for the effects of the
rubber cell membrane and the elevation difference. The
typical curve has three distinct phases commonly interpre-
tated as follows. The initial curved portion, Phase 1,
results from expansion of the membrane as it comes into
full contact with the sides of the predrilled borehole
at pressure P_o. The approximately linear portion of Phase
2 corresponds to pseudo-elastic deformation of the soil,
while Phase 3 starts with the onset of contained plastic
flow around the probe and continues to the limit pressure
P_l, generally taken as the pressure required to double the
initial volume of the cell.

---

* The material in this chapter was mainly obtained from
Ladd et al. (1977) and the book by Baguelin, Jezequel and
Shields (1978) entitled The Pressuremeter and Foundation
Engineering. The latter is a well written, most compre-
hensive treatise on the subject and should be required
reading for anyone seriously interested in pressuremeter
testing.

Based on theoretical considerations existing at the time of its development, the MPT was thought capable of yielding four soil parameters: the pressure P_O corresponding to the in situ total horizontal stress (σ_{ho}); the pressuremeter modulus (E_p) obtained from the slope of the Phase 2 curve; the pressure P_f corresponding to initial yielding; and the limit pressure P_1 used to estimate the strength of the soil. With the assumption that the guard cells minimize end effects, the test data can be interpreted in terms of radial expansion of a cylindrical cavity. For a linear elastic isotropic soil, the pressuremeter modulus is obtained using:

$$E_p = 2(1+\nu)(V_c+V_m)\,dP/dV \qquad \text{(Eq. 2-1)}$$

where ν is Poisson's ratio, V_c is the initial volume of the cell and V_m is the injected volume at the middle of the Phase 2 curve. And for an ideal elastic-plastic cohesive material, Bishop et al. (1945) derived the following theoretical expression for the limit pressure in terms of the undrained Young's modulus (E_u) and the undrained shear strength (c_u) of the soil:

$$P_1=P_O+c_u[1 + \ln \frac{E_u}{2c_u(1+\nu)}] \qquad \text{(Eq. 2-2)}$$

For a saturated soil ($\nu=0.5$), Eq. 2-2 can be rearranged to compute c_u by iteration as follows:

$$c_u = (P_1-P_O)/N_p \qquad \text{(Eq. 2-3a)}$$

where N_p = theoretical strength factor for pressuremeter test

$$= (1+\ln \frac{E_u}{3c_u}) \qquad \text{(Eq. 2-3b)}$$

Since E_u/c_u for most clays falls between 100 and 2000 (Ladd et al., 1977), N_p should theoretically equal 6.0 ± 1.5.

After returning to France, Menard and his co-workers devoted considerable effort to correlating MPT values of modulus and strength against data obtained from "conventional" tests, with rather discouraging results. They then decided that the test should be treated as a "model foundation test" and hence empirical scaling factors were eventually developed to permit the results of the MPT to be used directly to design both deep and shallow foundations. Baguelin et al. (1978) present and discuss such empirical design procedures in considerable detail based on the experience of Menard and the soil mechanics and foundations division of the Ponts et Chaussees, which became a principal user of the MPT. It is important to emphasize that the MPT is not recommended by Menard or Baguelin et al. (1978) to measure fundamental soil properties. Rather values of P_1-P_o and E_M ($=E_p$ with ν set equal to 0.33 in Eq. 2-1) are used directly in a strictly empirical fashion.*

Although the MPT really constitutes an entire design procedure, many engineers still employ the device for in situ measurements of soil properties for use with conventional theories to predict stability, deformations, in situ stresses, etc. This practice is ill-advised, for many factors essentially preclude rational interpretation of MPT data. The more important factors include: the substantial influence of soil disturbance; large end effects at high strains; indeterminate drainage conditions; and simplifications inherent to Eq. 2-1, 2-2 and related methods of interpretation.

---

* By analogy, standard penetration test N values are used directly to estimate the settlement of footings on sand via the Terzaghi and Peck (1967) empirically developed relationship given in Figure 54.4.

But two recent developments made the pressuremeter test concept very attractive as a potential method for reliable measurement of certain in situ soil properties, these being the self-boring pressuremeters (which greatly reduce the amount of disturbance) and theoretical advances in interpretation of the test data (which removed the rheological restriction of assuming elastic-plastic soil behavior). Ponts et Chaussees first used the self-boring pressuremeter test (SBPT) in 1967 and Baguelin et al. (1972) presented K_O, E_u and c_u data from these so-called "Autoforeur Probe" or PAF tests. Cambridge University in England was independently developing its self-boring device, later termed the CAMKOMETER, as reported by Wroth and Hughes (1973). The latter unit had a load cell for measurement of σ_{ho} in addition to an expandable membrane for conducting pressuremeter type tests. Meanwhile, Baguelin et al. (1972), Ladanyi (1972) and Palmer (1972) independently developed an analytical solution which enabled the complete <u>undrained</u> stress-strain curve of a saturated clay to be derived from the results of an undrained pressuremeter test. The solution assumes the soil to have a unique, but not pre-defined, stress-strain relationship which at small strains reduces to the simple expression:

$$\tau = 0.5(\sigma_r - \sigma_\theta) = \varepsilon_o \frac{dP}{d\varepsilon_o} \qquad \text{(Eq. 2-4)}$$

where σ_r = radial stress

σ_θ = circumferential stress

ε_o = strain = $\Delta r / r_o$

r_o = initial radius of measurement cell.

Δr = radial displacement of measurement cell.

Thus, at least in theory, $\sigma_{ho} = \sigma_r = P_o$ at $\varepsilon_o = 0$, c_u is the peak value of τ, and $E_u = 3G = 1.5\tau/\varepsilon_o$ for a perfectly executed SBPT in a saturated clay.

The next sections will summarize the basic equipment and procedures used to conduct self-boring pressuremeter tests in cohesive soils and methods commonly used to interpret SBPT data, followed by a brief discussion of some of the principal problems associated with this type of in situ testing.

2.2 EQUIPMENT AND PROCEDURES

Ponts et Chaussées and Cambridge University have both developed several self-boring pressuremeter devices. Though employing the same basic concept, important differences exist in the technical details of the methods used to accomplish self-boring and subsequent expansion of the cell and in the measurement systems. The self-boring principle has also been extended by the French to enable other types of in situ testing such as vane shear and permeability. The book by Baguelin et al. (1978) describes the various French devices and how they operate in considerable detail.

Figure 2-3 shows a schematic drawing of the PAFSOR (also called PAF-72), the second version developed by the French and the one used for the MIT test program in Boston Blue clay. The self-boring module contains a cutting tool rotated by a hydraulic motor, attached to the top of the device, that is connected via two hoses to a pump located on a drill rig. A drill rod pushes the probe into the ground and carries wash water that is jetted out from the cutting tool. The latter grinds up the soil which has entered the cutting edge and the slurried soil then flows up to ground surface through the space between the drill rod and the sides of the open borehole after passing through the measurement cell. The cutting tool configuration and its location within the cutting module, the volume of wash

12

water and location of the jet holes, and the force applied to
the drill rod (e.g. rate of advance) can all be varied in
order to achieve minimal displacement of soil around the
probe during the self-boring process. But this requires
considerable experience at each new site before one can
establish appropriate operating procedures. Since soil
displacements cannot be measured during self-boring,
one must evaluate data from trial tests to ascertain which
methods appear to give the best results.

Chapter 6 of Baguelin et al. (1978) describes variations
on the above technique. For example, the hydraulic motor
in the latest French device (PAF-76) is located within the
cutting module below the measurement cell. In contrast,
the CAMKOMETER employs a double string of rods. The hollow
central rod serves two functions: it carries the wash
water to the cutting module and also rotates the cutting
tool (i.e. the rotating motor is located at ground surface,
not within the actual device). The outer drill rod is
slightly smaller than the diameter of the hole and return
wash water and soil cuttings flow up to ground surface be-
tween it and the central rod.

Description of the measurement cell and conduct of an
expansion test follows, first for the French device and
then for the English unit. The inflatable part of the
PAFSOR probe consists of only one cell, having a diameter
of 5.2 inches (13.2 cm), whose outer surface is a longi-
tudinally reinforced rubber membrane (also protected by
vertical metal strips when used in stiff soils). A small
plastic tube connects the cell to a "control unit" located
at ground surface. This unit meters the volume of water
pumped into the measurement cell and reads the applied
pressure via conventional pressure gages. Note that the

13

measured pressure must be corrected for the difference in elevation between the probe and the control unit, for the membrane resistance and head losses in the plastic tube.

The measurement cell is inflated prior to insertion to have an initial volume such that the average diameter equals the outer diameter of the cutting shoe. However, during insertion the diameter at various locations along the measurement cell can vary due to compliance of the system (e.g. the plastic tubing and pressure gages) and/or due to variable in situ horizontal stresses acting along the measurement cell. In any case, the cell pressure is monitored during the self-boring process. Once the desired test level is reached, the vertical force on the drill rod is first released, the hydraulic motor is stopped and then the wash water cut off. The variation in cell pressure is recorded during the subsequent "relaxation" period, this typically being about 30 min., to obtain the initial pressure P_o.

The actual expansion test is strain controlled. A small electric motor attached to the control unit injects water down the small plastic tube and into the measurement cell. The expansion pressure is monitored by one of the control unit pressure gages. The PAFSOR used by MIT could inject water at different rates (6, 20 and 60 cc/min were used) with a total volume expansion of 750 to 1000 cc. After reaching the desired expansion, the motor is reversed and the pressure recorded as water is pumped out of the measurement cell.

The PAF-76 model offers the following advantages compared to the above PAFSOR (=PAF-72):

1) The measurement module has two guard cells in addition to the measurement cell (like the original

Menard device) and thus should be less influenced by end effects.

2) The cell pressure can be more accurately measured via an electric transducer located within the probe.

3) The volume of the measurement module is kept absolutely constant during insertion by a remote control valve located within the probe. Items (2) and (3) are especially important for evaluation of P_O.

4) Coaxial tubing and a special burette system provide more accurate measurements of volume change during expansion of the measurement cell.

Wroth and Hughes (1973) describe a self-boring device developed at Cambridge University that contained a total stress cell located between the cutting head and an upper section having an expandable membrane. The total stress cell, used to measure σ_{ho}, contained electrical resistance strain gages and operated on the principles of the boundary load cells developed at Cambridge (Arthur and Roscoe, 1961). Wroth and Hughes (1974) report that "a few hours are usually adequate" for the total stress cell to come into equilibrium with the lateral stress exerted by the soil on account of the small excess pore pressures generated during insertion of the probe.

The Mk 3 version of the CAMKOMETER, as described by Wroth and Hughes (1974), has a diameter of 2.5 in. (6.35 cm) and contains either a total pressure cell or an expandable section for performing pressuremeter tests [the latter version has an overall length of 30 in. (75 cm)]. During insertion, the rubber membrane is held firmly against a thick walled tube via a partial vacuum such that the outside diameter of the membrane is the same as the diameter

15

of the cutting head. An internal gas pressure is then
applied to the membrane in increments (say at 30 sec inter-
vals) by a hand-operated reducing valve attached to a high
pressure nitrogen cylinder. The pressure is measured both
by an electrical transducer within the probe and also by
a standard pressure gage next to the control valve. The
radial expansion of the membrane is monitored by three
separate hinged feelers which are kept in contact with the
rubber membrane by the action of thin leaf springs. Electric
resistance strain gages measure the movement of each feeler
and the results combined internally to give an average mem-
brane expansion. As with the French devices, small
pore pressure transducers can be attached to the rubber
membrane for measurements of pore water pressures at the
cell-soil interface during testing.

The Mk 3 CAMKOMETER and PAFSOR devices differ in the
following respects:

1) Better control of cell radius during insertion
with the former since the cell membrane rests on
a rigid inner tube. This should make the CAMKO-
METER unit somewhat better suited for measurements
of in situ lateral stress. However, the thin
rubber membrane of the CAMKOMETER is probably
more liable to damage during self-boring.

2) The PAFSOR uses water to expand the probe and to
record volume changes rather than gas pressure and
a feeler system. Baguelin et al. (1978) discuss
the relative advantages and drawbacks of these two
methods (see pp. 469-470).

3) The CAMKOMETER test is stress controlled rather
than strain controlled which causes a number of
added complications according to Baguelin et al.
(1978) (see p. 473).

16

2.3 THEORETICAL INTERPRETATION OF UNDRAINED TESTS IN SATURATED COHESIVE SOILS

Baguelin et al. (1978) review and extend analytical solutions developed by Baguelin et al. (1972), Ladanyi (1972) and Palmer (1972) for computation of the stress-strain relationship obtained from an undrained self-boring pressuremeter test run in a saturated cohesive soil. Table 2-1 summarizes various definitions of strain at the wall of the cavity (i.e. at the cell membrane) and corresponding equations used to compute the shear stress $\tau=0.5(\sigma_r-\sigma_\theta)$ at this location. As previously noted, at small strains Eq. 2-6a reduces to

$$\tau = \varepsilon_O \ dP/d\varepsilon_O \qquad \text{(Eq. 2-4)}$$

and the peak value of τ is taken to be equal to the undrained shear strength c_u of the clay.

Expressions for modulus are:

$$\text{Shear modulus:} \quad G = \tau/\gamma=\tau/2\varepsilon_O \qquad \text{(Eq. 2-7)}$$

$$\text{Undrained Young's modulus:} \quad E_u=2(1+\nu)G=3G \qquad \text{(Eq. 2-8)}$$

where $\gamma=2\varepsilon_O$ is the engineering shear strain.

Various graphical, numerical and analytical techniques are employed to obtain stress-strain curves from actual test data. The subtangent method, illustrated in Figure 2-4, is one common graphical procedure. It utilizes Eq. 2-4 since the subtangent distance y is equal to $\tau=\varepsilon_O \ dP/d\varepsilon_O$. A somewhat more involved graphical technique, based on Eq. 2-6b (Table 2-1), determines slopes from P versus log $\Delta V/V$ plots, i.e. $\tau=0.434 \ dP/d\log(\Delta V/V)$. Baguelin et al. (1978) describe a numerical method employing Eq. 2-6d. In its simplest form, the tangent to the P vs ΔV curve at a given point is assumed to have the same slope

as a straight line which passes through two adjacent points.
This procedure, however, often yields very erratic stress-
strain curves due to experimental scatter in the test data.
Thus   analytical techniques are widely used in order to
smooth out the scatter in derived stress-strain curves.
In these techniques, the actual expansion curve is repre-
sented by a mathematical relationship and the shear curve
then found by simple differentiation. For example, Baguelin
et al. (1972) employ the following empirical equation:

$$P-P_o = \frac{1}{2b}[a\log(1+\varepsilon_o^2) + \arctan\varepsilon_o]$$ (Eq. 2-9)

where the constants a and b are obtained using linear
regression. More recently, Jamiolkowski and Lancellotta
(1977) used theoretical equations based on stress-strain
relationships postulated by Prevost and Hoeg (1975) for
undrained shear of strain softening and strain hardening
soils.

2.4 DISCUSSION

The only assumption inherent to the equations presented
in Table 2-1, other than those stated in its title, is that
all the soil surrounding the probe which is influenced
by the test have a unique stress-strain relationship. But
for this to be absolutely true during a self-boring
pressuremeter test, the following conditions must exist:

1) The surrounding soil is completely homogeneous and
    saturated.
2) The stress-strain relationship of the soil is not
    affected by variations in the strain rate (the
    strain rate varies inversely with the square of
    the radial distance from the center of the cavity).
3) No disturbance of the soil during insertion of
    of probe. Since soil is not elastic, this

also implies zero horizontal strain in the soil adjacent to the measurement cell and hence P_O should equal the in situ lateral stress σ_{ho}.

4) Expansion occurs at a sufficiently rapid rate to preclude any drainage, i.e. flow of water, within the soil mass.

5) The length to diameter ratio of the measurement cell is sufficiently large to satisfy the plane strain assumption.

In reality, essentially none of the above conditions can be completely satisfied. Some of these factors have been studied theoretically as isolated variables (often with simplifying assumptions), while others have been investigated experimentally. Nevertheless, serious questions still exist regarding the practical significance of deviations from the ideal case, both individually and as a whole.

The above uncertainty concerning the reliability of the SBPT has resulted in large part from comparison of c_u values measured in that test with those obtained by more conventional methods. For example, the data summarized in Table 2-2 indicate that the SBPT usually yields peak strengths significantly larger than those measured with the field vane. Since the latter c_u values are generally too large for use in stability analyses with clays having a plasticity index greater than 20 to 40% (e.g. Ladd et al., 1977), it therefore appears that the SBPT will greatly overestimate the in situ c_u appropriate for evaluating bearing capacity and stability with most cohesive soils. Though Baguelin et al. (1978) reached a similar conclusion, they apparently feel that the discrepancy may be caused by deficiencies in present day methods of bearing capacity and stability analysis rather than errors in c_u values obtained from the SBPT.

Nevertheless, the fact exists that results of SBPT in clays generally show the following:

1) Peak c_u values considerably larger than expected.
2) Very small strains at the peak strength, ε_o typically being only 1 to 2%.
3) Significant strain softening, i.e. large decreases in the post peak shear stress.

Possible reasons for this behavior and other potential problems associated with the SBPT are summarized below under three principal headings: disturbance; strain rate; and other factors.

Disturbance

Disturbance due to lateral and vertical strains adjacent to the cavity affects the initial cell pressure. As a general rule with "good quality" tests (e.g. Baguelin et al., 1978), P_o increases during the self-boring process and then decays during the subsequent relaxation period. Several hours are often required for stabilization of P_o, although shorter relaxation periods are frequently used in practice. In any case, the value of P_o at the start of the test will seldom exactly equal the in situ lateral stress σ_{ho}. The magnitude of the error varies considerably with the precise installation technique and is generally thought to be greatest in "stiff" clays (e.g. Baguelin et al., 1974, and Windle and Wroth, 1977).

The magnitude of P_o has been found to have a significant effect on the stress-strain curve derived from the expansion curve using Eq. 2-4 or 2-6 (e.g. Schmertmann, 1975; Jamiolkowski and Lancellotta, 1977; Baguelin et al., 1978). If P_o is too low, the computed τ vs. ε_o and peak strength are too high and vice versa. The change in

20

strength can be very significant since relatively small variations in ε_O at failure (say by a few tenths of a percent) cause a large change in the magnitude of $\tau = \varepsilon_O dP/d\varepsilon_O$. Experience indicates that a 20% reduction in P_O produces an overestimate of c_u by about 20 to 40%.

In many cases, disturbance is sufficiently severe to alter the basic shape of the expansion curve such that the initial portion resembles Figure 2-2 rather than Figure 2-4, i.e. a reverse curvature. This greatly complicates selection of the appropriate P_O and hence stress-strain data derived from "corrected" expansion curves are liable to serious error (Jamiolkowski and Lancellotta, 1977). Baguelin et al. (1978) state that no attempt should be made to derive stress-strain curves in such situations (p. 570).

Baguelin et al. (1978) present a theoretical analysis of the case where an annulus of remolded soil having a reduced modulus and strength exists around the probe. They conclude that the derived stress-strain curve (i.e. using Eq. 2-6) leads to an overestimate of c_u which could be double the real strength if the thickness of the remolded zone approaches half the radius of the cavity. Such a large remolded zone is considered unlikely. However, the analysis neglects any changes in P_O due to disturbance, which if reduced could also contribute to a further overestimate of c_u.

Unless the expansion curve exhibits reverse curvature or very erratic behavior, how can one assess the quality of a test? Baguelin et al. (1978) suggest using a "displacement index" to ascertain the success of the self-boring technique. It equals $\Delta P_O/P_O'$ where ΔP_O is the decrease in the cell pressure during the relaxation period and P_O' is

the stabilized value of P_O minus the in situ equilibrium pore pressure. They assume P_O' will equal σ_{ho}' (in situ effective horizontal stress) and state that the displacement index should be less than two. Although the recommended limits on ΔP_O may be reasonable, the stabilized P_O might still differ from σ_{ho} and hence cause errors in the derived shear curve.

In the opinion of the writers, the precise effects of disturbance remain unresolved and requires considerable further research.

Strain Rate

The rate at which the cell is expanded obviously affects the amount the drainage, i.e. the degree of pore pressure dissipation, that can occur within the soil mass. The large changes in stress near the cell membrane cause high pore pressure gradients. Any resultant pore pressure dissipation would produce volume changes and also alter the stress-strain relationship of the soil. No existing analyses can account for these effects and thus theory has not provided guidelines regarding suitable rates as a function of the consolidation characteristics of various soil types. Baguelin et al. (1978) recommend using $d\varepsilon_O/dt = 1\%/min.$ so that "the test will be undrained in clay and drained in sand" (p. 517) but do not give supporting data. Also note that an appropriate rate cannot be established experimentally. Moreover, Wood and Wroth (1977) present results suggesting that significant pore pressure dissipation may occur when high gradients exist near the cell membrane during the latter stages of a typical SBPT. Thus, in the opinion of the writers, the exact effects of partial drainage remain unresolved.

Even when the cell is expanded at a constant rate, the strain rate within the soil mass varies inversely with the square of the radial distance. Since both undrained modulus and c_u decrease with decreasing strain rate (e.g. Ladd et al., 1977), substantial variations in the stress-strain relationship can exist within the soil mass whereas Eq. 2-6 assumes a unique relationship. Prevost (1976) analyzed this problem using a theoretical model that closely approximates the rheological properties of clays during undrained shear. He demonstrated that stress-strain curves derived from a standard SBPT using Eq. 2-6 will generally exhibit strain-softening even when the soil is actually strain-hardening for constant strain rate loading conditions. In addition, the strain rate in the soil adjacent to the expanding cavity (i.e. $d\varepsilon_o/dt=1\%/min.$) is one to two orders of magnitude faster than that employed in typical consolidated-undrained laboratory tests. The combined effect produces derived curves having pronounced strain-softening and an excessive peak c_u according to Jamiolkowski and Lancellotta (1977) and Baguelin et al. (1978). This conclusion agrees with the experimental evidence previously cited although other factors such as disturbance may exacerbate the effect.

Ladanyi (1977) claims that the effects of having a variable strain rate within the soil mass can be avoided by conducting stage loaded pressuremeter creep tests and analyzing the results using an elastic-nonlinear-viscous soil model. He used this procedure for evaluating creep properties of frozen soil where it may well be applicable. But with saturated clays, partial drainage during creep would also affect the deformations and hence greatly complicate interpretation of the results.

23

Other Factors

Conventional laboratory shear tests such as triaxial compression measure an undrained strength for vertical loading $c_u(V)$, i.e. the major principal stress always acts in the vertical direction (assuming K_o less than unity, a reasonable assumption for lightly overconsolidated clays). The SBPT causes a very different mode of failure, i.e. a vertical <u>failure</u> surface with the major and minor principal stresses at failure acting in the horizontal plane, and one should not expect the SBPT to yield strengths equal to $c_u(V)$. However, considerations of anisotropic behavior (Ladd et al., 1977) suggest that the stress path followed during a SBPT should lead to strengths less than $c_u(V)$ whereas the opposite is generally observed. Wood and Wroth (1977) support this view via data on kaolin from "true" triaxial tests performed to simulate the stress conditions imposed during a pressuremeter test.

Self-boring pressuremeter tests with measurements of pore pressure at the cell membrane (e.g. Baguelin et al., 1973; Wood and Wroth, 1977) indicate development of zones of negative circumferential effective stress in most of the tests and hence the possibility of resultant radial cracking. Ladanyi (1977) suggests that radial cracking should be expected during pressuremeter tests in overconsolidated clays, sensitive clays and frozen soils. With such soils, he states that the test "produced first a radial cracking of the soil around the borehole, followed by a nearly unconfined compression failure of the blocks between the cracks". Such behavior, if true, obviously violates the assumption of a unique stress-strain relationship for the entire soil mass.

Finally, analysis of the SBPT assumes that the intermediate principal stress at failure acts in the vertical direction. According to Wood and Wroth (1977), this assumption should be valid except perhaps in very heavily overconsolidated clays when K_o exceeds $1/(1-\sin\phi')$, ϕ' being the friction angle of the soil.

2.5 SUMMARY

The self-boring pressuremeter test (SBPT) offers the theoretical potential of making measurements of in situ lateral stress and undrained stress-strain properties of saturated clays in greater detail and more accurately than heretofore possible. This is an exciting prospect which has received well-deserved acclaim. But the test requires a very high level of technical expertise and experience and is costly compared to other in situ procedures. Serious uncertainties also exist regarding the reliability and true meaning of data obtained from a SBPT. For example, most tests show considerably more strain-softening and much higher peak strengths than expected based on conventional test methods. Thus, before the full potential of the test can be evaluated, a number of important topics require further theoretical and experimental research. These include the following questions:

1) How to assess and control the effects of disturbance during the self-boring process? This is especially important regarding the value of P_o vis-a-vis the actual in situ horizontal stress σ_{ho} and how variations in P_o affect the derived stress-strain curve.

2) Is partial drainage an important consideration? If so, what expansion rates are required to achieve acceptable results.

3) Do strain rate effects significantly alter the
   stress-strain relationship of most clays so as to
   invalidate the use of Eq. 2-6 (Table 2-1)? If so,
   what interpretation procedures should be employed
   to derive data from the expansion curve.
4) If radial cracks do develop during a SBPT, how does
   this affect the results?

TABLE 2-1 THEORETICAL RELATIONSHIPS FOR
UNDRAINED AXI-SYMMETRIC PLANE STRAIN
CAVITY EXPANSION IN SATURATED
COHESIVE SOIL (From Baguelin et al., 1978)

A. Circumferential Strain at Wall of Cavity

   1. Cauchy Strain: $\varepsilon_o = \dfrac{\Delta r}{r_o} = (1 - \Delta V/V)^{-1/2} - 1$ (Eq. 2-5a)

   2. Green Strain: $g_o = \dfrac{1}{2} \dfrac{\Delta V}{V_o} = \dfrac{1}{2}[(1 + \varepsilon_o)^2 - 1]$ (Eq. 2-5b)

   3. Almansi Strain: $a_o = \dfrac{1}{2} \dfrac{\Delta V}{V} = \dfrac{1}{2}[\dfrac{(1 + \varepsilon_o)^2 - 1}{(1 + \varepsilon_o)^2}]$ (Eq. 2-5c)

B. Shear Stress at Wall of Cavity $\tau = 0.5(\sigma_r - \sigma_\theta)$

   1. $\tau = \dfrac{1}{2}\varepsilon_o(1 + \varepsilon_o)(2 + \varepsilon_o) dP/d\varepsilon_o$ (Eq. 2-6a)

      $= dP/d\ln(\Delta V/V)$ (Eq. 2-6b)

   2. $\tau = g_o(1 + 2g_o) dP/dg_o$ (Eq. 2-6c)

      $= \Delta V(1 + \Delta V/V_o) dP/d\Delta V$ (Eq. 2-6d)

   3. $\tau = a_o dP/da_o$ (Eq. 2-6e)

      $= dP/d\ln(\Delta V/V)$ (Eq. 2-6b)

SITE	SOIL TYPE	PI (%)	$\dfrac{\text{Pressuremeter } C_u}{\text{Field Vane } C_u}$	REFERENCE
Cran	Soft clay	80	1.2	Baguelin et. al. (1974)
	Med. plastic silt	30	1.5	
Plancoet	Med. silt	20	0.75	
Provins	Med. clay	10	1.25	
	Med. silt w/peat	—	1.25	
St. André de Cubzac	Stiff plastic silt	35	1.5	
	Soft plastic silt	50	1.46	
Bosse Galin	Stiff clay	60	0.78	
	Med. clay	80	1.8	
Gothenburg	Soft clay	53 ?	1.3 – 2.5	Wroth & Hughes (1974)
King's Lynn	Soft clay	—	2.0	Wroth & Hughes (1973)

TABLE 2-2. COMPARISON OF UNDRAINED STRENGTHS MEASURED BY THE SELF-BORING PRESSUREMETER TEST AND THE FIELD VANE TEST (Ladd et al., 1977)
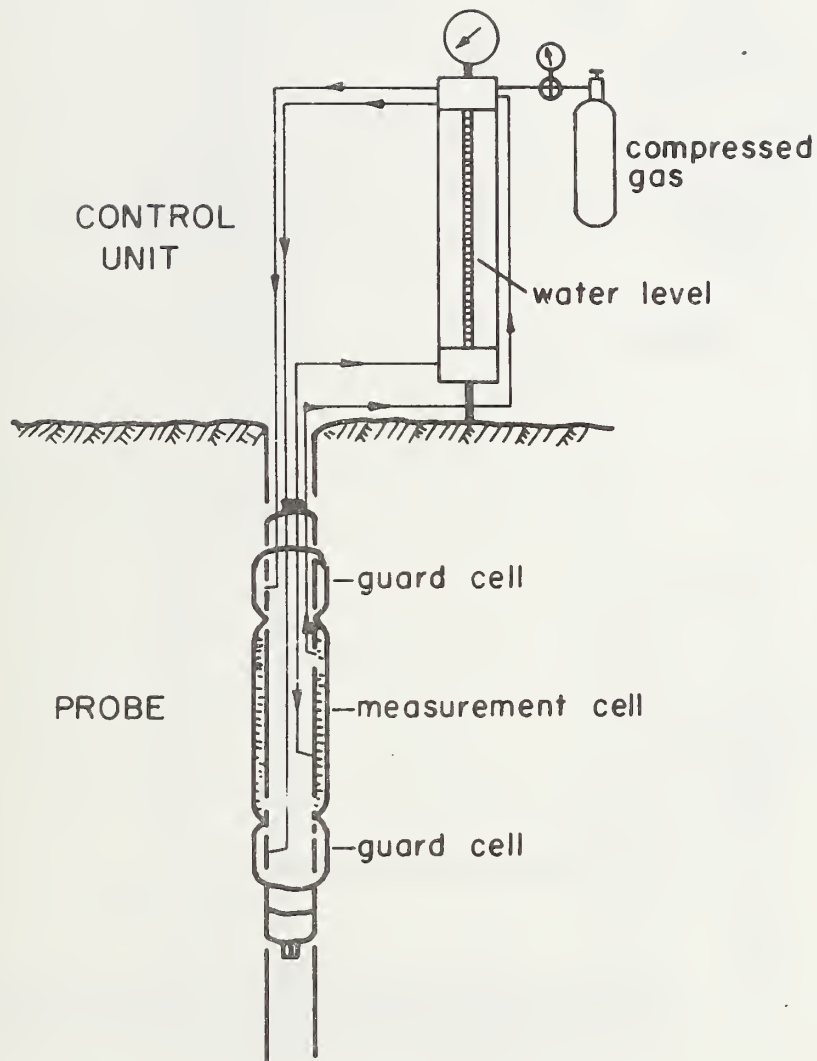
FIGURE 2-1. SCHEMATIC DRAWING OF MENARD PRESSUREMETER
TEST (Supplied by F. Schlosser in Ladd
et al., 1977)

29
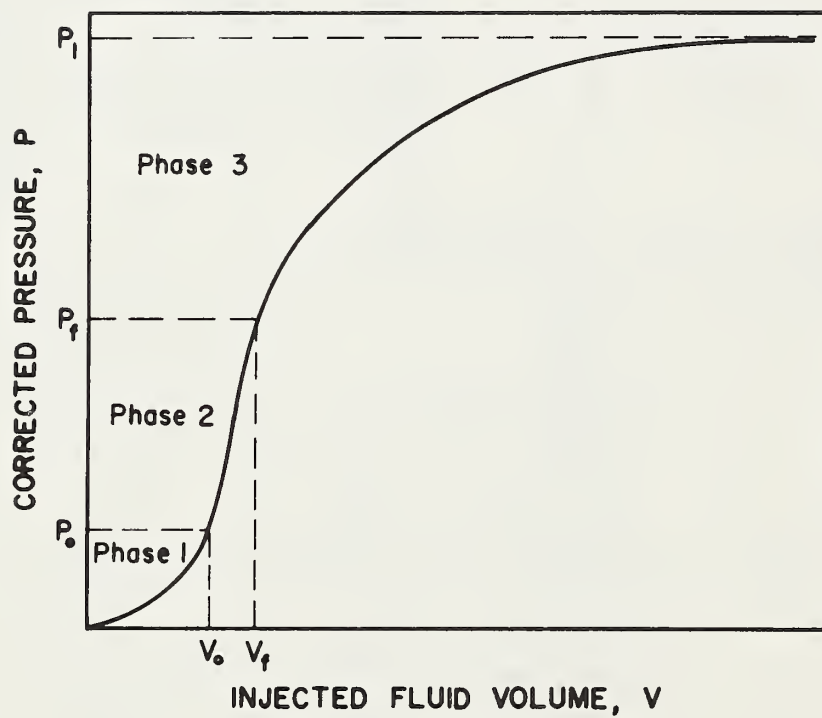
FIGURE 2-2. TYPICAL SHAPE OF PRESSURE VERSUS VOLUME
CURVE FROM MENARD PRESSUREMETER TEST
(Ladd et al., 1977)

30

Hydraulic
engine

Pressure
gauge

Measurement
cell

A

Tool

Cutting
edge

A

Slim pilot hole

Self boring in stiff soils

A

Guard

Self boring in soft soils
Normal guard & cutter
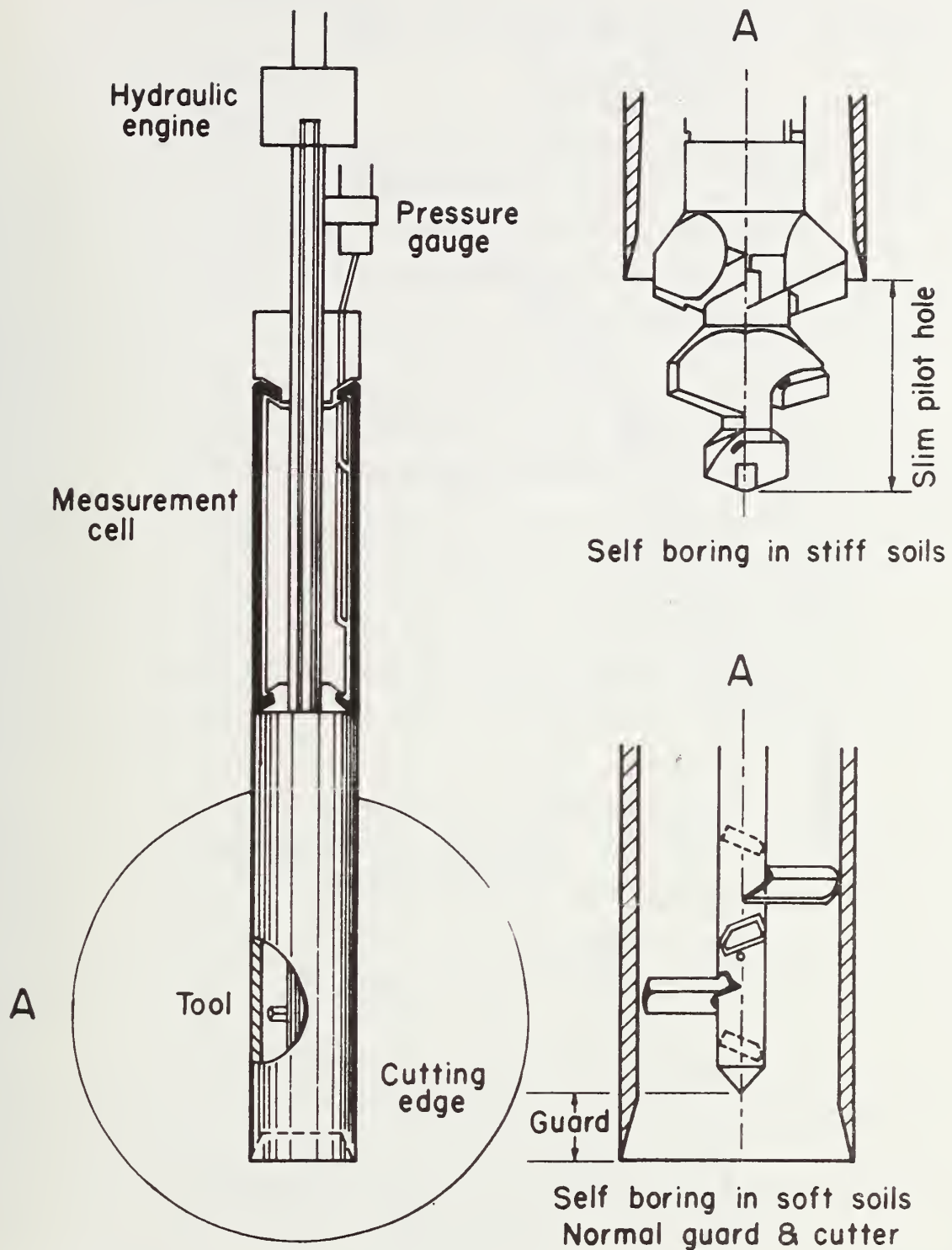
FIGURE 2-3.   SCHEMATIC DRAWING OF PAFSOR DEVICE (Supplied
by F. Schlosser in Ladd et al., 1977)

31
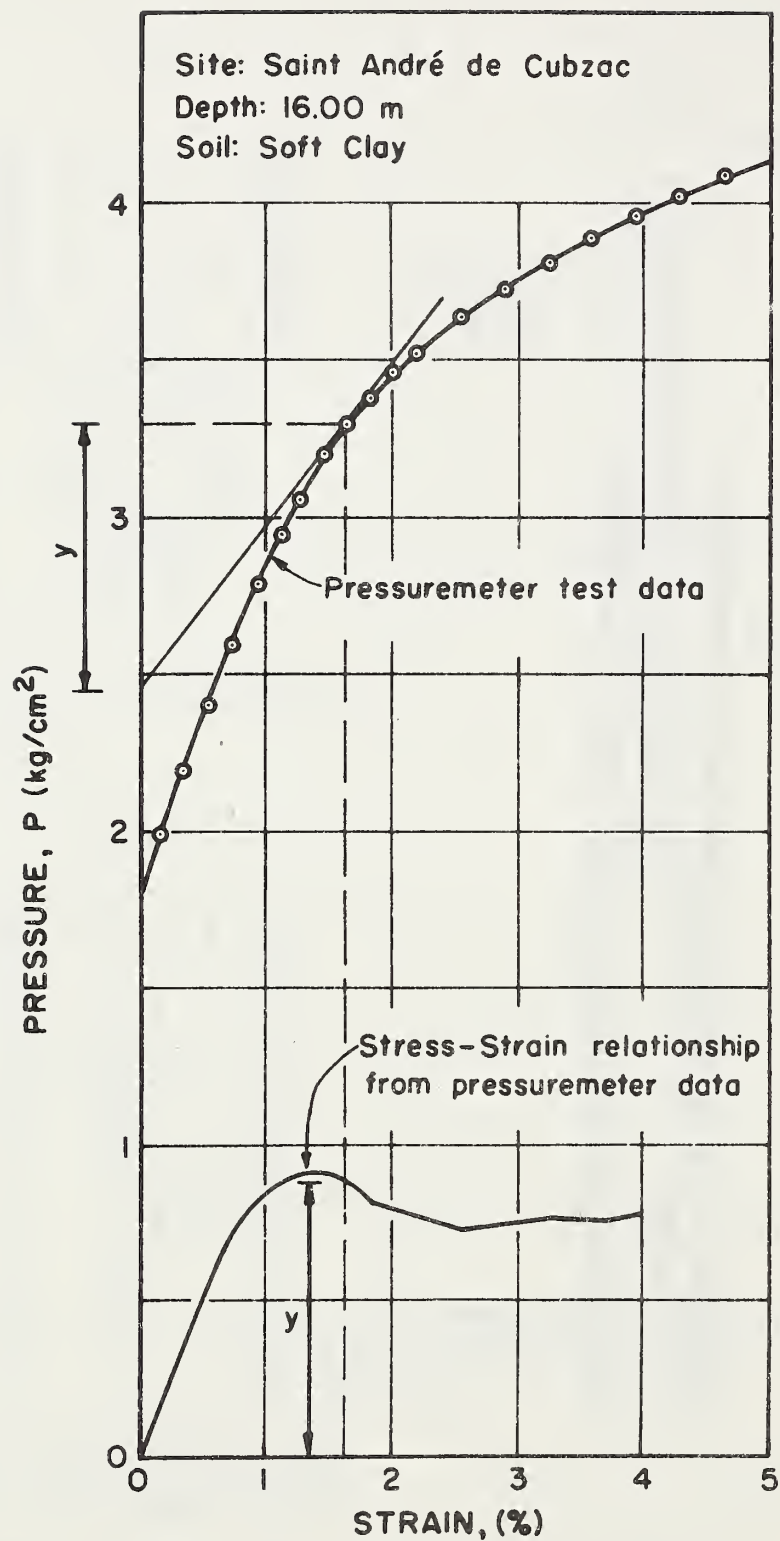
FIGURE 2-4. DATA FROM UNDRAINED SELF-BORING PRESSURE-
METER TEST ON CLAY (Supplied by F. Schlosser
in Ladd et al., 1977)

32

3. SITE CONDITIONS, TEST PROGRAMS AND SOIL PROPERTIES

3.1 SITE CONDITIONS

A portion of the partially completed Interstate High-
way I-95 in Saugus, Massachusetts passes through a tidal
marsh overlying deep deposits of Boston Blue clay. The
design incorporated preloading of the foundation soils
with surcharge fills in order to reduce post-construction
settlements. Construction of 35 ft (10.7 m) high embank-
ments began in 1967 and was terminated in May 1969. Ini-
tial plans called for removal of the surcharge and comple-
tion of construction in 1973. However a moratorium on high-
way construction cancelled further progress. Prior to this
change of plans, MIT in cooperation with the Massachusetts
Department of Public Works (MDPW) had instrumented two ex-
perimental test sections at Sta. 246 and 263 (see location
plan in Figure 3-1). Field vane tests and extensive labor-
atory investigations of the properties of Boston Blue clay
were also carried out.

In 1974, MIT and MDPW proceeded to remove the fill at
Sta. 246 to load the section at Sta. 263 until failure in
order to obtain insight in to the profession's ability to
predict stability and deformations. Predictions by eleven
geotechnical specialists were presented at a Symposium held
at MIT in 1974 (MIT, 1975).

In 1974, 1977 and 1978, MIT conducted testing programs
at both Sta. 246 and 263, including CAMKOMETER, PAFSOR,
Dutch cone penetrometer and piezometer probe tests. Figures
3-2 and 3-3 present plan and cross-sectional views of the
two test sites and location of the in situ tests.

Figures 3-4 and 3-5 summarize "virgin" soil conditions
at the two test sites. Relatively thin layers of peat, sand
and stiff overconsolidated clay cover up to 100 ft (30 m) or

33

more of medium to "soft" Boston Blue clay*. The Wisconsin
glaciation era deposited a layer of till over shale bedrock.
Glacial clay sediments were probably deposited in brackish
water some 14,000 years ago. Subsequently, during the
Valder's glacial substage, sea level fell with respect to
land, causing the clay sediments to emerge from below sea
level. Erosion, weathering and desiccation resulted in the
formation of the overconsolidated medium to stiff Boston
Blue clay. During warmer climates, sea level rose rapidly,
depositing sand on the clay surface. As the sea level con-
tinued to rise to its present level, organic silt, shells
and peat covered the entire area. Kenney (1964) presents
a detailed description of the geologic history of the post
glacial marine deposits in the Boston area.

In recent history, the water table stood at approxima-
tely El.+2. However an artesian pressure has been consis-
tently observed in the underlying glacial till. The cur-
rent magnitude of this artesian head is still under inves-
tigation, but for purposes of calculations a 10 ft (3.1 m)
artesian head in the till was selected based on piezometer
readings and results of piezometer probe tests.

The Atterberg limits of the illitic Boston Blue clay
plot near the A-line on Casagrande's plasticity chart in
the CL zone with a plasticity index (PI) typically equal to
21±3%. The liquidity index averages about 0.8 in the medium
clay and about 1.05 in the underlying soft clay. The pore
fluid salt concentration decreases with depth, perhaps
as a result of leaching via the artesian pressure in
the till layer.

---

* The bottom portion of the Boston Blue clay deposit is
  called soft based on standard penetration test blow
  counts, but actually has the undrained strength of a
  medium clay.

Results of undisturbed and remolded field vane tests indicate a very consistent sensitivity (S_t) of 5 at Sta. 246, whereas the value of S_t increases to 7 in the soft clay layer at Sta. 263. In the upper medium clay at this station, the sensitivity averages approximately 5.

Maximum past pressure profiles plotted in Figures 3-4 and 3-5 (more details are given in Figures 3-8 and 3-9 and Section 3.3) indicate a lightly overconsolidated deposit below El.-70 at Sta. 246, whereas the deposit below El.-70 at Sta. 263 appears to be normally consolidated. The undisturbed field vane strengths summarized in Figures 3-4 and 3-5 represent strengths averaged over 5 ft (1.5 m) intervals. At Sta. 246, the data (based on several test holes) apply to "virgin ground" conditions prior to any stress increase due to embankment construction. At Sta. 263, two vane test holes were conducted in 1973, 160 ft (48.8 m) east and west of the centerline when the ground elevation was at El.+12 on the west side and at El.+6 on the east side. These field vane c_u values also apply to "virgin ground" conditions. Section 3.5 further discusses the strength of the Saugus Boston Blue clay.

3.2 TEST PROGRAMS

As already mentioned and illustrated in Figure 3-2, numerous in situ and laboratory test programs were conducted at the two test sites. Table 3-1 lists the various in situ test programs. For the purpose of the present report, only the PAFSOR, CAMKOMETER and Earth Pressure Cell programs will be discussed in detail, although results of the other test programs will be used for comparison. Vivatrat (1978) and Lacasse et al. (1978) give details on the test procedures and results of the other investigations.

35

3.2.1 PAFSOR Tests

Prior to carrying out the pressuremeter tests, piezo-
meter probe profiles (Wissa et al., 1975) some 5 to 10 ft
(1.5 to 3.1 m) from the location of the PAFSOR tests were
made in order to detect sand lenses and other heterogeneities
in the clay stratum. Figure 3-6 summarizes the profiling
results at Sta. 246 and 263*. An 18° cone was used for
penetration, with the porous stone at the tip (Sta. 246)
or mid-tip (Sta. 263). The sharp decreases in the pore
pressures generated during penetration indicate a more
pervious (sandy) material. For example, the profiling at
Sta. 246 detected sand at El.-28, -40, -47, -49, and -53.
With this knowledge, an attempt was made to keep the PAFSOR
tests in the more homogenous clay layers. Figure 3-6
locates each PAFSOR test: 15 at Sta. 246 and five at Sta.
263 in May and June 1977. Typical variables in the test
procedures included membrane expansion rate, initial fluid
volume injected into the membrane before start of test,
delay time between self-boring and expansion, and the self-
boring drilling rate. After completing these tests, 3 in.
(76 mm) diameter undisturbed fixed piston samples were
taken at the elevation of each PAFSOR test in an adjacent
hole.

3.2.2 CAMKOMETER Tests

Fourteen CAMKOMETER tests were carried out at Sta.
263 in 1973 by Drs. J.M.O. Hughes and W.A. Marr to evaluate
this newly designed apparatus. The device had the following
characteristics:

        Diameter of cell = 2.50 in. (6.35 cm)
        Length of expansion membrane = 14.8 in. (37.7 cm)
        Pressure supply = gas (stress controlled tests)
        Type of readout = manual and electronic

* Detailed results in Vivatrat (1978) and Lacasse et al.(1978)

Although some of these tests are difficult to interpret because of their preliminary and prototype nature, the report attempts to compare these findings to the results obtained with the French pressuremeter. Figure 3-6 shows the elevations of the CAMKOMETER tests. Note that these were run before the embankment failure whereas the PAFSOR tests were run one year after the embankment failure which had caused considerable ground heave at the test location.

3.2.3 Earth Pressure Cell Measurements

In the spring and summer 1978, MIT made measurements of horizontal stress (σ_h) and pore pressure (u) at Sta. 246 via three new earth pressure cells designed in cooperation with Dr. A.E.Z. Wissa of Ardaman and Assoc. Nine measurements of σ_h and three of u were taken at the elevations shown in Figure 3-6. Appendix A presents the equipment and test procedures used, the test program and the results obtained.

3.2.4 Laboratory Investigations

In addition to index and consolidation tests, laboratory investigations of the Saugus Boston Blue clay prior to 1977 included unconfined compression (UC), unconsolidated-undrained triaxial compression (UUC), consolidated-undrained triaxial compression (CIUC), K_o consolidated-undrained triaxial compression (CK_oUC) and triaxial extension (CK_oUE), K_o consolidated-undrained plane strain compression (CK_oUPSC) and plane strain extension (CK_oUPSE) and K_o consolidated-undrained direct simple shear tests (CK_oUDSS). In 1978, Atterberg limits, incremental oedometer and constant rate of strain consolidation (CRSC) tests and unconfined compression tests were run on the Boston Blue clay samples taken adjacent to the pressuremeter tests.

37

3.3 STRESS HISTORY

Figure 3-7 summarizes the in situ stresses σ_{vo}, u_o and σ'_{vo} for "virgin ground" conditions at Sta. 246. These values apply to the 200 ft (61.0 m) offset east of the embankment centerline, where the majority of in situ tests was run. Figure 3-8 presents the values of maximum past pressures (σ'_{vm}) obtained on undisturbed samples of the clay foundation based on oedometer and constant rate of strain consolidometer (CRSC) tests. These latter σ'_{vm} values already correspond to end-of-primary compressibility curves. The figure also shows the overconsolidation ratio (OCR) in the medium Boston Blue clay decreasing with depth. The soft layer below El.-70 is only slightly overconsolidated, with OCR varying from 1.5 to 1.2, based on the average σ'_{vm}. At the centerline of Sta. 246, the fill elevation, at +38.5 since 1969, was reduced to +18 in 1974. (The granular material was used to load Sta. 263 to failure). The increase in total vertical stress 200 ft (61.0 m) east of the centerline after centerline loading and unloading was considered negligible, based on finite element calculations and elastic theory predicting $\Delta\sigma_v \leq 0.05$ kg/cm^2 (5 kPa). The total horizontal stress increased only slightly more, with $\Delta\sigma_h$ on the order of 0.2 kg/cm^2 (20 kPa) at El.-100.

As mentioned previously, the pore pressure profile was selected on the basis of equilibrium pore pressures recorded by the piezometer probe that were shown in Figure 3-7.

At Sta. 263, the present stress history cannot be determined reliably because of the 1974 failure (which caused a 6 ft (1.8 m) heave of the ground surface at the location of the test program) and uncertainty in the degree of pore pressure dissipation thereafter. Figure 3-7

presents the in situ stresses in 1967 for "virgin ground" conditions (far offsets) at Sta. 263 and the magnitude of the total vertical stress (σ_{vo}) in 1978 at the offset of Dutch cone, piezometer probe and PAFSOR tests. The σ'_{vo} value applies to conditions before any embankment construc- tion. Discussion of the pressuremeter tests run prior to and after the embankment failure will however require knowledge of σ'_{vo} at the time of the tests. The long term vertical stress increase at the west offset will equal at most the equivalent of 6 ft (1.8 m) of fill (due to the small berm shown in Figure 3-3) or $\Delta\sigma_{v}(max)=0.35$ kg/cm^2 (34.5 kPa). Given that some pore pressure dissipation occurred after 1967, neglecting a fraction of $\Delta\sigma'_{v}$ will not introduce a large error on σ'_{vo}, especially after con- sideration of all the other uncertainties associated with the state of stress at Sta. 263. Oedometer and CRSC tests on specimens from Sta. 263 yielded the σ'_{vm} data in Figure 3-9. The deposit is normally consolidated below El.-70. Through normalization of the field vane test data and using a relationship between $c_u(FV)/\sigma'_{vo}$ and OCR, Lacasse et al. (1978) calculated the values of σ'_{vm} from field vane (FV) results shown in the figure.

3.4 HORIZONTAL STRESS

This section summarizes calculated values of total horizontal stress at Sta. 246 and compares the results to the σ_h measurements made with the new earth pressure cells. Appendix A gives more details on the design of the cells and the test program.

The earth pressure cell test program was aimed at obtaining field measurements of the in situ total horizontal

stress, (σ_h) and the in situ pore pressure, (u) in order to ascertain the value of the effective horizontal stress (σ_h'). Determination of the coefficient of earth pressure at rest, $K_o = \sigma_{ho}'/\sigma_{vo}'$, has always been difficult, both in the laboratory and the field. Figure 3-10 summarizes the data available for Boston Blue clay prior to the field test program. Important scatter is observed. At the present time, Lacasse et al. (1978) still give most credibility to the Ladd (1965) test data. The relationship between K_o and OCR is reproduced in Figure 3-11*.

3.4.1 Sta. 246

Figure 3-12 presents the range of predicted total horizontal stress at Sta. 246. The values are based on the following data:

a) effective overburden vertical stress versus depth, σ_{vo}' (Figure 3-7)

b) range of K_o values from laboratory tests (Figure 3-10)

c) in situ pore pressure, u_o (Figure 3-7)

d) increase in total horizontal stress ($\Delta\sigma_h$) at 200 ft (61m) east offset at Sta. 246 due to 1967 embankment construction and subsequent partial removal in 1974.

For comparison purposes, the calculated σ_h for K_o equal to 0.5 (K_o value for normally consolidated Boston Blue clay) is also shown. As measurements of pore pressures from the earth pressure cell test program became available, the calculated σ_h values were revised to reflect the measured value of pore pressure (see Appendix A), but this caused relatively little change. Figure 3-12 also shows

---

* The SHANSEP strength curves shown in the same plot are discussed in Section 3.5.

40

the pore pressure and horizontal stresses measured by what is considered to be the most reliable of the earth pressure cells (See Appendix A for the data).

Figure 3-13 plots the predicted K_O values and the in situ K values inferred from the earth pressure cell test program. The "best estimate" is based on the K_O vs OCR curve in Figure 3-11 and the average OCR in Figure 3-8, while the band reflects the range in σ'_{vm} values and uncertainties in $\Delta\sigma_h$ due to embankment construction and in the K_O vs OCR relationships. The in situ measurements show the importance of the earth pressure cell tip geometry on the K values obtained after equilibrium (see equilibration curves in Appendix A). The very low values of K recorded by the blunt (40°) and enlarged tips probably reflect increased disturbance during penetration. The measurements with the symmetrical 20° tip are considered most reliable.

The range of predicted σ_{ho} at Sta. 246 (Figure 3-12) will be used for comparison with values of initial pressure measured in the pressuremeter tests.

3.4.2 Sta. 263

At Sta. 263, the occurrence of the 1974 failure makes accurate prediction of horizontal stress thereafter more or less impossible. Figure 3-14 presents a cross-section of the failure geometry and the probable location of the failure zone. However, since the CAMKOMETER tests were run prior to the embankment failure, Figure 3-12 presents a range of values for the horizontal stress profile at Sta. 263. These values, obtained in the same manner as for Sta. 246, must be considered as only approximate. They represent the initial state of stress before any construction (1967) and the total horizontal stress after construction to El.+38.

41

3.5 UNDRAINED STRESS-STRAIN-STRENGTH PROPERTIES

This section summarizes the results of the following strength tests in Saugus Boston Blue clay:

a) field vane
b) unconfined compression (UC) and unconsolidated-undrained triaxial compression (UUC)
c) Dutch cone penetrometer
d) CK_oU laboratory tests
e) SHANSEP strength calculations

Figure 3-15 summarizes the results of field vane tests* at Sta. 246 and 263 and Figure 3-16 compares the "virgin ground" strengths (before embankment construction) at the two stations. At Sta. 246, the data indicate little or no strength increase in 1969 and 1972 under the centerline of the embankment. This might be expected since relatively little pore pressure dissipation occurred during the period so that the clay remained overconsolidated. These results also imply that the foundation soil used for the pressuremeter, Dutch cone penetrometer and piezometer probe testing programs, located 200 ft (61 m) east of the centerline, remains relatively unaffected by construction of the embankment and subsequent unloading in 1974.

The average field vane profile at Sta. 246 shows the strength gradually decreasing in the medium clay to reach a minimum at El.-70, where the "soft" Boston Blue clay begins, and then increasing with depth. The FV strengths exhibit rather modest scatter, especially in the "soft" clay where the coefficient of variation (=standard

---

* All field vane tests were run with the Geonor apparatus using the prescribed ASTM procedure.

42

deviation/mean) was only about 5% compared to 15% in the overlying medium clay.

At Sta. 263, the field vane testing program included three test holes, run in 1974 before addition of new fill; two of these were located at distant east and west offsets from the centerline. Although the data exhibit slightly more scatter than at Sta. 246, the centerline strength again appears little affected by consolidation under the 35 ft (10.7 m) high embankment during the 5 years after filling, except below El.-90. This is consistent with Ladd's (1975) interpretation of the vertical consolidation stress that existed at the time of the field vane tests, i.e. values of σ'_{vc} less than σ'_{vm} except in the bottom 20 ft (6.1 m) of clay.

Comparison of the FV data at the two stations indicates that Sta. 263 has slightly lower strengths than Sta. 246. Lacasse et al. (1978) normalized the field vane strength data and present a plot of $c_u(FV)/\sigma'_{vo}$ vs OCR.

Results of UC and UUC tests are compared to the field vane strengths in Figure 3-17. At Sta. 246, the points represent average values from UUC tests performed by CALDOT on one or more adjacent tubes. These samples were generally of very high quality and the strengths are only slightly lower than the average FV strengths. The data at Sta. 263 are from samples taken in 1974 prior to the embankment failure. These show more scatter, presumably due to greater effects of sample disturbance.

Figure 3-17 also presents strengths from several Dutch cone tests* performed at Sta. 246. Computation of the DCT undrained shear strength c_u considered the average

---

* Standard 60° Fugro electrical cone, $10cm^2$ cross-sectional area, pushed at a constant rate of 2 cm/sec.

cone resistance, q_c, and a cone factor, N_c, of 16 in the theoretical equation proposed by Baligh (1975):

$$c_u = \frac{q_c - \sigma_{ho}}{N_c}$$

where σ_{ho} = in situ total horizontal stress.

The value of σ_{ho} was derived from the effective vertical stress (Figure 3-7), the coefficient of earth pressure at rest, K_o, versus OCR (Figure 3-11) and the in situ pore pressure, u_o (Figure 3-7). Test data were taken at 5 ft (1.5 m) intervals. As shown in Figure 3-17, the Dutch cone strengths plot below the field vane strengths, especially in the upper more heavily overconsolidated clays. Lacasse et al. (1978) discuss the reasons for this difference.

Typical stress-strain curves for normally consolidated and overconsolidated (OCR=4) Boston Blue clay from three types of CK_oU tests are shown in Figure 3-18. The direct simple shear (DSS) and plane strain extension (PSE) tests, which involve a rotation of principal stresses during shear, resulted in much lower strengths than the plane strain compression (PSC) tests, which were failed by increasing the vertical stress. Thus, Boston Blue clay has a high degree of strength anisotropy, i.e. lower c_u and increasing strain at failure with rotation of the principal stresses. The PSC tests also exhibited significant strain softening.

Since Boston Blue clay exhibits undrained strength anisotropy (as well as strain-softening and strain rate effects), one cannot define a unique c_u. Rather the value depends on the type of stability problem under consideration. For example, when estimating active earth pressures, the appropriate c_u should be close to the peak strength

44

for vertical loading, i.e. the value of $q_f = 0.5(\sigma_1 - \sigma_3)_f$ measured in a plane strain compression (PSC) test. Figure 3-11 presents the relationship between q_f/σ'_{vc} and OCR from $CK_O UPSC$ tests performed on Boston Blue clay. Note that this strength should represent the <u>maximum</u> undrained strength for the clay (neglecting strain rate effects), i.e. other modes of failure involve a rotation of principal stresses and hence a reduced strength.

On the other hand, when evaluating the factor of safety of an embankment on a clay foundation via circular arc stability analyses, the appropriate strength is the "average" value that can be mobilized along a potential failure surface at the moment of rupture. For this case, the peak strengths along the potential failure surface should be reduced to provide "strain compatibility" and c_u is defined as $\tau_{ff} = q_f \cos \phi'$, i.e. the shear stress on the failure plane at failure (Ladd, 1975). Figure 3-11 presents the variation in $c_u(Ave)/\sigma'_{vc}$ with OCR for Boston Blue clay as developed by Azzouz (1977).

Table 3-2 presents calculations of the variation in c_u with elevation at Sta. 246 using the SHANSEP procedure. The computations are made for vertical loading $[c_u(V)]$, which should represent the maximum strength, and for circular arc stability analyses $[c_u(Ave)]$, which should represent the average strength along a potential circular surface. The range in computed c_u values corresponds to the range in σ'_{vm} shown in Figure 3-8. These strengths will be used for comparison with strengths derived from the pressuremeter test program as they represent approximate upper and lower limits for the c_u of Boston Blue clay.

Figure 3-17 presents plots of the SHANSEP $c_u(Ave)$ versus elevation at Sta. 246 and 263 based on the <u>average</u>

maximum past pressure profiles at these two locations. At Sta. 246, c_u(Ave) is about 10% less than the average field vane strengths in the upper medium clay and about 10% higher than the average field vane strength in the under- lying "soft" clay. Based on results of model footing tests (Kinner and Ladd, 1973) and the planned embankment failure at Sta. 263, Azzouz (1977) and Vivatrat(1978) concluded that the SHANSEP c_u(Ave) profiles in Figure 3-17 should yield fairly reliable estimates of the in situ c_u for circular arc stability analyses.

Ladd (1975) evaluated values of undrained shear modulus (G) from various types of CK_oU laboratory tests, the results of finite element analyses aimed at predicting undrained deformations, and field measurements of lateral deformations that occurred during construction of the embankments at Sta. 246 and 263. Figure 3-19 presents values of G for vertical and horizontal loadings divided by consolidation stress plotted versus OCR derived from this study wherein G corresponds to one half of the stress increment required to cause failure, i.e. at $\Delta q/\Delta q_f$=0.5. These data and the average stress history profiles at Sta. 246 and 263 result in the values of G plotted in Figure 3-20.

TABLE 3-1. SUMMARY OF IN SITU INVESTIGATIONS
AT SAUGUS I-95 EMBANKMENT

In Situ Test	Date	Sta.	Offset (ft)	Ground Condition	Remarks
PAFSOR	1977	246 263	200 East 160 West	"Virgin ground" conditions After embankment failure	15 tests in two holes 5 tests in one hole
CAMKOMETER	1973	263	160 West	After addition of 12 ft berm in 1969	14 tests in one hole
Earth Pressure Cell	1978	246	200 East	"Virgin ground" conditions	9 measurments of σ_{ho} with three differently shaped instruments
Field Vane	1967 1969 1972	245 244,245 244	₵ and 160 East " ₵ and 100 East	"Virgin ground" conditions End of construction	Before embankment construction Data for partially consolidated foundation
Dutch Cone Penetrometer	1977, 1978	246 263	180-220 East 160 West	"Virgin ground" conditions After embankment failure	Several test holes One test hole
Piezometer Probe	1977, 1978	246 263	180-220 East 160 West	"Virgin ground" conditions After embankment failure	Several test holes One test hole
Hydraulic Fracturing	1974	246-263	₵ and offsets	----	Measurement of σ_{ho} at various stations and offsets

1 ft = 0.305 m

47

TABLE 3-2. CALCULATION OF SHANSEP UNDRAINED STRENGTHS AT STA. 246
(Stresses in kg/cm^2 = 98.1 kPa)

El.	σ'_{vo} [1]	σ'_{vm} [1]	OCR	Vertical Loading		Circular Arc Average	
				c_u/σ'_{vc} [2]	$c_u(V)$	c_u/σ'_{vc} [2]	$c_u(Ave)$
-20	0.58	3.5-4.5	6.05-7.75	1.26-1.50	0.73-0.87	0.74-0.92	0.43-0.53
-30	0.82	3.1-4.0	3.8-4.9	0.92-1.10	0.75-0.90	0.53-0.64	0.43-0.52
-40	1.04	2.8-3.6	2.7-3.45	0.72-0.86	0.75-0.90	0.41-0.49	0.43-0.51
-50	1.28	2.5-3.35	1.95-2.6	0.56-0.70	0.72-0.90	0.32-0.40	0.41-0.51
-60	1.52	2.35-3.1	1.55-2.05	0.46-0.58	0.70-0.88	0.26-0.33	0.40-0.50
-70	1.76	2.3-2.85	1.3-1.6	0.40-0.48	0.70-0.84	0.22-0.27	0.39-0.48
-80	1.99	2.4-2.9	1.2-1.45	0.38-0.44	0.76-0.88	0.21-0.25	0.42-0.50
-90	2.22	2.65-3.1	1.2-1.4	0.38-0.43	0.84-0.95	0.21-0.24	0.47-0.53
-100	2.45	2.9-3.35	1.2-1.35	0.38-0.42	0.93-1.03	0.21-0.23	0.51-0.57
-110	2.68	3.1-3.6	1.15-1.35	0.37-0.42	0.99-1.13	0.20-0.23	0.54-0.62
-120	2.92	3.35-3.8	1.15-1.3	0.37-0.42	1.08-1.23	0.20-0.23	0.58-0.67

(1) From Figure 3-8   (2) From Figure 3-11
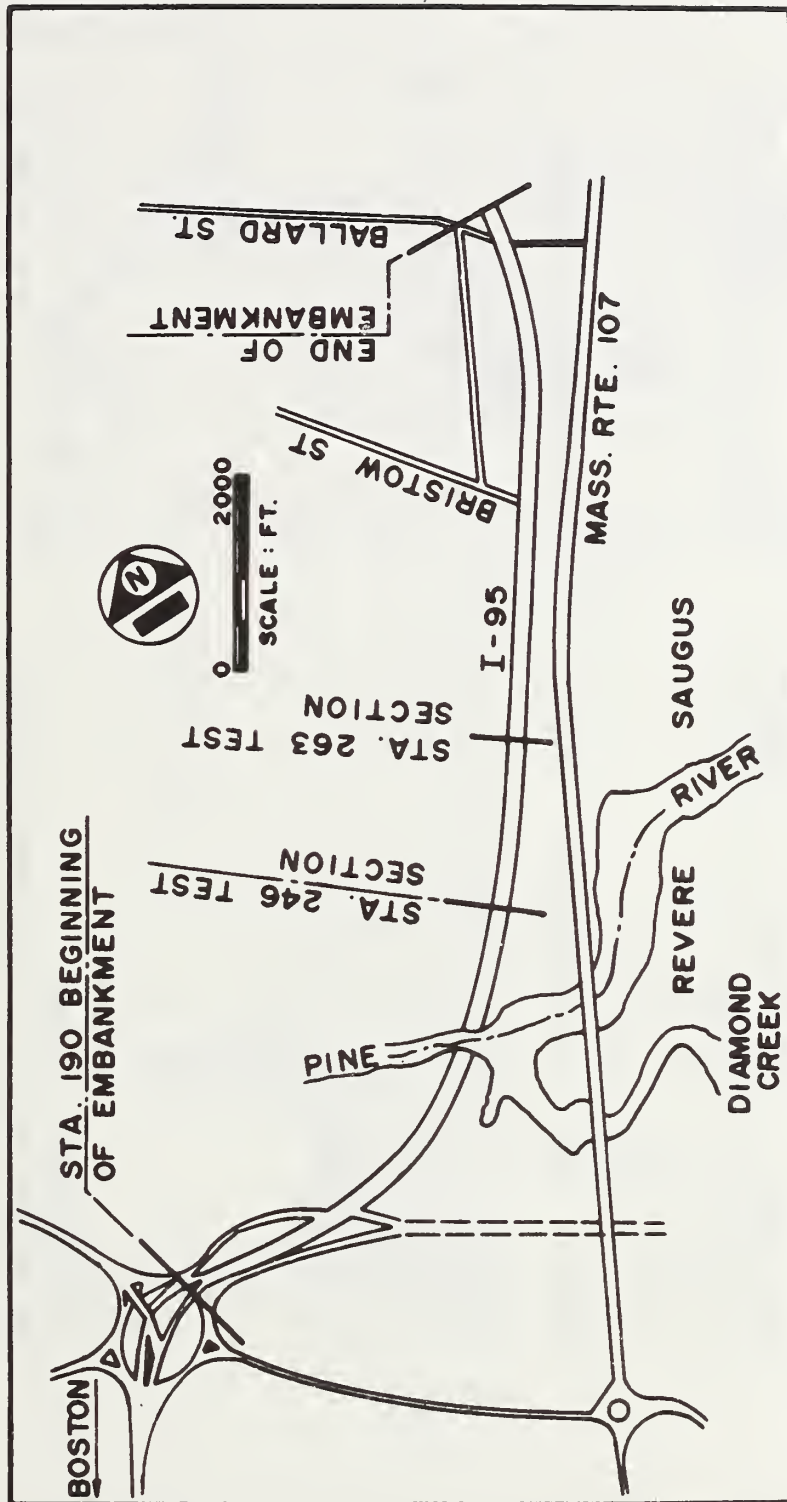
FIGURE 3-1 LOCATION MAP OF SAUGUS I-95 EMBANKMENT (1 ft=0.305m)

49
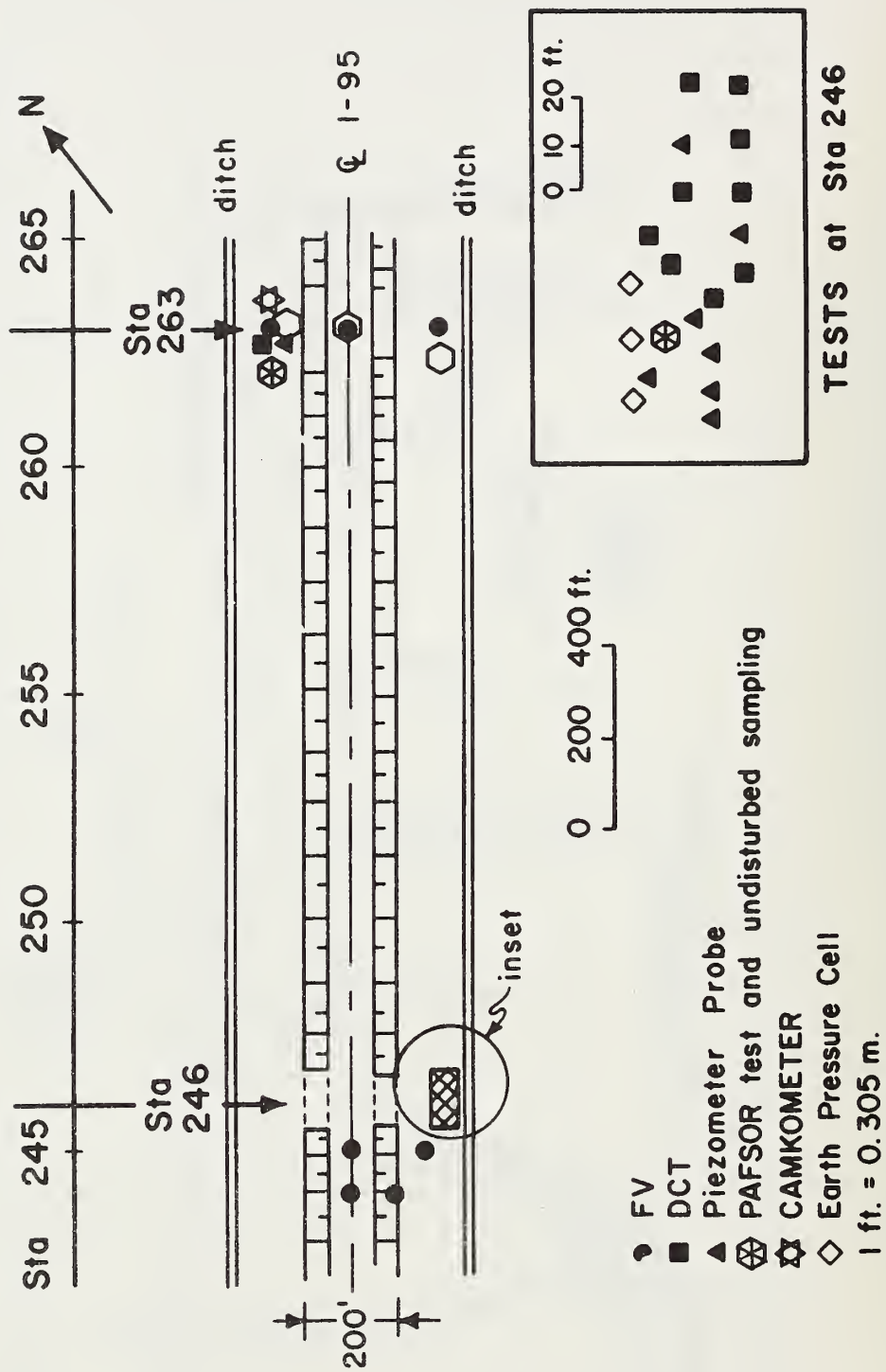
FIGURE 3-2 LOCATION OF IN SITU TESTS IN SAUGUS
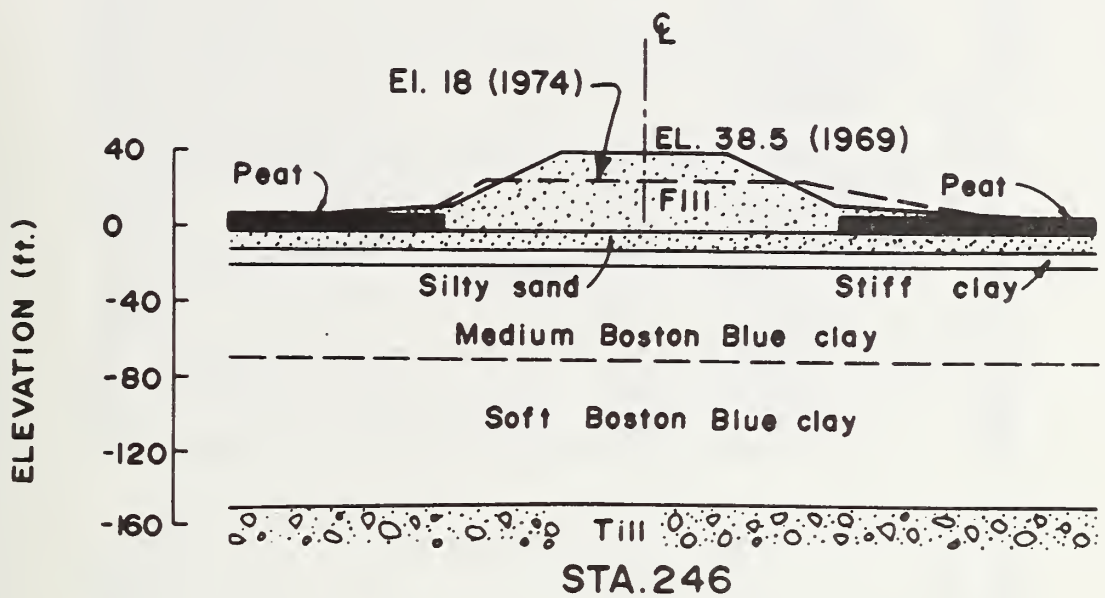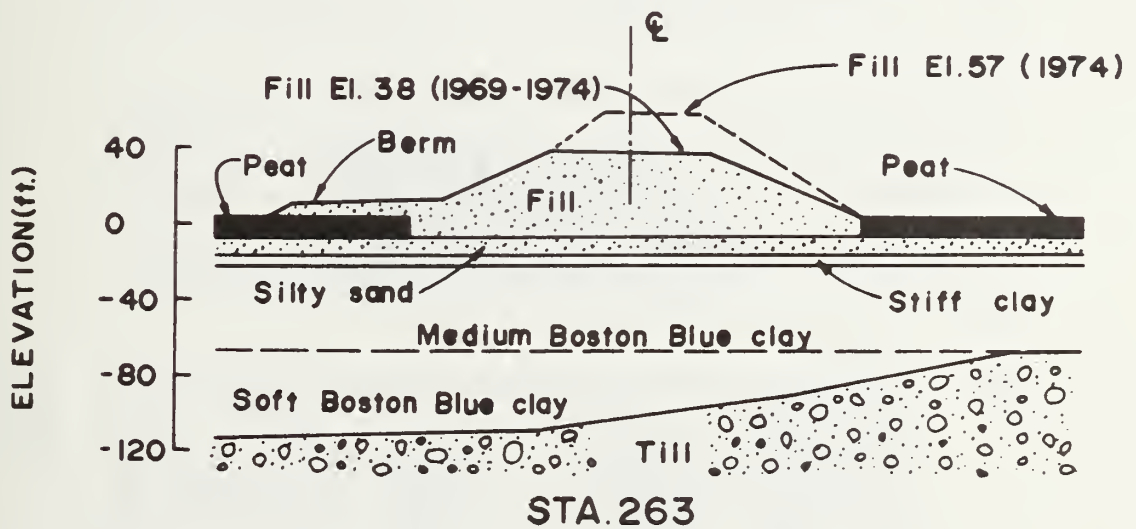
FIGURE 3-3 CROSS-SECTIONS AT STA. 246 and 263 AT SAUGUS

51
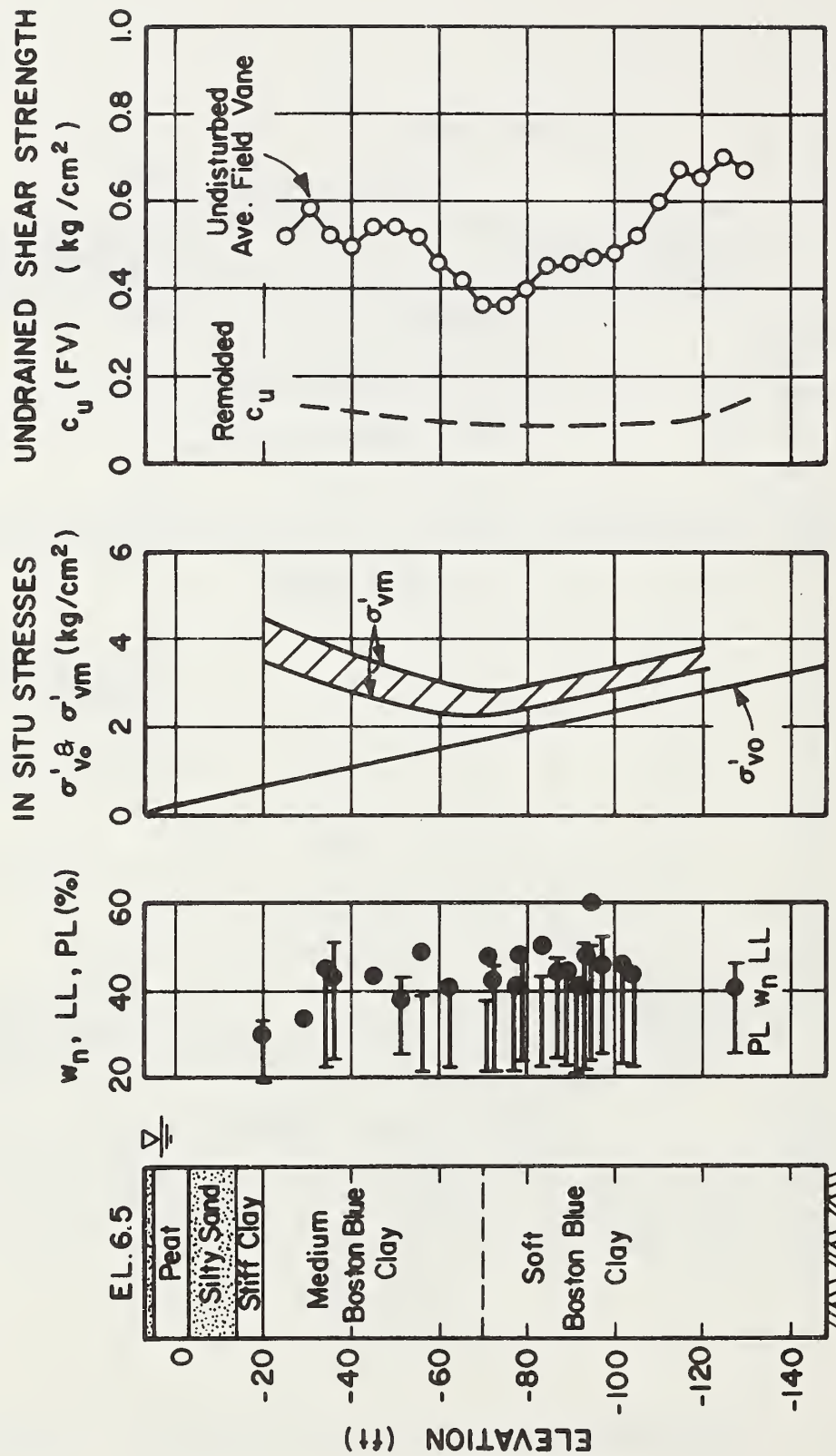
FIGURE 3-4 GENERAL "VIRGIN GROUND" CONDITIONS AT STA. 246

52
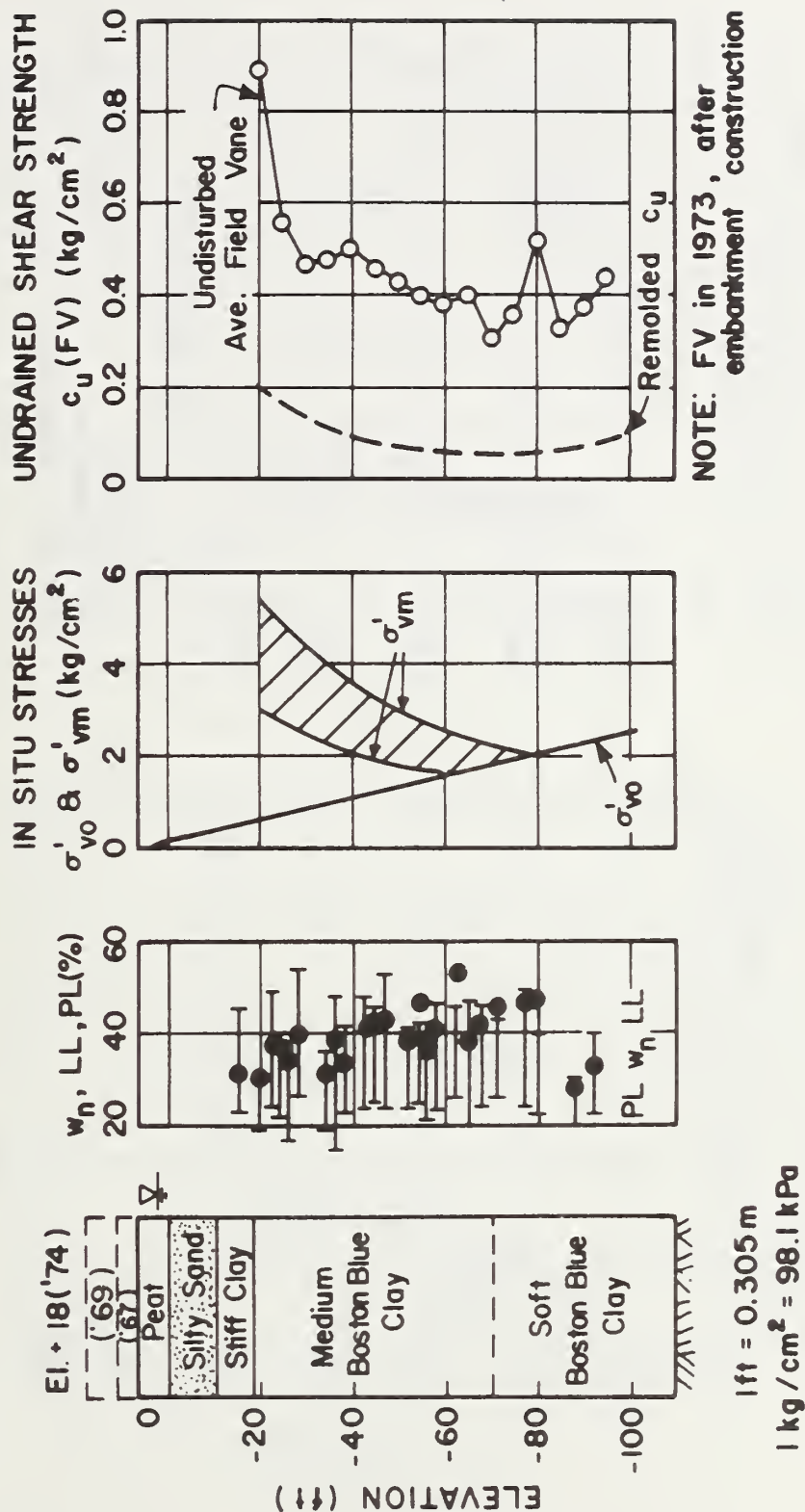
FIGURE 3-5 GENERAL "VIRGIN GROUND" CONDITIONS AT STA. 263
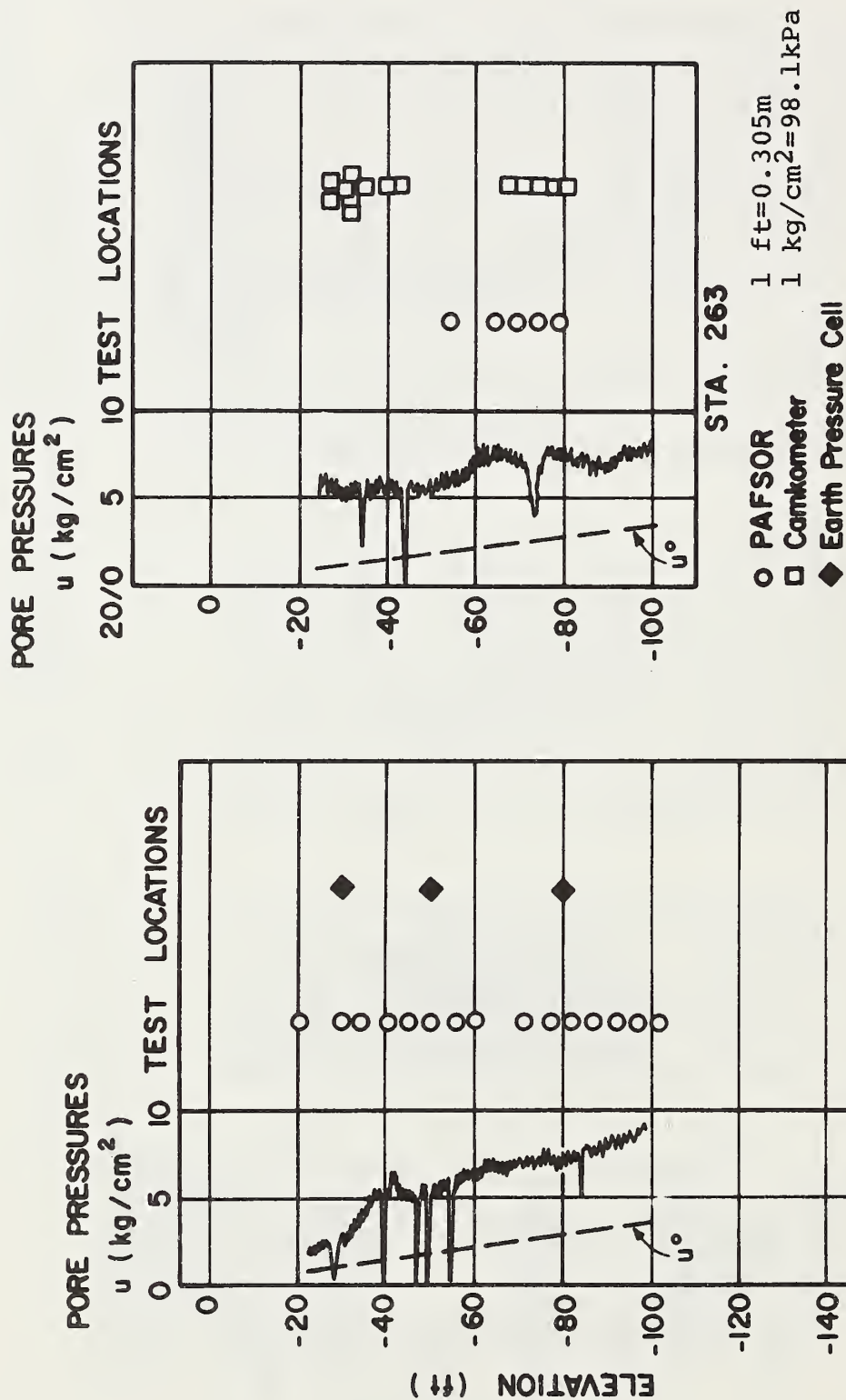
FIGURE 3-6 TEST PROGRAMS AND PIEZOMETER PROBE DATA AT STA. 246 and 263

NOTE: Piezometer probe with 18° tip

54
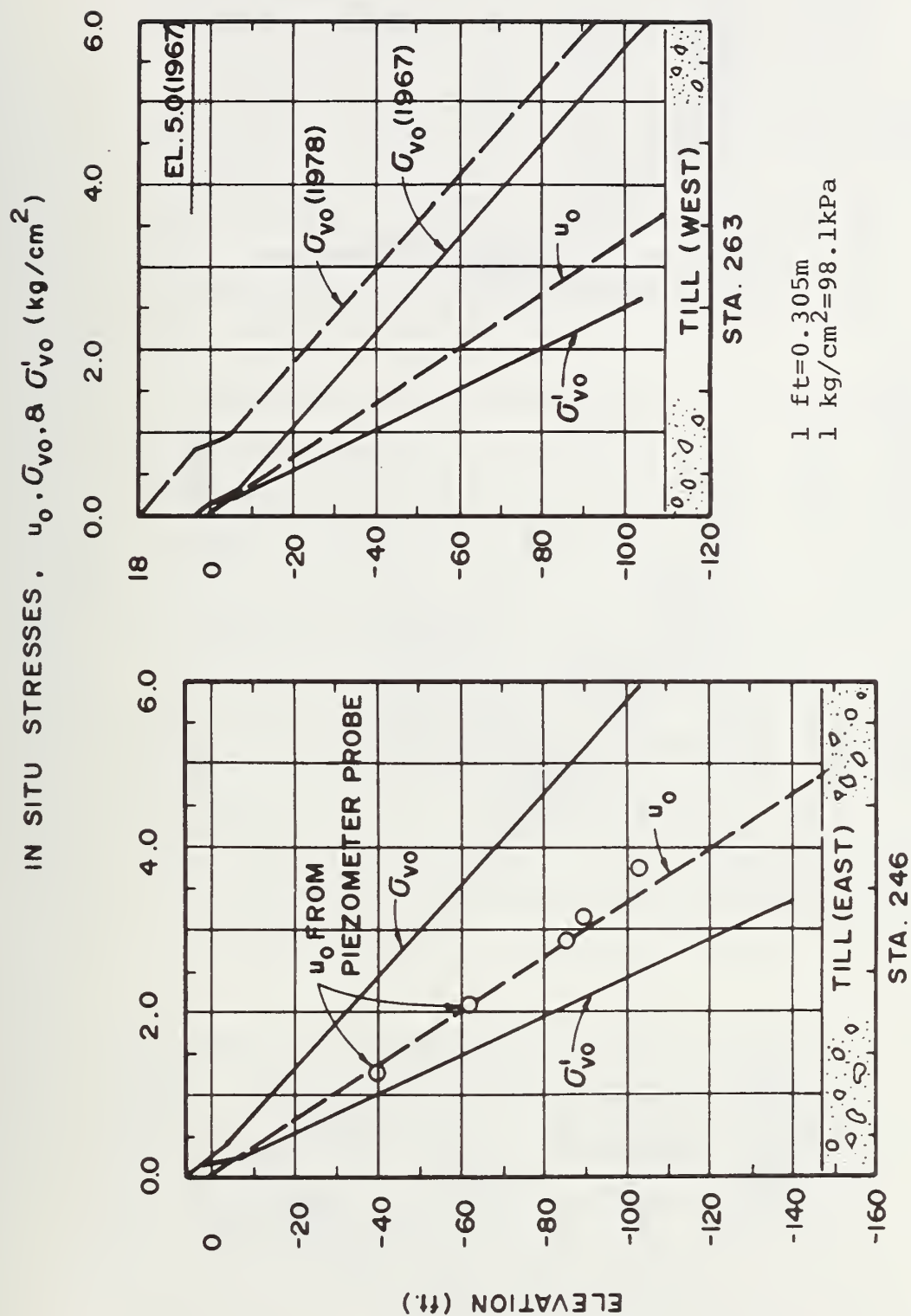
FIGURE 3-7 IN SITU STRESSES AT STA. 246 and 263

55
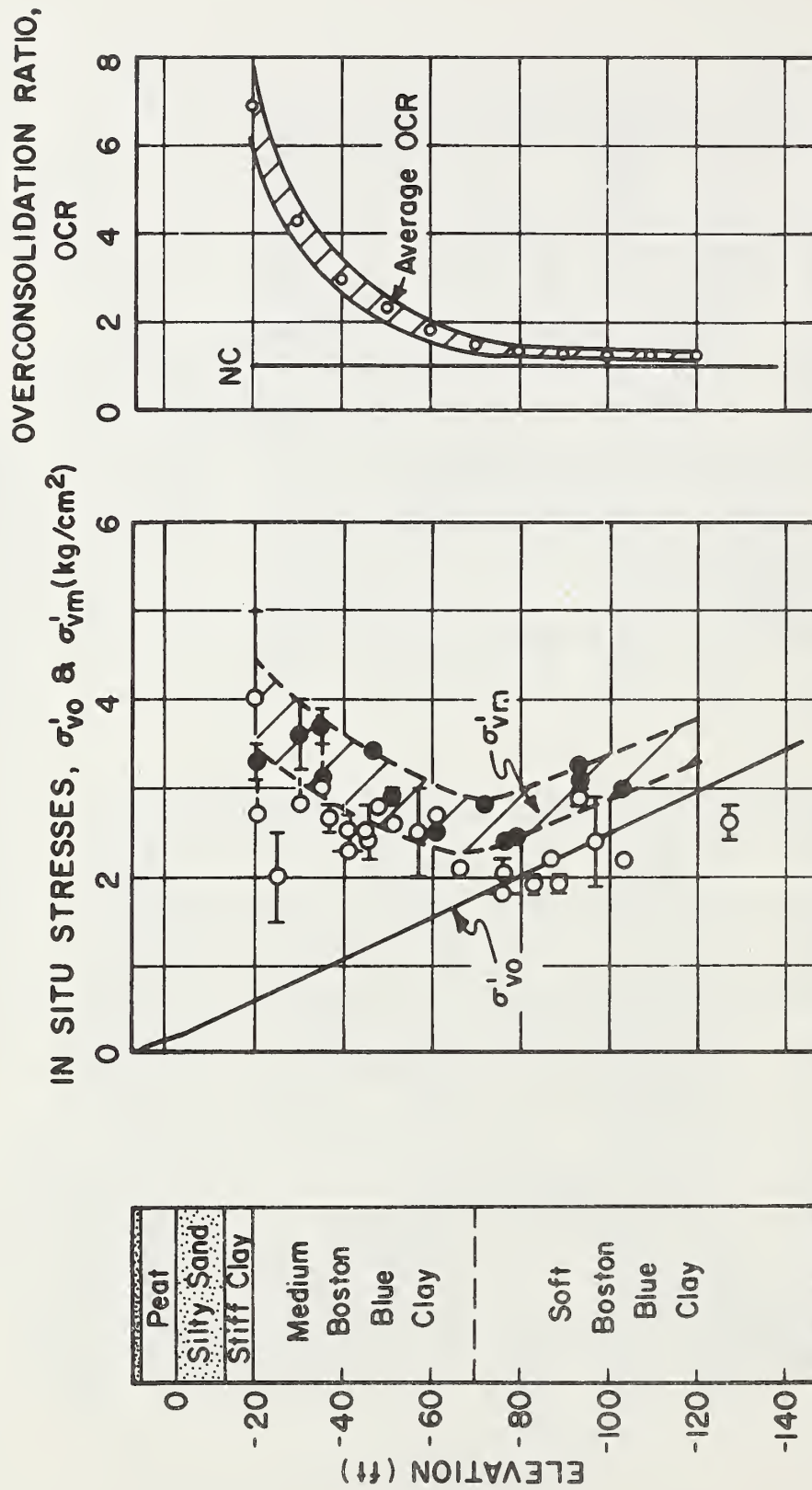
FIGURE 3-8   STRESS HISTORY AT STA. 246
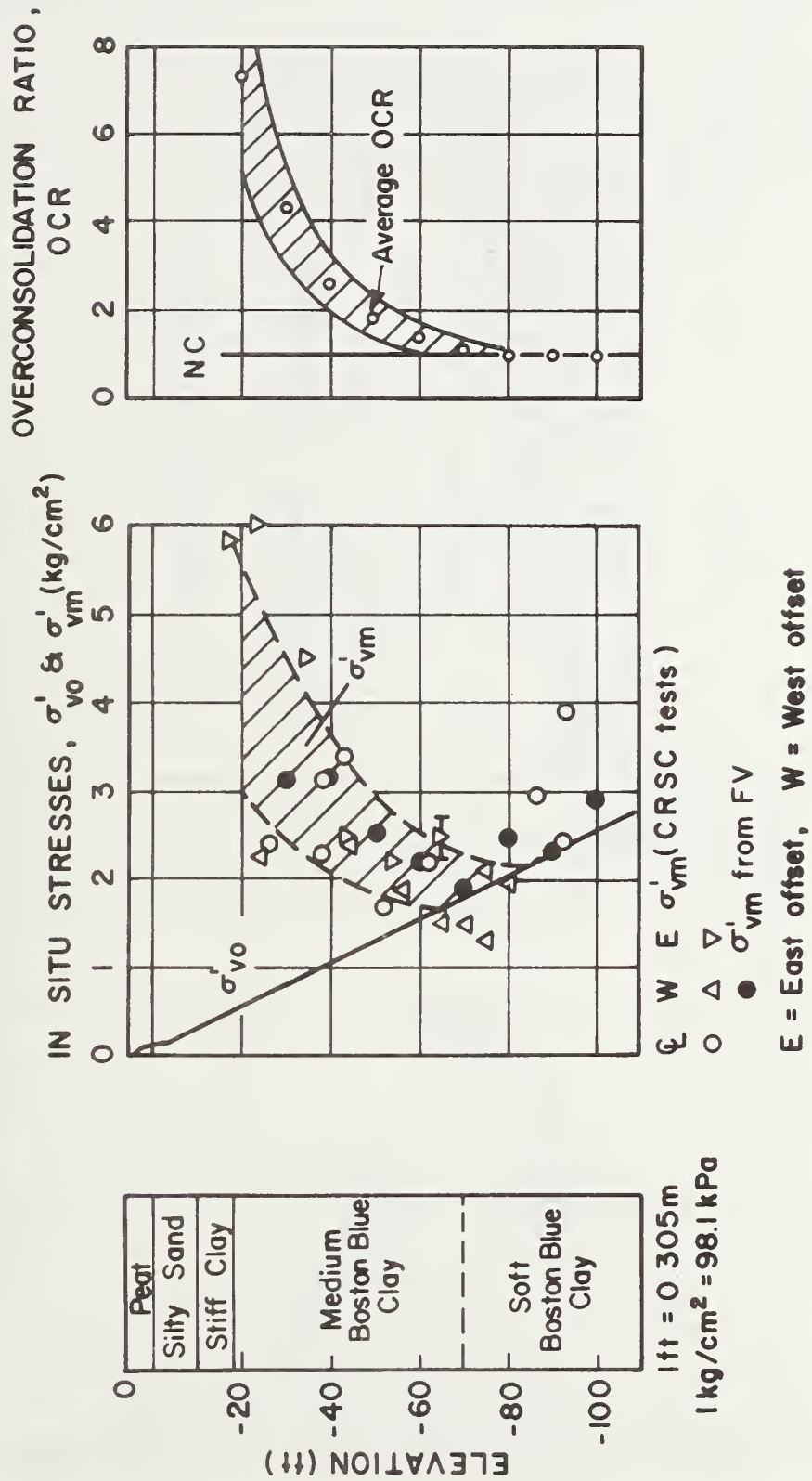
FIGURE 3-9 STRESS HISTORY AT STA. 263

57
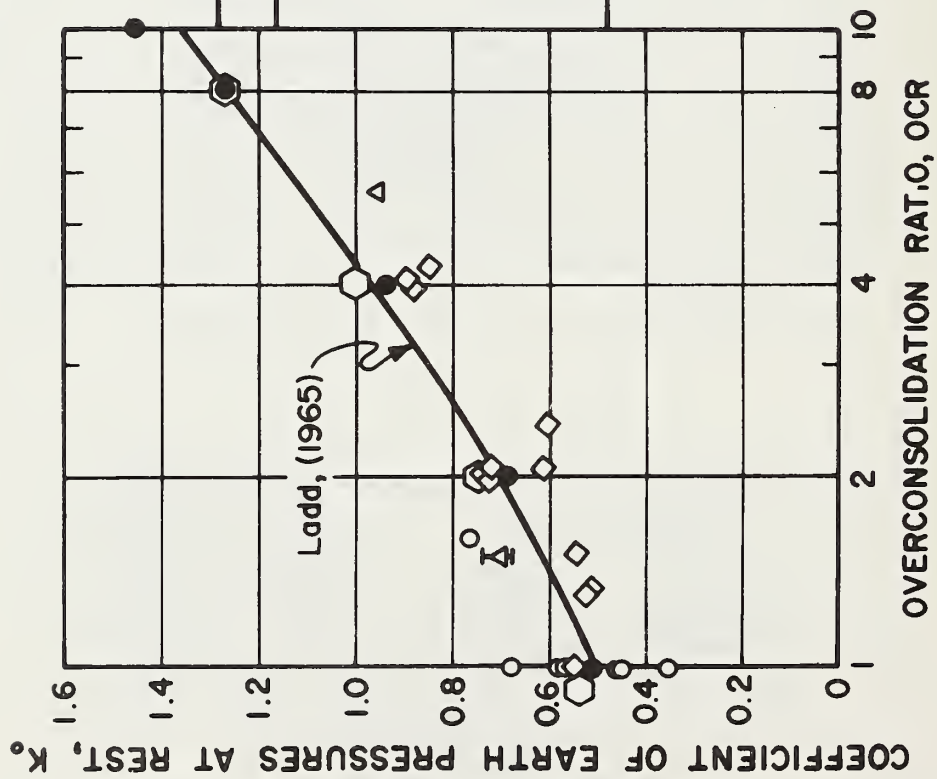
FIGURE 3-10 K_o FROM LABORATORY AND IN SITU TESTS ON BOSTON BLUE CLAY
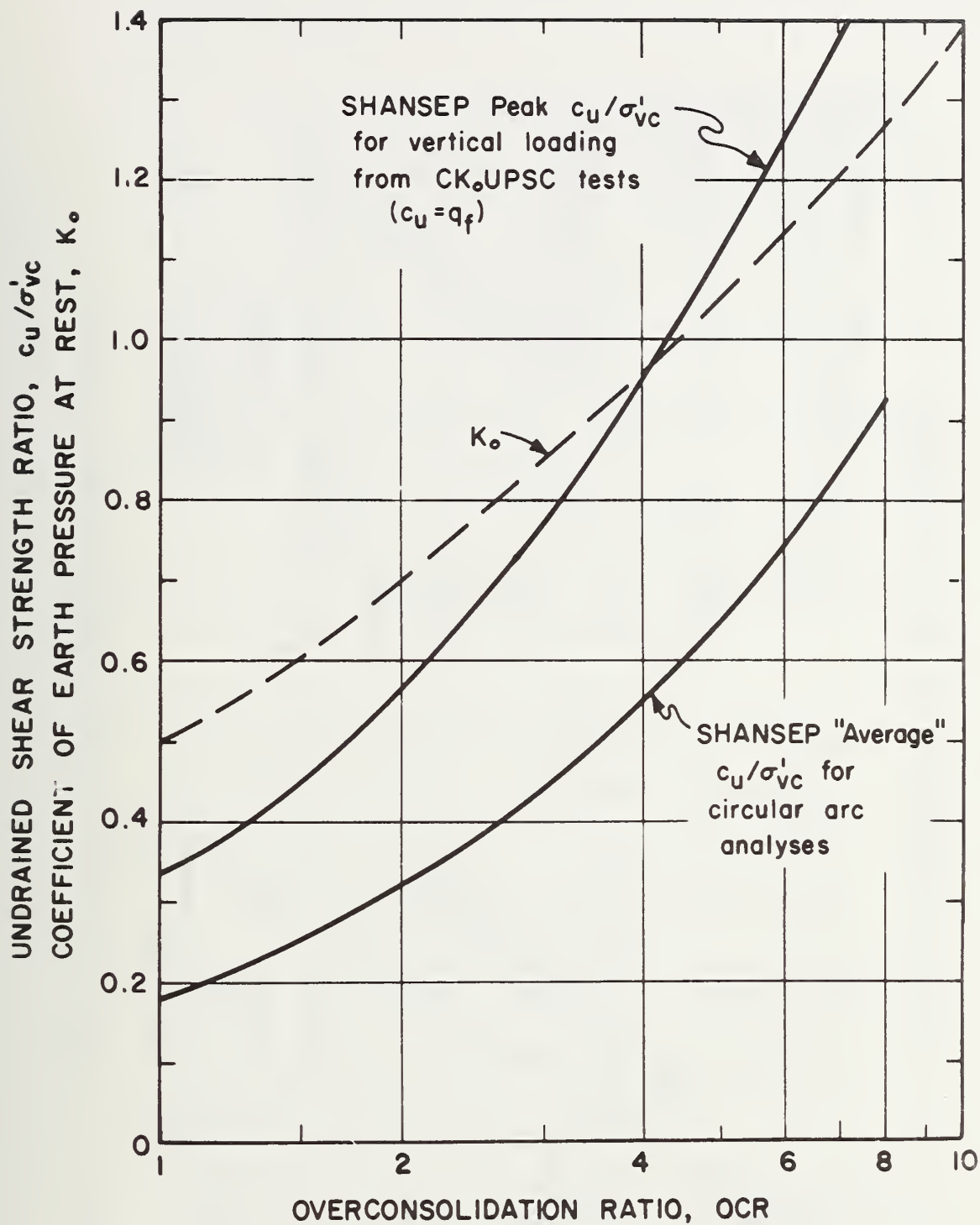
FIGURE 3-11   SHANSEP STRENGTH AND COEFFICIENT OF EARTH
PRESSURE AT REST FOR SAUGUS BOSTON BLUE CLAY
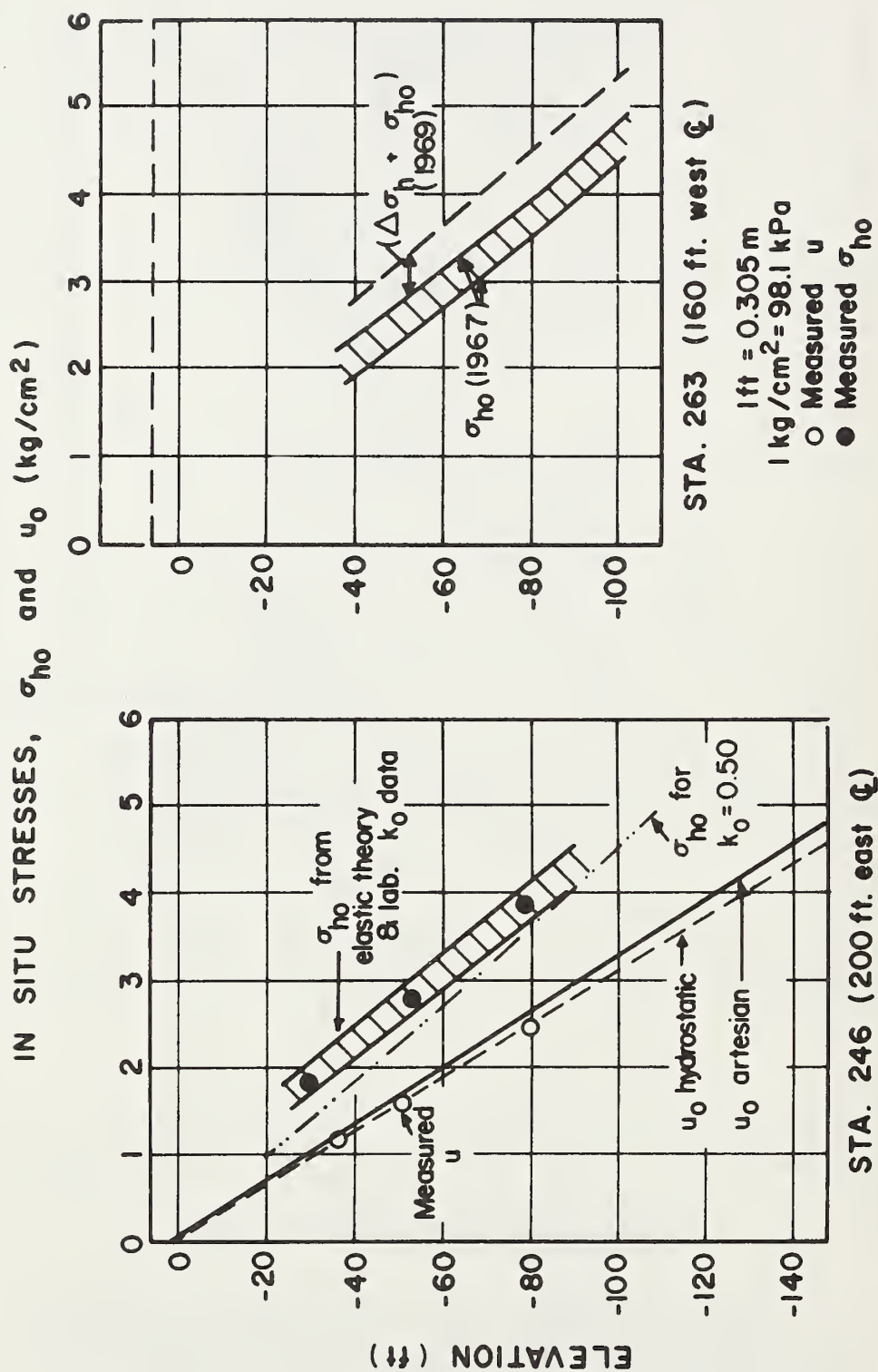
FIGURE 3-12 TOTAL HORIZONTAL STRESS IN SAUGUS BOSTON BLUE CLAY

60
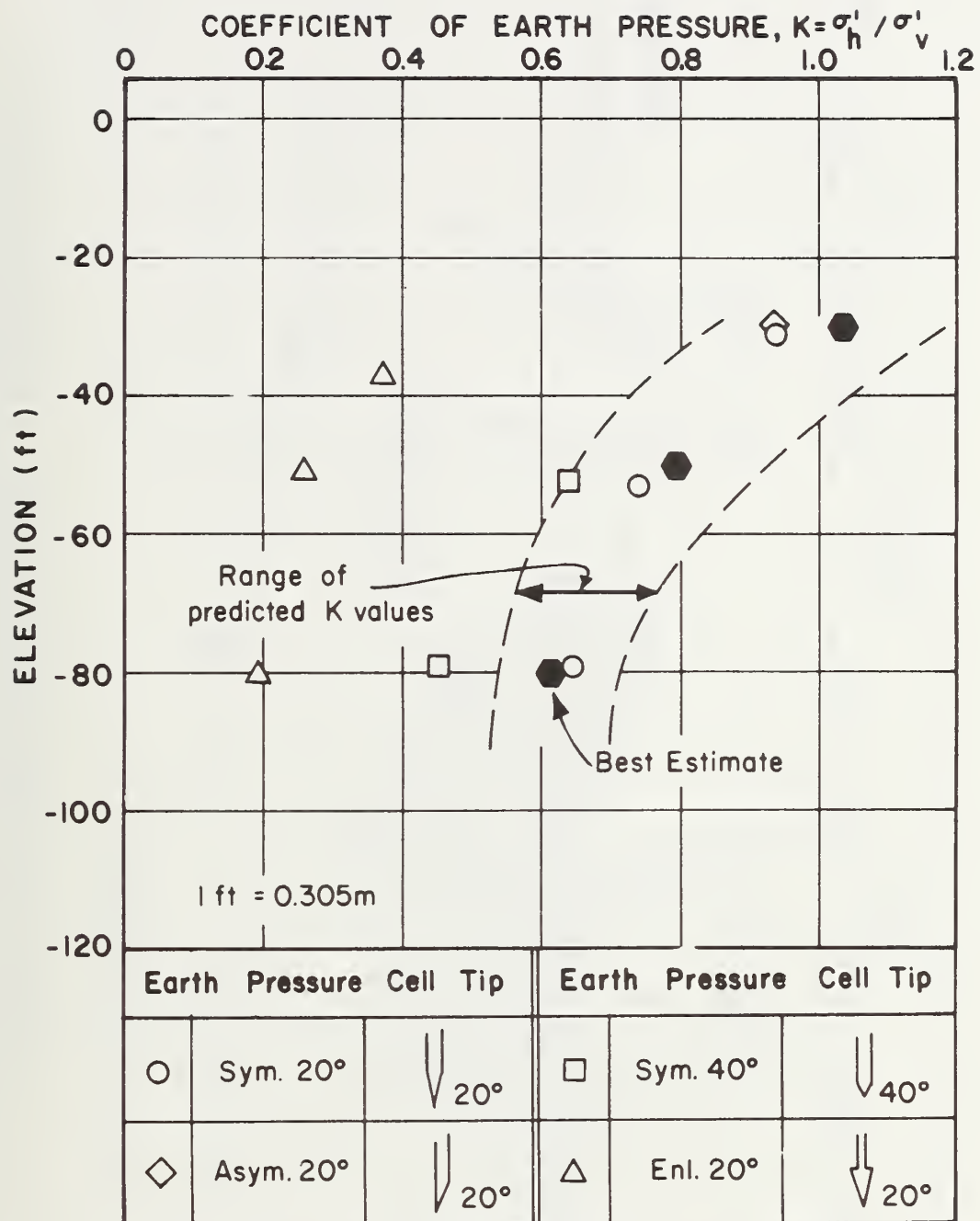
FIGURE 3-13 COEFFICIENT OF EARTH PRESSURE AT STA. 246
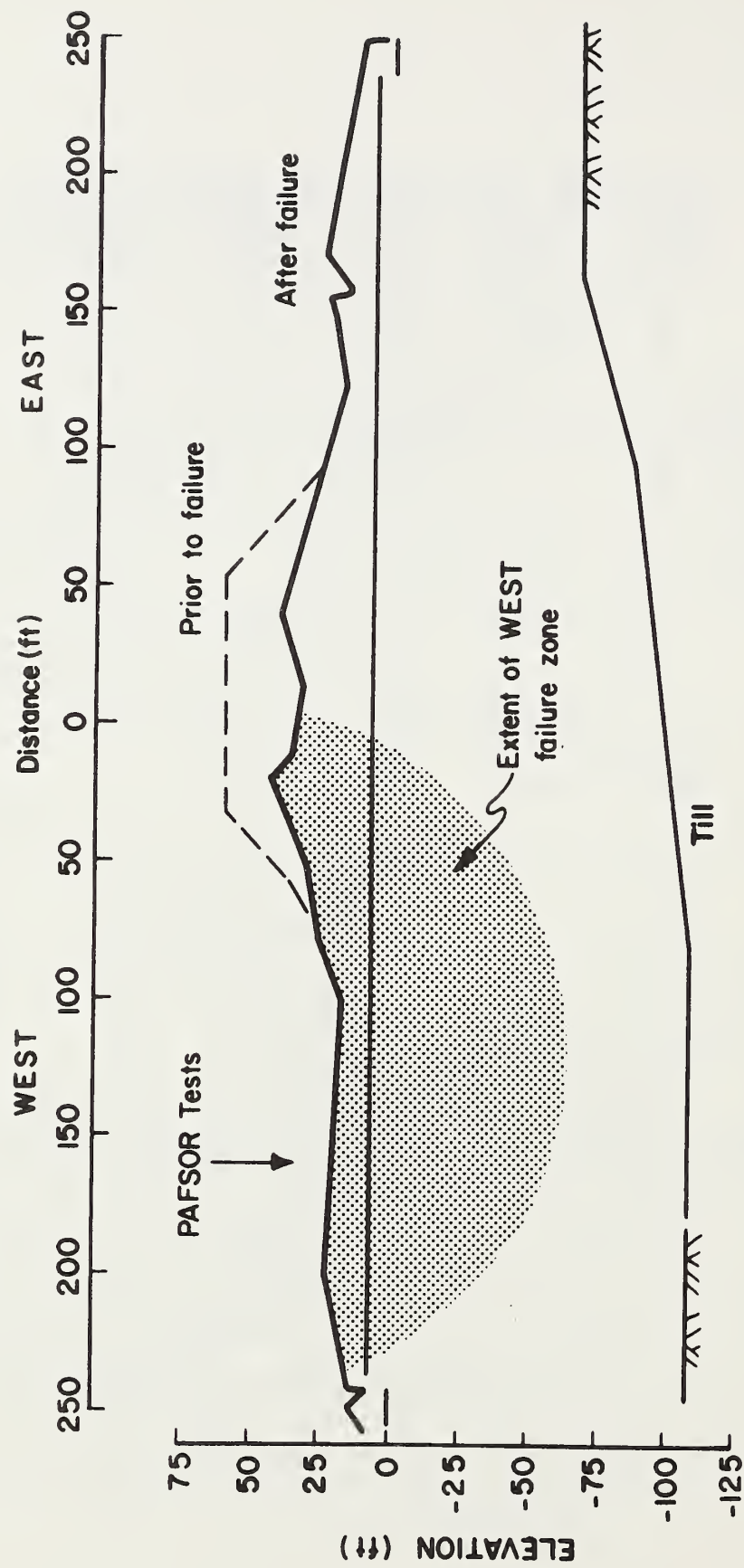
FIGURE 3-14   CROSS-SECTION AT STA. 263 AFTER 1974 FAILURE

1 ft = 0.305 m

62
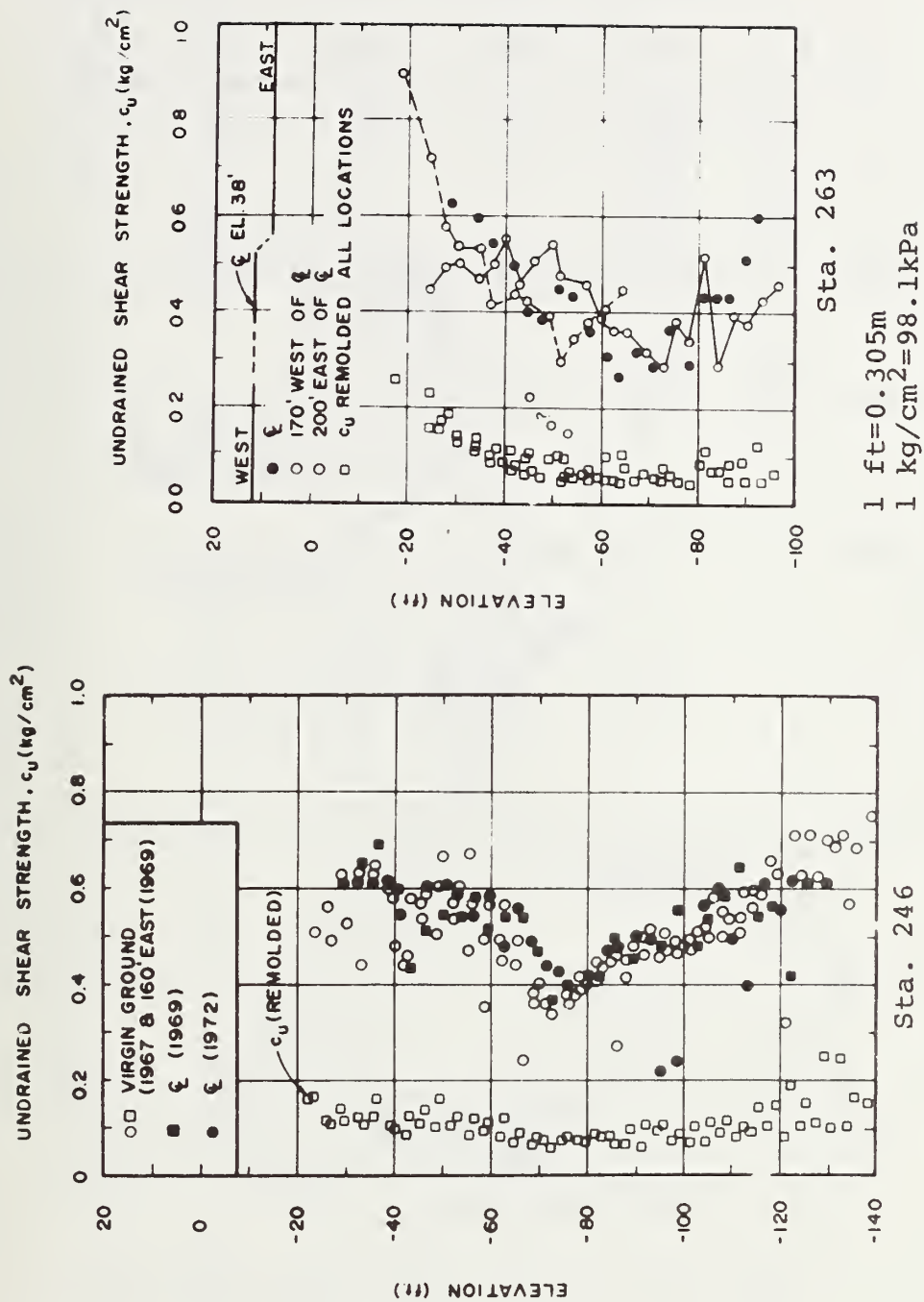
FIGURE 3-15 RESULTS OF FIELD VANE TESTS AT SAUGUS TEST SITES

63
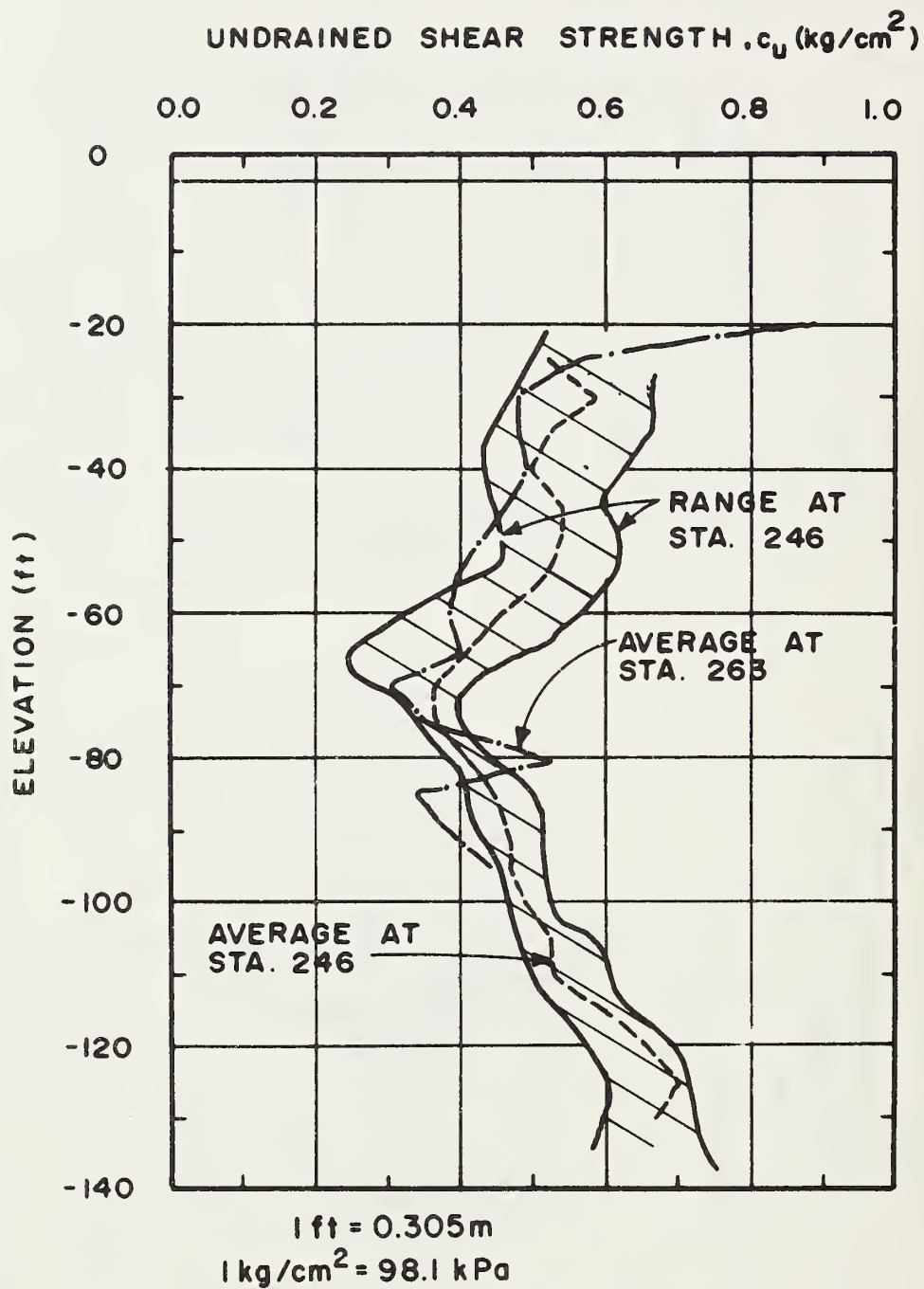
FIGURE 3-16   COMPARISON OF "VIRGIN GROUND" FIELD VANE
STRENGTH OF STA. 246 AND 263

64
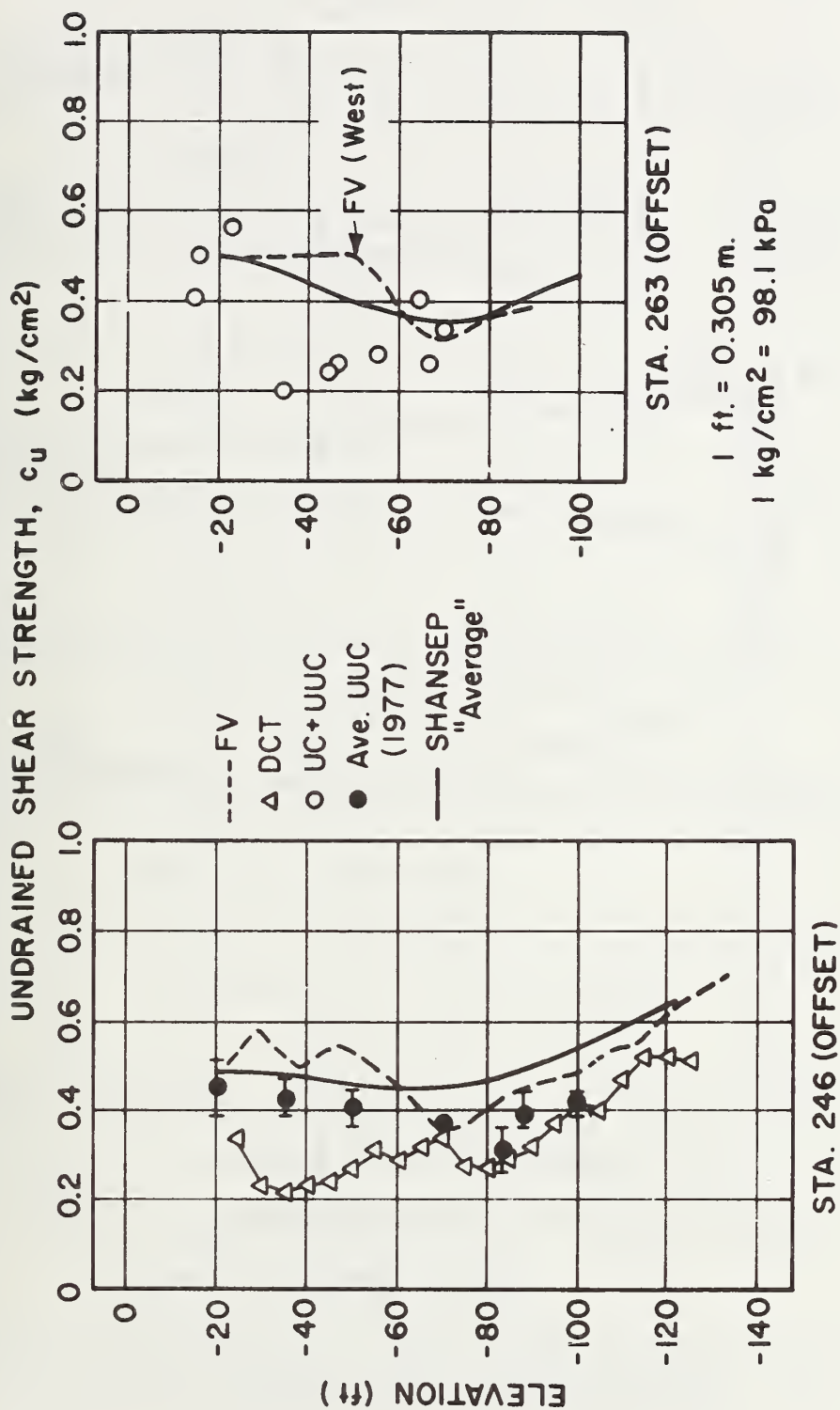
FIGURE 3-17 LABORATORY AND FIELD UNDRAINED SHEAR STRENGTHS IN SAUGUS
BOSTON BLUE CLAY

65
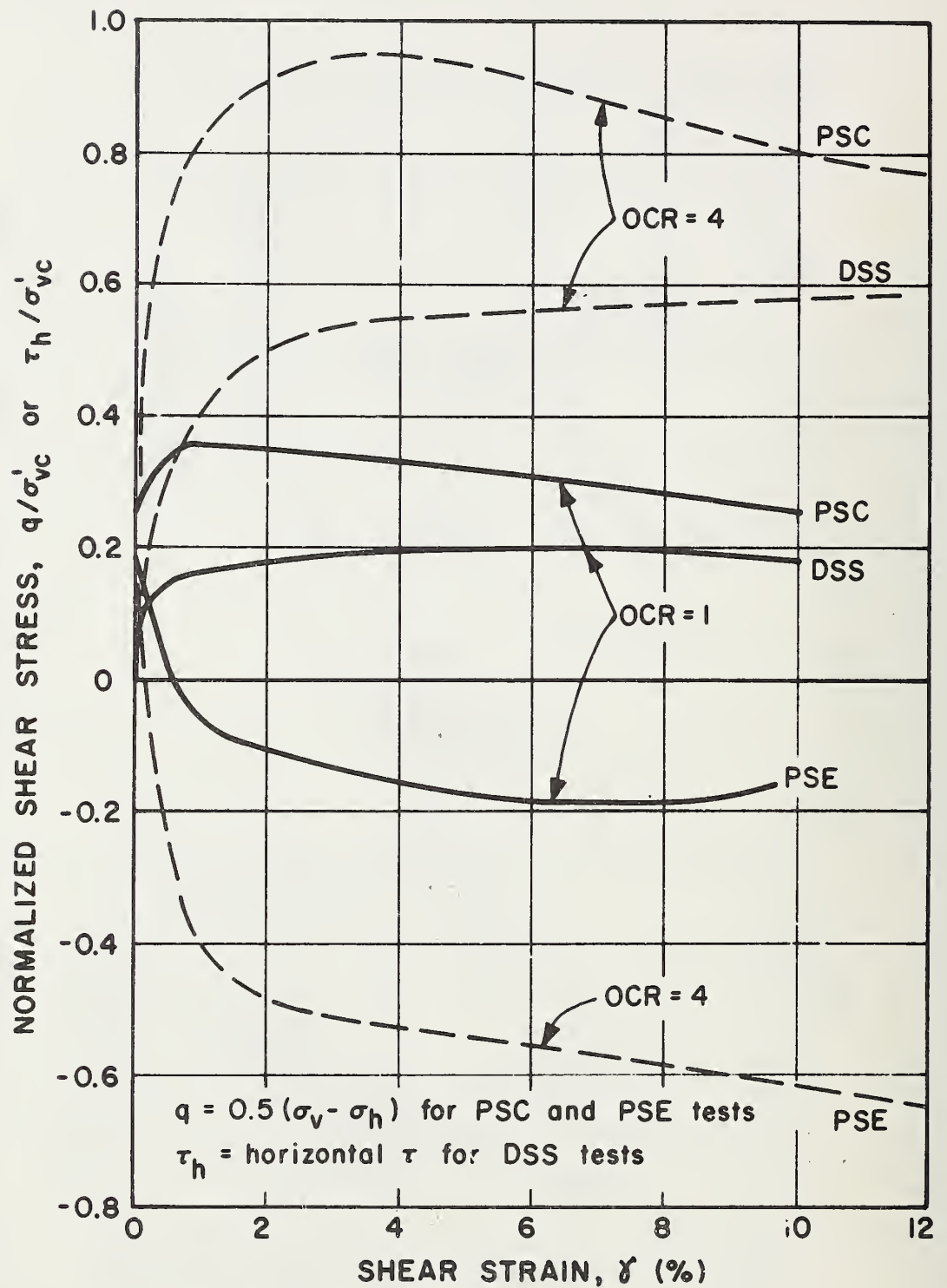
FIGURE 3-18   TYPICAL STRESS-STRAIN CURVES FROM CK_oU TESTS
ON BOSTON BLUE CLAY (OCR=1,4)
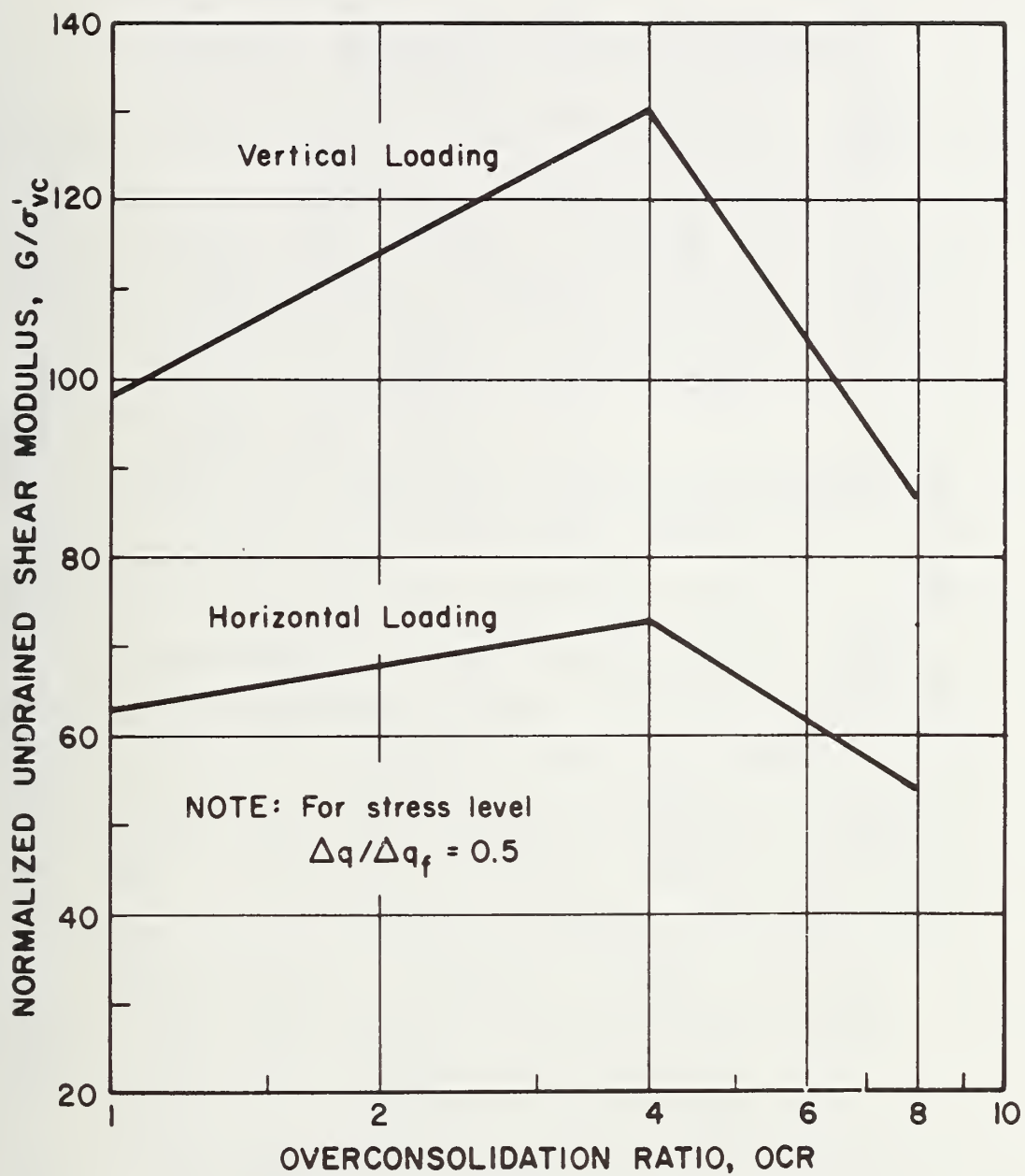
FIGURE 3-19   NORMALIZED UNDRAINED SHEAR MODULUS VS OCR FOR
BOSTON BLUE CLAY

67
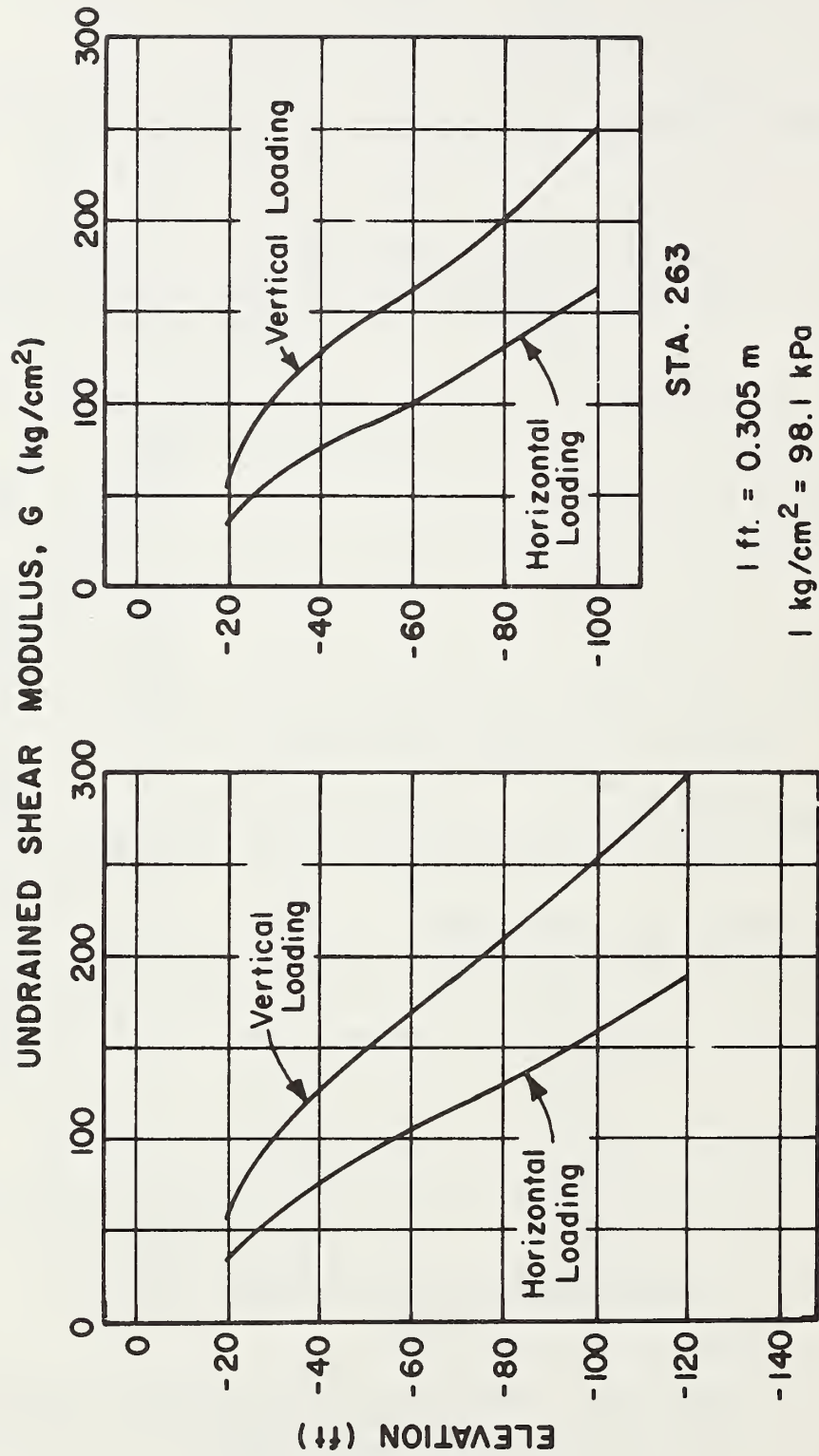
FIGURE 3-20   UNDRAINED SHEAR MODULUS PROFILES AT STRESS LEVEL $\Delta q/\Delta q_f = 0.5$ BASED
ON AVERAGE STRESS HISTORY

4. GENERAL RESULTS OF SELF-BORING PRESSUREMETER TEST PROGRAM

4.1 EQUIPMENT, PROCEDURES AND TEST VARIABLES

The overall program included 20 PAFSOR and 14 CAMKO-
METER tests conducted at the locations shown in Figures
3-2 and 3-6. The latter tests were performed at Sta. 263
in 1973 (i.e. prior to the planned embankment failure) by
Dr. Marr of MIT and Dr. Hughes of Cambridge University.
These gentlemen kindly supplied their test results but most
of the details regarding installation and testing techni-
ques are lacking.

The PAFSOR program was conducted during May 23-June 10,
1977 in cooperation with the California Department of
Transportation (CALDOT). Principal personnel included
Dr. Lacasse and Mr. Germaine of MIT, Messrs Bennett John
and James MacFarlane of CALDOT (who furnished the equipment,
specified "standard" operating procedures, and helped
conduct the tests) and Mr. Robert McGlashan, owner of
CON-TEC, Inc. of Concord, NH which provided the drilling
equipment. The test program included 15 PAFSOR tests at
Sta. 246, where soil properties are well defined, and five
tests in the deep "soft" clay at Sta. 263 adjacent to
the CAMKOMETER test location. However, the soil conditions
had changed, and became much more complex, due to the 1974
embankment failure (see Figure 3-14).

Section 2.2 presented a general description of the
PAFSOR and CAMKOMETER equipment and test procedures and
further details are contained in Appendices B and C.
Table 4-1 summarizes the main features of the two devices
which, as discussed in Section 2.2, differ in several
important respects. For example, the CAMKOMETER provides

69

better control of the cell radius during insertion since the cell membrane rests on a rigid inner tube. In contrast, the water filled PAFSOR cell can deform differentially and, if not properly inflated to start with, will not even have an average diameter equal to that of the cutting shoe. As noted below, this unfortunately occurred with most all of the PAFSOR tests run in Boston Blue clay. Important differences also exist in the expansion portion of the tests: the PAFSOR records average volume changes during strain controlled expansion whereas deformations are measured at mid-height of the CAMKOMETER cell during inflation via gas pressure increments, i.e. a stress controlled expansion

As originally planned, the principal variables in the PAFSOR test program would be:

(1) Tests at varying depth to investigate the influence of stress history, i.e. changes in effective overburden stress (σ_{vo}') and overconsolidation ratio (OCR= $\sigma_{vm}'/\sigma_{vo}'$).

(2) Variations in "equilibration time" to measure changes in P_o with time and its subsequent effect on the expansion curve.

(3) Tests with varying rates of expansion to investigate "strain rate-drainage" effects.

This program assumed that suitable procedures regarding the method of installation had already been established, based on CALDOT's past experience, for inserting the device with minimal disturbance to the surrounding soil. This was not the case however,* and thus the method of installation

---

* Based on subsequent discussions with Professor Jamiolkowski, one should expect the need for experimentation with installation techniques at each new test site.

turned out to be a major, yet ill-defined, variable. In
particular, the "initial" volume of the measurement cell
specified by CALDOT resulted in a concave inward shape
having a minimum diameter about 3.7% less than the diameter
of the cutting shoe. After noting the discrepancy and
the fact that P_O during installation was often less than
the hydrostatic pore pressure, the "initial" cell volume
was increased in some of the tests (in retrospect, it should
have been increased by 215 cc in all of the tests).
Attempts to vary the rate of advance during self-boring in
order to make P_O equal to the predicted in situ total hori-
zontal stress generally proved unsuccessful. Use of equil-
ibration times much larger than the CALDOT "standard"
10 to 15 min also proved unfeasible due to schedule and
financial limitations (two tests were equilibrated over-
night, but this required police guards to protect against
vandalism). Other potential installation variables such
as the type and location of the cutting tool and magnitude
of the oil and water pressure were kept essentially constant.

CALDOT had used 60 cc/min as their standard rate of
expansion, which is approximately equal to the $\dot{\varepsilon}=1\%/min$
recommended by Baguelin et al. (1978). However, definition
of the initial portion of the expansion curve proved
difficult with this rate. After running some initial tests
at 6, 20 and 60 cc/min, MIT generally adopted the follow-
ing procedure: 6 cc/min during initial "seating", 20 cc/
min during the steep portion of the P-ΔV curve, and then
60 cc/min during the last half of the test. This had
the advantage of providing better defined curves, but
usually caused discontinuities at each change in expansion
rate. Some of the PAFSOR tests included unload-reload
cycles.

71

The 1973 CAMKOMETER test program is thought to have employed the same cell expansion procedure for all tests, namely pressure increments of about 0.1 kg/cm^2 (10kPa) applied at approximately one minute intervals, and most included one or more unload-reload cycles. Details concerning variations in installation technique and equilibration time are lacking.

4.2 CLASSIFICATION OF EXPANSION CURVES

Although self-boring pressuremeter tests should ideally yield expansion curves like the one shown in Figure 2-4, many of the PAFSOR tests gave distinctly different shapes. A classification system was therefore developed to facilitate their description. Figure 4-1 presents these and possible reasons for such behavior are hypothesized below.

Type I: This represents the ideal curve, i.e. concave downward with gradually decreasing slope (though the initial portion may be almost linear). However, even with a Type I curve, P_O will not necessarily equal the in situ total horizontal stress σ_{ho}.

Type II: This shows an obvious seating problem that might occur from overcoring in a relatively stiff clay. The pressure remains essentially constant as water between the membrane and the soil is displaced, and then increases rapidly upon contact with the surrounding soil.

Type III: This S shaped curve is typical of results with the Menard pressuremeter test (see Figure 2-2) and indicates obvious disturbance in the surrounding soil. Though the inflection point might be taken as an adjusted starting point, Baguelin et al.(1978) state that no attempt should be made to obtain derived stress-strain curves from

72

such tests (p. 570). Jamiolkowski and Lancellotta (1977)
also conclude that stress-strain data derived from
"corrected" Type III curves are liable to serious error.

Type IV: This shape occurred in several of the PAFSOR
tests at Sta. 246, i.e. a "double curve" in the P-ΔV
relationship. As noted in the subsequent discussion,
it may have resulted from using an undersized cell volume
during insertion, at least in some of the tests.

Type V: This behavior is the predictable result of
increasing the expansion rate, i.e. an immediate increase
in pressure and perhaps slope. For the relatively small
rate increases employed in this test program (from 6 to 20
to 60 cc/min), the effect appears to damp out after about
2% further strain. Nevertheless, rate changes do complicate
application of the various procedures available to obtain
derived stress-strain curves.

In addition to the above classification, most of the
tests were also given a subjective designation as to their
overall "quality", this ranging from excellent to poor.
"Excellent" indicates a very smooth curve with a well
defined starting point such that there is little question
regarding how the results should be analyzed. It can apply
to Type I and II curves. "Good" suggests relatively minor
problems such as might be caused by a change in expansion
rate at a critical point in the test or somewhat ill-
defined starting conditions. "Fair" tests are difficult
to analyze and mainly apply to Type III and IV curves
wherein the initial portion of the test has obvious flaws.
A few of the tests exhibited extremely erratic expansion
curves and are labeled as "poor".

The next three sections give an overview of the test
results, concentrating on the test variables, the types of

curves and their general quality. Chapters 5, 6 and 7
then analyze the data regarding evaluation of in situ
horizontal stress, the pressure limit and undrained stress-
strain-strength parameters.

4.3 PAFSOR TESTS AT STA 246

Table 4-2 summarizes pertinent information regarding
the test procedures and the nature of the expansion curves
for the 15 tests performed at roughly 5 ft (1.5 m) intervals
between El.-19.7 and -101.7. The effective overburden
stress (σ'_{vo}) increased from 0.6 to 2.5 kg/cm^2 (59 to 245 kPa),
while the OCR=$\sigma'_{vm}/\sigma'_{vo}$ decreased from about 7 to 1.4±0.2
below El.-70. The self-boring process usually took
30 to 60 min and from 10 to 30 min was typically allowed
for "equilibration", except for Test No. 12 which was left
in the ground overnight. The measurement cell was partially
inflated during insertion in eight of the tests with nominal
(uncorrected) values of ΔV_o ranging from 12 to 220 cc.
With zero ΔV_o, the cell had a volume of only 3397 cc com-
pared to 3612 cc theoretically required to yield an average
diameter equal to that of the cutting shoe. This 215 cc
volume deficiency corresponds to an average negative
strain (Eq. 2-5, Table 2-1) of 0.5(215/3612)=3.0%. Thus
substantial unloading of the clay would be expected during
insertion with 11 of the 15 tests having ΔV_o significantly
less than 215 cc. Hence the values of P_o listed in
Table 4-2, equal to the measured P after equilibration,
should also be much less than the in situ total horizontal
stress (σ_{ho}) for these eleven tests (see Chapter 5 for
further discussion of this important point).

Only four tests employed a constant expansion rate,
i.e. dΔV/dt=$\Delta \dot{V}$=6, 20 or 60 cc/min (corresponding $\dot{\varepsilon}\approx 0.09$,

0.3 or 0.9%/min) throughout the entire expansion to a
nominal maximum $\Delta V=800$ cc ($\varepsilon=12\%$). Table 4-2 lists the
rates used in the other tests wherein $\Delta \dot{V}$ was typically
increased from 6 to 20 to 60 cc/min as the test progressed
[the numbers in ( ) give the nominal ΔV at each change in
rate]. Three tests contained unload-reload cycles.

Table 4-2 also classifies each curve according to
its shape (i.e. Type I, II, etc. after Figure 4-1),
assigns subjective judgement as to the quality of each test
(i.e. excellent to poor as described in Section 4.2) and
contains some additional remarks. Note that all tests with
a variable expansion rate have a dual classification.

Figures 4-2(a) through (d) show the basic expansion
curves for each of the tests wherein both the pressure P
and volume change ΔV have been corrected according to the
calibrations presented in Appendix B. These figures are
intended to give perspective rather than details (see
Appendix B for full scale plots), but also give the initial
inflation during insertion (ΔV_O, cc) and the rate of expan-
sion ($\Delta \dot{V}$, cc/min).

The tests will be grouped together according to the
type of curve for purposes of discussion. For perspec-
tive, it should first be noted that peak strengths derived
from the expansion curves using Eq. 2-6 (Table 2-1) usually
occur at strains of only 1 to 2%, which in turn corresponds
to a volume change of only 105 ± 35 cc. Thus a well defined
starting point and the precise shape of the initial portion
of the expansion curve are critical items.

Type I and I-V

Four tests fall in this category, Nos. 4 and 7 in the
medium clay and Nos. 9 and 12 in the deep "soft" clay,
all with good to excellent quality ratings. No. 4 has an

75

ideal shape, with an initial linear P vs ΔV relationship, as might be expected since its ΔV_O of 220 cc should have produced an average cell diameter equal to that of the cutting shoe. Moreover the expansion rate was kept constant at $\Delta \dot{V} = 20$ cc/min. Tests 7 and 9 have shapes very similar to No. 4 in spite of the fact that the initial inflation was much smaller ($\Delta V_O = 80$ and 12 cc respectively) and hence self-boring should have caused some unloading of the surrounding clay. Also the increase in expansion rate from 6 to 20 cc/min apparently had little effect on the initial portion of the curve, although noticeable jumps occurred at the subsequent rate increase.

Though Test 12 had a relatively large $\Delta V_O = 150$ cc and was equilibrated for a much longer period than usual (6 hr vs. 10-30 min), the P-ΔV data show a slight Type IV double curve. However, the increased slope occurred at the same point as the change in expansion rate, which might explain the double curvature. On the other hand, Tests 10 and 11 were inserted in a similar manner (but with much shorter equilibration) and they showed very pronounced Type IV curves.

Type II and II-V

Tests 2 and 5 exhibited this behavior, both being inserted into medium clay without any initial expansion. P_O for No. 5 is probably very close to the pressure in the wash water and the initial shape of the P-ΔV curve suggests that slurry was being displaced until the membrane came into contact with "undisturbed" clay. After this obvious seating problem, the subsequent curve had nearly an ideal shape. Test 2 behaved similarly, but with a somewhat less abrupt change in shape as slurry was presumably being squeezed out from between the membrane and relatively intact clay. The rate change from 6 to 20 cc/min also

76

produced a marked jump in the P-ΔV curve. In spite of the obvious seating problems, both tests were judged to be of good quality since corrected initial conditions are fairly well defined and the subsequent curves conform to the classical shape.

Type III-V

Test 1 showed a distinct reverse curvature after insertion in stiff clay with the undersized expansion cell ($\Delta V_O=0$). The P-ΔV curve resembles that of typical Menard pressuremeter tests (see Figure 2-2) which greatly complicates selection of an appropriate corrected starting point. The rate change also produced a modest jump in the expansion curve.

Type IV and IV-V

Four of the six tests in this category exhibited very pronounced "double curves", namely Nos. 10, 11, 13 and 15. These tests were all inserted into the "soft" clay with inflated membranes, ΔV_O ranging from 50 to 180 cc. The abrupt change in slope occurred very near the theoretical volume deficiency of 215 cc in Tests 11, 13 and 15 (perhaps fortuitously), but only at $\Delta V=160$ cc in Test 10. Moreover, the second curve in these tests generally had a shape close to that expected for an ideal test, although the rate change from 6 to 20 cc/min in Tests 11 and 15 caused an increased slope in the P-ΔV curve which complicates their interpretation. Thus, in spite of having double curves, the quality of these four tests is judged as fair to good.

Tests 3 and 6, run in medium clay without any initial expansion, exhibited much less pronounced double curves and the change in slope occurred at a volume change far below the theoretical 215 cc deficiency. The faster initial expansion rate used in these two tests (20 and 60 cc/min

vs 6 cc/min) might offer a partial explanation if the double curves are associated with expulsion of slurry from between the cell membrane and the surrounding soil. That is, the fast rate did not enable complete removal of slurry.

As previously discussed, Test 12 could be classified as having a Type IV curve. It is also rather surprising that Tests 7 and 9 did not exhibit double curves since they had test procedures very similar to those used for the six tests having Type IV curves.

"Poor Tests"

Tests 8 and 14 yielded such erratic initial P-ΔV data as to render the results useless. The cutting shoe became damaged and the metal strips partially ripped off the cell membrane as Test 8 was boring through a layer of coarse soil. This no doubt disturbed the surrounding clay. Why No. 14 behaved so erratically is unknown.

4.4 PAFSOR TESTS AT STA 263

Table 4-3 and Figures 4-3 (a) and (b) present results for the five PAFSOR tests run at Sta. 263 in the same format as used for the Sta. 246 test program. These tests were performed after the 1974 embankment failure, but presumably in relatively undisturbed "soft" clay located below the failure zone (see Figure 3-14). However, although the strength properties may be reasonably well defined (assuming little consolidation between 1974 and 1977), the in situ state of stress is subject to considerable uncertainty and no doubt differs in directions parallel and perpendicular to the embankment centerline.

Four of the five tests were inserted without any initial expansion, and hence had a volume deficiency of 215 cc, while a ΔV_O of only 50 cc was used in the other

test. Equilibration times ranged from 12 hr to only 15 min and the expansion rate was increased in all tests from 6 cc/min to 20 and/or 60 cc/min.

The results differ from those at Sta. 246 in two important respects. All five tests yielded Type I-V curves, i.e. the ideal shape except for jumps at changes in expansion rate, with substantially higher values of initial pressure, P_O [about 3.5 kg/cm^2 (345 kPa) versus 2.5 kg/cm^2 (245 kPa) at comparable elevations]. Station 263 has a somewhat higher total overburden stress [say about 0.5 kg/cm^2 (50 kPa)] and a slightly lower undrained strength (say 10 to 20%, unless the failure caused significant remolding), but these differences are thought to be relatively minor compared to the substantial change in measured behavior. However, the initial portion of the Sta. 263 P vs ΔV curves generally showed a marked decrease in slope with increasing strain, whereas many of the better tests at Sta. 246 had an almost linear initial P vs ΔV relationship. This does indicate different soil conditions at Sta. 263, and perhaps significant disturbance due to the massive embankment failure.

Increasing the strain rate generally produced a fairly marked jump in the expansion curve. However, except for Test 20, this should not adversely affect modulus and strength values derived from the initial portion of the curves.

4.5 CAMKOMETER TESTS AT STA 263

Table 4-4 and Figures 4-4 (a) through (d) summarize the results of the 14 CAMKOMETER tests performed in 1973 prior to the embankment failure. For these test elevations, the average overconsolidation ratio decreased uniformly with depth from about five to unity (Figure 3-9),

79

the last five tests being run in "soft" clay. Unfortunately, most of the details regarding specific test procedures are lacking, such as the equilibration periods and the stress increment and the time interval used during incremental loading in these stress controlled tests. The literature suggests 0.1 kg/cm^2 (10 kPa) and about 0.5 to one minute as typical during cell expansion. The "cell pressure" is negative during insertion in order to keep the cell membrane in contact with the inner rigid tube via a partial vacuum, and thus values of initial cell pressure (P_O) are not quoted. Three of the 14 tests were run on soil that had been previously tested (Nos. 22, 25 and 26) and all tests conducted on "virgin" soil had at least one unload-reload cycle performed after achieving maximum cell expansion.

Though electric feelers directly measure the radial expansion in CAMKOMETER tests, the results are presented in terms of an equivalent volume change*. For these tests, 1% strain corresponds to $\Delta V \approx 25$ cc. Most tests were expanded to $\Delta V = 200-300$ cc.

As with the Sta. 263 PAFSOR tests, all of the CAMKOMETER tests exhibited Type I shapes judged of good to excellent quality. However, as discussed in later Chapters, Type I curves do not necessarily mean that the results can be easily interpreted, especially regarding measurements of in situ horizontal stress. For example, questions exist concerning the reliability of the strains measured during the very early portion of the expansion curves.

---

* Based on an assumed initial volume of 1282 cc, whereas the actual initial volume was probably about 1195 cc. However, this causes little significant error.

TABLE 4-1   GENERAL INFORMATION ON EQUIPMENT USED

PAFSOR(=PAF-72)

Dimensions

1.   Overall: diameter = 13.2 cm; length = 1.7 m

2.   Measurement cell: radius=6.60 cm; length=26.4 cm
                        initial volume=3612 cc.

   NOTE: Actual initial volume was only 3397 cc for
           tests run with zero ΔV_O.

Self-Boring

1.   Cutting tool rotated by hydraulic motor located above
     measurement cell with hoses to oil pump on drill rig.

2.   Single drill rod supplies wash water and force to
     advance cutting shoe.

Measurement Cell

1.   Longitudinally reinforced rubber membrane covered with
     vertical metal strips ("Chinese lantern").

2.   Cell should be inflated prior to insertion so that its
     average diameter equals the outer diameter of the cut-
     ting shoe (determined from calibration tests prior
     to field testing). However, actual diameter was too
     small in most of the MIT tests.

3.   Cell usually expanded at constant rate during test
     (but rate was changed in most of the MIT tests). Small
     electric motor on surface "control unit" pumps metered
     water through plastic tubing connected to cell.

4.   Pressure gage in control unit records applied pressure
     that must be corrected for: difference in elevation
     between probe and control unit; membrane resistance;
     and head losses in plastic tube.

TABL

CRYOMETER (MK3 Version)

Dimen

1. .... length=.75 m

2. .... h=37.7 cm
   ..(....) volume=195 cc.

   .... the actual dimen-
   ....in were
   ... . cell volume of
   .... 195 cc. ....

Self

1. .. .. driven by
   .. .. and also
   ....

.. . . ater and applies
   ..ng shoe.

Measu..... ...

1. T.. ..... membrane held firmly ....lled
   t.. ..... .acuum so that ... .
   . ..... cutting ..... during ....

2. .. .. by applying internal gas
   .... i.e. stress controlled expansion.

3. .... measured via transducer and radial
   ..... by three electric feelers located
   ..... (result. ...... averaged).

4. ....

8

TABLE 4-2 PAFSOR TESTS AT STA 246

Test No.	El. (ft)	σ'_{vo} (kg/cm²)	Ave OCR	Initial ΔV_0 (cc)	Equilibration Time (min)	Measured P_g (kg/cm²)	Expansion Rate cc/min[to ΔV(cc)]	Unload Reload Cycle	Type of Curve	Quality	Remarks
1	-19.7	0.58	7.0	0	30	0.67	20(180)60(800)	No	III-IV	Fair	Slight inflection
2	-28.7	0.78	4.6	0	13	1.00	6(280)20(750)	No	II-V	Good	Obvious seating problem
3	-33.7	0.90	3.9	0	10	1.15	20(800)	Yes	IV	Fair	Seating problem
4	-39.7	1.04	3.1	220	12	1.60	20(800)	No	I	Excellent	
5	-44.7	1.15	2.7	0	25	1.67	6(800)	No	II	Good	Obvious seating problem
6	-49.7	1.26	2.3	0	30	1.93	60(800)	No	IV	Fair	
7	-54.7	1.38	2.0	80	15	2.07	6(105)20(640)60(800)	No	I-V	Good	
8	-59.7	1.50	1.8	0	15	2.43	6(220)20(490)60(800)	No	?-V	Poor	V. erratic curve. Lost cutting shoe
9	-71.1	1.77	1.45	12	30	2.27	6(60)20(400)60(800)	No	I-V	Good	35 min for boring
10	-76.7	1.90	1.35	110	15	2.62	6(210)20(470)60(800)	No	IV-V	Fair-Good	32 min for boring
11	-81.7	2.02	1.3	150	30	2.87	6(260)20(510)60(800)	No	IV-V	Fair	43 min for boring
12	-86.7	2.13	1.3	150	720	3.02	6(240)20(460)60(800)	No	I-V	Good	Might be IV-V curve
13	-91.7	2.25	1.3	50	29	3.15	6(300)20(440)60(800)	No	IV-V	Fair-Good	62 min for boring
14	-96.7	2.37	1.25	0	70	3.30	6(270)20(490)60(800)	Yes	IV-V	Poor	Very erratic initial loading
15	-101.7	2.49	1.25	180	16	3.50	6(280)20(420)60(800)	Yes	IV-V	Fair	36 min for boring

1 ft = 0.305 m
1 kg/cm² = 98.1 kPa

83

TABLE 4-3   PAFSOR TESTS AT STA 263

Test No.	El. (ft)	σ'_{vo} (kg/cm^2) (1)	Ave OCR (1)	Initial ΔV_o (cc) (2)	Equili- bration Time(min)	Measured P_o (kg/cm^2)	Expansion Rate cc/min[to ΔV (cc)]	Unload- Reload Cycle	Type of Curve	Quality
16	-54.3	1.43	1.6	0	720	3.28	6(25)20(320) 60(680)	No	I-V	Good
17	-64.3	1.68	1.25	0	40	3.20	6(240)60(760)	No	I-V	Good
18	-69.3	1.80	1.1	0	112	3.60	6(120)20(300) 60(800)	No	I-V	Good
19	-74.3	1.92	1.05	50	15	3.65	6(120)20(300) 60(800)	No	I-V	Good
20	-79.3	2.04	1.0	0	42	3.85	6(70)20(200) 60(800)	No	I-V	Good

(1) For "virgin" ground prior to construction.
(2) 20 to 70 min. required for self-boring.

1 ft=0.305 m   1 kg/cm^2=98.1 kPa

84

TABLE 4-4   CAMKOMETER TESTS AT STA 263

Test No.	El. (ft)	σ'_{vo} [1] (kg/cm^2)	Ave. [1] OCR	Unload-Reload Cycle	Type of Curve	Quality	Remarks
21	-27	0.75	5.0	Yes	I	Excellent	
22	-27	0.75	5.0	No	I	-	Reload of No. 21
23	-30	0.82	4.3	Yes	I	Good	
24	-32	0.87	3.8	Yes-Two	I	Excellent	
25	-32	0.87	3.8	Yes	I	-	Reload of No. 24
26	-32	0.87	3.8	No	I	-	Reload of No. 25
27	-35	0.94	3.2	Yes	I	Excellent	
28	-40	1.08	2.6	Yes	I	Excellent	
29	-42.5	1.14	2.3	Yes	I	Good	
30	-67	1.74	1.2	Yes	I	Excellent	
31	-70.5	1.82	1.1	Yes	I	Good	
32	-74	1.91	1.05	Yes	I	Good	
33	-77.5	2.00	1.0	Yes	I	Good	
34	-80.5	2.07	1.0	Yes	I	Excellent	

[1] For "virgin" ground

1 ft=0.305 m   1 kg/cm^2=98.1 kg/cm^2
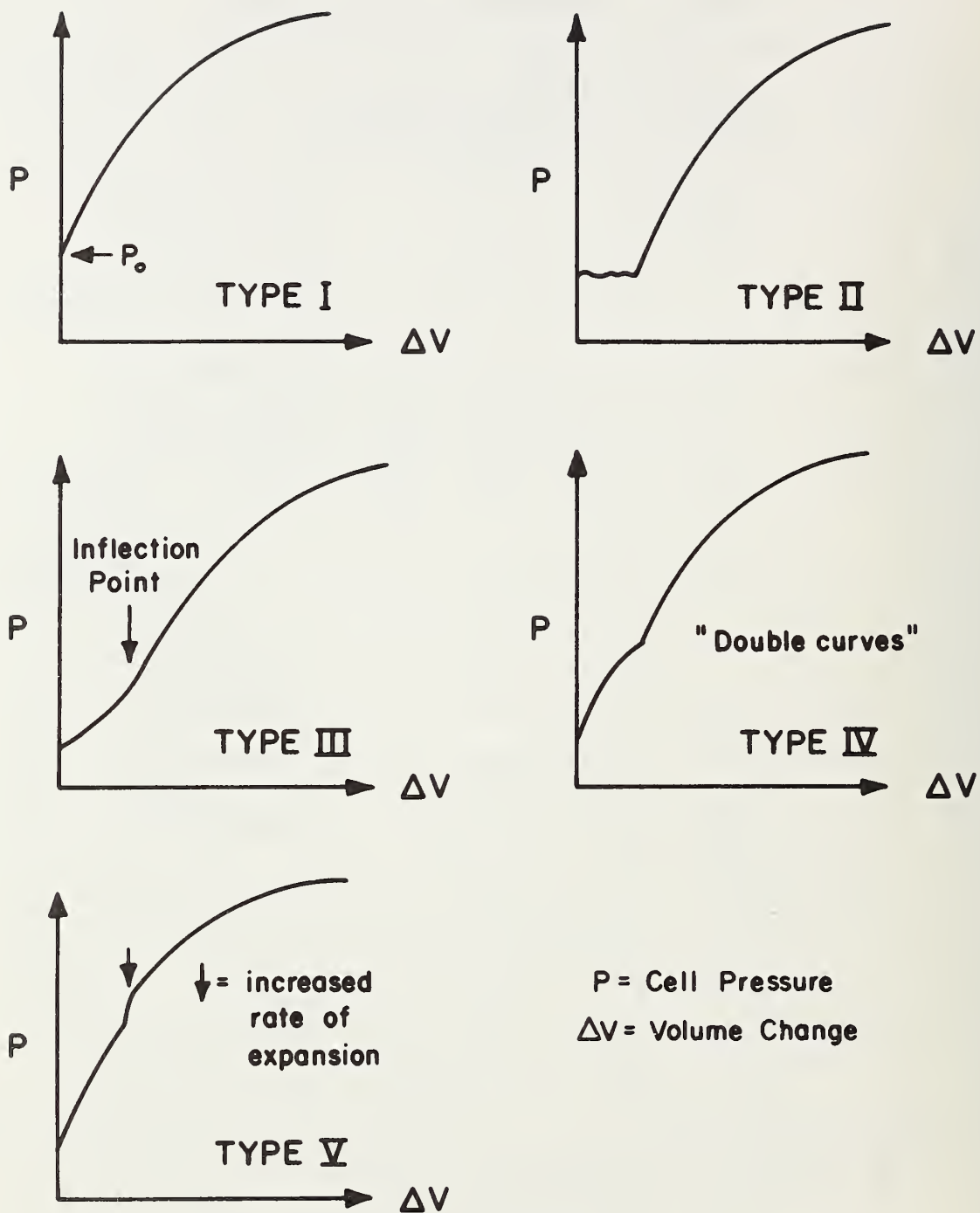
FIGURE 4-1 CLASSIFICATION OF EXPANSION CURVES
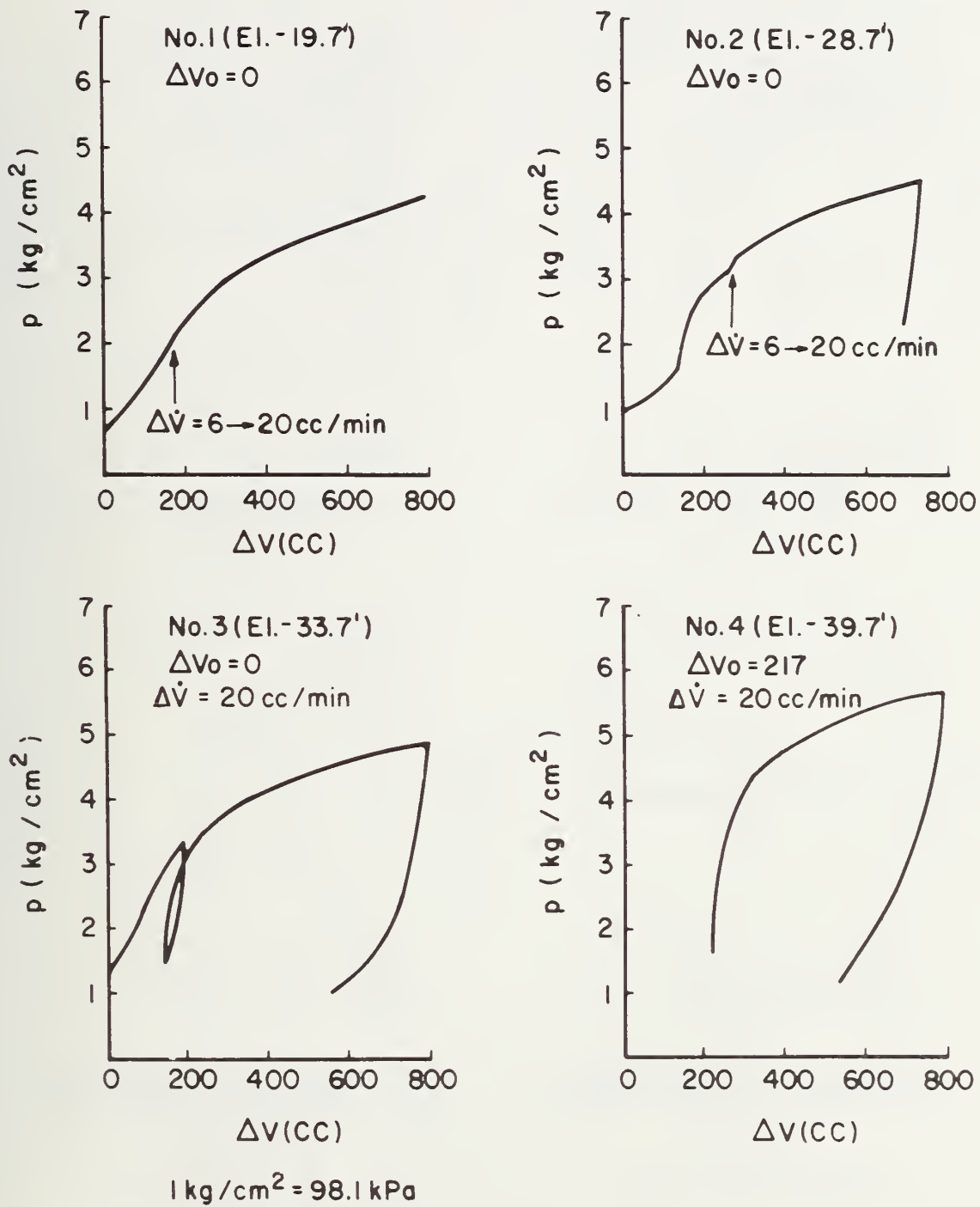
FIGURE 4-2   EXPANSION CURVES FROM PAFSOR TESTS AT STA. 246
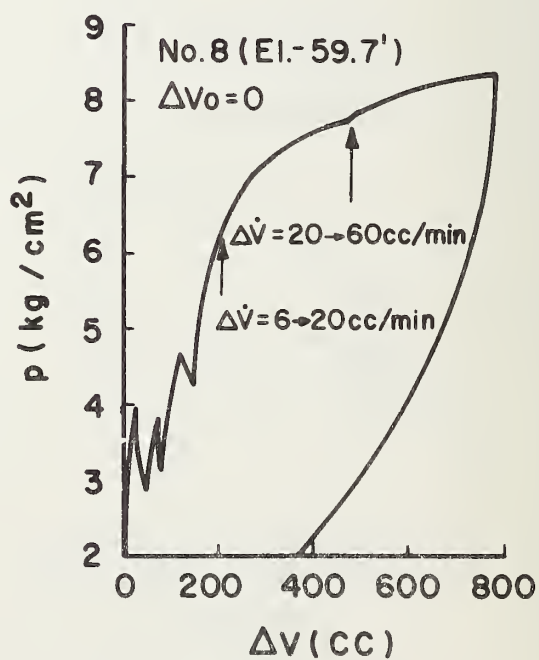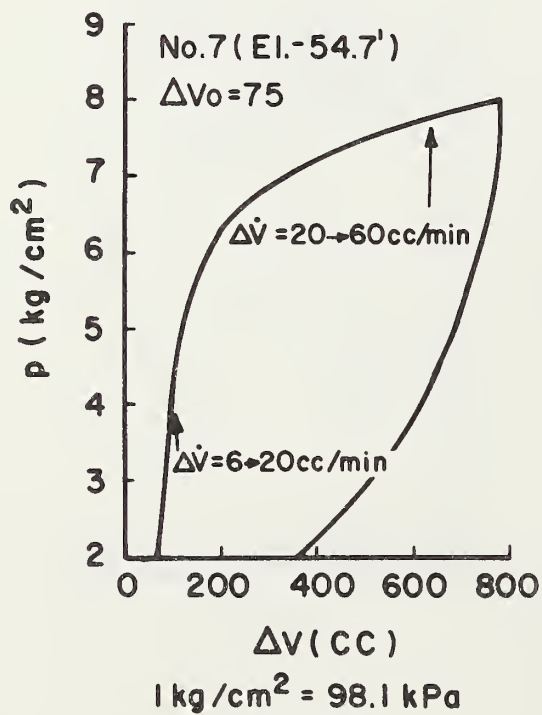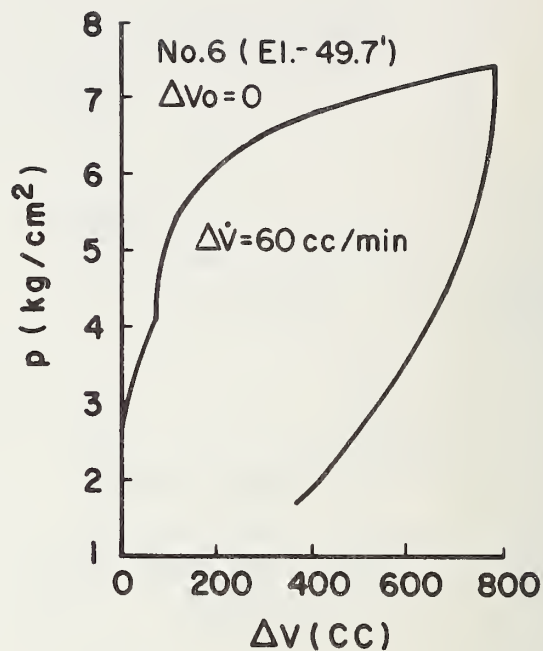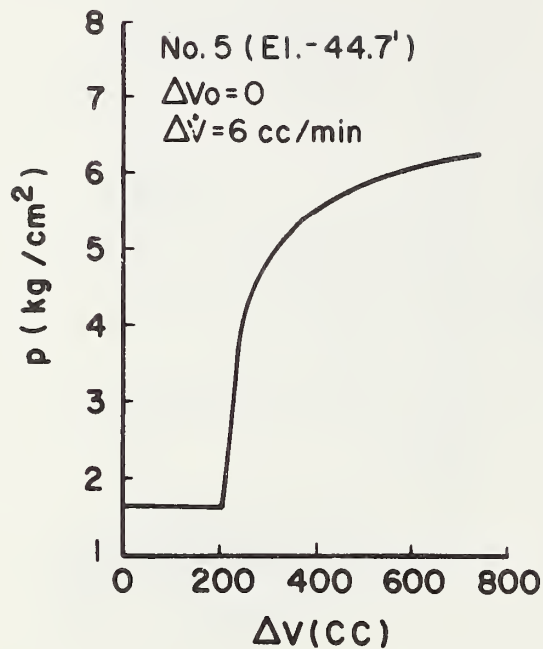
87

FIGURE 4-2 (cont.)   EXPANSION CURVES FROM PAFSOR TESTS AT STA. 246

88

FIGURE 4-2(cont.)   EXPANSION CURVES FROM PAFSOR TESTS AT
STA. 246

89
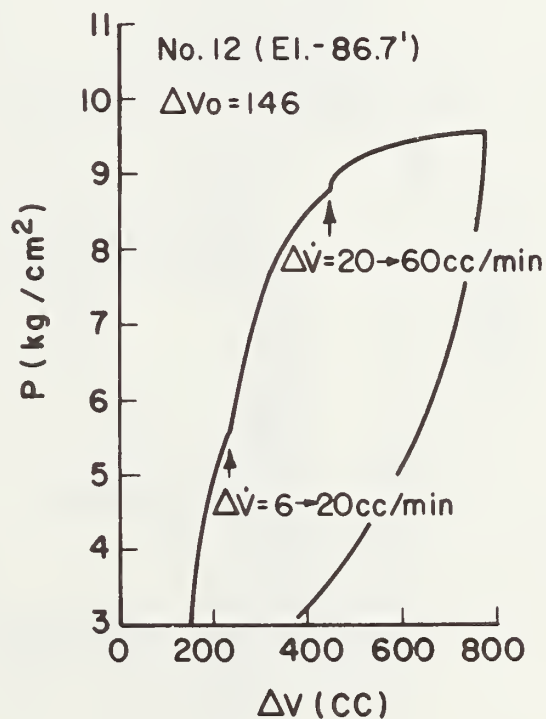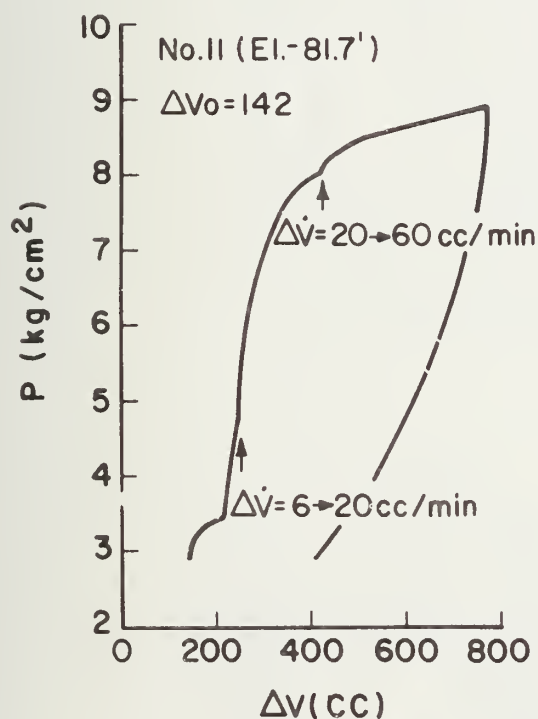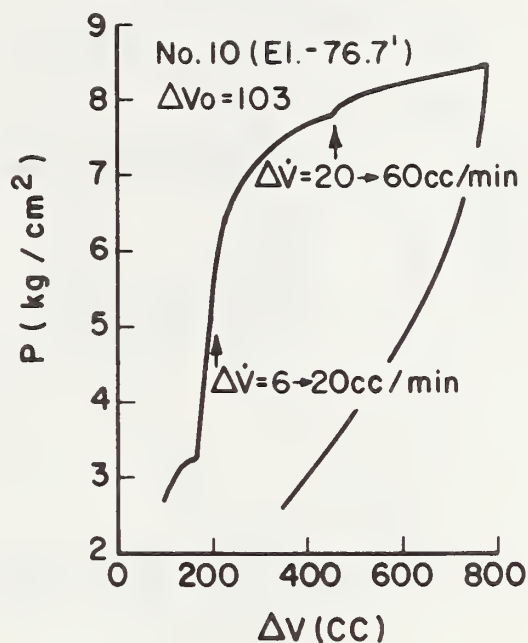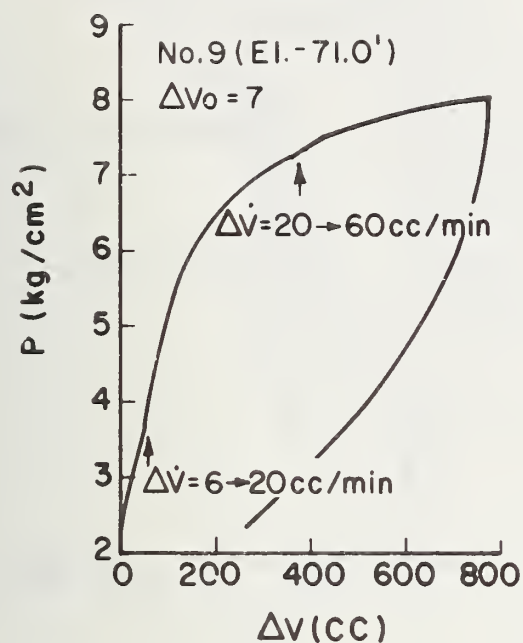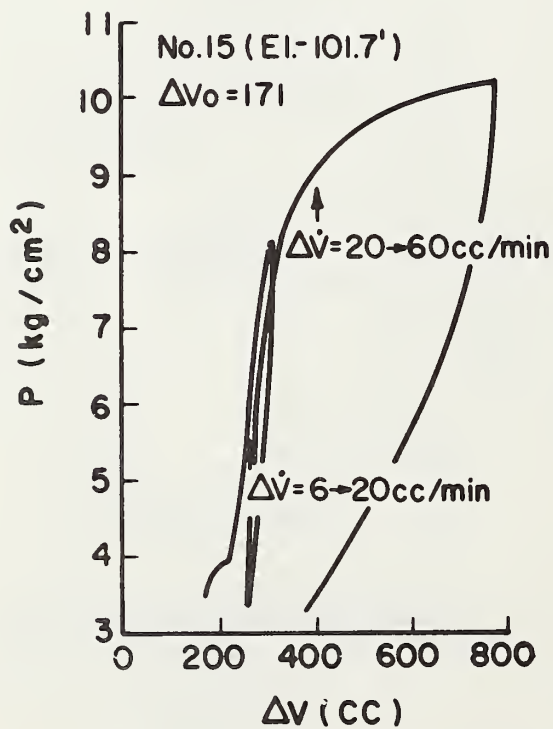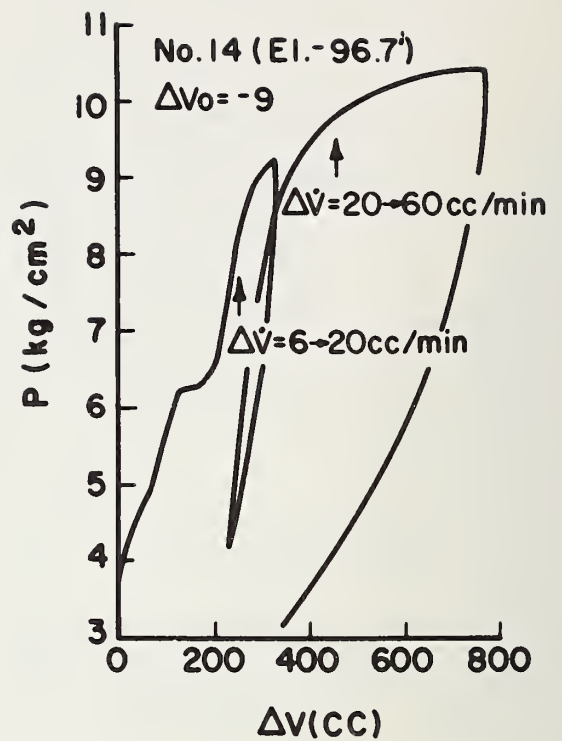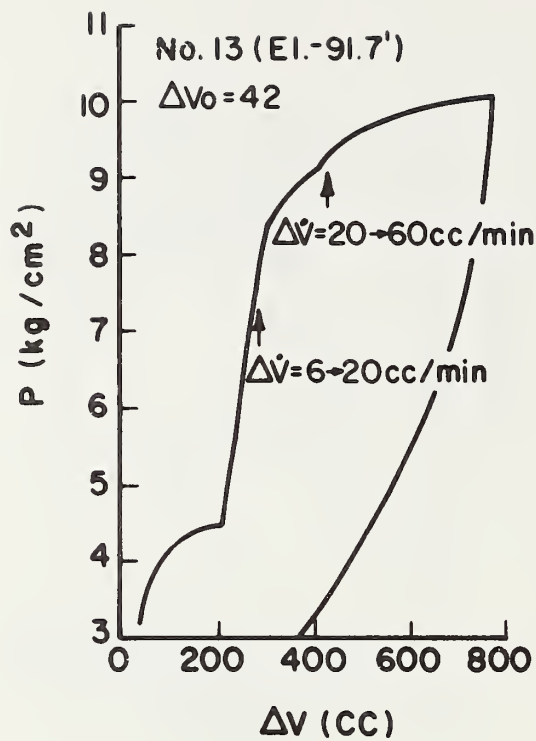
FIGURE 4-2 (cont.)   EXPANSION CURVES FROM PAFSOR TESTS AT
STA. 246
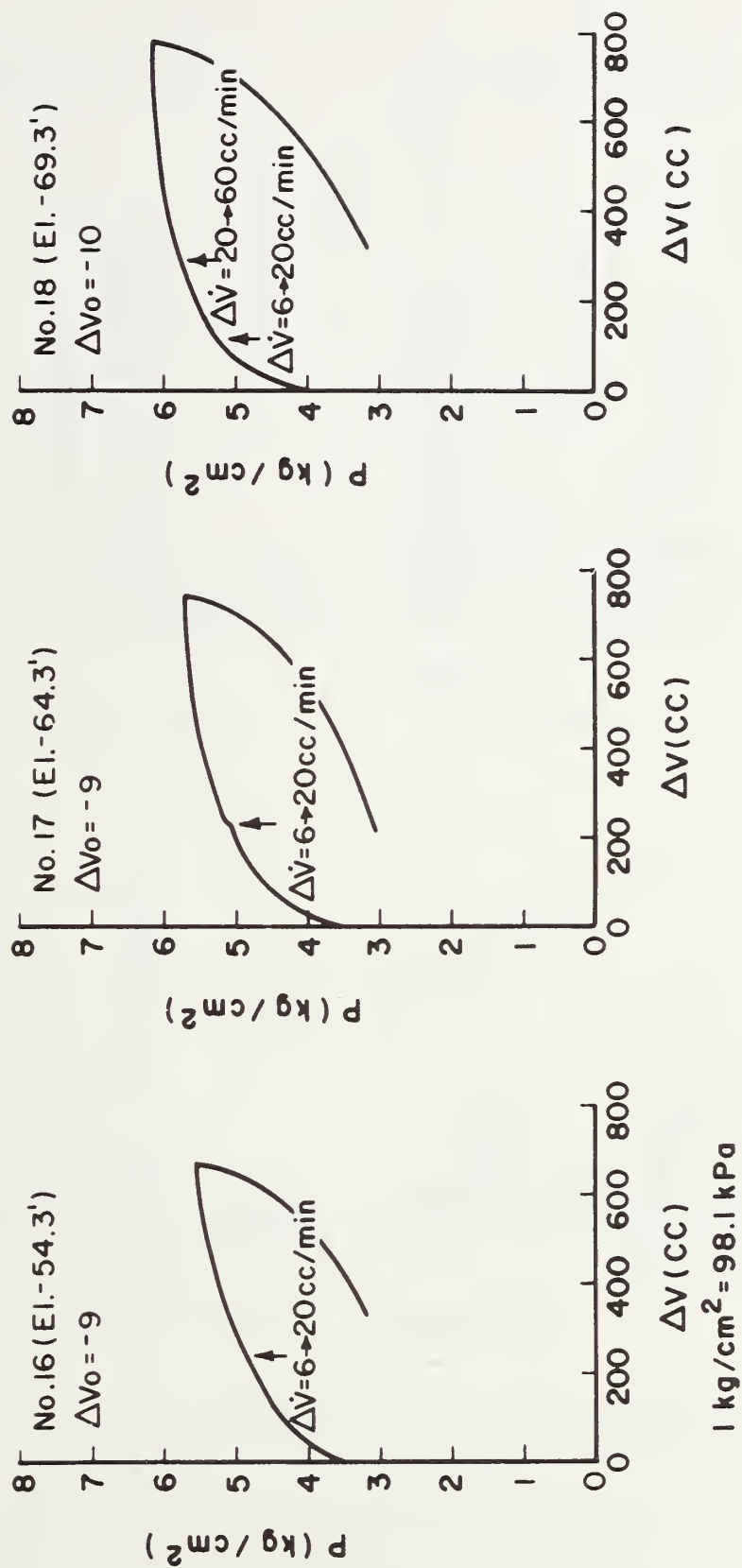
FIGURE 4-3   EXPANSION CURVES FROM PAFSOR TESTS AT STA. 263
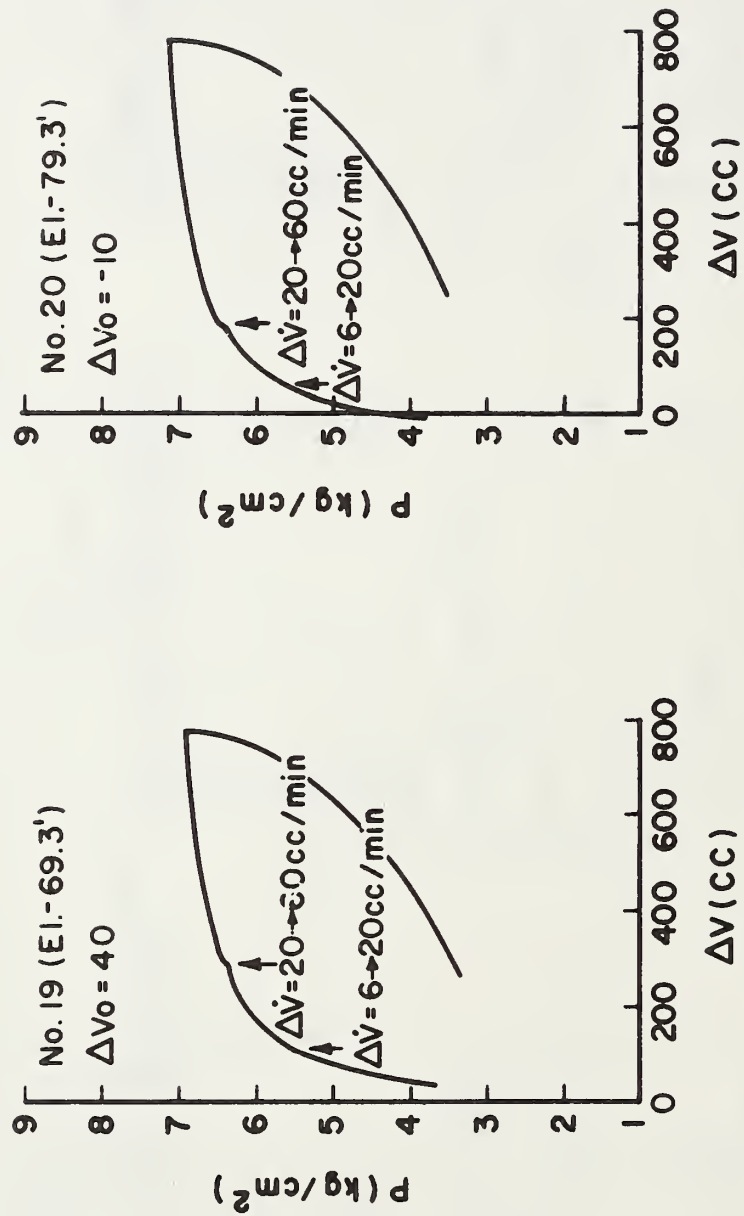
FIGURE 4-3 (cont.) EXPANSION CURVES FROM PAFSOR TESTS AT STA. 263

92
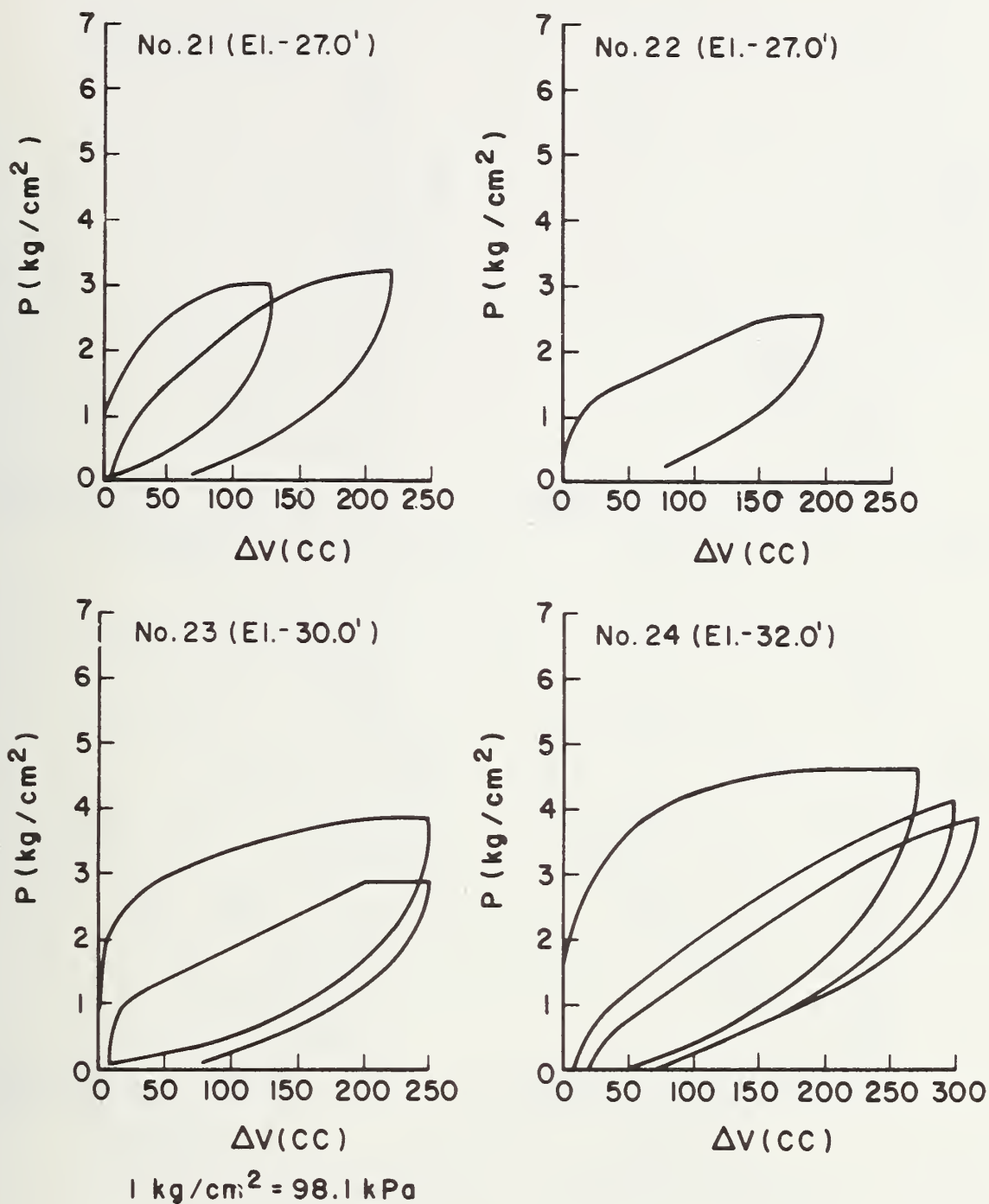
FIGURE 4-4   EXPANSION CURVES FROM CAMKOMETER TESTS AT
STA. 263
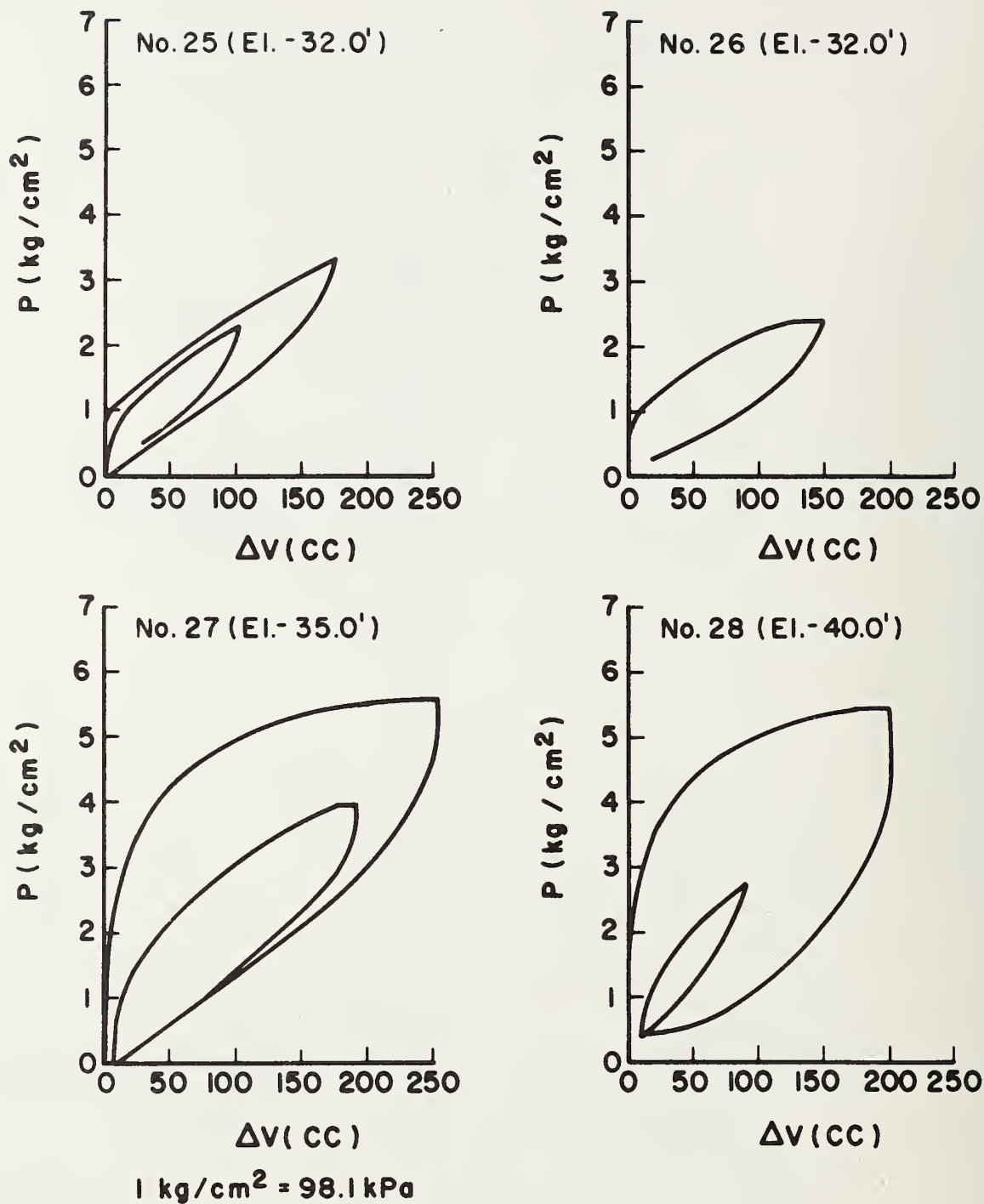
93

FIGURE 4-4 (cont.) EXPANSION CURVES FROM CAMKOMETER TESTS AT
STA. 263
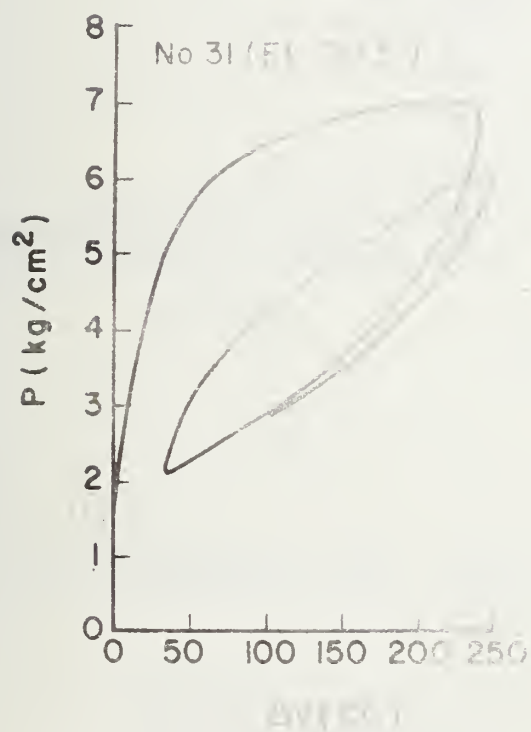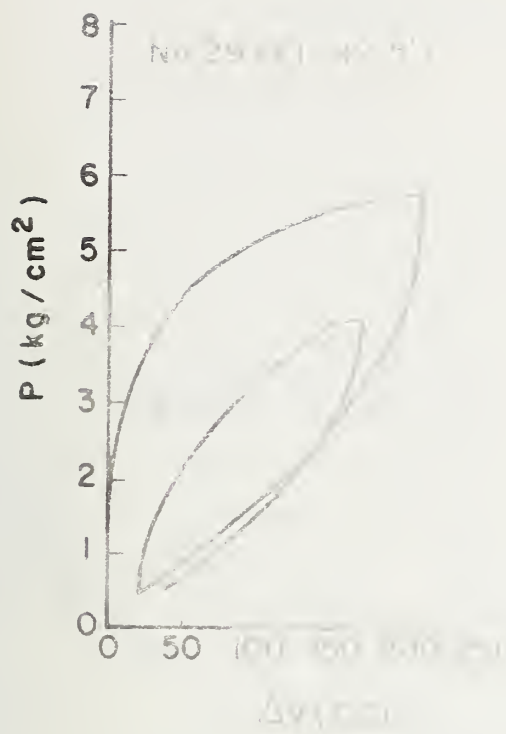
94

No 29 (F ...)

No 31 (F ...)

$1 kg/cm^2 = 98.1 kPa$

FIGURE ... STS ...

FIGURE 4-4(cont.)   EXPANSION CURVES FROM CAMKOMETER TESTS AT
STA. 263

96
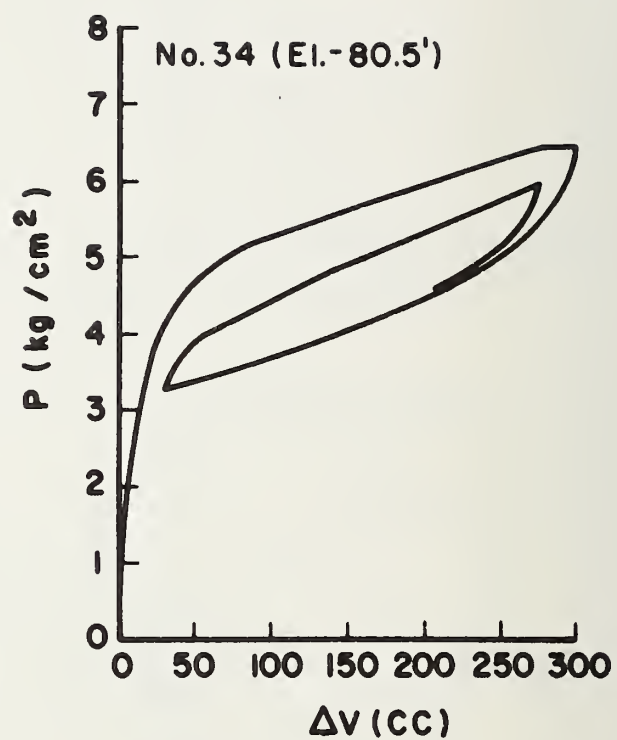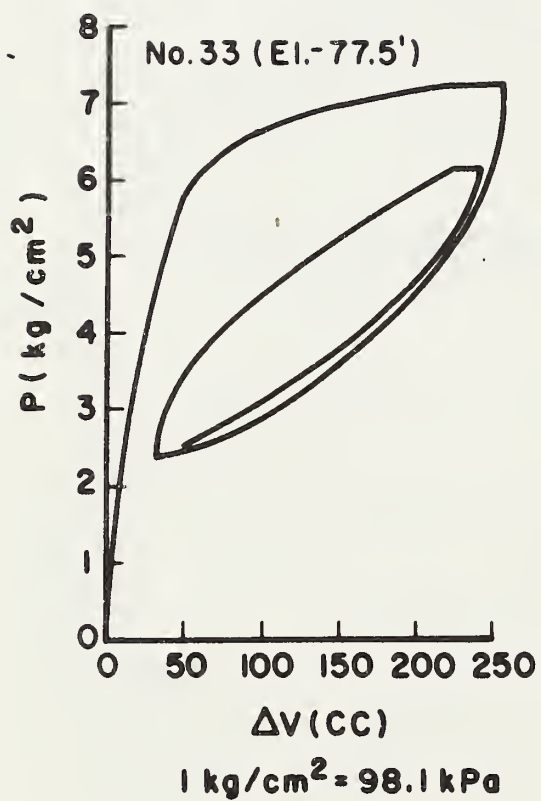
5. EVALUATION OF IN SITU HORIZONTAL STRESS

5.1 INTRODUCTION

Evaluation of in situ horizontal stress (σ_{ho}) is certainly amongst the most important but difficult tasks in geotechnical engineering. If the self-boring pressure-meter test can indeed provide reliable estimates of σ_{ho}, this by itself represents a major development since other procedures (namely hydraulic fracturing, earth pressure cells and laboratory testing) are known to be expensive, time consuming and/or subject to considerable uncertainty (e.g. Wroth, 1975, and Ladd et al., 1977). Thus much prior research with the SBPT has focused on evaluation of in situ stress, especially that using the CAMKOMETER.

The stress acting on the measurement cell after inser-tion and the strain history of the surrounding soil also influence stress-strain-strength data derived from the expansion curve, i.e. via the equations presented in Table 2-1. In particular, values of the peak strength are very sensitive to relatively small changes in the starting point of the P-ΔV curve.

Let us first consider the situation wherein the ex-pansion curve has an ideal shape with a well defined initial starting point, i.e. the Type I curve illustrated in Figure 4-1. For such cases, P_O is the initial cell pressure* in PAFSOR tests or the "lift-off" pressure in CAMKOMETER tests. The only question, then, is whether or not this value of P_O gives a reliable estimate of the

---

* After correction for membrane resistance, compliance in the system, etc.

97

in situ σ_{ho}. Some possible reasons why P_O may not equal σ_{ho} are listed below:

(1) Shear stresses must act along the circumference of the measurement cell even with perfect self-boring (no radial straining).

(2) The soil may be further disturbed due to significant radial straining during insertion. For example, several of the PAFSOR tests had Type I curves even though the measurement cell was significantly under-sized.

(3) The PAFSOR measurement cell can deform differentially along its axis even when the overall cell volume remains constant*.

(4) Even though all CAMKOMETER tests had Type I curves, the precise lift-off pressure was difficult to determine (perhaps due to problems with the electric feelers at very low strains).

Further complications arise with expansion curves that do not have well defined initial conditions and/or show an obvious seating problem such as illustrated by the Type II, III and IV curves shown in Figure 4-1. Thus one is frequently confronted with two problems: how to select an appropriate value of P_O; and how will the value of P_O (even if well defined) compare with the in situ σ_{ho}.

5.2 METHODS OF INTERPRETATION

This section presents five methods currently available for evaluating P_O. Some have no theoretical basis while others attempt to compensate, at least partially, for the

---

* Actually the volume decreases slightly (a few cc) due to compliance in the system, but this effect is considered unimportant.

likely effects of disturbance which inevitably occur in most pressuremeter testings. It should be noted that all but the first of these procedures were developed to interpret Menard, not self-boring, pressuremeter test data.

5.2.1   Initial Pressure at Start of Test

The approach simply selects the pressure measured after the equilibration period. This equals the cell pressure at the start of PAFSOR tests and the lift-off pressure in CAMKOMETER tests. The latter may be somewhat difficult to measure accurately if the initial portion of the expansion curve is very steep or if the electric feelers record initial strains that are too large. This value of P_O should be less than the true in situ stress whenever disturbance causes Type II, III and IV curves. It may also be erroneous even with Type I curves as discussed in Section 5.1.

5.2.2   Inflection Point Method

This method was developed in the early days of Menard pressuremeter testing when it was thought that σ_{ho} would equal P at the start of the "straight line" portion of a Type III expansion curve (Baguelin et al., 1978, p. 573) as illustrated in Figure 5-1. It has since been abandoned with the Menard device as this form of testing is known to cause excessive disturbance to the soil. Though the method has no theoretical or empirical basis for use with the SBPT, which should produce only Type I curves, it was used as one procedure for selecting a corrected initial pressure in those PAFSOR tests having Type II, III and IV expansion curves. Figure 5-1 shows how the writers applied the method. There is no real reason why this value should equal σ_{ho}, but it at least gives a more reasonable starting

point for obtaining stress-strain-strength data. Its
application to Type IV curves may be questionable unless
the inflection point occurs at a volume change approxi-
mately equal to the initial volume deficiency in the PAFSOR
measurement cell.

5.2.3 Inverse Volume Method

Van Wambeke and d'Hemricourt (1975) proposed this
method, illustrated in Figure 5-2, wherein pressure is
plotted versus the reciprocal of the volume change. Though
primarily developed to provide a more accurate estimate of
the limit pressure at infinite expansion ($1/\Delta V=0$) with
Menard pressuremeter tests, the authors infer that it
can also be used to evaluate P_O. The P vs $1/\Delta V$ plot has
three portions where AB represents initial expansion for
a Type III curve, BC corresponds to the "pseudo-elastic
phase" of the test and CD the "plastic phase". Sections
BC and CD are presumed linear, which implies that P vs ΔV
must follow two different hyperbolic curves between points
B and D. Point B defines P_O, i.e. the pressure at the
start of the first linear segment.

This research mainly used the inverse volume method
for evaluating limit pressures, though it was also employed
to estimate P_O with the CAMKOMETER tests.

5.2.4 Numerical Iteration Method

Gibson and Anderson (1961) developed a theoretical
approach for estimating P_O using an elasto-plastic stress-
strain model to describe soil behavior during a Menard
pressuremeter test. Though details of their model will be
discussed in Chapter 7, the pertinent equations and steps
in this "numerical iteration" method are briefly outlined
below.

The authors present the following equations to describe the P vs ΔV expansion curve:

In "elastic" range;

$$G = \Delta P / (\Delta V / V_O) \qquad \text{(Eq. 5-1)}$$

After "initial" yielding;

$$P = P_O + c_u + c_u \ln\left[\frac{G}{c_u}\left(\frac{\Delta V}{V}\right) - \left(1 - \frac{\Delta V}{V}\right)\frac{P_O}{c_u}\right] \qquad \text{(Eq. 5-2)}$$

$$P = P_1 + c_u \ln\left[\frac{\Delta V}{V} - \left(1 - \frac{\Delta V}{V}\right)\frac{P_O}{G}\right] \qquad \text{(Eq. 5-3)}$$

where $V = V_O + \Delta V$. From Eq. 5-3 for two points on the yielded portion of the expansion curve, one obtains;

$$c_u = \frac{P_2 - P_1}{\ln\left[\frac{\Delta V/V_2 - (1 - \Delta V/V_2)P_O/G}{\Delta V/V_1 - (1 - \Delta V/V_1)P_O/G}\right]} \qquad \text{(Eq. 5-4)}$$

where P_1, V_1 and P_2, V_2 are points on the expansion curve separated by $\Delta V = V_2 - V_1$.

The iterative procedure involves the following steps:

(1) Assume a value for P_O and hence V_O and then compute G using Eq. 5-1.

(2) From two points on the yielded portion of the expansion curve, calculate c_u using Eq. 5-4.

(3) For either of these two points, now solve for P_O in Eq. 5-2 and compare this value with that assumed in step (1).

(4) Repeat the process until convergence is obtained.

The numerical iteration method differs from the three previous approaches since it accounts, at least in theory, for the effects of unloading which always occur with

Menard pressuremeter tests. Note that some unloading presumably occurred in all PAFSOR tests where the measurement cell was inserted with a volume deficiency. Though Gibson and Anderson (1961) assumed that the unloading process was linear, their method should provide a better (i.e. higher) estimate of P_O than the previous methods.

MIT did not use the numerical iteration technique because the next method, though based on similar reasoning, is less restrictive in its assumptions. Also MIT computerized the procedure to facilitate its use.

5.2.5 Graphical Iteration Method

Marsland and Randolph (1977) developed this new method, though in concept it resembles the Gibson and Anderson (1961) technique, for application to Menard pressuremeter test data in stiff clays. They make the following assumptions (see Figure 5-3):

(1) Small positive or negative increments of pressure from P_O will cause similar volume changes, i.e. the P vs ΔV relationship behaves elastically near P_O.

(2) Therefore P_O should lie within the central portion of the approximately linear P vs ΔV curve and not at the start of the linear region as assumed by the inflection method (Section 5.2.2).

(3) For an elastic perfectly plastic material, plastic yielding occurs in the clay next to the measurement cell at a pressure increment of c_u above P_O, where c_u is the peak strength derived from the expansion curve using Eq. 2-6 in Table 2-1. A marked increase in the curvative of the P vs ΔV relationship therefore should occur when P exceeds P_O+c_u.

Since P_O must be determined in order to calculate the derived peak c_u, the method requires iteration until the value of $P_O + c_u$ obtained corresponds to the pressure at which the P vs ΔV curve exhibits a marked increase in curvature. Figure 5-3 illustrates the procedure which involves the following steps:

(1) Select a trial P_O, which also establishes a corrected origin [e.g. $(\Delta V)_a$ equals zero strain in Trial a].

(2) Compute the corresponding derived peak strength using Eq. 2-6.

(3) Compare $P_O + c_u$ with the value of P at the point of marked increase in curvature (this value requires subjective judgement).

(4) Repeat the process until $P_O + c_u$ agrees with the above value of P.

Trial b in Figure 5-3 shows perfect agreement, whereas Trials a and c had assumed values of P_O that were too low and too high respectively.

MIT developed a computerized procedure for applying this method, which is described in Appendix D, and used it for the PAFSOR tests at Sta. 246 and some of the CAMKOMETER tests at Sta. 263.

5.3 RESULTS OF ANALYSES

This section presents estimates of horizontal stress from the PAFSOR and CAMKOMETER tests based on the following methods:

PAFSOR at Sta. 246

    (1) Initial pressure at start of test
    (2) Inflection point
    (3) Graphical iteration

103

PAFSOR At Sta. 263

    (1) Initial pressure at start of test = inflection
        point

CAMKOMETER at Sta. 263

    (1) Inverse volume

    (2) Graphical iteration

The results are compared to values of in situ horizontal stress (σ_{ho}) developed from laboratory tests and generally confirmed by the earth pressure cell measurements. Problems encountered in using the various methods are also discussed. Data from the Sta. 263 PAFSOR tests received relatively little attention since the in situ stresses are unknown due to the embankment failure.

5.3.1 PAFSOR Tests at Sta. 246

Table 5-1 summarizes the results and Figure 5-4 plots initial pressure and inflection point data versus elevation. This figure also presents for comparison: values of hydrostatic pore pressure (for water table at El.+2); σ_{ho} computed for $K_O=0.5$ (a lower bound corresponding to normally consolidated clay); and the estimated range in the actual σ_{ho} taken from Section 3.4.

The initial pressure values all plot well below the σ_{ho} line for $K_O=0.5$ and generally equal or only slightly exceed the hydrostatic pore pressure. As noted in Chapter 4, the measurement cell usually had a significant volume deficiency during insertion. Insertion with $\Delta V_O=0$ corresponds to a 215 cc deficiency (negative strain of 3%). As shown in Table 5-1, one test (No. 4) had $\Delta V_O=220$ cc, four had $\Delta V_O=150-180$ cc and most used $\Delta V_O=0$. It is some-what surprising that both the changes in P during equili-bration and the final values of P appear almost unrelated

to the insertion condition. Moreover the ΔP values in Table 5-1 were generally quite small with both positive and negative changes with time. Based on these observations, one might conclude that the pressure in the wash water (which flowed out of the casing at El.+7) was the major factor controlling the initial P_O.

Three of the writers (Germaine, Lacasse and Ladd) independently applied the inflection point method. They obtained very similar results for tests with Type I, II and III curves and their average values are reported. A much larger scatter resulted with most of the Type IV curves, as some selected the first inflection point and others the second one. After considering the ΔV at which the second curve started with respect to the volume deficiency in the measurement cell, the inflection point for the second curve was finally selected as being most reasonable for these tests, except for No. 6 where the change in curvature occurred at a very high stress.

Although the inflection point method often yielded significant increases above the initial pressure, all but one of the values plotted in Figure 5-4 still fall below the lower estimate of σ_{ho}. In fact most are still significantly less than σ_{ho} computed for $K_O=0.5$ and again there appears little relation between the values and the conditions that existed during insertion. Hence the inflection point method gives very unsatisfactory and un-predicable results for this test series wherein the self-boring process generally caused significant unloading within the soil adjacent to the measurement cell.

MIT did not apply the inverse volume procedure in the belief that it offered little advantage over the inflection point method which already gave estimates of horizontal stress generally much too low.

105

As discussed in Section 5.2.5, MIT developed a computer program to facilitate application of the Marsland and Randolph (1977) graphical iteration method. The program uses a modified version of the Prevost and Hoeg (1975) equation for strain-softening materials (see Chapter 7 and Appendix D) to represent the expansion curve data by a smooth curve and requires the following input data (see Figure 5-3): (1) expansion curve data; (2) the point representing the "marked increase in curvature" which remains fixed for a given analysis; and (3) a first estimate of P_O. The program then best fits the modified Prevost-Hoeg equation to the data for this P_O, calculates the derived peak c_u, substracts this value from the "curvature point" to obtain a new P_O and compares it to the original P_O. The process continues until convergence, i.e. two successive iteration steps produce the same P_O.

The above procedure applies to only one value for the "curvature point", which was selected on the basis of judgement. This point could be defined with reasonable accuracy in some tests, but was subject to considerable uncertainity in others. Thus, depending upon the shape and quality of the expansion curve, the method was generally performed for a range of curvature points*.

Table 5-1 and Figure 5-5 present values of in situ horizontal stress predicted by the graphical iteration method based on lower bound, upper bound and/or best estimates of the location of the "point of marked increase in curvature" on the measured expansion curve. Table 5-1 also contains comments on problems encountered in applying the method. For example, the phrases "$\Delta\dot{V}$ causes problem,

---

* First selected independently by Germaine and Ladd, who then agreed on "most reasonable" values.

$\Delta \dot{V}$ real problem", etc. mean that an increase in the rate of volume expansion affected the shape of the curve. This caused a problem, to varying degrees, in selecting the curvature point and sometimes produced erratic changes in the modified Prevost-Hoeg curve fitting parameters (Had this method been known during the test program*, the expansion rate would not have been increased until after reaching the curvature point). The table also notes when the shape of the curves either precluded using the method or cast serious doubt on the results, i.e. for Tests 6, 8, 13, 14 and 15.

Thus the results presented in Table 5-1 and plotted in Figure 5-5 should be divided into two groups: values considered highly questionable because of erratic curves and/or serious problems caused by changing the expansion rate; and data from tests wherein the method could be applied in a reasonably straightforward fashion. Tests 2 through 5, and to a lesser degree Nos. 1, 7 and 9, belong in the latter category. These tests generally yielded consistent results, with "best estimates" usually falling within or very near the range of the in situ σ_{ho} values. In fact, the agreement is considered exceptionally good on an absolute basis since the self-boring process was far from ideal in most of these tests. In any case, this method gave far better results than obtained from the inflection point method.

On the other hand, results from tests falling in the first category (i.e. highly questionable) yielded a wide range of values that often plotted well below and especially far above the estimated in situ σ_{ho}. However, these

---

* It was published after completing the tests.

results do not necessarily invalidate the graphical iteration procedure since the scatter primarily results from changes in the rate of expansion. In particular, we know that the very high upper bound data are erroneous because the peak strengths computed by the modified Prevost-Hoeg curve fitting procedure are much too low, as explained in Chapter 7 (the procedure simply cannot handle changes in slope when the expansion rate was increased). Thus, since P_O equals the curvature point P minus c_u(peak), an underestimate of c_u(peak) must yield a P_O that is too large. But in spite of this error, even a simple average of the data from these tests is better than the initial P_O values and often superior to the inflection point data.

In conclusion, the graphical iteration method appears to offer a very promising approach for estimating σ_{ho}. It gave very reasonable results in those PAFSOR tests where the "curvature point" fell within a relatively narrow band even though the soil surrounding most of these tests experienced considerable unloading during the self-boring process. The method does require, however, smooth expansion curves having a fairly well defined curvature point that can be reasonably fitted by the modified Prevost-Hoeg equation. This did not occur with most of the deeper tests at Sta. 246 because the expansion rate was changed at an inappropriate time and/or due to unexplained erratic behavior. In particular, the very high values plotted in Figure 5-5 from Tests 11, 13 and 15 are known to be too large due to underestimates of the peak c_u.

5.3.2 PAFSOR Tests At Sta. 263

These five tests all showed Type I curves even though self-boring occurred with $\Delta V_O \leq 50$ cc such that the measurement cell was seriously undersized. With Type I curves,

108

P_O at the start of the test and from the inflection point method are the same. Table 4-3 gives the values* which are plotted in Figure 5-6. Though the embankment failure precludes a reliable estimate of the actual in situ horizontal stress, the figure shows an approximate range. This band equals the range plotted in Figure 3-12 for 1969 plus 0.35 kg/cm^2 (34 kPa), the latter number representing a rough estimate of the increased vertical stress due to ground heave (see Figure 3-14). The figure also shows corresponding data for the PAFSOR tests at Sta. 246.

The Sta. 263 tests gave P_O values about 1 kg/cm^2 (98kPa) higher than those at Sta. 246 at comparable elevations. These data also plot somewhat closer to the estimated in situ stress, though the actual values may lie above the indicated range. Moreover, the horizontal stress acting perpendicular to the embankment axis probably exceeds that acting parallel to the embankment. Thus no definitive conclusion can be drawn other than to state that the Sta. 263 inflection point P_O values are undoubtedly too low and the error can logically be attributed to self-boring with an undersized measurement cell, though this may not be the sole reason.

5.3.3 CAMKOMETER Tests at Sta. 263

Table 5-2 and Figure 5-7 summarize the results from applying the inverse volume and graphical iteration methods to the 11 CAMKOMETER tests performed prior to the embankment failure on "virgin" soil(i.e. excluding reloading

---

* ΔP during equilibration equalled +0.46 kg/cm^2 (45kPa)in Test 16 and ranged from +0.2 to -0.14 kg/cm^2 (+20 to -14kPa) in the other tests.

tests). The tests all had Type I curves, but also generally exhibited significant strains at stresses well below the estimated in situ σ_{ho}. Values of "lift-off" pressure, i.e. the pressure when strain first occurred, were rather ill-defined and also very low, usually falling between 1 and 2 kg/cm^2 (100-200 kPa).

The inverse volume method yielded results considered unsatisfactory even though most of the curves had shapes similar to the AB-BC portions shown in Figure 5-2, i.e. the method could be applied in a relatively consistent fashion. As seen in Figure 5-7, the predicted horizontal stresses are all too high in the upper overconsolidated clay (OCR=3±1), whereas in the low OCR clay the values generally fall well above or below the estimated in situ σ_{ho} range. Also note that the inverse volume curves in the deep clay were all judged to have a "fairly good shape" (Appendix C presents the curves).

Horizontal stresses predicted by the graphical iteration method were based on lower bound, upper bound and/or best estimates of the location of "curvature point" and Table 5-2 comments on this selection process. As for the Sta. 246 PAFSOR tests, Germaine and Ladd made independent selections before deciding on final values of "curvature points" to be used in the analyses. The results plotted in Figure 5-7 generally show a wide variation in the predicted limits of horizontal stress, especially in the deep "soft" clay. However, 8 of the 11 "best estimate" values fall within or very near to the estimated range for the in situ σ_{ho}. Judgement regarding these "best estimate" values was probably influenced somewhat by prior knowledge of what the answer should be. Nevertheless, the writers hold the view that the graphical iteration method shows considerable promise.

5.4 DISCUSSION

Since most of the PAFSOR tests were inserted with a significantly undersized measurement cell (volume deficiency of 75-225 cc in 16 of the 20 tests), it is not surprising that the inflection point method predicted horizontal stresses (Figures 5-4 and 5-6) much less than the estimated in situ σ_{ho} in almost all cases. However, the measured behavior had several unusual features. For example, changes in pressure during equilibration, the equilibrium values of P_o and the shape of the expansion curves all appeared to be unrelated to the amount of volume deficiency during self-boring. Also, although many of the tests met the "displacement index" criteria proposed by Baguelin et al. (1978) (see Section 2.4), they still predicted horizontal stresses much too low.

"Lift-off" pressures measured in the CAMKOMETER, though generally rather ill-defined, were all less than the estimated in situ σ_{ho}, especially in the deep "soft" clay. The reason for this behavior is not clear: it might be due to problems with the electric feelers and/or the installation technique, about which little is known. The inverse volume method, while predicting much larger stresses, still yielded unsatisfactory results. As shown in Figure 5-7, these exceeded σ_{ho} in the upper overconsolidated clay and varied from being too high to too low in the normally consolidated clay.

MIT applied the Marsland and Randolph (1977) graphical iteration method to the PAFSOR tests at Sta. 246 (Figure 5-5) and the CAMKOMETER tests at Sta. 263 (Figure 5-7). The method requires judgement in selecting the point of marked increase in curvature on an expansion curve (see Figure 5-3) and thus the analyses used upper and lower bounds

111

and/or a best estimate for the "curvature point". In those tests having a smooth expansion curve with a reasonably well defined "curvature point", the predicted best estimate value usually fell within or very near to the estimated in situ σ_{ho} band. This was generally the case for tests in the upper overconsolidated clay with both the PAFSOR and CAMKOMETER tests, while results in the deep "soft" clay were less satisfactory. Changes in the expansion rate in the Sta. 246 PAFSOR tests provide a logical explanation for why these tests gave poorer results, particularly those values which are much too high.

Marsland and Randolph (1977) developed the graphical iteration method to predict σ_{ho} from Menard tests in the stiff fissured London clay and obtained excellent agreement with values of K_O estimated from laboratory tests. Their test program involved eight pairs of Menard tests at depths of 4 to 25 m where the predicted and estimated K_O decreased with depth from about 3.5 down to 2.0.

The graphical iteration method certainly appears to offer great potential for predicting reasonable values of σ_{ho} from pressuremeter test data and should be further evaluated for a variety of soil types. It may be best suited for use in more heavily overconsolidated clays, which is almost ideal since these deposits also have the greatest uncertainty in K_O predicted by other methods.

TABLE 5-1 HORIZONTAL STRESS MEASUREMENTS FROM PAFSOR
TESTS AT STA 246

| Test No. | El. (ft) | ΔV_o (cc) | Equilibration | | Type of Curve | Horizontal Stress (kg/cm^2) | | | | | Comments on Graphical Iteration |
| | | | t(min) | ΔP (kg/cm^2) | | Initial Pressure | Inflection Point | Graphical Iteration | | | |
								Lower	Best Est.	Upper	
1	-19.7	0	12	+0.02	III-V	0.67	1.2	0.85?	1.55	1.55	$\Delta\dot{V}$ causes problem
2	-28.7	0	13	+0.05	II-V	1.00	1.25	-	1.5	-	Good
3	-33.7	0	10	+0.05	IV	1.15	1.65	-	2.0	-	Fair
4	-39.7	220	12	-0.02	I	1.60	1.65	2.0	2.15	2.25	Good
5	-44.7	0	25	-0.06	II	1.67	1.7	2.45	2.7	2.9	Good
6	-49.7	0	30	+0.15	IV	1.93	2.0	-	-	-	Shape prohibits
7	-54.7	80	15	+0.11	I-V	2.07	2.15	-	3.0	3.0	$\Delta\dot{V}$ may cause problem
8	-59.7	0	15	+0.05	?	2.43	-	-	-	-	Shape prohibits
9	-71.7	12	30	+0.36	I-V	2.27	2.3	2.95	3.4?	3.85	$\dot{V}$ may cause problem
10	-76.7	110	15	+0.02	IV-V	2.62	3.25	3.5	-	5.0?	$\Delta\dot{V}$ causes problem
11	-81.7	150	30	-0.12	IV-V	2.87	3.45	3.5?	-	5.2?	$\dot{V}$ real problem
12	-86.7	150	720	-0.19	I-V	3.02	3.0	2.7?	-	4.7	$\Delta\dot{V}$ real problem
13	-91.7	50	29	-0.05	IV-V	3.15	4.55	4.5?	-	6.55?	Erratic curve
14	-96.7	0	70	+0.18	IV-V	3.30	-	-	-	-	Shape prohibits
15	-101.7	180	16	+0.16	IV-V	3.50	3.95	4.25?	-	6.3?	Erratic curve $+\Delta\dot{V}$ problem

1 ft=0.305 m   1 kg/cm^2=98.1 kPa

TABLE 5-2   HORIZONTAL STRESS MEASUREMENTS FROM CAMKOMETER TESTS AT STA 263

Test No.	El. (ft)	Inverse Volume Method		Graphical Iteration Method			
		Horiz. Stress (kg/cm²)	Remarks	Horizontal Stress (kg/cm²)			Remarks (CP=Curvature Point)
				Lower	Best Est.	Upper	
21	-27	2.4	Fairly Good Shape	1.70	2.05	-	CP poorly defined
23	-30	-	Plot has wrong shape		1.95		CP well defined
24	-32	2.9	Fairly good shape	2.2	2.85	3.05	Initial P-ΔV curved
27	-35	-	Entire plot curved	1.7	2.45	3.2	CP poorly defined
28	-40	2.8-3.5	Poorly defined	2.50	2.6	2.75	CP fairly well defined
29	-42.5	3.3-3.85	Poorly defined	2.5	3.0	3.4?	Double curvature?
30	-67	4.4	Fairly good shape	2.35	3.45	4.4	Lower limit well defined
31	-70.5	4.5	Fairly good shape	2.35	3.3	5.15?	Upper limit well defined
32	-74	3.5-4.0	Fairly good shape	2.4	3.6	4.8	Wide selection of CP possible
33	-77.5	3.0-3.4	Fairly good shape	2.6	3.85	5.5	Both limits well defined
34	-80.5	3.0	Fairly good shape	2.65	3.15	3.5	Lower limit well defined

1 ft=0.305 m   1 kg/cm²=98.1 kPa
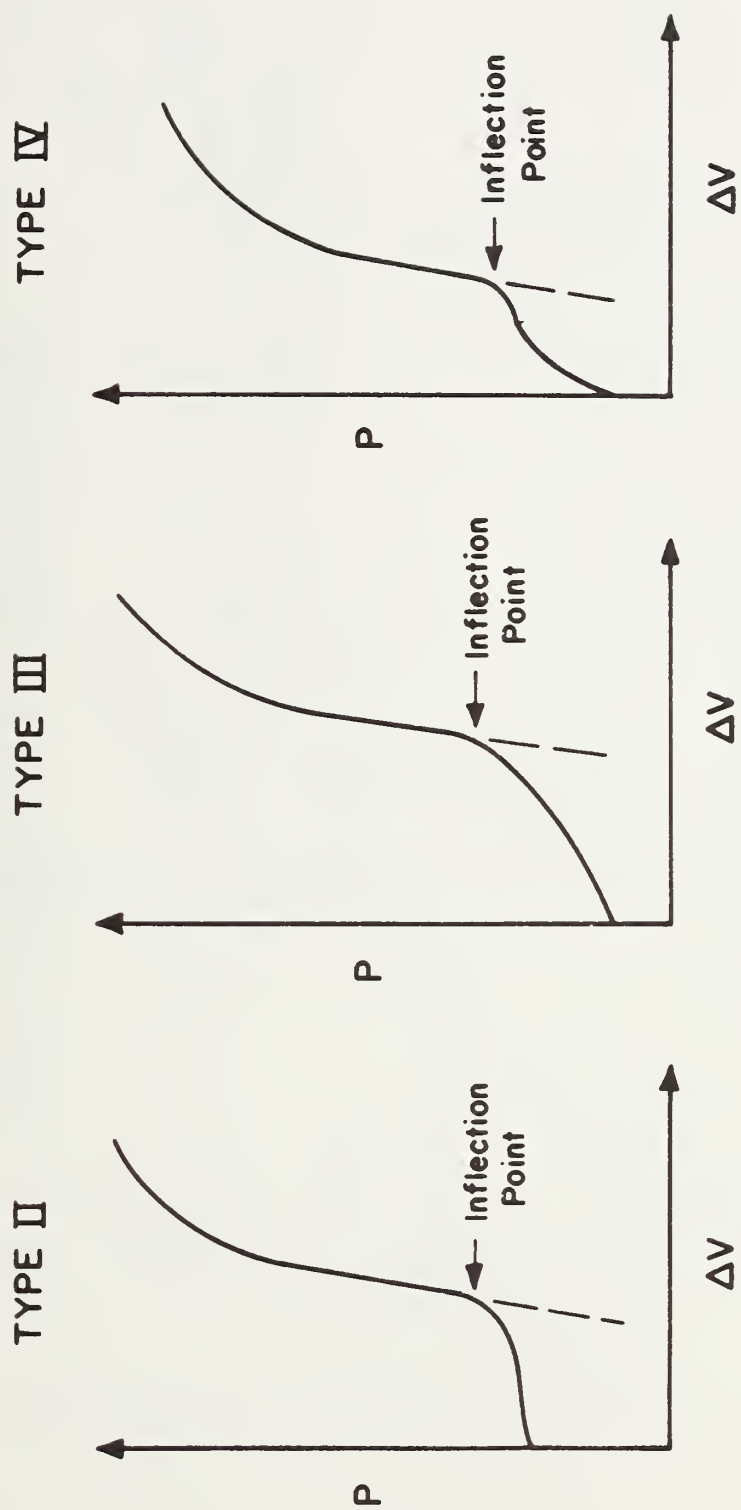
FIGURE 5-1   INFLECTION POINT METHOD FOR ESTIMATING P_o

115
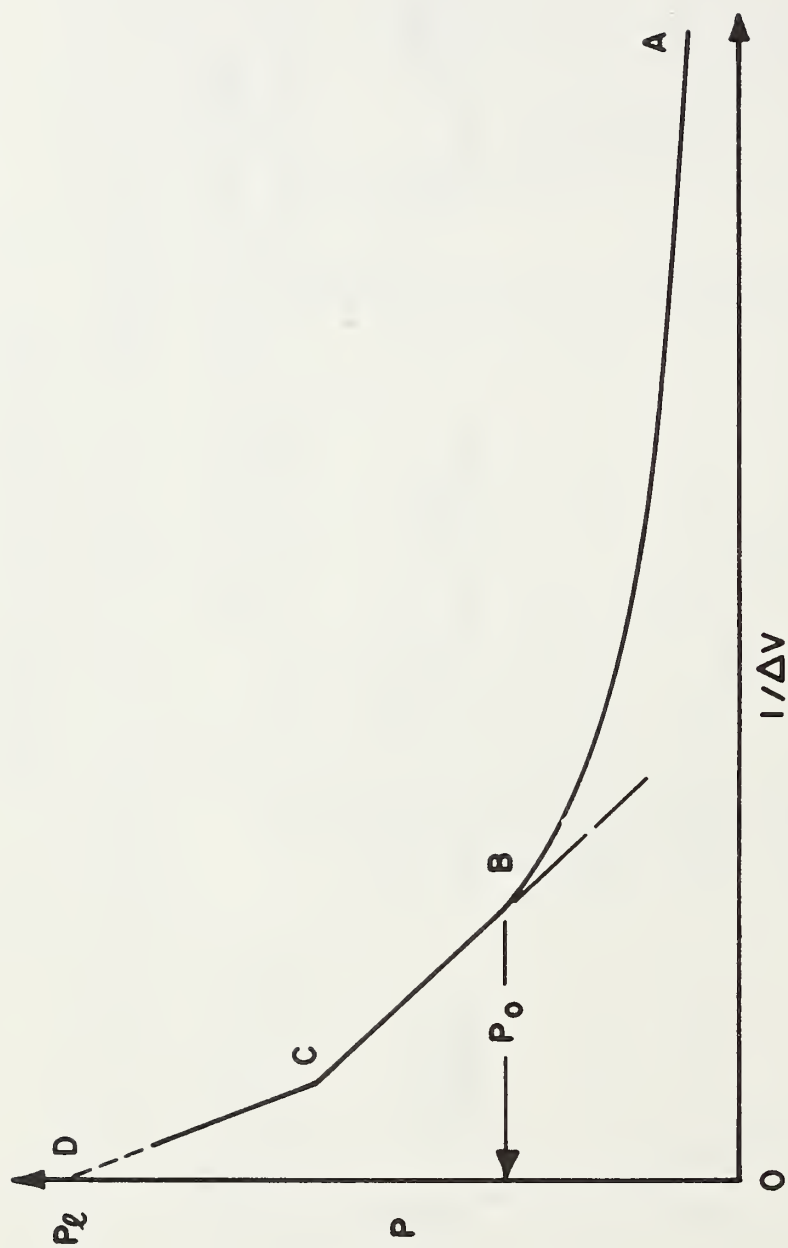
FIGURE 5-2 INVERSE VOLUME METHOD FOR ESTIMATING P_o
(After VanWambeke and d'Hemricourt, 1975)

116
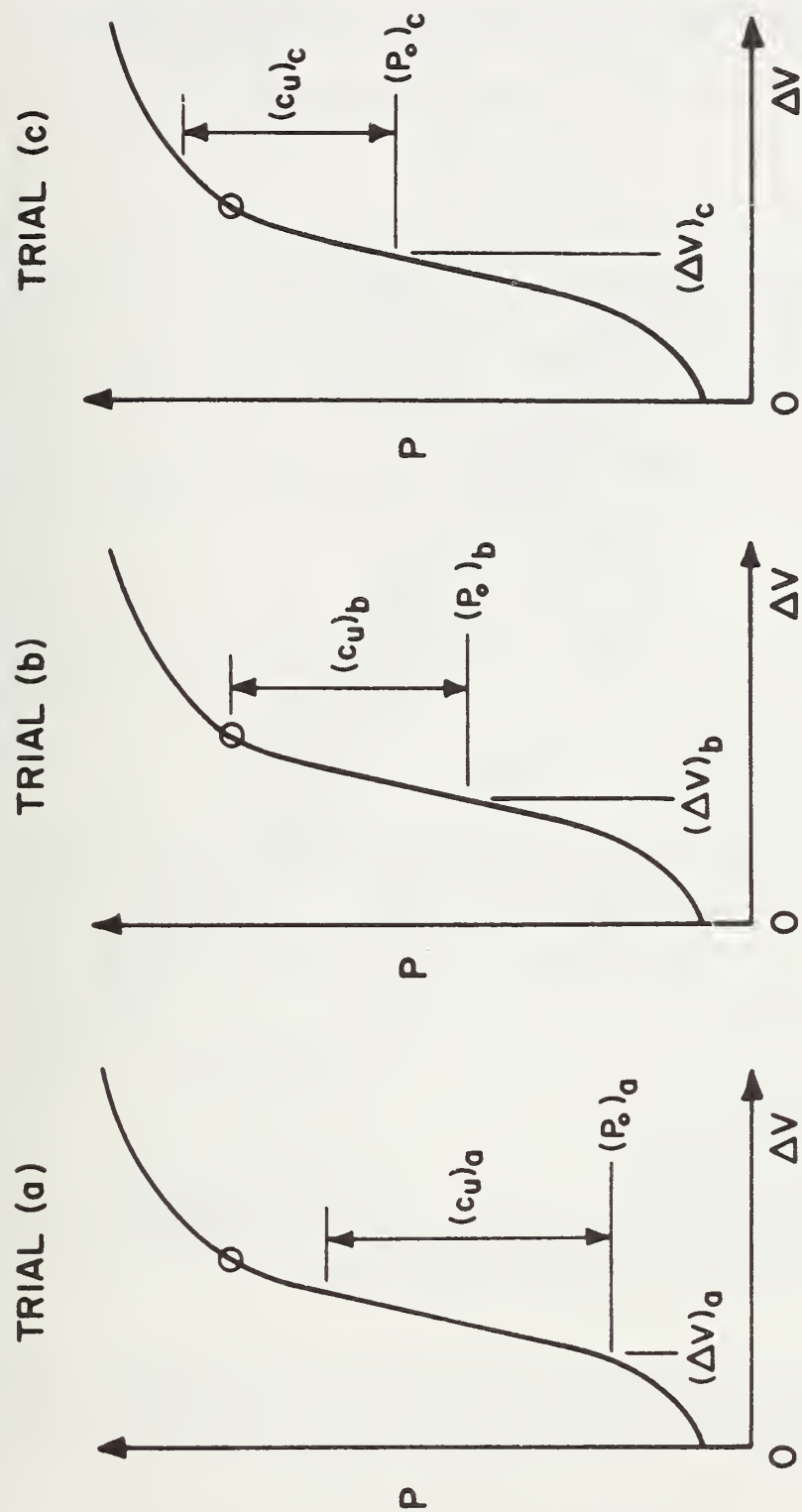
FIGURE 5-3 GRAPHICAL ITERATION METHOD FOR ESTIMATING P_O
(After Marsland and Randolph, 1977)

O Point of marked increase in curvature

117
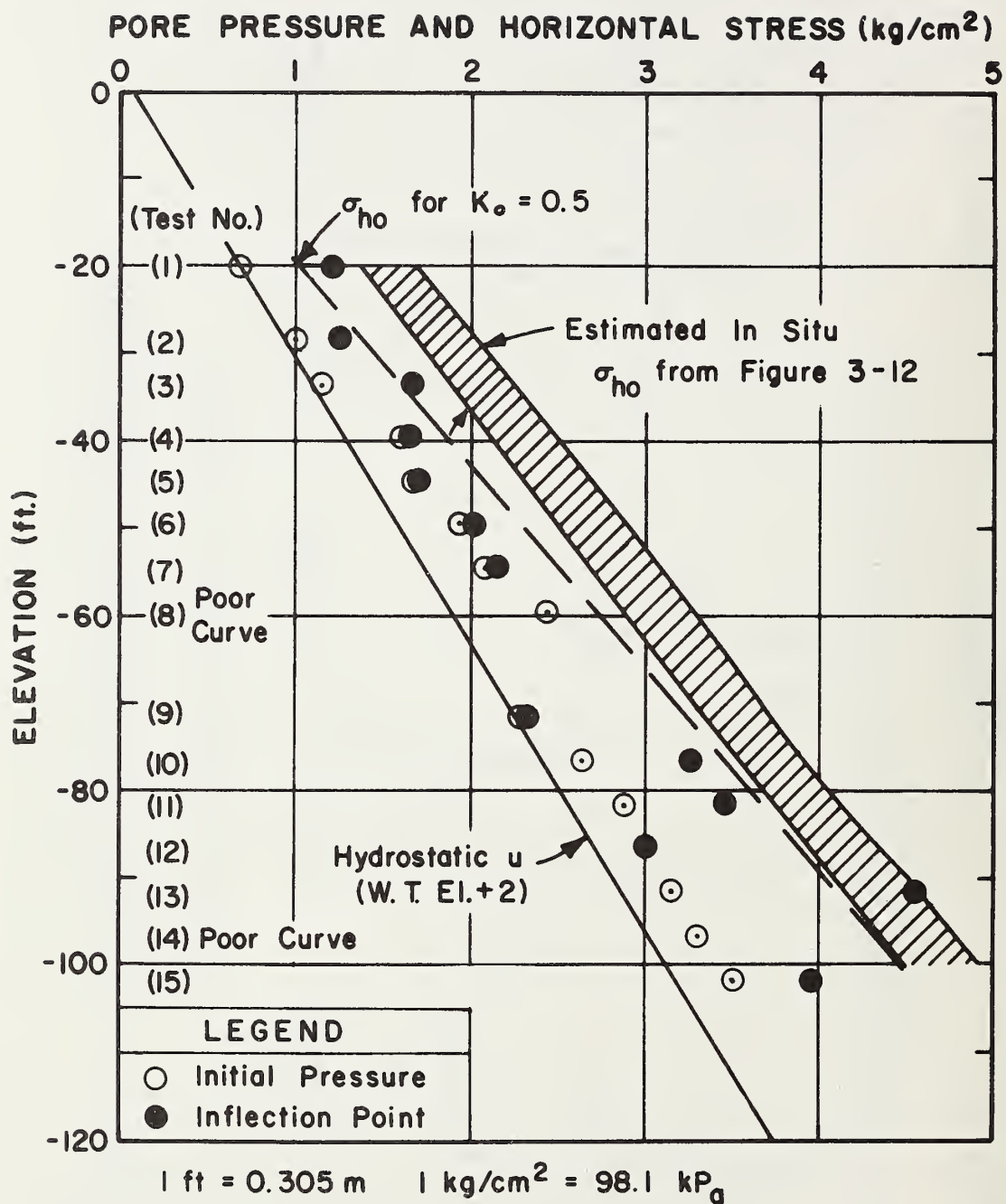
FIGURE 5-4   HORIZONTAL STRESS FROM PAFSOR TESTS AT STA. 246
BASED ON INITIAL PRESSURE AND INFLECTION POINT
METHODS

118
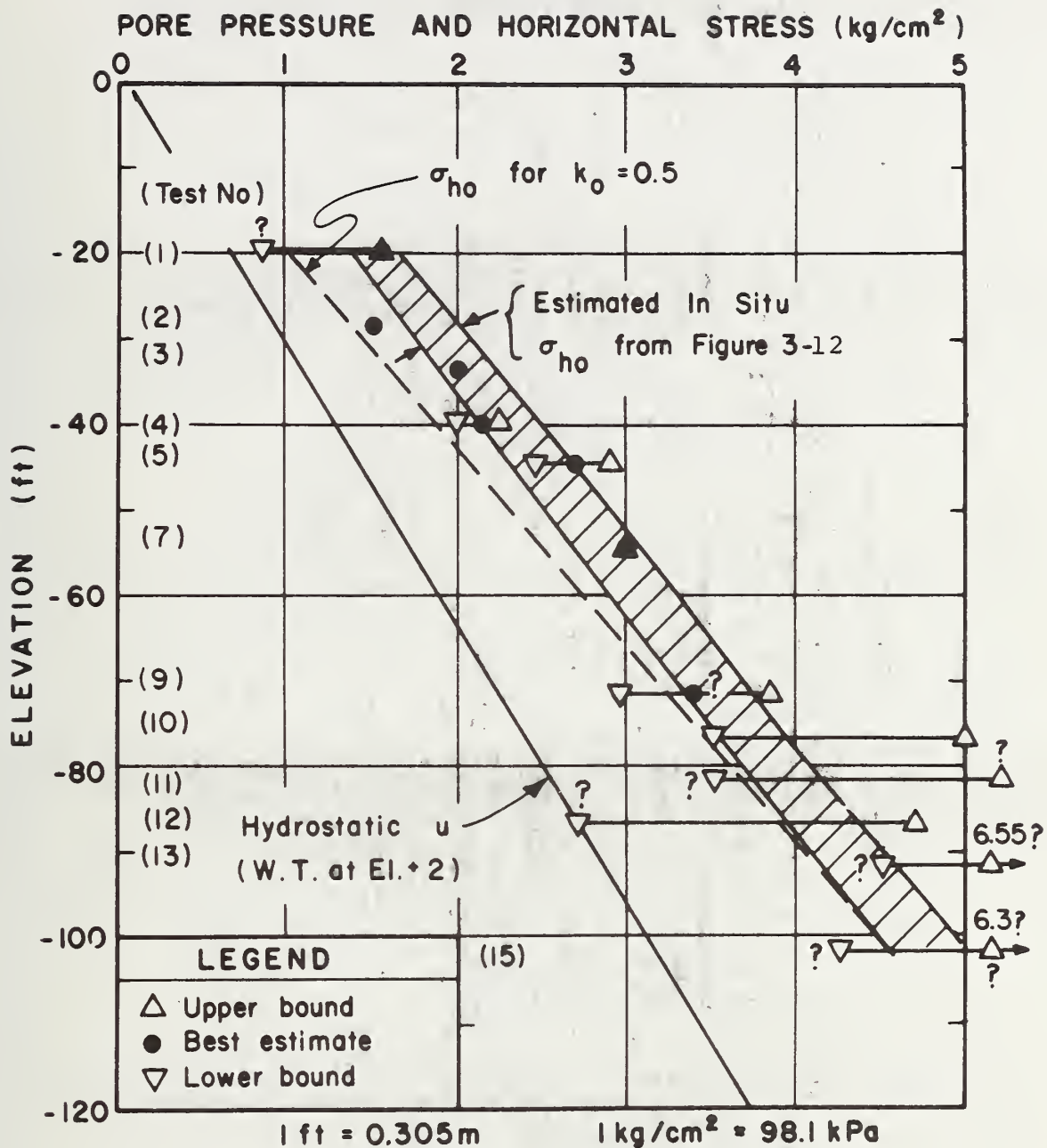
FIGURE 5-5   HORIZONTAL STRESS FROM PAFSOR TESTS AT STA.
246 BASED ON GRAPHICAL ITERATION METHOD

119
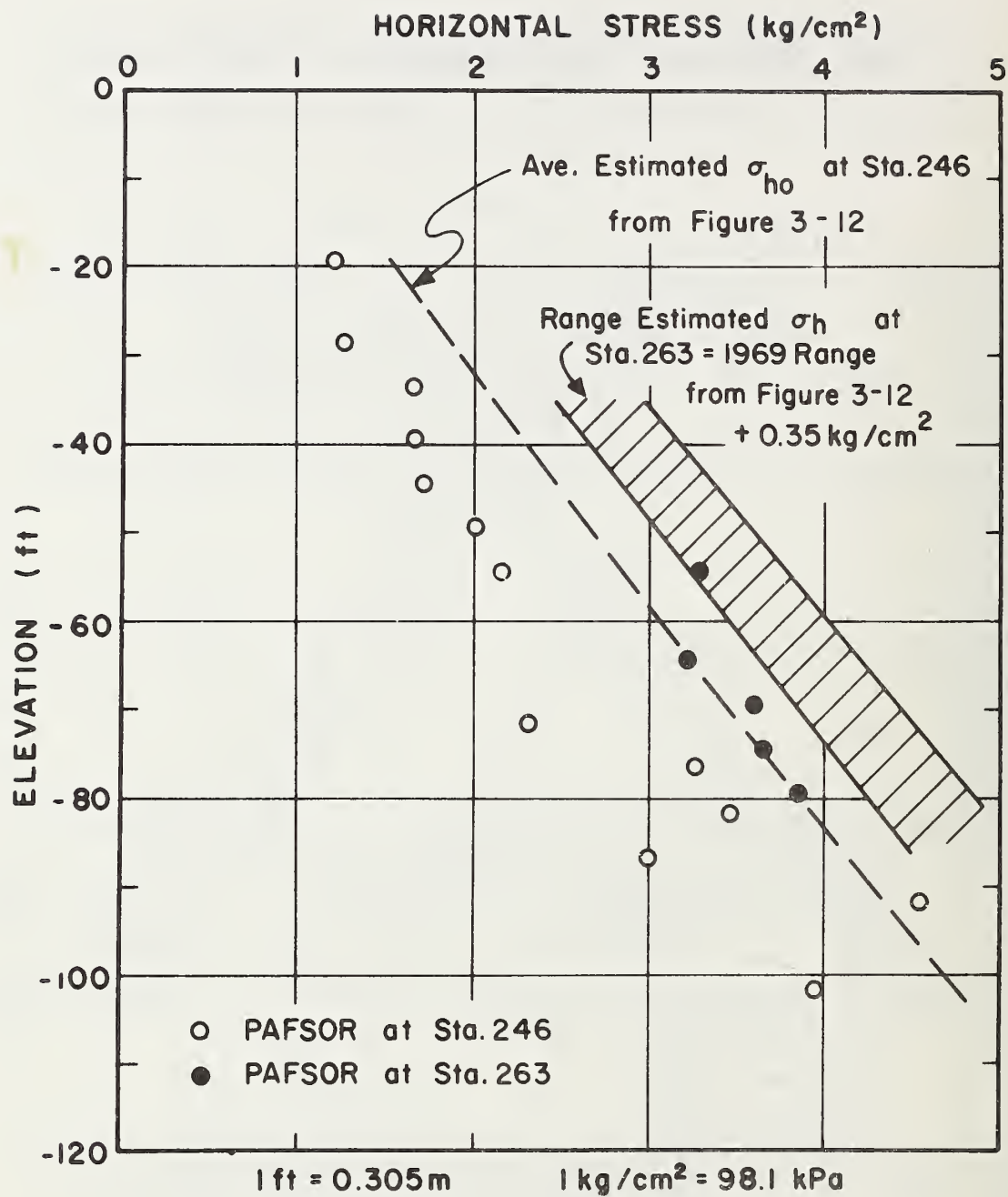
FIGURE 5-6   HORIZONTAL STRESS FROM PAFSOR TESTS AT STA. 246
AND 263 BASED ON INFLECTION POINT METHOD

120
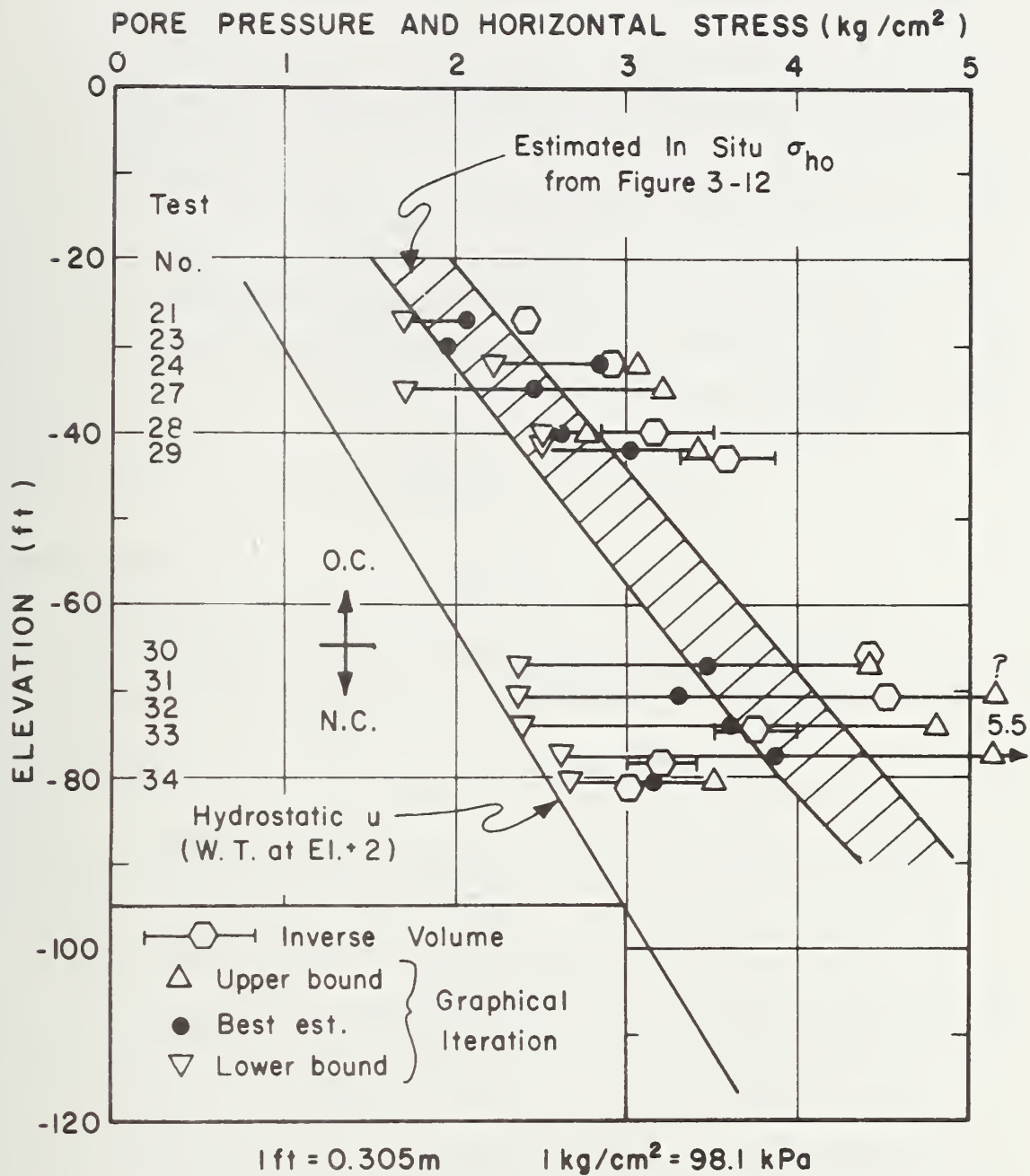
FIGURE 5-7   HORIZONTAL STRESS FROM CAMKOMETER TESTS AT
STA. 263 BASED ON INVERSE VOLUME AND GRAPHICAL
ITERATION METHODS

121

6. EVALUATION OF LIMIT PRESSURE

6.1 INTRODUCTION

Bishop et al. (1945) defined the "theoretical" limit pressure as the pressure corresponding to an infinite expansion of the cylindrical cavity around the pressure-meter. For undrained expansion in an ideal elastic-plastic cohesive material, they derived the following theoretical expression for P_1 in terms of the initial pressure (P_o), the undrained shear strength (c_u) and the undrained modulus [$G=E_u/2(1+\nu)$] of a saturated clay:

$$P_1=P_o+c_u[1+\ln \frac{E_u}{2c_u(1+\nu)}] \qquad \text{(Eq. 2-2a)}$$

or
$$P_1=P_o+c_u[1+\ln \frac{G}{c_u}] \qquad \text{(Eq. 2-2b)}$$

Equation 2-2 also provides a method for calculating c_u from pressuremeter tests via:

$$c_u=(P_1-P_o)/N_p \qquad \text{(Eq. 2-3)}$$

where N_p theoretically equals 6.0±1.5 (see Section 2.1) and P_o corresponds to the in situ total horizontal stress, σ_{ho}.

In reality, no test can achieve infinite expansion and thus P_1 must be determined by extrapolation to the pressure existing when $\Delta V/V$ approaches unity (note that $V=V_o+\Delta V$). Section 6.2 will present extrapolation methods.

As discussed by Baguelin et al. (1978), users of the Menard pressuremeter test developed a different limit pressure for evaluating pressuremeter data in engineering practice. This "conventional" P_1 equals the pressure required to double the initial volume of the measurement cell, i.e. the value of P at $\Delta V/V_o = 1$ (or $\Delta V/V=0.5$). This

122

again requires extrapolation employing methods presented in Section 6.2. Also experience with the Menard test developed an empirical approach for applying Eq. 2-3, using N_p=5.5 with P_o obtained from the inflection point method (Section 5.2.2).

Section 6.3 evaluates different methods for estimating the "theoretical" limit pressure, assesses the effect of using various starting points on the expansion curve and compares these results to the "conventional" limit pressure. Since values of P_1 per se have little practical significance, these data are mainly used in Chapter 7 for predicting c_u values via Eq. 2-3.

6.2 METHODS OF EXTRAPOLATION

Chapter 5 of Baguelin et al. (1978) summarizes various methods that have evolved for obtaining the conventional limit pressure, some of which can also be used to obtain the theoretical P_1 at infinite expansion. Figure 6-1 illustrates four methods. The first extends the usual P-ΔV expansion curve by eye and gives the conventional P_1 at $\Delta V = V_o$, i.e. the pressure required to double the initial cell volume, V_o. Though simple, it involves judgement and should only be used for limited extrapolation. A more objective approach uses a log P vs log ($\Delta V/V_o$) plot to obtain the conventional P_1, as shown in Figure 6-1(b).

Marsland and Randolph (1977) extended the analyses of Gibson and Anderson (1961) to show that a plot of P vs $\ln(\Delta V/V)$ should be linear for the later stages of an undrained pressuremeter test run in an elastic-plastic material. The same conclusion also results from Eq. 2-6 (Table 2-1) if the derived shear stress at large strains remains constant. Thus extrapolating the presumed linear

123

portion of a P vs $\ln(\Delta V/V)$ curve to $\Delta V/V=1$, i.e. $\ln \Delta V/V=0$, gives the theoretical P_1 at infinite expansion. $\text{Log}(\Delta V/V)$ is more convenient to use than $\ln(\Delta V/V)$ and also yields the theoretical P_1 at $\log(\Delta V/V)=0$. The data handling computer program developed by MIT actually gives semi-log plots (natural P vs $\Delta V/V$ to log scale) that were used to obtain P_1 at $\Delta V/V=1$ as illustrated in Figure 6-1(c). Appendices B and C present the semi-log plots of measured data used to apply this method by two or more persons. This procedure generally required little judgement, except in a few cases where the expansion rate was changed very late in the test, and resulting values of P_1 seldom differed by more than a few percent.

The last method, illustrated in Figure 6-1(d), uses the inverse volume curve proposed by VanWambeke and d'Hemricourt (1975) to evaluate the theoretical limit pressure. Section CD should be linear according to these authors, so that this linear portion can be extrapolated to find P_1 at $1/\Delta V=0$. MIT applied the method to most of the curves presented in Appendices B and C, but considered it rather unsatisfactory since the values obtained were often controlled by the last two or three data points.

Politecnico di Torino (Jamiolkowski, 1979) uses a variation of the above method to obtain the theoretical P_1 by plotting $1/\varepsilon_0$ rather than $1/\Delta V$ (see Eq. 2-5(a), Table 2-1 for definition of ε_0). This approach, though perhaps better than the original inverse volume method, was not used however since MIT only learned about it as this Chapter was being written.

Section 6.3 presents limit pressure values obtained by the following methods:

124

(1) Theoretical P_1 from P vs $\log(\Delta V/V)$ plot [$\log(\Delta V/V)=0$ method].

(2) Theoretical P_1 from P vs $1/\Delta V$ plot [$1/\Delta V=0$ method].

(3) Conventional P_1 from P vs $\log(\Delta V/V)$ plot [$\Delta V/V_o=1$ method].

Also, since the conditions after self-boring can influence the location and shape of the expansion curve, values of the theoretical P_1 obtained via the $\log(\Delta V/V)=0$ method were determined for three initial conditions.

6.3 RESULTS

6.3.1 <u>AT Sta. 246</u>

Table 6-1 summarizes P_1 values obtained by the above three techniques for the 15 PAFSOR tests performed at this location. We shall first discuss the effect of varying the initial conditions on P_1 determined by the $\log(\Delta V/V)=0$ method. The table presents these P_1 data for three initial conditions: (1) measured P_o at start of test; (2) inflection point P_o; and (3) upper bound estimate of the in situ σ_{ho}. It also lists values of the measured P_o and the upper σ_{ho} (also see Figure 5-4) to demonstrate the large difference in these pressures.

Figure 6-2 plots the range in theoretical P_1 values resulting from varying the initial conditions. The range is generally quite small (always less than 10% and usually less than 5%) in spite of the fact that the initial pressure varied by 50 to 100%. Increasing P_o should theoretically reduce P_1 since $\log(\Delta V/V)$ becomes smaller at the same P and the results in Table 6-1 follow this trend. Figure 6-2 also notes the type and quality of the expansion curve (but not including Type V due to changes in expansion rate) which indicates little correlation between P_1 and general nature

125

of the curve. Hence, varying amounts of disturbance during insertion and substantial changes in the starting points used for the P-log($\Delta V/V$) plots have a relatively small effect on measured values of the theoretical P_1. This observation agrees with general experience reported in the literature.

Since varying P_0 has relatively little effect on P_1, the evaluation of different methods is based on using the inflection point P_0. Figure 6-3 compares theoretical P_1 data from the log($\Delta V/V$)=0 and $1/\Delta V$=0 methods*. The inverse volume approach yields values 15±10% smaller, the difference decreasing with depth of test, as does the OCR of the clay. These same data are plotted versus elevation in Figure 6-4, but also including values of the conventional limit pressure, i.e. P_1 at $\Delta V/V_0$=1 extrapolated from P vs log($\Delta V/V$) curves. The conventional P_1 should by definition be less than the theoretical P_1 since they correspond to P at $\Delta V/V$=0.5 and 1.0 respectively. When both values are determined from P-log($\Delta V/V$) curves, the ratio P_1(conventional)/P_1(theoretical) averages about 0.9 in the upper medium clay and 0.95 in the lower "soft" clay. But values of the theoretical P_1 obtained via the $1/\Delta V$=0 method all plot below the conventional limit pressure. This strongly indicates that the inverse volume approach predicts a P_1 for infinite expansion that is too low and the method probably has a rather dubious theoretical basis. Also the method selected to estimate the theoretical P_1 can be more important than the effects of disturbance.

---

* Section 6.3.2 discusses the data from Sta. 263.

6.3.2 At Sta. 263

Tables 6-2 and 6-3 summarize P_1 data at Sta. 263 from the five PAFSOR tests carried out after the embankment failure (which altered the soil conditions) and the 11 CAMKOMETER tests performed in "virgin" ground at the same location. All tests had Type I curves and thus no analysis was made of the effect of varying the initial conditions.

Figures 6-3 and 6-5 plot the results which show the same trends regarding methods of extrapolation as observed at Sta. 246, namely:

(1) The inverse volume method predicts lower values of the theoretical P_1 than the $\log(\Delta V/V)=0$ method. The greatest difference again exists in the upper more overconsolidated clay and overall is somewhat larger for the Sta. 263 CAMKOMETER tests than for the Sta. 246 PAFSOR tests (Figure 6-3).

(2) The ratio P_1 (conventional)/P_1(theoretical) determined from P-$\log(\Delta V/V)$ curves averages about 0.9 for the CAMKOMETER tests (little variation with depth) and about 0.95 for the PAFSOR tests (all run in the deep "soft" clay).

The CAMKOMETER tests gave substantially higher limit pressures than the PAFSOR tests when compared on the same basis. Disturbance to the soil due to the massive embankment failure provides a reasonable explanation for the lower PAFSOR P_1 values. Figure 6-6, which compares theoretical P_1 data at both stations, supports this hypothesis. The Sta. 246 PAFSOR and Sta. 263 CAMKOMETER P_1 values agree quite well, especially in the upper stiffer clay, and they greatly exceed the Sta. 263 PAFSOR P_1 values obtained after the embankment failure.

127

6.4 DISCUSSION

The following conclusions can be drawn from the limit pressure data at Sta. 246 and 263:

(1) The CAMKOMETER and PAFSOR tests probably give essentially the same results.

(2) Varying amounts of disturbance during self-boring and adjustments to the starting point of the test have relatively little effect on P_1 values extrapolated from P vs $\log(\Delta V/V)$ plots (e.g. Figure 6-2).

(3) The inverse volume method predicts values of the theoretical P_1 at infinite expansion less than those obtained by the P-$\log(\Delta V/V)$ method (Figure 6-3). The ratio appears to decrease with increasing OCR from 0.85 ± 0.05 down to about 0.7 ± 0.1.

(4) Theoretical P_1 values for infinite expansion from the inverse volume method are also less that the "conventional" P_1 corresponding to a doubling of cell volume obtained from P vs $\log(\Delta V/V)$ plots. The writers therefore conclude that the $1/\Delta V=0$ method underpredicts the correct theoretical limit pressure.

(5) Disturbance due to the embankment failure provides a logical explanation for the low P_1 values measured by the PAFSOR tests at Sta. 263.

TABLE 6-1   EVALUATION OF LIMIT PRESSURE FROM
PAFSOR TESTS AT STA 246

Test No.	El. (ft)	ΔV_o (cc)	Type of Curve	Quality of curve	Initial Stress (kg/cm²)		Limit Pressure, P_l (kg/cm²)				
					Measured P_o	Upper σ_{ho}	$\Delta V/V_o=1$ Inflect. P_o	Log$(\Delta V/V)=0$ Meas. P_o	Infl. P_o	Upper σ_{ho}	$1/\Delta V=0$ Inflect. P_o
1	-19.7	0	III-V	Fair	0.67	1.65	5.65	6.65	6.55	6.45	5.1
2	-28.7	0	II-V	Good	1.00	2.00	5.6	6.8	6.35	6.25	4.7
3	-33.7	0	IV	Fair	1.15	2.25	6.0	6.9	6.85	6.55	5.7
4	-39.7	220	I	Excellent	1.60	2.50	6.7	7.3	7.3	7.25	6.2
5	-44.7	0	II	Good	1.67	2.72	7.35	8.8	8.3	8.1	7.0
6	-49.7	0	IV	Fair	1.93	2.92	8.4	9.15	9.15	9.1	8.3
7	-54.7	80	I-V	Good	2.07	3.15	8.9	9.65	9.7	9.5	8.9
8	-59.7	0	?-V	Poor	2.43	3.30	-	-	10.2	-	9.1
9	-71.7	12	I-V	Good	2.27	3.75	9.0	9.7	9.7	9.6	8.7
10	-76.7	110	IV-V	Fair-Good	2.62	3.90	9.35	9.9	9.9	9.85	8.9
11	-81.7	150	IV-V	Fair	2.87	4.15	9.9	10.5	10.3	10.0	9.3
12	-86.7	150	I-V	Good	3.02	4.40	10.3	10.7	10.7	10.7	10.3
13	-91.7	50	IV-V	Fair-Good	3.15	4.60	11.0	11.85	11.4	11.25	10.6
14	-96.7	0	IV-V	Poor	3.30	4.80	-	-	11.9	-	11.4
15	-101.7	180	IV-V	Fair	3.50	5.00	11.4	12.0	12.0	11.8	10.8

1 ft = 0.305 m   1 kg/cm² = 98.1 kPa

TABLE 6-2. EVALUATION OF LIMIT PRESSURE FROM
PAFSOR TESTS AT STA 263

Test No.	El. (ft)	ΔV_o (cc)	Type of Curve	Quality of curve	Initial stress (kg/cm^2)	Limit Pressure, P_1^* (kg/cm^2)	
						$\Delta V/V_o=1$	$\log(\frac{\Delta V}{V})=0$
16	-54.3	0	I-V	Good	3.3	6.1	6.6
17	-64.3	0	I-V	Good	3.2	6.2	6.6
18	-69.3	0	I-V	Good	3.6	6.6	7.0
19	-74.3	50	I-V	Good	3.65	7.4	7.8
20	-79.3	0	I-V	Good	3.85	7.5	7.9

* Starting from inflection P_o

1 ft=0.305 m   1 kg/cm^2=98.1 kPa

TABLE 6-3.   EVALUATION OF LIMIT PRESSURE FROM
CAMKOMETER TESTS AT STA 263

Test No.	El. (ft)	Type of curve	Quality of curve	"Lift-Off" P_O (kg/cm^2)	Limit Pressure, P_1 (kg/cm^2)		
					$\Delta V/V_O=1$	$\log(\frac{\Delta V}{V})=0$	$1/\Delta V=0$
21	-27	I	Excellent	1.10	4.8*	5.3*	3.4*
23	-30	I	Good	1.50	≈5.0	≈5.5	4.35
24	-32	I	Excellent	1.70	5.65	6.1	5.0
27	-35	I	Excellent	1.20	6.85	7.55	6.05
28	-40	I	Excellent	1.7	6.95	7.65	5.6
29	-42.5	I	Good	2.0	7.3	8.1	6.4
30	-67	I	Excellent	1.7	8.4	9.2	7.5
31	-70.5	I	Good	1.8	8.15	8.9	7.5
32	-74	I	Good	1.6	8.1	8.75	7.1
33	-77.5	I	Good	0.8	8.3	8.95	7.6
34	-80.5	I	Excellent	0.8	≈7.5	≈8.35	7.1

*Required considerable extrapolation since initial loading
 stopped at $\Delta V/V=0.08$

1 ft=0.305 m   1 kg/cm^2=98.1 kPa
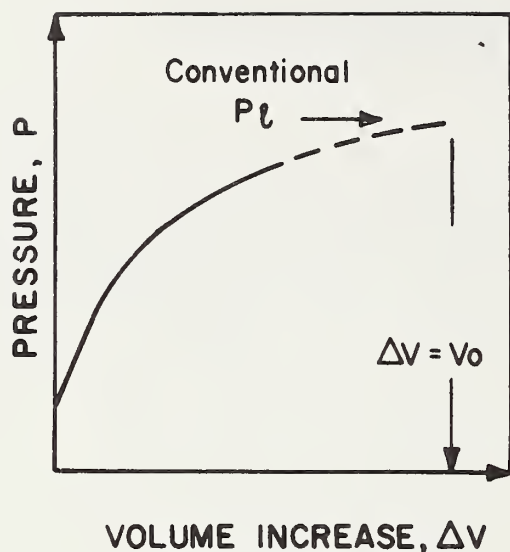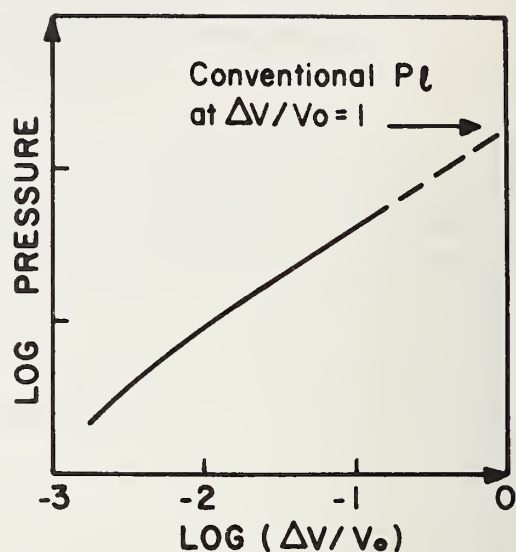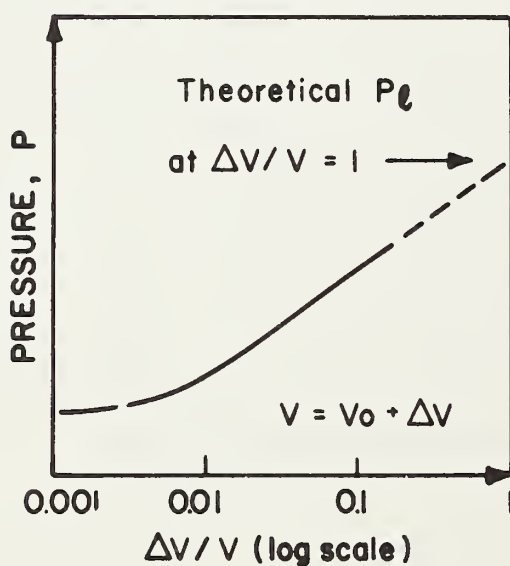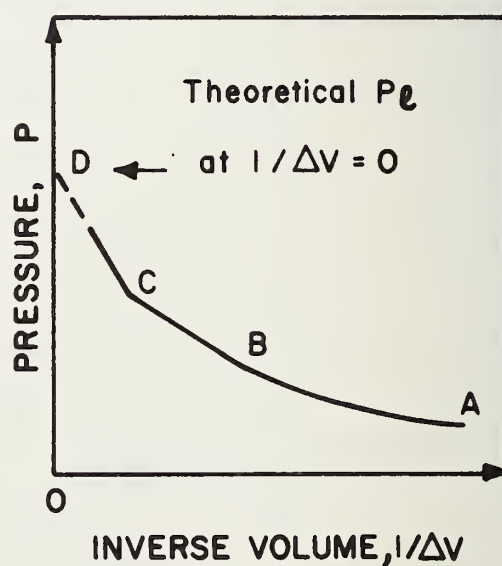
FIGURE 6-1 METHODS FOR ESTIMATING LIMIT PRESSURE
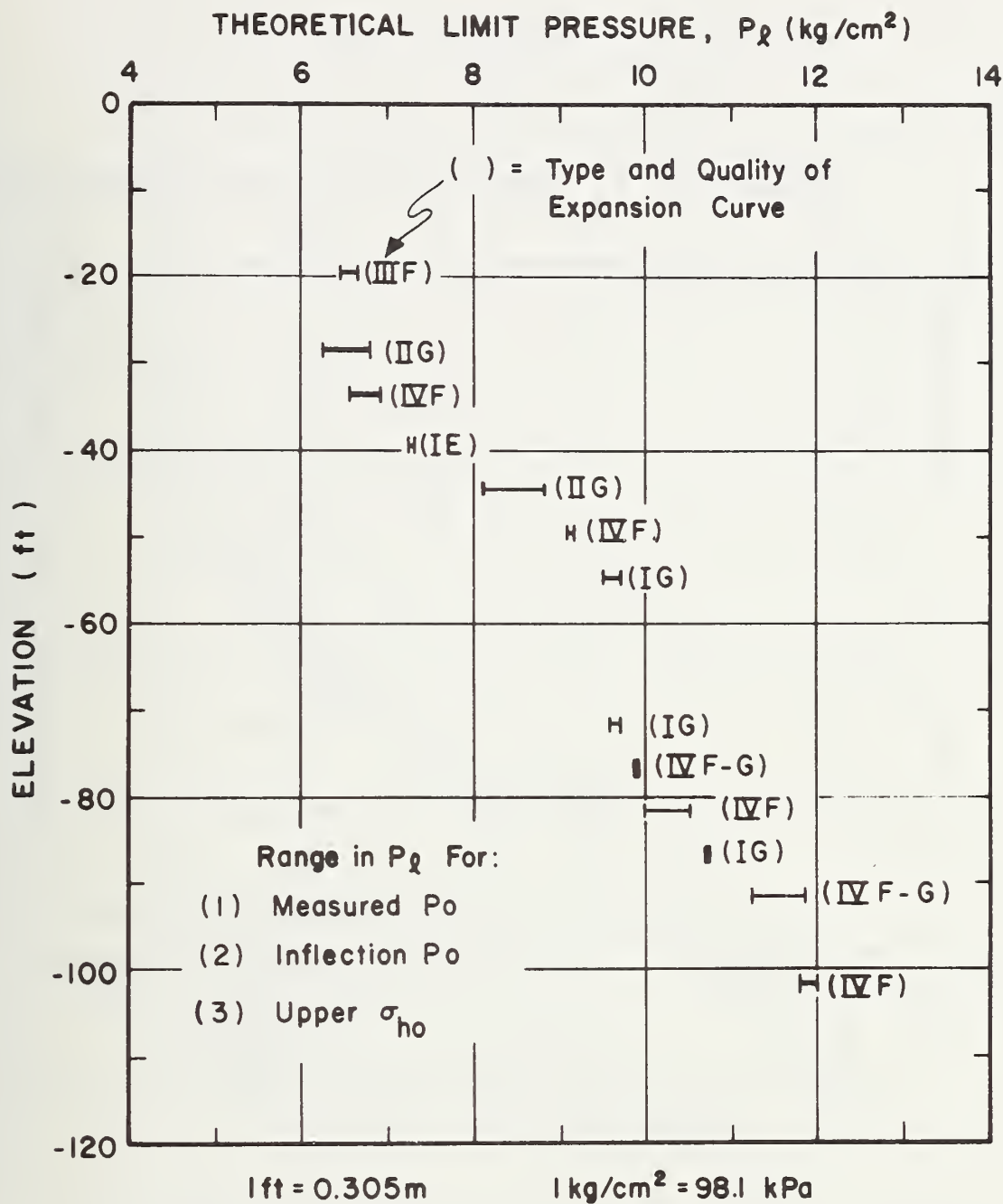
FIGURE 6-2 EFFECT OF VARYING INITIAL CONDITION ON THEORETI-
CAL LIMIT PRESSURE USING LOG ($\Delta V/V$)=0 METHOD FOR
PAFSOR TESTS AT STA. 246

133
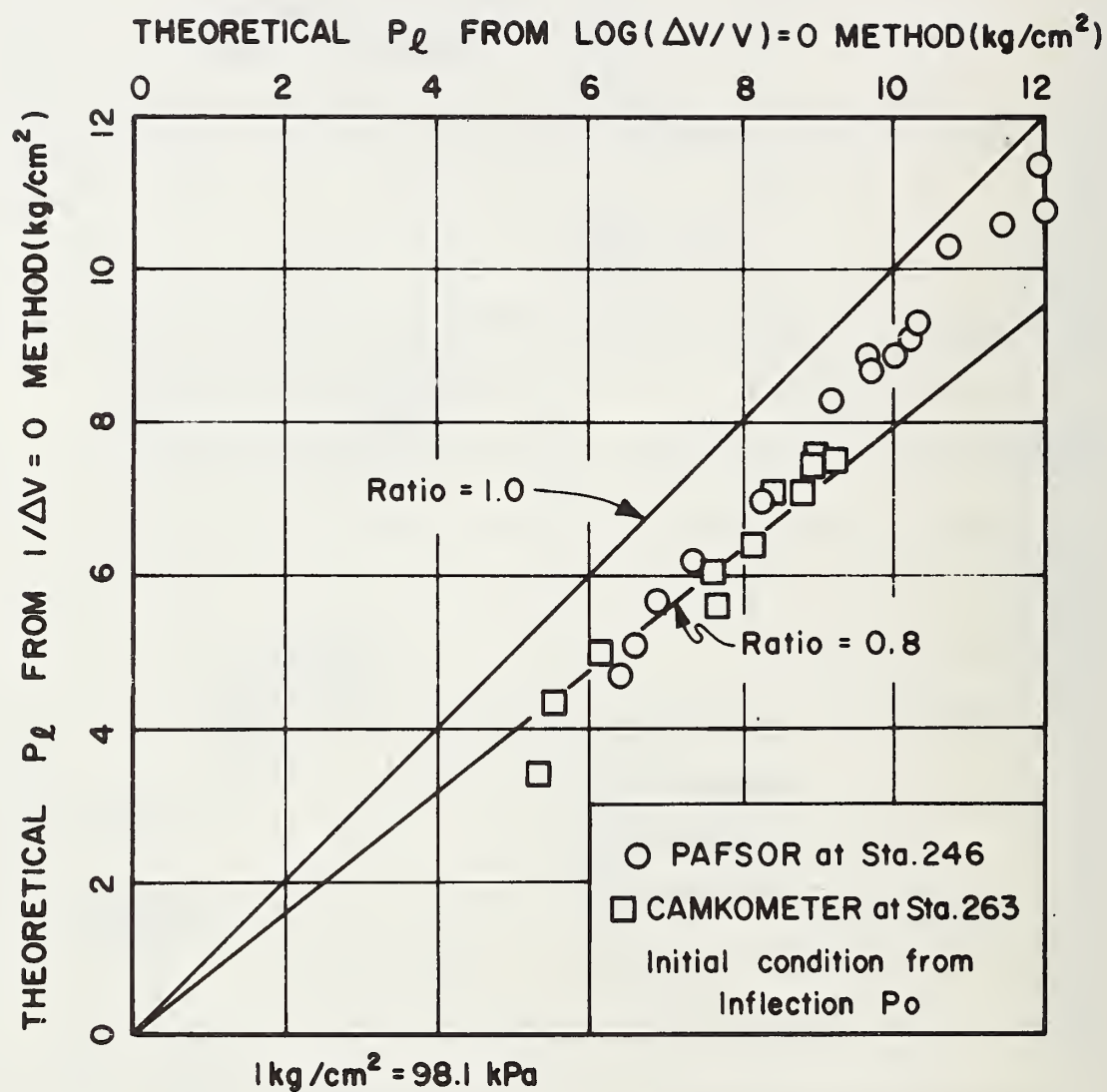
FIGURE 6-3   COMPARISON OF THEORETICAL LIMIT PRESSURE BY
LOG(ΔV/V)=0 and 1/ΔV=0 METHODS AT STA. 246
AND 263

134
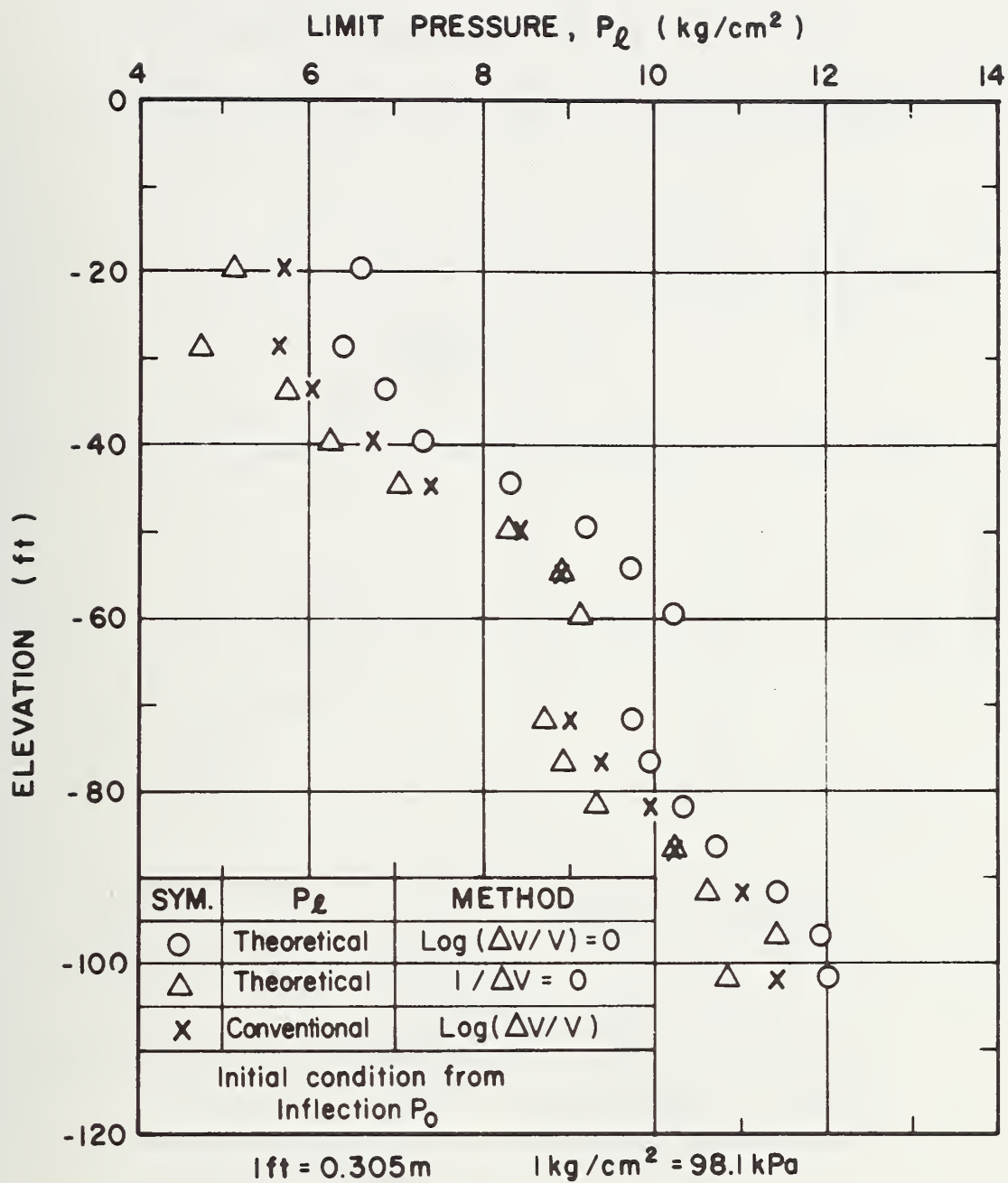
FIGURE 6-4   THEORETICAL AND CONVENTIONAL LIMIT PRESSURE
FROM PAFSOR TESTS AT STA. 246

135
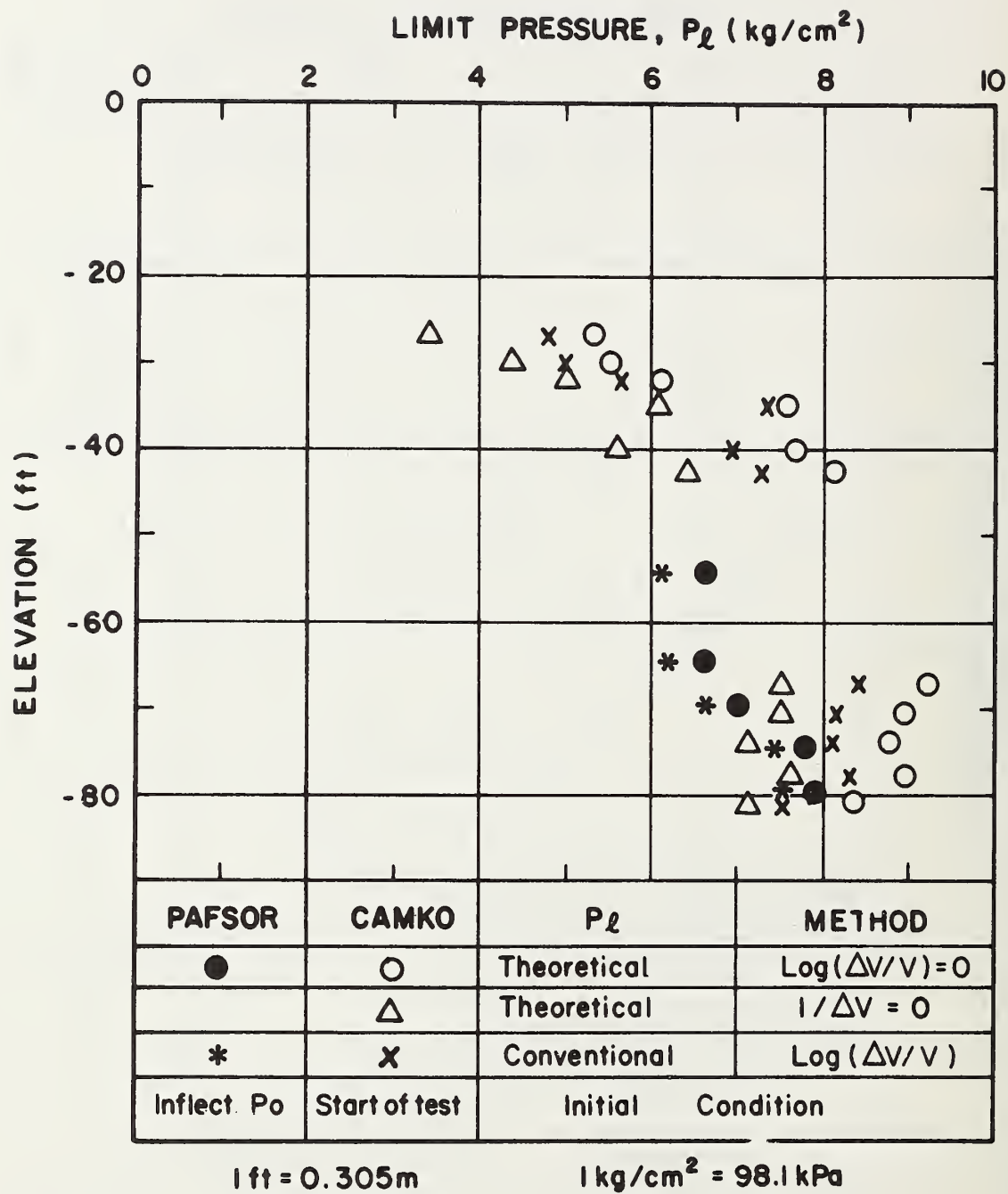
FIGURE 6-5 THEORETICAL AND CONVENTIONAL LIMIT PRESSURE
FROM PAFSOR AND CAMKOMETER TESTS AT STA. 263
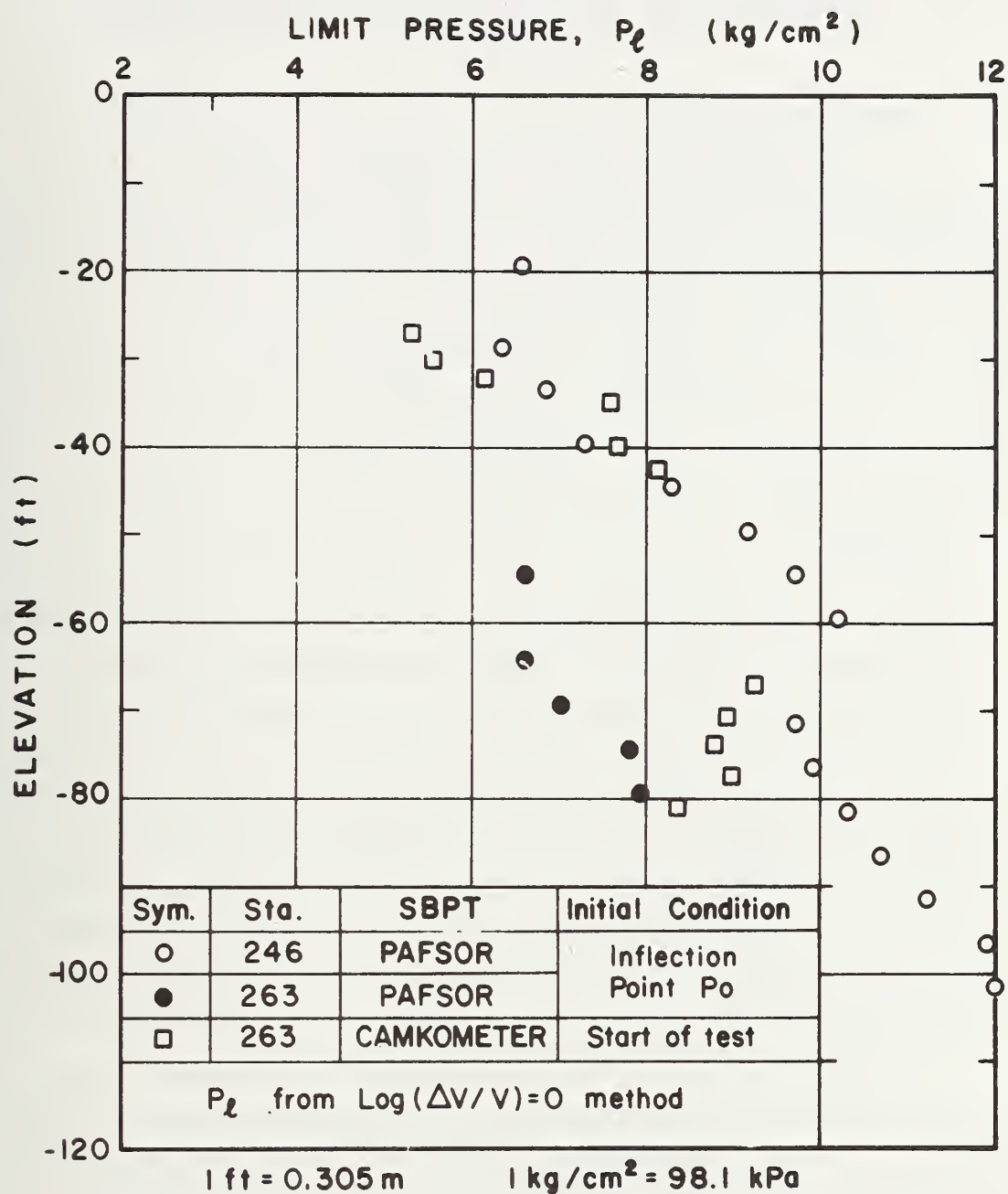
FIGURE 6-6   THEORETICAL LIMIT PRESSURE FROM PAFSOR AND
CAMKOMETER TESTS AT STA. 246 AND 263

137

7. EVALUATION OF UNDRAINED STRESS-STRAIN-STRENGTH PARAMETERS

7.1 INTRODUCTION

As discussed in Chapters 1 and 2, two major developments in 1972-73 caused much renewed interest in the pressuremeter device for in situ measurements of undrained stress-strain-strength properties in saturated clays. One was the self-boring concept which ideally enables inserting the probe without disturbance to the surrounding soil. The other was a theoretical solution that allows the complete undrained stress-strain curve to be _derived_ from pressuremeter test data providing the surrounding soil has a unique, but not pre-defined, stress-strain relationship. But for reasons still not fully understood, values of the peak c_u derived from SBPT data usually greatly exceed values predicted by other methods (e.g. Table 2-2). This observation caused considerable concern amongst developers and users of the SBPT, along with a reevaluation of procedures that should or might be employed to obtain more reliable strength data. In fact, Baguelin et al. (1978) have even recommended that SBPT data be used with semi-empirical design rules similar to those developed for the Menard pressuremeter test (p. 572).

Nevertheless, for purposes of this research, the writers restricted the methods of interpretation to those having some reasonable theoretical basis and Section 7.2 describes the methods used. Section 7.3 presents results interpreted via an elastic-plastic model of soil behavior, as is frequently done in connection with the Menard pressuremeter test. These data are compared to "reference" values developed in Chapter 3. Results based on "derived"

parameters are similarly presented and compared in Section
7.4, followed by general discussion in Section 7.5.

7.2 METHODS OF ANALYSIS

7.2.1 Elastic-Plastic Methods of Analysis

Values of undrained shear modulus (G) and strength (c_u)
were calculated using the following equations:

$$G = V_O (\Delta P / \Delta V) \qquad \text{(Eq. 7-1)}$$

$$c_u = (P_1 - P_O) / N_p \qquad \text{(Eq. 7-2a)}$$

where
$$N_p = [1 + \ln(\frac{G}{c_u})] \qquad \text{(Eq. 7-2b)}$$

Equation 7-1 is identical to Eq. 5-1 presented in conjunc-
tion with the analyses developed by Gibson and Anderson
(1961) and it applies, in theory, to the expansion curve
at pressures less than the point of marked increase in
curvature (Figure 5-3). It assumes elastic soil behavior
if unloading occurs during self-boring. Initial tangent
values of G were obtained from the measured P-ΔV curves to
use in Eq. 7-2(b).*

Equation 7-2 is identical to Eqs. 2-2 and 2-3 obtained
by Bishop et al. (1945) and later by Gibson and Anderson
(1961), but G now replaces $E_u/2(1+\nu) = E_u/3$ for undrained
shear. Since c_u appears on both sides of the equation, a
simple program was used with a hand calculator to obtain
convergence. Appropriate values of the limit pressure (P_1)
and the initital pressure (P_O) pose a more serious problem,
however. The analyses therefore used a range of values,
as discussed in Section 7.3.

---

* Politecnico di Torino suggested this approach (Jamiolkowski,
  1979).

139

7.2.2 <u>Derived Methods of Analysis</u>

Section 2.3 and Table 2.1 present the basic equations developed independently by Baguelin et al. (1972), Ladanyi (1972) and Palmer (1972) to obtain derived stress-strain-strength data from an undrained SBPT run in a saturated cohesive soil and Section 2.4 discussed the inherent assumptions. MIT used three methods based on these equations to compute peak strengths from the PAFSOR and CAMKOMETER data. Since the results are extremely sensitive to the origin of the expansion curve, the analyses include a range of starting conditions. Estimates of "ultimate" strength, i.e. the derived shear stress at large strains, and shear modulus at 50 percent of the peak strength also used one or two of these methods.

The basic difference in the three methods lies in the fact that they employ numerical, graphical and analytical techniques respectively, as described below.

<u>Numerical Subtangent Method</u>

This technique used the following equation to obtain complete stress-strain curves:

$$\tau = \frac{1}{2}(\sigma_r - \sigma_\theta) = \frac{1}{2}\varepsilon_O(1+\varepsilon_O)(2+\varepsilon_O)dP/d\varepsilon_O \qquad \text{(Eq. 7-3)}$$

It is identical to Eq. 2-6(a), which at small strains simplifies to;

$$\tau = \varepsilon_O dP/d\varepsilon_O \qquad \text{(Eq. 2-4)}$$

and thus is the basis for the subtangent graphical method described in Section 2.3 and Figure 2-4. The actual

procedure followed by MIT involved the following steps
(see Appendix D for details)*

(1) Digitized P-ΔV data fed into computer program.
(2) Actual data smoothed out to produce a less erratic
    P-ΔV curve using a "moving window" technique (moving
    average of four points).
(3) ΔV values converted to strain via Eq. 2-5(a).
(4) τ vs. ε_O values computed via Eq. 7-3 using data points
    from the smoothed expansion curve.
(5) Results presented as a plot of individual points to
    form a complete stress-strain "curve" which is used to
    select values of peak and ultimate strength and to
    compute a secant modulus at the 50% stress level.

Graphical P-Log(ΔV/V) Method

The data handling routine developed by MIT produced
semi-log plots of P versus ΔV/V [see Figure 6-1(c)] for
all tests. Since;

$$\tau = dP/d\ln(\Delta V/V) \qquad \text{(Eq. 2-6b)}$$

the shear stress at any point during a test can be computed
from the slope of a P-log(ΔV/V) plot by the equation:

$$\tau = 0.434 \, dP/d\log(\Delta V/V) \qquad \text{(Eq. 7-4)}$$

This graphical procedure was used to obtain the peak
strength, derived from the maximum slope, and the ultimate
strength determined from the average slope of the approxi-
mately linear final portion of the curve. The semi-log

---

* In retrospect, it would have been more straightforward
  to use Eq. 2-6(d) directly, though the results would
  still be the same.

141

plots use data filtered by the "moving window" technique
and some additional "smoothing" may also come from judge-
ment in selecting appropriate slopes.

Analytical Modified Prevost-Hoeg Method

Stress-strain data directly derived from experimental
expansion curves often yield erratic results. Such scatter
can be eliminated by differentiating a mathematical rela-
tionship that replaces the actual expansion curve. The
reliability of such analytical techniques depends, of
course, on how well the relationship matches the actual
curve.

Section 2.3 presented the empirical curve fitting
equation employed by Baguelin et al. (1972) and mentioned
that Jamiolkowski and Lancellotta (1977) used equations
based on stress-strain relationships postulated by Prevost
and Hoeg (1975). MIT adopted the "strain-softening" version
of the latter approach, but modified it by adding a third
constant to enable modelling stress-strain curves with peak
strains less than one percent. The method uses the
standard least squares fitting technique and Eq. 7-5 to
represent the measured expansion curves.

$$P = P_O + \frac{AB}{2\sqrt{3C}} \ln(1 + C\varepsilon_O{}^2) + \frac{A}{\sqrt{3C}} \arctan(\sqrt{C}\varepsilon_O) \qquad \text{(Eq. 7-5)}$$

The stress-strain curve is then computed from:

$$\tau = A\frac{(B\varepsilon_O{}^2 + \varepsilon_O)}{(1 + C\varepsilon_O{}^2)} \qquad \text{(Eq. 7-6)}$$

and the strain at failure given by:

$$\varepsilon_{Of} = (B + \sqrt{B^2 + C})/C \qquad \text{(Eq. 7-7)}$$

142

For C=1, the above equations reduce to those presented by Prevost and Hoeg (1975).

The Modified Prevost-Hoeg method was used to derive peak strengths and was also part of the graphical iteration technique presented in Chapter 5 to estimate in situ horizontal stress.

7.3 RESULTS OF ELASTIC-PLASTIC METHODS OF ANALYSIS

Reference to Eq. 7-2 shows that values of undrained strength based on an elastic-plastic model of soil behavior depend on three test variables: the initial pressure (P_o); the limit pressure (P_1); and the shear modulus (G). The initial pressure should theoretically equal the in situ total horizontal stress (σ_{ho}), but Chapter 5 demonstrated that P_o was highly variable, depending both on the installation technique (e.g. amount of disturbance) and the method of interpretation. The analyses used the inflection point P_o, the upper estimate of σ_{ho} and/or the "best estimate" from the Marsland and Randolph (1977) graphical iteration method as representative values.

The limit pressure in Eq. 7-2 is the theoretical value corresponding to infinite expansion. Chapter 6 showed this quantity to be relatively unaffected by the starting condition (Figure 6-2), and hence disturbance to the soil, but highly dependent on the extrapolation procedure (Figures 6-3, 4 and 5). Although Chapter 6 concluded that the $\log(\Delta V/V)=0$ method provided more reasonable (and often much higher) P_1 values than the $1/\Delta V=0$ method, the strength analyses included both approaches. Also note that the conventional P_1, used to interpret Menard pressuremeter data and corresponding to $\Delta V/V_o=1$ rather than infinite

143

expansion, always fell within the above range of theoretical limit pressures.

Finally, all analyses used initial tangent values of G obtained via Eq. 7-1 from actual expansion curve data as suggested by Jamiolkowski (1979). The starting point was varied to be consistent with the value of P_O used in each analysis. With most of the tests, G either decreased or remained almost constant with increasing P_O.

Tables 7-1 and 2 present values of c_u and N_p from the analyses, while Figures 7-1 and 2 plot the strength data versus elevation. These figures also show two SHANSEP strengths: the peak $c_u=q_f$ for plane strain compression, which should represent the maximum possible in situ strength (neglecting strain rate effects); and the much lower average c_u, which considers strength anisotropy and strain compatibility. The later strength is appropriate for circular arc stability analyses and is generally within ±10% of the measured field vane strength. For the mode of failure and strain rate imposed by the SBPT, its strength should fall between the two SHANSEP c_u values.

The SHANSEP strengths at Sta. 263, though computed based on the stress history existing in 1967, should apply at the time of the 1973 CAMKOMETER tests. The 1974 embankment failure, however, probably disturbed the clay and caused lower in situ strengths at the time of the 1977 PAFSOR tests.

The results from the Sta. 246 PAFSOR tests show the following (Table 7-1 and Figure 7-1):

(1) Analyses using the inflection point P_O and the $\log(\Delta V/V)=0$ limit pressure give the highest c_u, and all but one of these values exceed the peak c_u for

144

vertical loading. This might be expected since the inflection point P_O is generally much lower than the in situ σ_{ho} (see Figure 5-4).

(2) Analyses using the same theoretical P_1, but with P_O increased to the upper bound estimate of σ_{ho} obviously give lower strengths, often by a substantial amount. However, these values are still considered too high, especially in the "soft" clay where they exceed the peak $c_u(V)$ by about 20%.

(3) Analyses using the upper bound σ_{ho} and the $1/\Delta V = 0$ limit pressure give the lowest c_u. These values are generally reasonable in the upper medium clay, but are still too large in the deep "soft" clay. Also note that the method used to estimate P_1 often has a greater effect than changes in P_O.

(4) None of the analyses gives an especially good estimate of the variation in strength with depth, even though essentially all N_p values fell within the theoretically acceptable bounds of 6.0 ± 1.5. In fact, N_p averaged 5.95 and 6.15 for P_1 estimated via the $\log(\Delta V/V) = 0$ and $1/\Delta V = 0$ methods respectively.

Turning to Sta. 263 and Figure 7-2, one first observes that the "after failure" PAFSOR strengths are much less than all other values based on similar definitions of P_O and P_1 and hence further discussion is restricted to the CAMKOMETER data. These analyses used "best estimates" of P_O from the graphical iteration method and the upper bound σ_{ho}. This caused relatively minor changes in c_u, as might be expected from the horizontal stress data plotted in Figure 5-7. However, as was the case at Sta. 246, the procedure used to estimate the limit pressure proved very important, with $P_1(1/\Delta V = 0)$ giving strengths

averaging only 60% of those based on P_1 (log($\Delta V/V$)=0). The latter analyses yielded c_u values about equal to the SHANSEP peak c_u(V) in the upper overconsolidated clay, but 30% greater than the peak c_u(V) in the lower normally consolidated material. The same trend occurred at Sta. 246. Strengths based on the inverse volume P_1 were often less than the SHANSEP c_u(Ave.) at shallow depths and fell between the two limits in the underlying clay. Although these strengths are more reasonable, it must be somewhat fortuitous since the $1/\Delta V=0$ method underestimates the theoretical limit pressure for infinite expansion. Finally the values of N_p shown in Table 7-2 again fall within the expected range.

Section 7.5 will compare results of the elastic-plastic analyses with "derived" peak and ultimate strengths.

7.4 RESULTS OF DERIVED STRESS-STRAIN-STRENGTH METHODS OF ANALYSIS

7.4.1 Scope of Analyses and Problems Encountered

Section 7.2.2 presented the three basic methods of analysis used to obtain "derived" data. A summary of these methods and pertinent comments follow.

(1) Subtangent = numerical differentiation of "smoothed" expansion curve data computed via Eq. 7-3. A computer program performs the analysis and plots individual stress-strain (τ-ε_0) data points. These plots were then used to obtain values of peak and ultimate strength and the secant shear modulus (G_{50}) at 50% of the peak strength.

(2) P-Log($\Delta V/V$) = a graphical procedure wherein peak and ultimate strengths are obtained via Eq. 7-4 from the slopes of semi-log plots prepared by a computer

146

using "smoothed" data. As noted before, this process may involve some judgement.

(3) Modified Prevost-Hoeg = an <u>analytical</u> method wherein a computer program first uses Eq. 7-5 to represent the actual expansion curve and then it differentiates that mathematical relationship to obtain a complete stress-strain curve via Eq. 7-6. The curve fitting procedure emphasizes the initial portion of the expansion curve and hence the method is better suited to evaluate peak strength and G_{50} than the ultimate strength.

Table 7-3 summarizes the scope of the final anlayses. The analyses first compared results from the three different methods using the inflection point P_O with the PAFSOR tests and the start of the test with the CAMKOMETER tests as the "initial condition". This showed one or more of the methods to have definite limitations, as discussed below. The more suitable methods were then employed to investigate the importance of varying the initial condition for the Sta. 246 PAFSOR and Sta. 263 CAMKOMETER tests.

Two PAFSOR tests, No. 4 and 10, are selected to demonstrate the application of the three methods of analysis and to illustrate the types of problems encountered in making each analysis. Figure 7-3 shows the measured expansion curves. Test No. 4 represents an "ideal" test, the cell having been inserted wtih no volume deficiency* and then expanded at a constant rate. Test No. 10 typifies the opposite end of the spectrum (other than extremely erratic data such as in Test No. 8 and 14), namely: insertion with a significant volume deficiency (103 vs 215 cc) which

_____

* However, P_O was still about 0.7 kg/cm^2 (70kPa) less than the average estimated in situ σ_{ho} (see Figure 5-4).

147

caused a Type IV double curve; and two changes in expansion rate, the one at $\Delta V=196$ cc being most critical.

The results from analyzing the two tests are presented in Figures 7-3 through 7-5. Both analyses used an initial condition based on the inflection point P_O, this corresponding to $\Delta V_O=217$cc and 161cc respectively. Consider Test No. 4 first, where the results in Figure 7-5 show excellent agreement (within 10%) amongst the values of peak and ultimate strength obtained by the three methods. The subtangent data points exhibit little scatter about the calculated Modified Prevost-Hoeg curve and the latter relationship closely follows the measured expansion curve (Figure 7-3). Slopes obtained from Figure 7-4 also involve little judgement. Moreover, even the values of $G_{50}*$ derived from the subtangent and Modified Prevost-Hoeg methods agree within $\pm 25\%$ of 250 kg/cm^2 (24,500 kPa).

Now consider Test No. 10, which shows a very different picture even though the first "curve" in Figure 7-3 was eliminated since the corrected test starts from $\Delta V_O=161$cc. These results show the following:

(1) The subtangent method yields absurd stress-strain data (Figure 7-5). The very large peak strength, followed by extreme strain-softening, results mainly from the effects of the first increase in expansion rate from 6 to 20 cc/min. A secondary peak also occurred when the rate was increased to 60 cc/min.

(2) Even discounting the predictable general effects of changes in expansion rate, the subtangent method gave very erratic data at strains exceeding $\varepsilon_O\approx 0.5\%$. In fact, almost all of the "deep" tests at both locations exhibited erratic subtangent data beyond the

---

* $G=\tau/\gamma=\tau/2\varepsilon_O$

148

peak strength. Whether this is caused by depth per se
or a decrease in the overconsolidation ratio of the
clay is unclear.

(3)   Although the graphical P-log(ΔV/V) method shown in
Figure 7-4 yields a fairly well defined maximum
slope, and hence peak c_u, the result is very misleading
because the maximum slope occurs immediately after an
increase in expansion rate. That is, the slope would
undoubtedly have been much smaller if the expansion
rate had not been increased at ΔV/V$\approx$0.011. This same
rate change phenomena occurred in Test No. 11, 12 and
15 and hence the peak c_u values measured in these tests
are also too large. These strengths are therefore
discounted, as is that for Test No. 6 wherein the
Type IV curve caused an extreme change in slope during
the early portion of the test [Figure 4-2(b)].

(4)   The stress-strain curve in Figure 7-5 obtained by the
Modified Prevost-Hoeg method gave a much lower, and
more reasonable, peak strength. But this is fortui-
tous because the corresponding "theoretical" expansion
curve plotted in Figure 7-3 has a much flatter slope
than the measured curve in the region of interest.
Similar problems occurred in Test No. 6, 11, 12 and
15 wherein changes in expansion rate and/or Type IV
curves produced expansion curves that simply cannot
be adequately modeled by Eq. 7-5. It should be
emphasized, however, that the basic fault lies in the
nature of the test data and not with the method of
analysis. It also means that one should look at all
aspects of the data before drawing conclusions
regarding the reliability of any method of anlaysis.

Results presented in subsequent Sections exclude peak
strengths (and sometimes modulus) from those tests wherein

changes in expansion rate and/or certain Type IV curves are thought to have seriously affected the results. These Sections also: compare results from the different methods of analysis and further comment on their relative merits; show the effect of varying the initial condition; compare SBPT strength and modulus data to in situ properties predicted from the SHANSEP approach (Chapter 3); and compare "derived" c_u values with those presented in Section 7.3 from the elastic-plastic method of analysis. Appendicies B and C give the results in tabulated form.

7.4.2 Derived Peak Strengths

Figure 7-6 compares peak c_u values obtained by the graphical P-Log($\Delta V/V$) and analytical Modified Prevost-Hoeg methods from tests at both stations. The open symbols represent analyses using the inflection point P_o or start of the test as the initial condition, whereas the solid symbols denote the Sta. 246 PAFSOR and Sta. 263 CAMKOMETER test results using the upper limit σ_{ho} (Figure 5-4) and the best estimate graphical iteration P_o (Figure 5-7) as the starting points respectively for the analyses. The two methods give almost identical peak strengths from the Sta. 263 PAFSOR tests performed in relatively deep clay that had probably been disturbed by the 1974 embankment failure. For the other tests however, the P-Log($\Delta V/V$) method consistently yielded peak c_u values 1.25±0.25 times larger than the Modified Prevost-Hoeg method, more or less independent of the depth of test or the initial condition. Although not shown, strengths from the subtangent and P-Log($\Delta V/V$) methods usually agreed within ±10%. Thus replacing measured data by Eq. 7-5 produces lower computed

peak strengths.* Also, at least for most of these tests,
the P-Log($\Delta V/V$) approach is preferred over the subtangent
method as the latter frequently gave erratic results.

Figure 7-7 plots peak c_u data from the Sta. 246
PAFSOR tests versus elevation and shows the effect of
varying the initial condition with the graphical and
analytical methods of analysis. The figure also plots two
SHANSEP strengths and the writers believe that ideal SBPT
should theoretically yield peak c_u values falling between
these two limits for Boston Blue clay. However, analyses
starting from the inflection point P_o (i.e. the open
symbols) give much higher strengths, especially in the deep
clay, though this might be expected since the initial
stresses usually fell well below the estimated in situ σ_{ho}
(Figure 5-4). Hence, changing the initial condition to
correspond to the estimated upper limit σ_{ho} decreases the
computed strengths (the solid symbols), often by a substan-
tial amount. Nevertheless, except for some of the tests
in the highly overconsolidated clay, the c_u values still
greatly exceed the maximum SHANSEP strength.

Figure 7-8 presents corresponding data from the tests
performed at Sta. 263. The PAFSOR peak strengths agree
very well with the SHANSEP peak c_u(V), but this must be
fortuitous since the in situ strength was undoubtedly
decreased by the 1974 embankment failure. We shall there-
fore restrict the discussion to the CAMKOMETER results
which employed two initial conditions, the start of the
test and the best estimate from the graphical iteration.
The former yielded peak strengths agreeing reasonably well
with the SHANSEP peak c_u(V) in the upper heavily overcon-
solidated clay, whereas in the lower normally consolidated

---

* See end of Section 7.4.3 for further discussion of this
  important point.

151

clay the derived strengths are about two to three times larger than the SHANSEP peak $c_u(V)$. The excessive strengths in the deep clay are perhaps predictable since the "lift-off" pressures at the start of the test were only one-half to one-third of the estimated in situ σ_{ho}. Thus analyses starting from the graphical iteration best estimate of the in situ σ_{ho}, which generally gave reasonable results (Figure 5-7), produced substantially lower peak c_u values in deep clay, although they are still about 100±50% larger than the SHANSEP peak $c_u(V)$. Changing the initial condition in the upper clay had much less effect and there the derived strengths generally appear quite reasonable compared to the SHANSEP strengths.

The peak strength occurred at very small strains ($\varepsilon_o \approx 1.0 \pm 0.5\%$) in the deep tests at both Stations, which is consistent with the observation that changes in the initial condition (i.e. the point on the expansion curve corresponding to zero strain) caused substantial changes in the derived peak strength.* Tests in the upper more overconsolidated clay usually had larger strains at c_u (peak), say in the range of 2 to 5%, and thus the derived peak strengths were generally less sensitive to changes in the initial condition.

7.4.3 Derived Ultimate Strengths

The analyses used the approximately linear final portion of the P-Log($\Delta V/V$) plots to graphically determine ultimate strengths. These values should theoretically equal the average shear stress at large strains computed via the subtangent method, but these τ-ε_o data were usually too erratic to make meaningful comparisons.

---

* For a linear P-ε_o expansion curve, c_u(peak) is proportion to ε_o since $\tau \approx \varepsilon_o dP/d\varepsilon_o$.

Figures 7-9 and 7-10 plot ultimate c_u data versus elevation at the two test sites, along with profiles of the SHANSEP c_u(Ave.) and peak c_u(V). Based on considerations of strength anisotropy, the writers would expect that c_u(Ult.) should be closer to c_u(Ave.) than peak c_u(V), at least in the deeper "soft" clay. The Sta. 246 PAFSOR tests yielded ultimate c_u values that quite consistently decreased with depth and were relatively unaffected by the initial condition. In any case, the derived c_u(Ult.) in the upper clay is larger than expected, averaging 15% higher than the peak c_u(V), while in the lower clay it appears to be more reasonable.

Ultimate strengths from the Sta. 263 CAMKOMETER tests were almost constant with depth and also more seriously affected by the initial condition. Although the best estimate graphical iteration reduced c_u(Ult.) by about 15%, these values are still considered too large, especially in the lower clay where they exceed the peak c_u(V) by 20%. Figure 7-10 also shows quite reasonable data from the PAFSOR tests, but this is probably fortuitous.

Figure 7-11 plots the ratio c_u(Peak)/c_u(Ult.) versus elevation from the Sta. 246 PAFSOR and Sta. 263 CAMKOMETER tests for two initial conditions, the higher starting point data (i.e. the solid symbols) being considered more reliable. These results show no strain softening in the upper heavily overconsolidated clay, i.e. c_u(Peak)=c_u(Ult.), whereas the derived stress-strain curves generally exhibit appreciable strength loss at large strains in the underlying "soft" clay.

Figure 7-6 showed that the analytical Modified Prevost-Hoeg method gave peak strengths averaging about 20% less than those obtained by the graphical P-Log(ΔV/V)

method. Comparison of the c_u(Peak) data in Figures 7-7 and 7-8 with the c_u(Ult.) data in Figures 7-9 and 7-10 indicates that the analytical approach usually leads to derived peak strengths that are <u>less than</u> the graphical ultimate strengths for tests performed in the upper clay. The results are summarized below:

Test Series	$\dfrac{\text{Modified P-H Peak } c_u}{\text{Graphical Ultimate } c_u}$
Sta. 246 PAFSOR Above El.-60 (Using Upper σ_{ho})	0.95(0.7-1.3)
Sta. 263 CAMKOMETER Above El.-60 (Using B.E.G.I.)	0.8(0.7-0.9)

This finding casts some doubt on the validity of using the Modified Prevost-Hoeg method to analyze SBPT data in heavily overconsolidated Boston Blue clay, at least this particular set of tests that was hampered by many experimental problems. The same doubt may also apply to tests in the deep clay since the trend shown in Figure 7-6 did not appear to vary with depth.

7.4.4 Derived Shear Modulus

Figures 7-12 and 7-13 present values of secant shear modulus at the 50% stress level, at Stations 246 and 263 respectively, computed via the subtangent and Modified Prevost-Hoeg methods for two initial conditions. The figures also plot for comparison profiles of G_{50} for vertical and horizontal loading developed from a combination of SHANSEP plane strain tests and finite element analyses of foundation deformations under embankment

154

loadings (Section 3.5 and Figures 3-19 and 3-20).

Given the fact that estimation of undrained modulus is generally considered to be amongst the most difficult tasks in geotechnical engineering, the overall agreement between the SBPT and SHANSEP G_{50} data is really amazingly good. The results at Sta. 246 are especially encouraging since these tests were generally inserted with a significant volume deficiency and yet most of the modulus values still fall near the SHANSEP band. Station 263 shows somewhat more scatter, but much of this is due to the PAFSOR tests that should be discounted. Also changing the initial condition had a larger effect with the CAMKOMETER tests.

The Modified Prevost-Hoeg G_{50} values were generally $25\pm25\%$ greater than those computed by the subtangent method. Though not shown, most of the values of G obtained using Eq. 7-1 for the elastic-plastic strength analyses were within $\pm20\%$ of the subtangent G_{50} data.

In summary, the SBPT appears to yield quite reasonable estimates of undrained shear modulus for Boston Blue clay. Politechnico di Torino (Jamiolkowski, 1979) reached a similar conclusion from PAFSOR and CAMKOMETER tests at several sites.

7.5 DISCUSSION

We shall first discuss the strength data based on the following assumptions:

(1) Problems due to improper insertion can be overcome, or at least minimized, but selecting an appropriate initial condition, namely the upper limit σ_{ho} for the Sta. 246 PAFSOR tests and the best estimate graphical iteration P_O for the Sta. 263 CAMKOMETER tests.

(2) Strengths determined from the elastic-plastic analyses should use limit pressures obtained by the $\text{Log}(\Delta V/V)=0$ method since the $1/\Delta V=0$ approach gives P_1 values that are obviously too low.

(3) Derived peak and ultimate strengths are best determined graphically from $P\text{-Log}(\Delta V/V)$ plots since the subtangent method gave data that were frequently too erratic, while the analytical Modified Prevost-Hoeg approach yielded peak c_u values that were often too low (based on the results presented at the end of Section 7.4.3).

(4) Based on considerations of strength anisotropy (and to a lesser degree strain rate effects), derived peak strengths should be somewhat less than the SHANSEP peak strength for vertical loading, i.e. the peak $c_u(V)$, while derived ultimate strengths should probably be closer to the SHANSEP $c_u(\text{Ave})$, at least in the deep "soft" clay.

We shall further eliminate derived peak strengths from those Sta. 246 PAFSOR tests wherein changes in the expansion rate obviously affected the results. The Sta. 263 PAFSOR tests are also eliminated since the 1974 embankment failure decreased the in situ strength to an unknown degree.

In essence, the above selects those methods of analyses believed to have the soundest theoretical basis for a "perfect" SBPT performed in an "ideal" clay. In other words, the surrounding soil is completely undisturbed and homogeneous, expansion starts from the in situ σ_{ho}, the clay has an unique stress-strain relationship unaffected by variations in strain rate and no drainage occurs, end effects are negligible, no significant errors

156

or scatter in the expansion curve, etc. (see Section 2.4).
Inconsistencies in the results from these analyses, both
amongst themselves and compared to the SHANSEP reference
strengths, therefore indicate deviations from the idealized
set of assumptions. These can be due to problems caused
by the SBPT equipment and procedures, nonuniform soil
conditions, deficiencies in the theoretical model of soil
behavior, etc.

Figures 7-14 and 7-15 plot undrained strength data
from the elastic-plastic and derived methods of analysis
selected above as being most appropriate, along with the
SHANSEP c_u profiles, at Sta. 246 and 263 respectively.
Let us first consider the results in the upper more heavily
overconsolidated clay (say above El.-60) where the derived
analyses gave identical peak and ultimate strengths in
11 of the 13 tests. Since the derived data indicate little
or no strain-softening, one should expect close agreement
between the elastic-plastic and derived strengths. In
fact, the CAMKOMETER results agree very well, with average
c_u values considered generally reasonable compared to
the SHANSEP strengths. The PAFSOR results are less satis-
factory. The derived strengths exceed the elastic-plastic
values and also have an average some 20% higher than the
SHANSEP peak $c_u(V)$. Test No. 4 at El.-40 was the only
test inserted with the correct cell volume and it gave
the best results. However, the data are too limited to
show whether or not disturbance is the major reason for
the excessive strengths from both methods of analysis.

The results in the clay below El.-60 show a very
different picture. The derived strength analyses indicate
considerable strain-softening, as might be expected for
the more sensitive deep clay. The elastic-plastic strengths

157

also fall between the derived peak and ultimate values, as they probably should. However, except for the Sta. 246 PAFSOR ultimate strengths, all other strength data are too large. This is especially true of the derived peak strengths which are about double the SHANSEP peak $c_u(V)$. Even the elastic-plastic c_u values exceed the SHANSEP peak $c_u(V)$ by an average of 20 to 30%, as do the CAMKOMETER derived ultimate strengths.

The writers would like to be in a position to explain these results, but cannot other than to reiterate the possibilities already discussed in Section 2.4. One could, or course, recommend other methods of analysis that would lead to lower and more reasonable c_u values such as the elastic-plastic approach using P_1 data obtained by the $1/\Delta V=0$ method (Figures 7-1 and 7-2). But this is an empirical approach that may not apply at other sites. Moreover, it does not address the main issue of why these SBPT yielded such unreasonable strength data in the deep Boston Blue clay.

TABLE 7-1 UNDRAINED SHEAR STRENGTH FROM PAFSOR TESTS
USING ELASTIC-PLASTIC ANALYSES

Test No.	El. (ft)	P_o = Inflection Point				P_o=Upper Limit σ_{ho}			
		P_1 from Log($\Delta V/V$)=0		P_1 from $1/\Delta V$=0		P_1 from Log($\Delta V/V$)=0		P_1 from $1/\Delta V$=0	
		c_u(kg/cm^2)	N_p	c_u(kg/cm^2)	N_p	c_u(kg/cm^2)	N_p	c_u(kg/cm^2)	N_p
1	-19.7	1.22	4.4	0.81	4.8	1.06	4.55	0.68	4.95
2	-28.7	0.95	5.35	0.59	5.85	0.75	5.65	0.37	6.35
3	-33.7	1.13	4.6	0.83	4.9	0.83	5.15	0.63	5.45
4	-39.7	0.84	6.75	0.65	7.0	0.69	6.85	0.51	7.15
5	-44.7	0.96	6.85	0.75	7.1	0.78	6.9	0.59	7.15
6	-49.7	1.14	6.25	0.98	6.4	1.07	5.8	0.88	6.0
7	-54.7	1.10	6.85	0.97	7.0	0.92	6.9	0.81	7.05
9	-71.7	1.37	5.4	1.15	5.55	1.03	5.65	0.82	5.9
10	-76.7	1.07	6.25	0.88	6.45	0.94	6.35	0.77	6.55
11	-81.7	1.14	6.0	0.94	6.2	0.96	6.1	0.83	6.25
12	-86.7	1.34	5.75	1.25	5.8	1.12	5.65	0.98	5.75
13	-91.7	1.15	5.95	0.99	6.1	1.11	6.0	0.98	6.1
15	-101.7	1.37	5.9	1.13	6.1	1.12	6.1	0.93	6.25
16	-54.3	0.55	6.05	–	–	–	–	–	–
17	-64.3	0.54	6.3	–	–	–	–	–	–
18	-69.3	0.53	6.45	–	–	–	–	–	–
19	-74.3	0.61	6.8	–	–	–	–	–	–
20	-79.3	0.57	7.15	–	–	–	–	–	–

1 ft=0.305 m   1kg/cm^2=98.1 kPa

TABLE 7-2   UNDRAINED SHEAR STRENGTH FROM CAMKOMETER
TESTS USING ELASTIC-PLASTIC ANALYSES

| Test No. | El. (ft) | P_o = Best Est. Graphical Iteration | | | | P_o = Upper Limit σ_{ho} | | | |
| | | P_1 from $Log(\Delta V/V)=0$ | | P_1 from $1/\Delta V=0$ | | P_1 from $Log(\Delta V/V)=0$ | | P_1 from $1/\Delta V=0$ | |
		c_u (kg/cm^2)	N_p	c_u (kg/cm^2)	N_p	c_u (kg/cm^2)	N_p	c_u (kg/cm^2)	N_p
21	-27	0.69	4.7	0.23	5.8	0.62	4.85	0.18	6.1
23	-30	0.59	6.0	0.37	6.45	0.72	4.35	0.40	4.9
24	-32	0.60	5.4	0.37	5.9	0.65	5.4	0.43	5.8
27	-35	0.87	5.85	0.57	6.25	0.85	5.85	0.55	6.25
28	-40	0.84	6.0	0.45	6.6	0.79	6.05	0.41	6.75
29	-42.5	0.88	5.85	0.54	6.3	0.90	5.7	0.56	6.2
30	-67	0.99	5.85	0.65	6.25	0.94	5.6	0.59	6.05
31	-70.5	0.96	5.8	0.68	6.15	0.82	5.8	0.55	6.2
32	-74	0.80	6.45	0.51	6.9	0.73	6.2	0.42	6.75
33	-77.5	0.92	5.55	0.63	5.9	0.81	5.65	0.51	6.1
34	-80.5	0.82	6.3	0.60	6.65	0.83	4.65	0.50	5.15

1 ft=0.305 m   1 kg/cm^2=98.1 kPa

TABLE 7-3 SCOPE OF DERIVED METHODS OF ANLAYSIS

Test Program	Method of Analysis	Initial Condition	Property (*=Yes)		
			Peak c_u	Ultimate c_u	Modulus G_{50}
PAFSOR Sta. 246	Subtangent	Inflection P_o	*	(2)	*
	P-Log($\Delta V/V$)	Inflection P_o	*	*	-
	P-Log($\Delta V/V$)	Upper σ_{ho}(1)	*	*	-
	Modified	Inflection P_o	*	-	*
	Prevost-Hoeg	Upper σ_{ho}(1)	*	-	*
PAFSOR Sta. 263	Subtangent	Inflection P_o	*	(2)	*
	P-Log($\Delta V/V$)	Inflection P_o	*	*	-
	Mod. P-H		*	-	*
CAMKOMETER Sta. 263	Subtangent	Start of Test	*	(2)	*
	P-Log($\Delta V/V$)	Start of Test	*	*	-
	P-Log($\Delta V/V$)	Best Est. Graph. Iter.	*	*	-
	Modified	Start of Test	*	-	*
	Prevost-Hoeg	Best Est. Graph Iter.	*	-	*

(1) Also Lower σ_{ho}, but results not presented

(2) If data not too erratic.
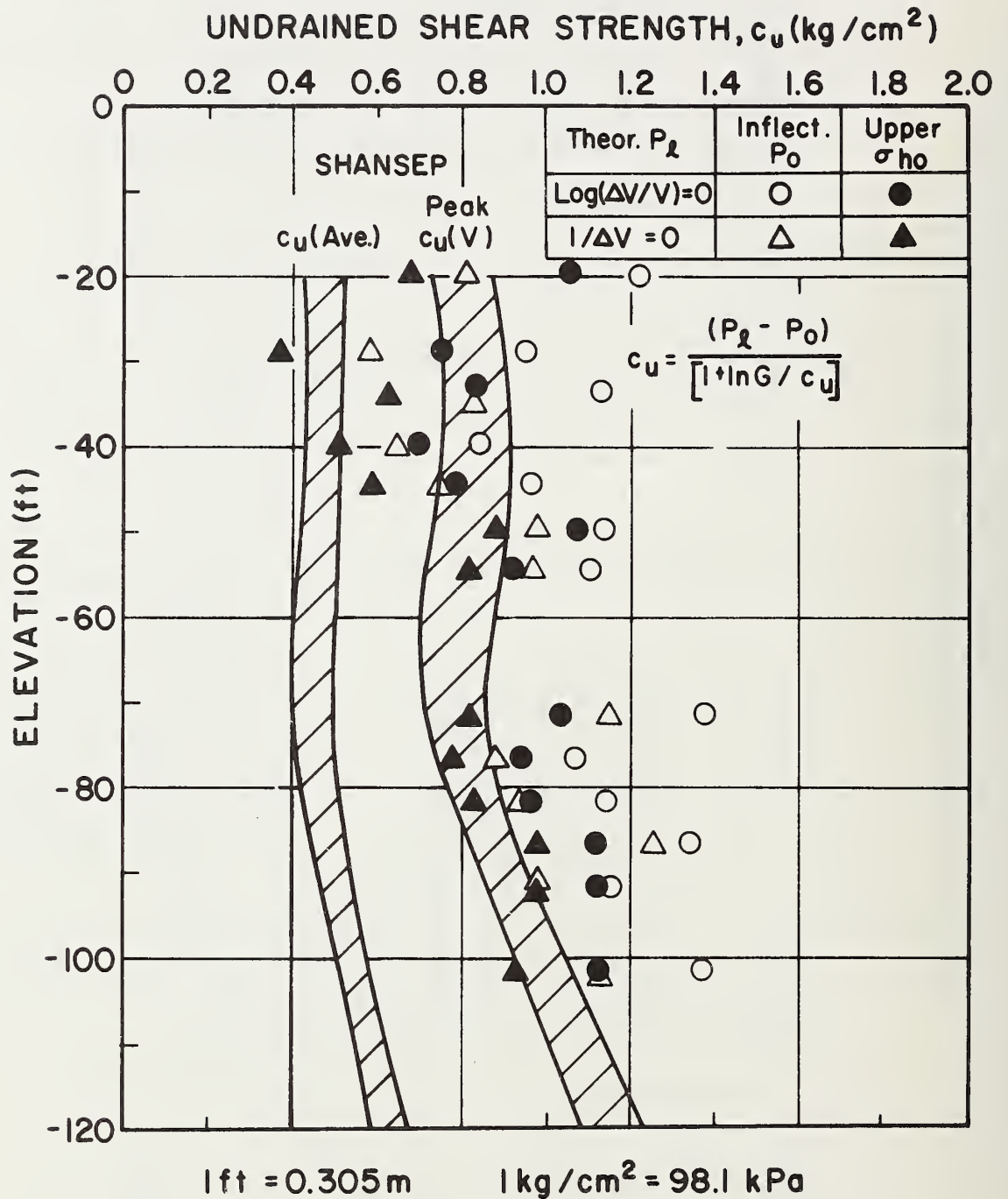
FIGURE 7-1   UNDRAINED SHEAR STRENGTH FROM PAFSOR TESTS
AT STA. 246 USING ELASTIC-PLASTIC ANALYSIS
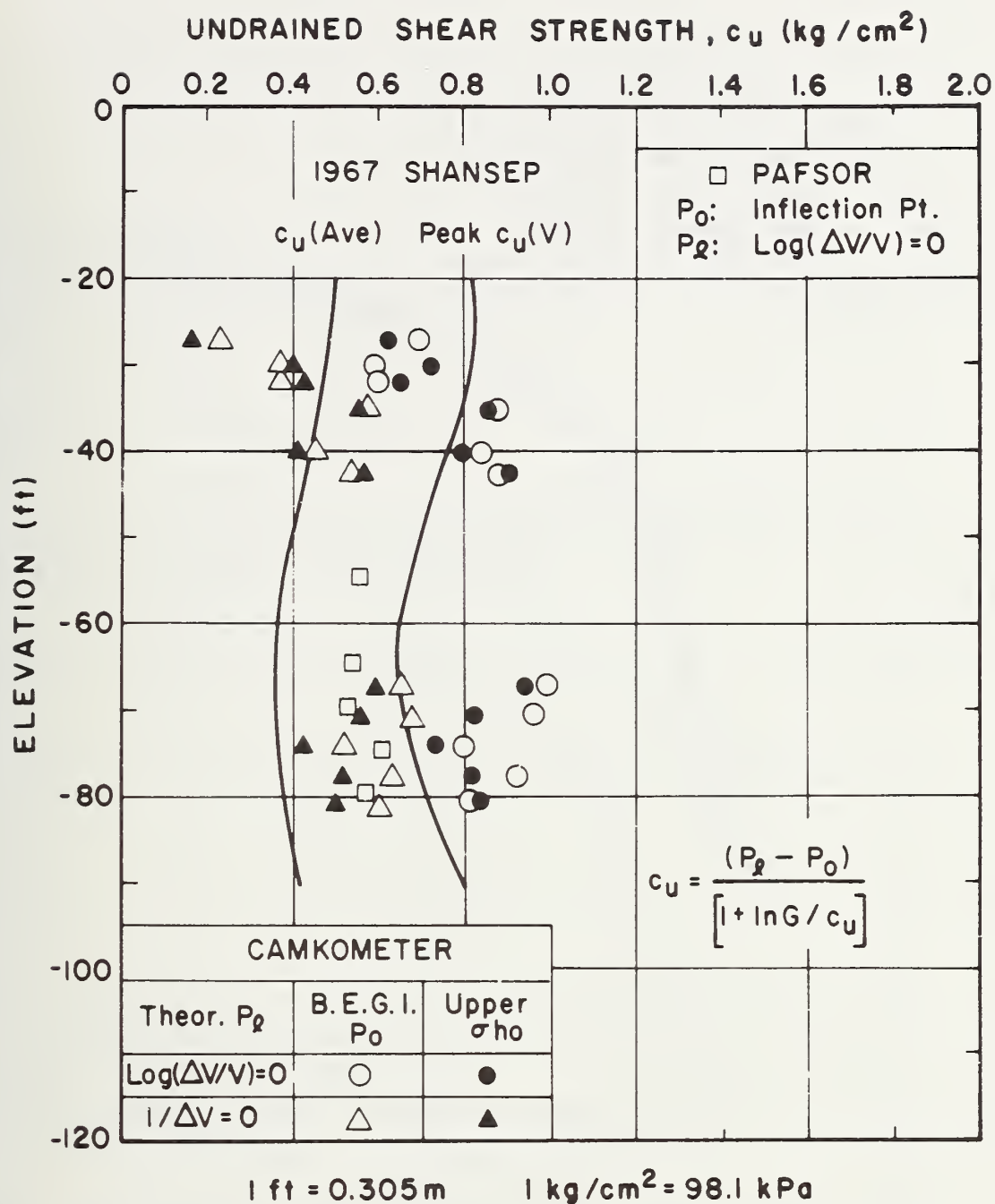
FIGURE 7-2   UNDRAINED SHEAR STRENGTH FROM PAFSOR AND
CAMKOMETER TESTS AT STA. 263 USING ELASTIC-
PLASTIC ANALYSIS

163
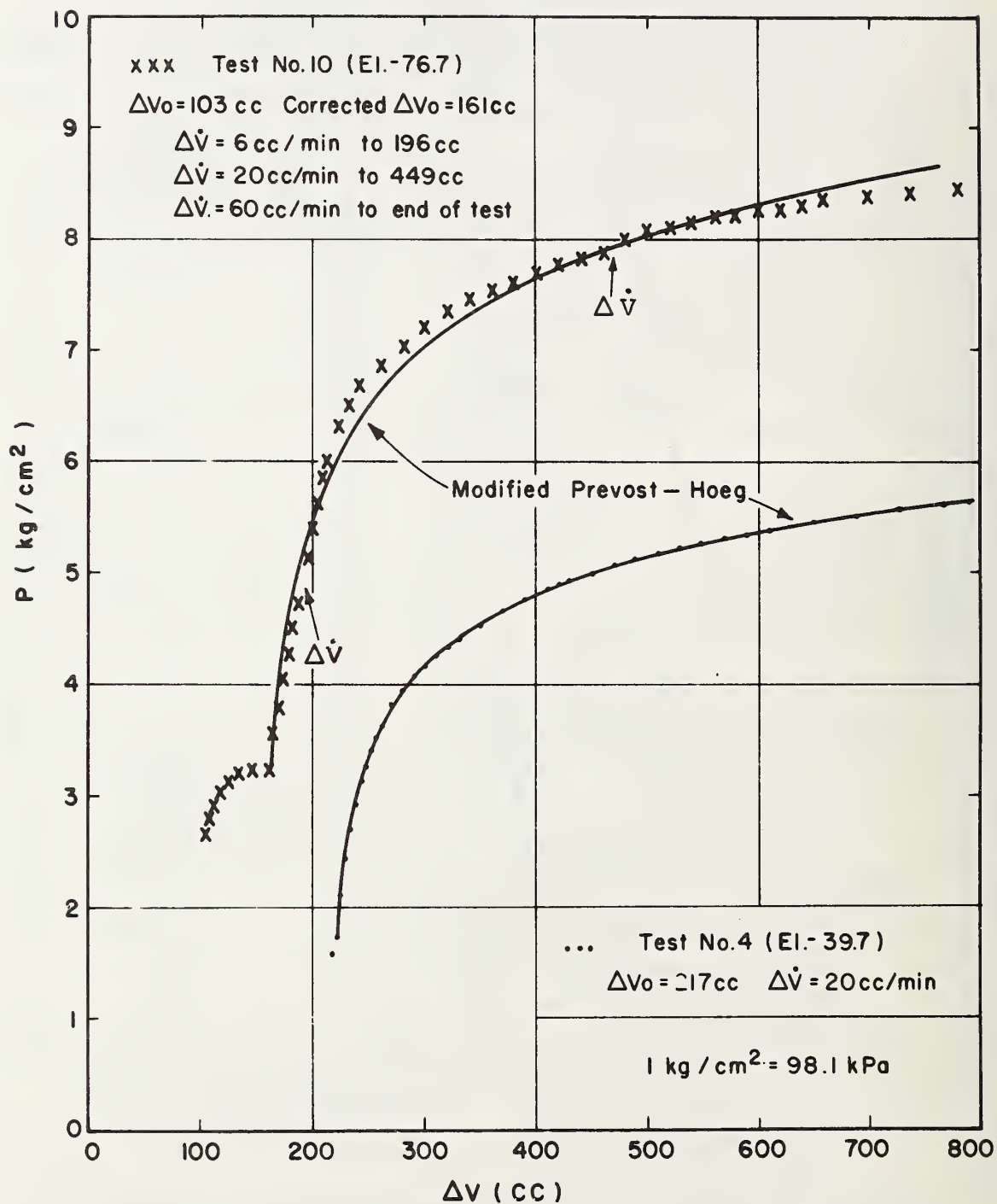
FIGURE 7-3   MEASURED AND MODIFIED PREVOST-HOEG EXPANSION
CURVES FOR PAFSOR TESTS NO. 4 and 10

164
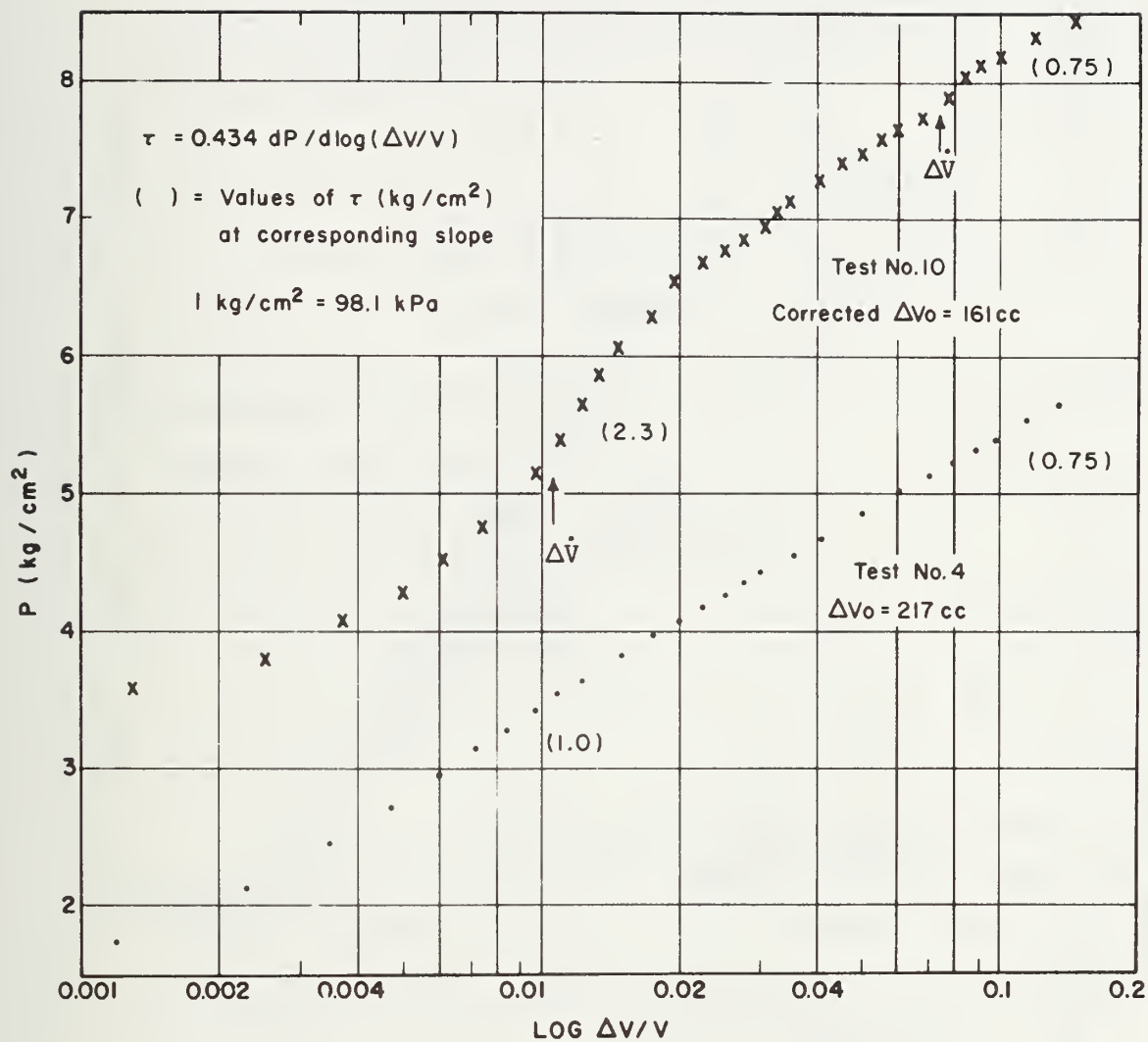
FIGURE 7-4   PRESSURE VS. LOG(ΔV/V) CURVES FROM PAFSOR
TESTS NO. 4 AND 10

165
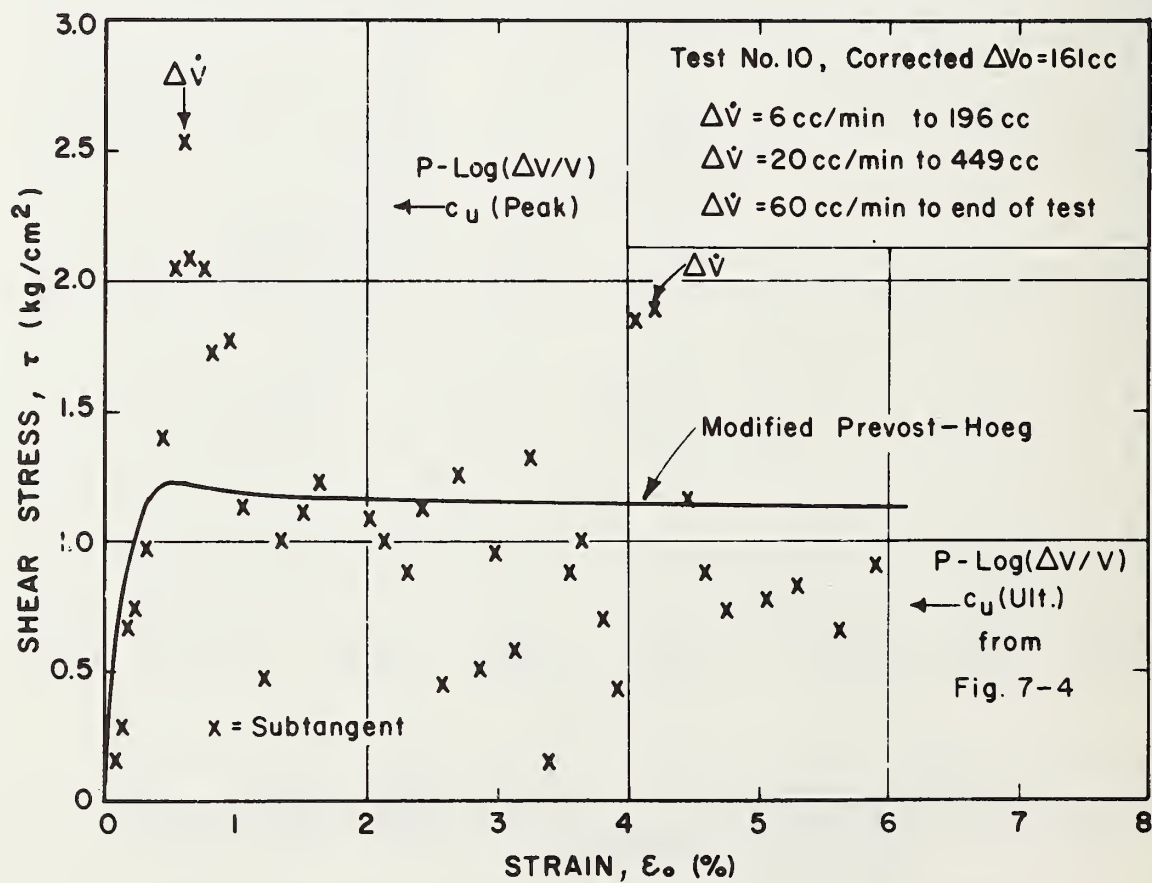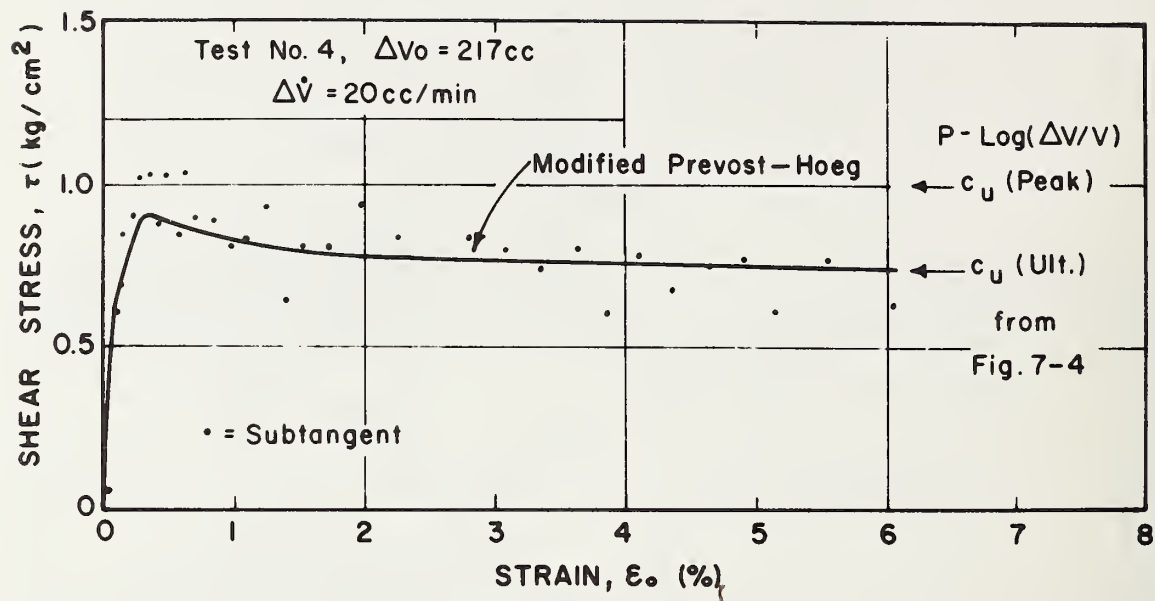
FIGURE 7-5   DERIVED STRESS VS. STRAIN FROM PAFSOR TESTS
NO. 4 and 10

166
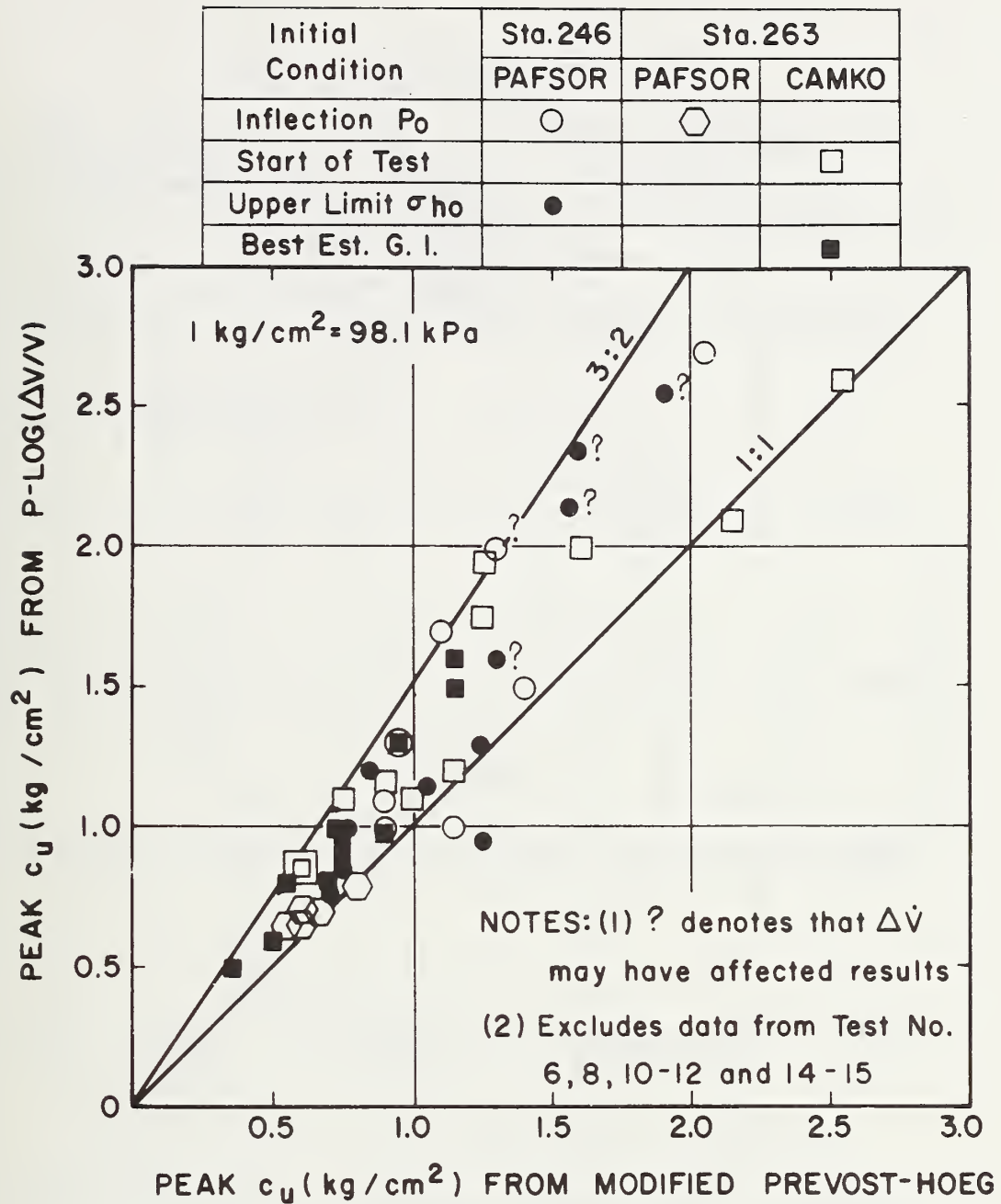
FIGURE 7-6   COMPARISON OF PEAK STRENGTHS USING P-LOG (ΔV/V)
AND MODIFIED PREVOST-HOEG METHODS FROM PAFSOR
AND CAMKOMETER TESTS
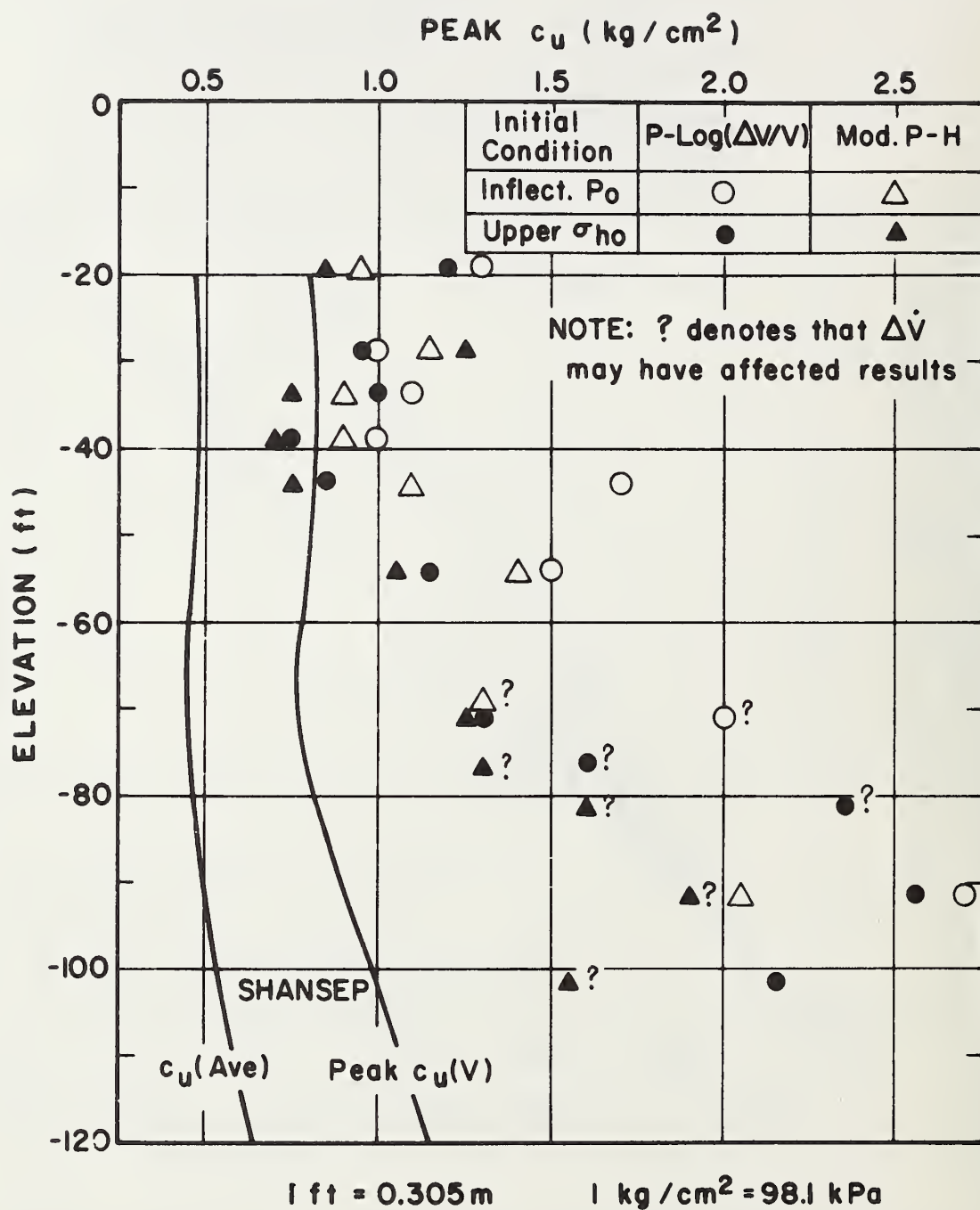
FIGURE 7-7   EFFECT OF INITIAL CONDITION ON DERIVED PEAK
STRENGTHS FROM PAFSOR TESTS AT STA. 246

168
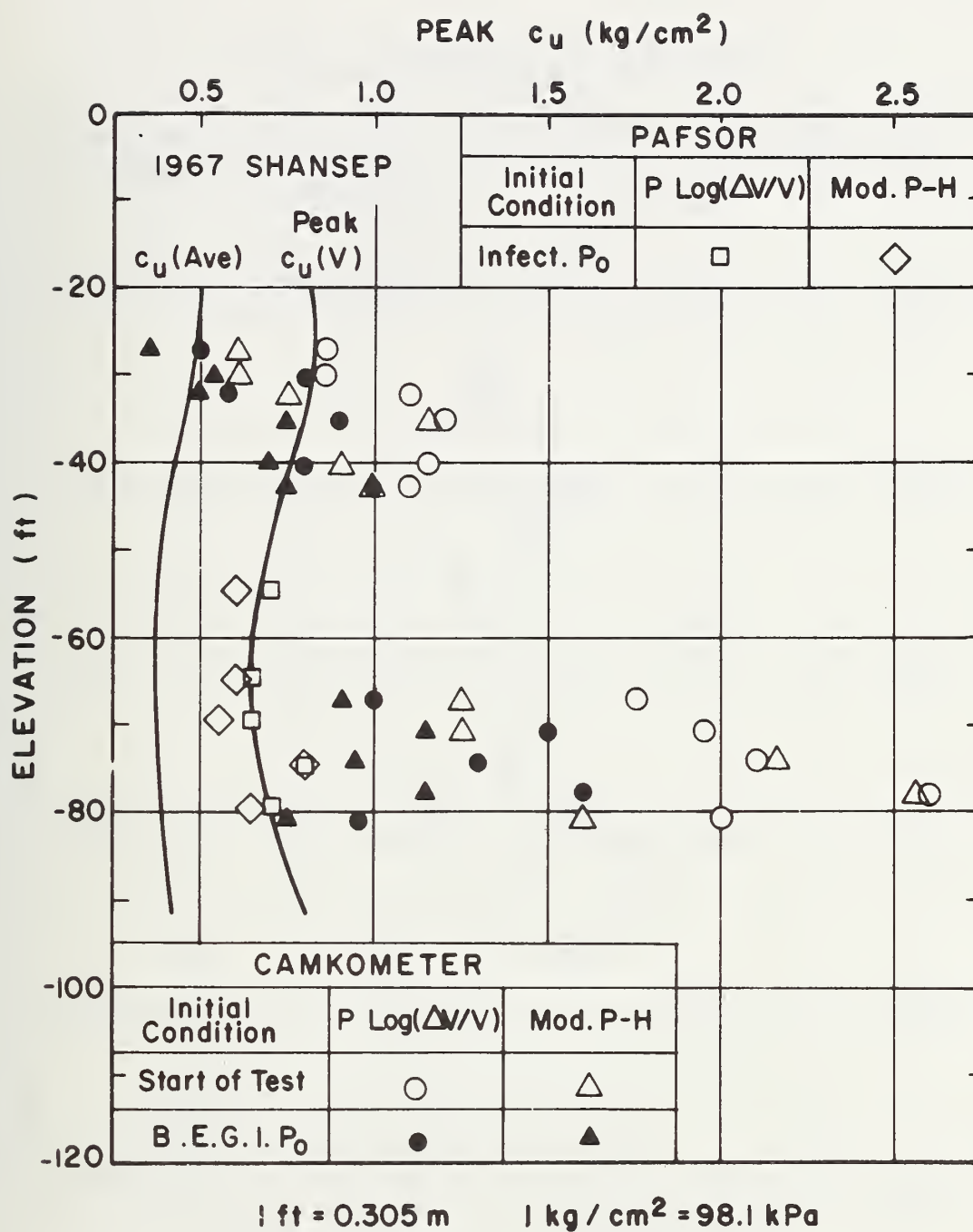
FIGURE 7-8   EFFECT OF INITIAL CONDITION ON DERIVED PEAK
STRENGTHS FROM PAFSOR AND CAMKOMETER TESTS
AT STA. 263

169
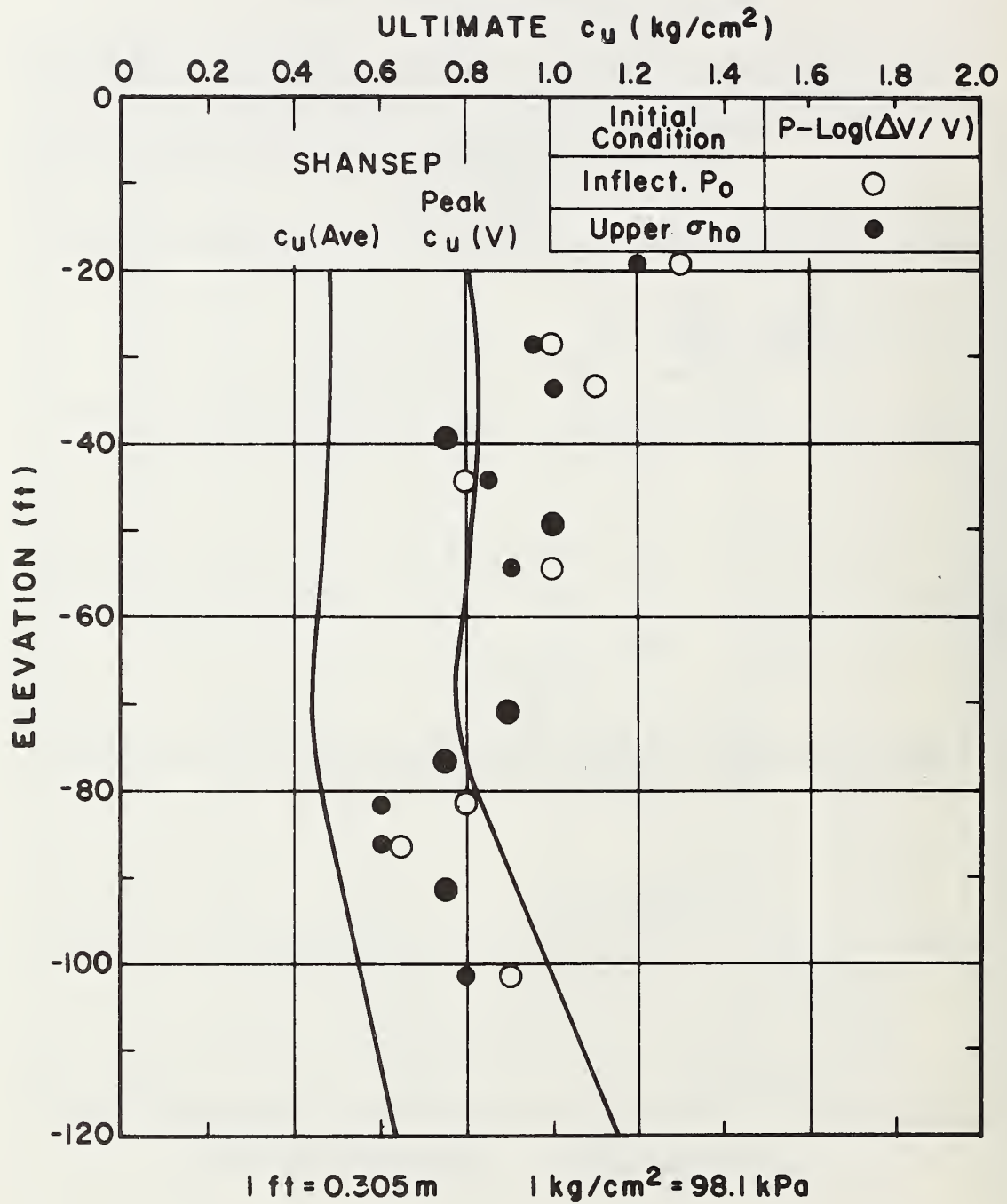
FIGURE 7-9   ULTIMATE STRENGTH FROM PAFSOR TESTS AT STA. 246
USING P-LOG(ΔV/V) METHOD
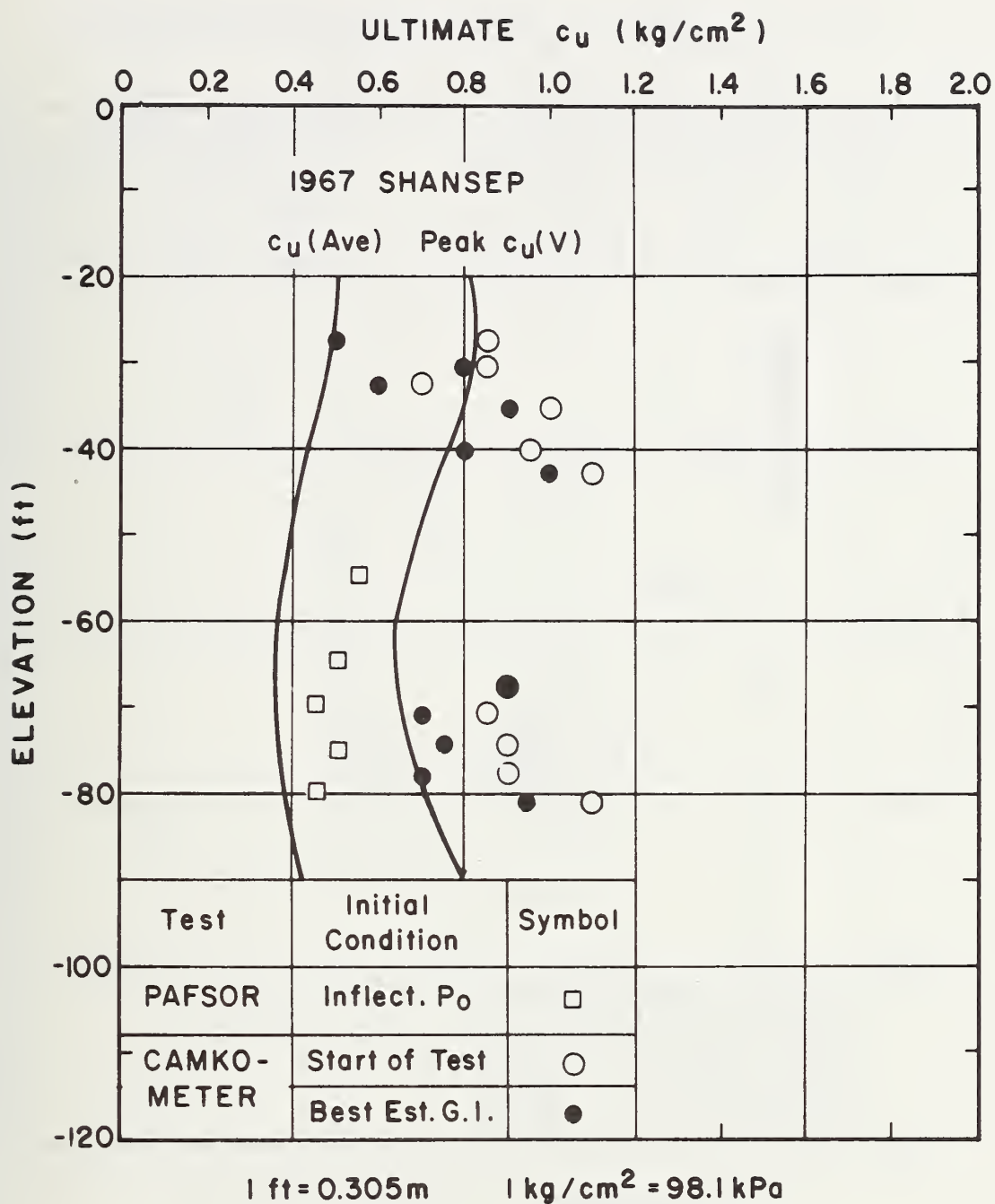
FIGURE 7-10   ULTIMATE STRENGTH FROM PAFSOR AND CAMKOMETER
TESTS AT STA. 263 USING P-LOG(ΔV/V) METHOD

171
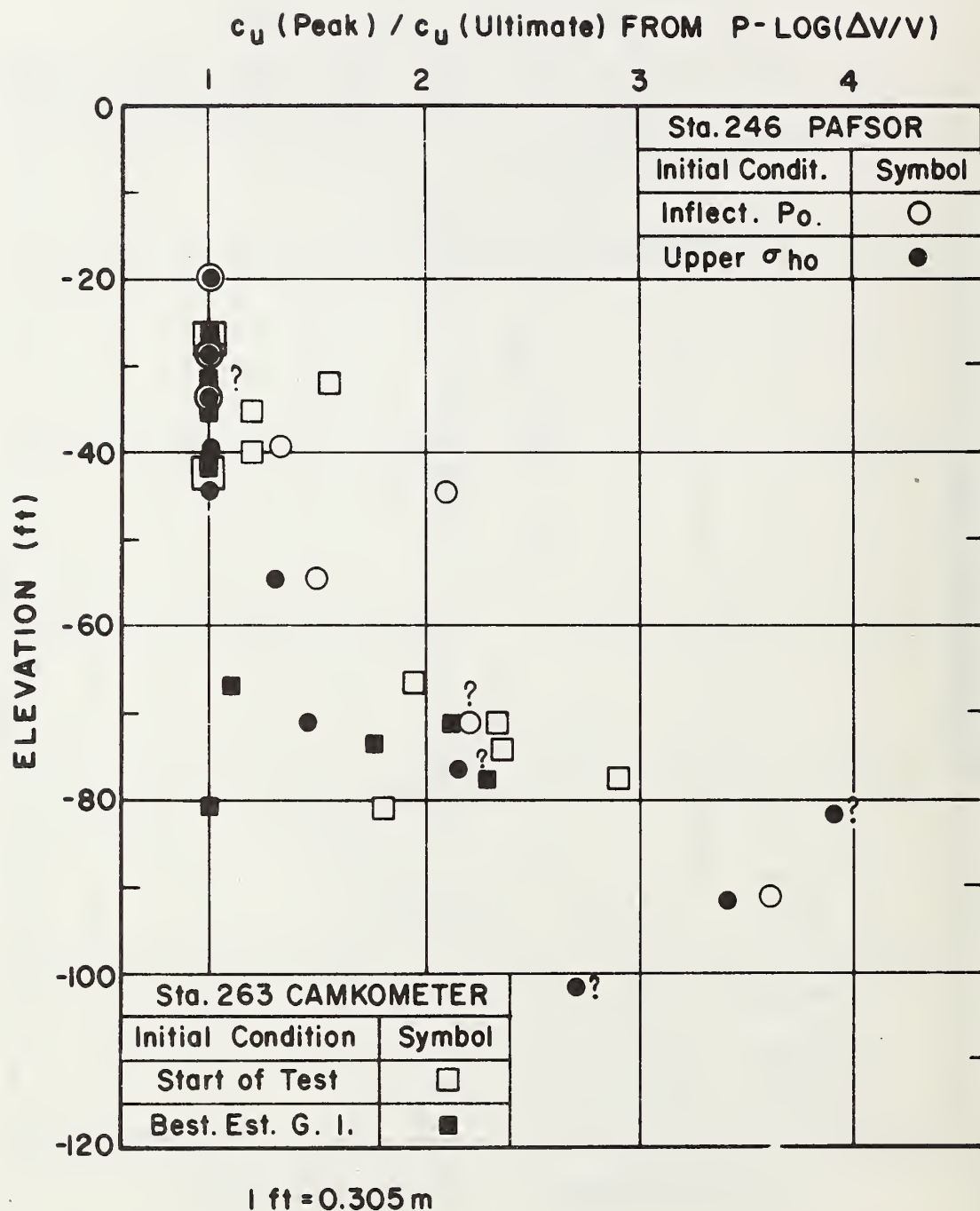
FIGURE 7-11 RATIO OF DERIVED PEAK TO ULTIMATE STRENGTHS
FROM PAFSOR AND CAMKOMETER TESTS
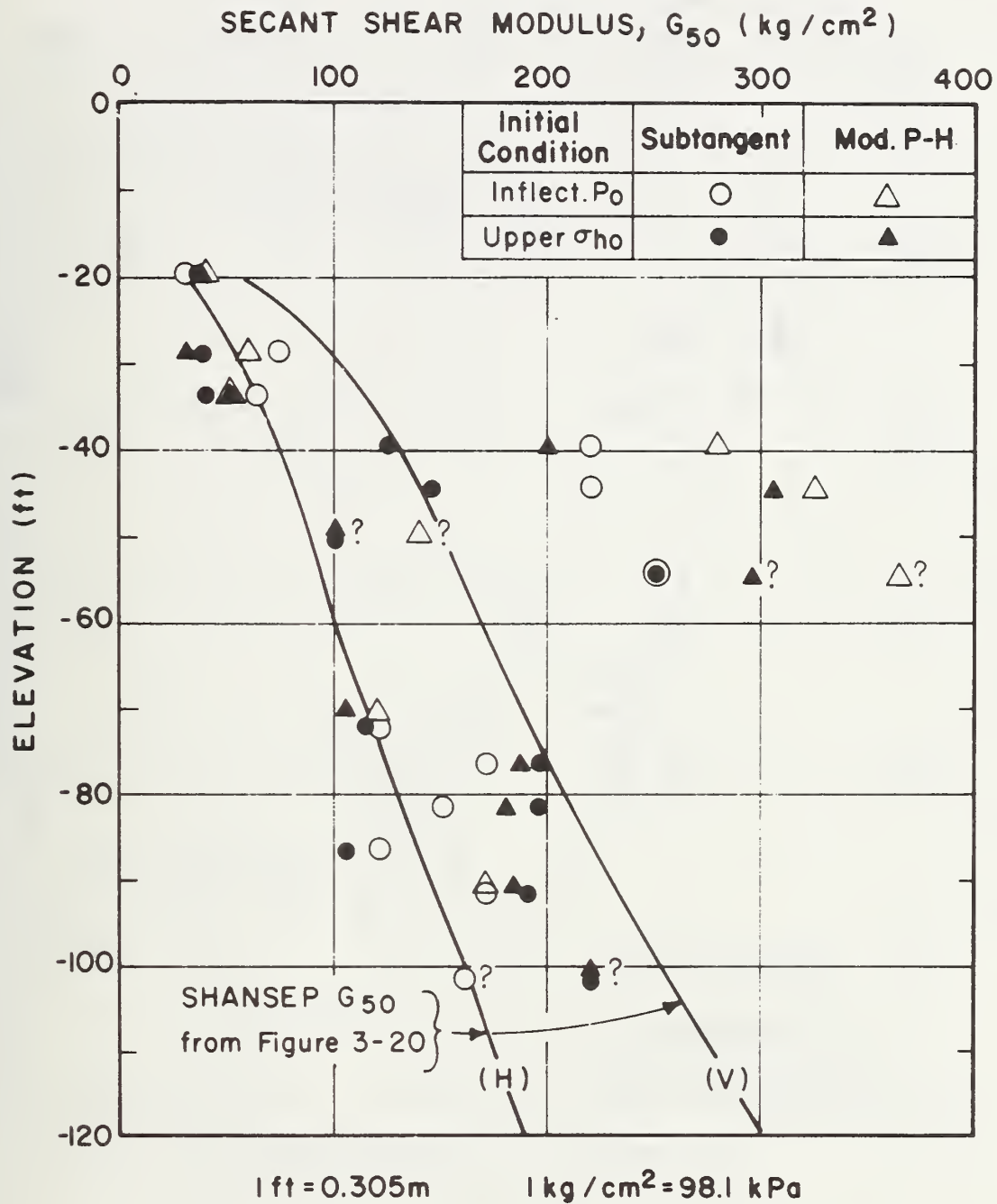
FIGURE 7-12   UNDRAINED SHEAR MODULUS FROM PAFSOR TESTS
AT STA. 246

173
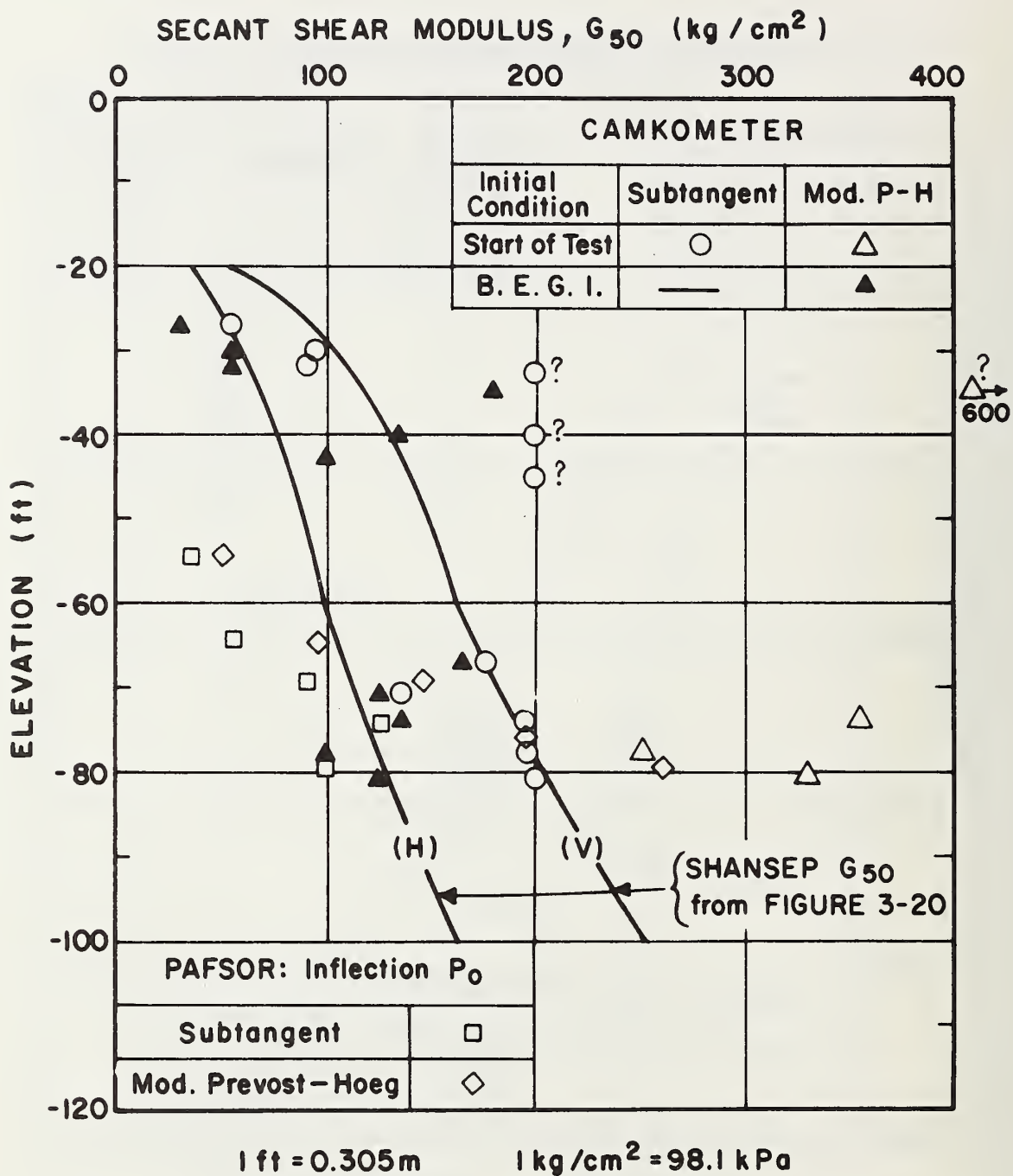
FIGURE 7-13   UNDRAINED SHEAR MODULUS FROM PAFSOR AND
CAMKOMETER TESTS AT STA. 263
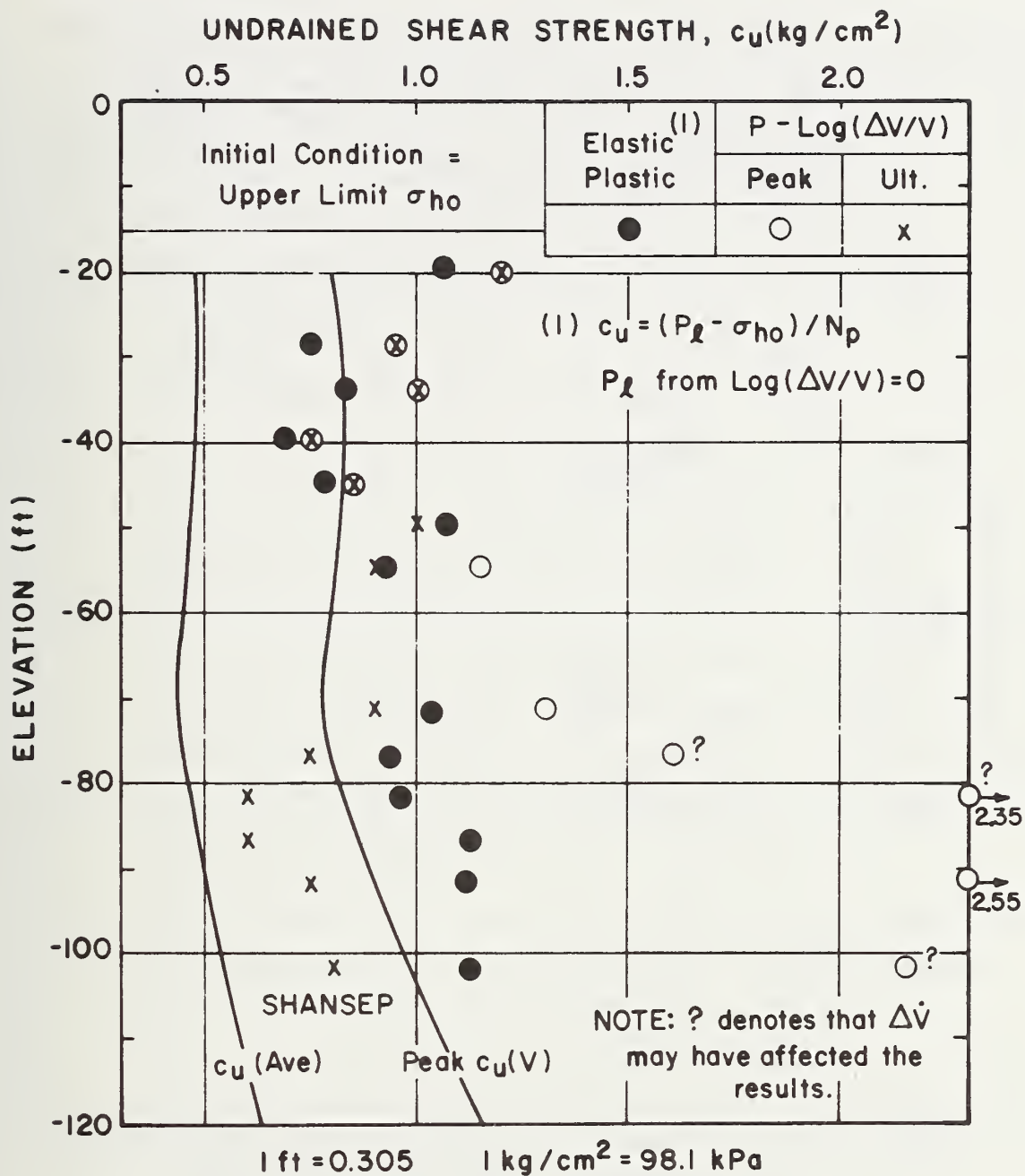
FIGURE 7-14   ELASTIC-PLASTIC AND DERIVED UNDRAINED SHEAR
STRENGTHS FROM PAFSOR TESTS AT STA. 246

175
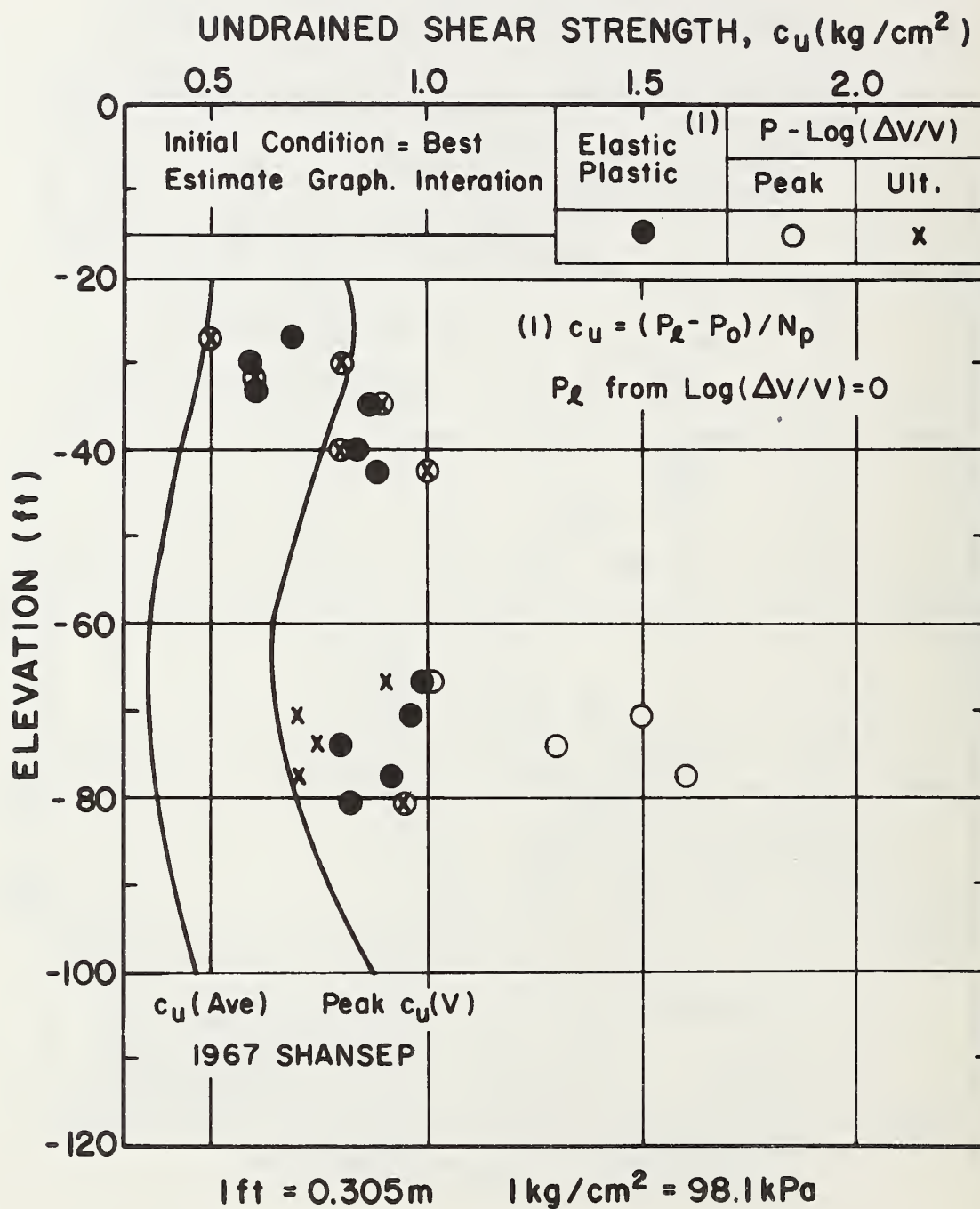
FIGURE 7-15   ELASTIC-PLASTIC AND DERIVED UNDRAINED SHEAR
STRENGTHS FROM CAMKOMETER TESTS AT STA. 263

176

8. SUMMARY, CONCLUSIONS AND RECOMMENDATIONS

8.1 BACKGROUND

The self-boring pressuremeter test (SBPT) represents one of the most exciting prospects for in situ testing of saturated cohesive soils as it has the theoretical potential of measuring the in situ total horizontal stress (σ_{ho}), and hence the coefficient of earth pressure at rest (K_o), and the complete undrained stress-strain curve, e.g. values of shear modulus (G) and the shear strength (c_u). However, serious questions exist as to whether the full potential of the SBPT can be readily achieved in practice. For example:

(1) The precise installation technique (e.g. disturbance) may not only affect the measured σ_{ho}, but also the values of G and c_u derived from data obtained during subsequent expansion of the cylindrical probe;

(2) The influence of other factors, such as variations in the rate of strain imposed within the soil mass and potential effects of partial drainage, are poorly understood;

(3) The various methods used to interpret test data often yield very different results (as might be expected in light of the above);

(4) The SBPT requires a high level of technical expertise and experience and is costly compared to most other in situ testing procedures.

The engineering profession therefore needs to further evaluate and assess the capabilities and limitations of the SBPT. The Federal Highway Administration (FHWA) recognized this research need and hence supported an experimental evaluation program wherein parameters derived from self-boring pressuremeter tests could be compared to "correct" results established via laboratory tests, other types of

177

in situ tests and/or full scale field testing. The
Massachusetts Institute of Technology (MIT) cooperated in
this research by conducting experiments in Boston Blue
clay, one of the most highly tested and best known clay
deposits in the world. This Interim report presents results
from that program. A subsequent report to be prepared by
Politecnico di Torino in Italy, under a subcontract with MIT,
will present results from similar test programs at several
other sites.

8.2 SCOPE OF WORK

8.2.1 Site Conditions

A portion of the partially completed Interstate Highway
I-95 in Saugus, Massachusetts passes through a tidal marsh
overlying a deep deposit of Boston Blue clay (BBC). The
SBPT program was conducted about 100 ft (30m) from the toe
of the embankment sections at Sta. 246 and 263 shown in
Figure 3-3.

The upper portion of the marine illitic CL clay (above
El.-70) has been precompressed via desiccation such that the
overconsolidation ratio (OCR=$\sigma_{vm}'/\sigma_{vo}'$) decreases with depth
(Figures 3-4 and 3-5). The clay below El.-70 is slightly
overconsolidated at Sta. 246 and is normally consolidated
at Sta. 263. Figure 3-12 shows the in situ total horizontal
stress (σ_{ho}) variation with depth and Figure 3-17 presents
undrained shear strength (c_u) data from various types of
field and laboratory tests.

8.2.2 Experimental Program

Part A of Table 8-1 summarizes the essential features
of the two SBPT devices employed. The CAMKOMETER (devel-
oped at Cambridge University, England) is inserted with the
cell membrane held firmly against a thick walled tube.

178

An internal gas pressure then expands the measurement cell in stress controlled increments. The PAFSOR (developed at Ponts et Chaussees, France) should be inserted with the cell inflated with water such that the average cell diameter equals that of the cutting shoe. However, due to misinformation, the initial cell volume was too small in most tests, this creating a concave shape having a minimum diameter up to 3.7% less than the diameter of the cutting shoe. After insertion, a motor pumps metered water into the measurement cell. Though a constant expansion rate of 60cc/min is typically used, this corresponding to a radial strain of about 1%/min, MIT usually employed slower rates during the initial portion of each test. This had the advantage of producing better defined P-ΔV curves, but also caused discontinuities at each change in expansion rate.

Part B of Table 8-1 summarizes the scope of the test program. Details concerning the exact procedures used for the 14 CAMKOMETER tests performed at Sta. 263 in 1973 (e.g. prior to initiation of this research) are lacking. The California Department of Transportation furnished the PAFSOR equipment, specified "standard" operating procedures, and helped conduct the tests. As noted, the cell was generally inserted with too small a volume and the expansion rate was usually increased from 6 to 20 to 60cc/min. These two factors resulted in expansion curves having various shapes as shown in Figure 4-1 and described in Section 4.2. The soil properties at the location of the 15 PAFSOR tests at Sta. 246 are well defined, whereas the 1974 embankment failure at Sta. 263 (see Figure 3-14) apparently caused a significant "softening" in the BBC at the location of the five PAFSOR tests run in 1977. The results of these latter tests are therefore ignored in this Chapter.

179

As shown in Part C of Table 8-1, MIT also installed three specially designed earth pressure cells, having variable tip geometries, at three different elevations in the clay at Sta. 246. The results supported the estimated in situ σ_{ho} profile plotted in Figure 3-12. Laboratory index, consolidation and strength tests were also run on undisturbed samples taken adjacent to the PAFSOR tests.

8.2.3 Analyses

Table 8-2 summarizes the various analyses made of the SBPT data in order to obtain estimates of in situ total horizontal stress (σ_{ho}), the limit pressure (P_l) and values of undrained modulus (G) and shear strength (c_u). The data evaluation represented a major portion of the research effort and involved the development of new procedures for: data handling and reduction; computerized plotting of the results; and analytical analyses to estimate σ_{ho} using the graphical iteration method and to derive values of G and c_u using a modified version of the Prevost-Hoeg (1975) method.

8.3 EVALUATION OF IN SITU HORIZONTAL STRESS

Evaluation of the in situ total horizontal stress (σ_{ho}) is certainly amongst the most important but difficult tasks in geotechnical engineering. If the SBPT can provide reliable estimates of σ_{ho}, this by itself represents a major development since other procedures (such as hydraulic fracturing, earth pressure cells and laboratory testing) are known to be expensive, time consuming and/or subject to considerable uncertainty. But a proper assessment of the SBPT's ability to correctly predict σ_{ho} involves several complicating factors.

Unless the self-boring process produces obvious problems, e.g. Type II, III or IV curves in Figure 4-1, one

180

has little basis for judging whether or not the soil has been disturbed and how this might affect interpreted values of σ_{ho}. For example, some of the PAFSOR tests had Type I expansion curves (the "ideal" shape), with well defined initial pressures (P_O), even though the cell had been inserted with a significant volume deficiency. This fact and other considerations discussed in Section 5.1 indicate that the initial pressure (P_O) will seldom yield a reliable estimate of σ_{ho}, even with Type I curves. Other methods used to infer σ_{ho} values, such as the inflection point (Figure 5-1) and the inverse volume approach (Figure 5-2), are strickly empirical procedures developed to interpret Menard pressure-meter data. Whether or not they can be applied to SBPT data having Type II, III or IV curves is highly questionable. Thus about the only way to judge whether or not the SBPT can reliably predict σ_{ho} is to compare results in clay deposits having known values of K_O.

MIT used the four methods of interpretation listed in Table 8-2 and described in detail in Section 5.2. The principal findings, partially summarized in Figure 8-1, are as follows:

(1) The initial pressure values from the Sta. 246 PAFSOR tests all plot well below the σ_{ho} line for $K_O = 0.5$ (a lower bound corresponding to normally consolidated clay) and generally equal or only slightly exceed the hydrostatic pore pressure. However, these low values of P_O should be expected since all but one test (El.-39.7) had volume deficiencies during self-boring ranging from 35 to 215 cc. It was surprising, though, that both the changes in P during equilibration and the final P_O appear almost unrelated to the insertion condition. Also the four tests having Type I expansion curves (denoted by the arrow) still yielded P_O values much too low.

181

(2) Although the inflection point method (see Figure 5-1) often gave significant increases above the PAFSOR initial P_o, all but one of these values still fall below the estimated in situ σ_{ho} range. In fact, most are significantly less than σ_{ho} computed for K_o=0.5 and again little relation appears between these values and the cell volume during insertion.

(3) Although all of the Sta. 263 CAMKOMETER tests had Type I curves, values of "lift-off" pressure (i.e. the pressure when strain first occurred) were ill-defined and very low, usually only 1 to 2 kg/cm^2 (100-200 kPa). Application of the empirical inverse volume method to these tests also produced results considered unsatisfactory. As shown in Figure 5-7, the predicted values are all too high in the upper overconsolidated clay (OCR=3±1), whereas in the deeper low OCR clay the values generally plot well above or below the estimated in situ σ_{ho} range.

(4) The graphical iteration method proposed by Marsland and Randolph (1977) shows great promise for estimating σ_{ho}. MIT computerized this procedure, as described in Section 5.2.5, which is based on a fairly realistic model of soil behavior. The method does require some judgement in selecting the "point of marked increase in curvature" on the expansion curve (see Figure 5-3) and is really only applicable to tests having a smooth expansion curve with a reasonably well defined curvature point. For example, results were not satisfactory in the "deep" Sta. 246 PAFSOR tests where changes in expansion rate caused an artificial "curvature point". But otherwise, the best estimate values plotted in Figure 8-1 are considered very reasonable, especially in the upper more heavily overconsolidated clay. It should also be emphasized that significant unloading

occurred during self-boring in six of the seven PAFSOR tests shown in Figure 8-1. In fact, the improper procedures used in most of the PAFSOR tests produced some advantages as one could apply the graphical iteration method to tests where the surrounding soil was known to be disturbed during self-boring.

In summary, the most important conclusions from the SBPT program in BBC are that:

(1) The initial pressure will seldom equal the in situ σ_{ho}, even with seemingly ideal tests having Type I expansion curves.

(2) The empirical inflection point and inverse volume procedures give unreliable estimates of σ_{ho}.

(3) The graphical iteration method appears very promising as a reliable procedure for predicting in situ horizontal stress, especially in overconsolidated clay. This approach may be fairly insensitive to moderate disturbance during self-boring (as certainly occurred in most of the PAFSOR tests), but requires tests having a smooth expansion curve with a reasonably well defined "point of marked increase in curvature".

8.4 EVALUATION OF LIMIT PRESSURE

There are two limit pressures (P_l): the "conventional" P_l required to double the initial cell volume (i.e. the value of P at $\Delta V/V_o=1$ or $\Delta V/V=0.5$); and the "theoretical" P_l corresponding to infinite expansion of an cylindrical cavity (i.e. the value of P at $\Delta V/V=1$). Both involve extrapolation of measured data. The research evaluated two methods for estimating the theoretical P_l, assessed the effect of varying the initial condition on the results and compared the values to the conventional P_l.

Evaluation of P_1 data from the SBPT program in BBC lead to the following conclusions:

(1) Varying amounts of disturbance during self-boring and substantial changes in the initial condition (from the initial P_O to the upper bound estimate of σ_{ho}) has relatively little effect on P_1 values extrapolated from P vs. $\log(\Delta V/V)$ plots of the Sta. 246 PAFSOR test data (Figure 6-2).

(2) The inverse volume method predicts theoretical P_1 values substantially less than those obtained by the P-log $(\Delta V/V)$ method (Figure 6-3).

(3) The $1/\Delta V=0$ method gives theoretical P_1 values less than the conventional P_1 and thus probably underpredicts the pressure at infinite expansion.

8.5 EVALUATION OF UNDRAINED STRESS-STRAIN-STRENGTH PARAMETERS

8.5.1 Analyses

Though semi-empirical procedures exist for estimating undrained modulus and strength values from pressuremeter test data, the writers restricted their evaluation to the "elastic-plastic" and "derived" methods of analysis summarized in Table 8-2 and described in Section 7.2.

Equations pertinent to the elastic-plastic analyses are:

$$G = V_O (\Delta P/\Delta V) \qquad\qquad\qquad \text{(Eq. 7-1)}$$

$$c_u = (P_1 - P_O)/N_p \qquad\qquad\qquad \text{(Eq. 7-2a)}$$

$$N_p = [1 + \ln(\frac{G}{c_u})] \qquad\qquad\qquad \text{(Eq. 7-2b)}$$

and the principal variables were selected as follows:

184

(1) Values of P_O taken as the inflection point P_O, the upper estimate of σ_{ho} and/or the best estimate from the graphical iteration method.

(2) Values of the theoretical P_1 corresponding to infinite expansion obtained by the $\log(\Delta V/V)=0$ and the $1/\Delta V=0$ methods to provide upper and lower bound estimates.

(3) Values of G obtained from the initial tangent portion of actual expansion curves using Eq. 7-1.

Note that the strength calculation requires iteration since c_u appears on both sides of Eq. 7-2.

The various "derived" solutions allow one to obtain complete stress-strain curves provided that the surrounding soil has a unique, but not pre-defined, stress-strain relationship. MIT used three types of analyses based on numerical, graphical and analytical techniques as summarized below.

(1) The subtangent method involved <u>numerical</u> differentiation of "smoothed" expansion curve data computed via Eq. 7-3.

$$\tau=\frac{1}{2}(\sigma_r-\sigma_\theta)=\frac{1}{2}\varepsilon_o(1+\varepsilon_o)(2+\varepsilon_o)dP/d\varepsilon_o \qquad (Eq.\ 7-3)$$

where σ_r and σ_θ are the radial and circumferential normal stresses and ε_o is the circumferential strain. A computer program performs the analysis and plots individual τ-ε_o data points. These plots were then used to obtain values of peak and ultimate strength [c_u(Peak) and c_u(Ult.)] and the secant shear modulus (G_{50}) at 50% of the peak strength.

(2) The P-$\log(\Delta V/V)$ method is a <u>graphical</u> procedure wherein peak and ultimate strengths are obtained via Eq. 7-4 from the slopes of semi-log plots prepared by a computer using "smoothed" data.

$$\tau=0.434dP/d\log(\Delta V/V) \qquad (Eq.\ 7-4).$$

185

(3) The Modified Prevost-Hoeg method is an <u>analytical</u> tech-
nique wherein a computer program first uses Eq. 7-5
to represent the actual expansion curve and then
differentiates that mathematical relationship to obtain
a complete stress-strain curve via Eq. 7-6 (See Section
7.2.2 for these equations which are based on the strain-
softening version of the Prevost and Hoeg (1975) rela-
tionship). The curve fitting procedure emphasizes the
initial portion of the expansion curve and hence is
better suited to evaluate c_u(Peak) and G_{50} than c_u(Ult.).

Derived values of c_u(Peak) are very sensitive to the point
on the expansion curve assumed to represent zero strain and
hence the analyses varied the initial condition as summarized
in Table 7-3.

Strengths calculated from the elastic-plastic and
derived methods of analysis are compared to two reference
strengths obtained via the SHANSEP approach, as described
in Section 3.5, and denoted as the peak c_u(V) and the c_u
(Ave.). The former corresponds to the peak $q_f = 0.5(\sigma_1 - \sigma_3)_f$
from plane strain compression tests and should represent
an upper limit for the in situ c_u (neglecting strain rate
effects). The much lower c_u(Ave.) considers strength
anisotropy and strain compatibility and is the appropriate
strength for use in circular arc stability analyses. It
also generally plots within ±10% of the measured field vane
strengths (see Figure 3-17). For the mode of failure and
strain rate imposed by the SBPT, the writers believe that
the peak c_u value derived from an <u>ideal</u> test run in Boston
Blue clay should theoretically be somewhat less than the
SHANSEP peak c_u(V), while the derived c_u(Ult.) should pro-
bably be closer to the SHANSEP c_u(Ave.).

8.5.2 Results

The results presented in Chapter 7 clearly demonstrate
that the various methods of analysis frequently yield very
different strengths and that most analyses are extremely
sensitive to the assumed initial condition. Improper
test procedures and the relatively high sensitivity of Boston
Blue clay no doubt exacerbated the problems encountered in
these analyses.   Nevertheless, the overall results rein-
force what others frequently conclude, namely that c_u values
obtained from self-boring pressuremeter tests are often
unreliable. In particular, derived peak strengths tend to
greatly exceed the in situ c_u appropriate for bearing capa-
city and stability analyses.

Regarding the three different derived methods of
analysis, the graphical P-Log($\Delta V/V$) procedure generally
yielded the most <u>consistent</u> c_u results since: (1) stress-
strain data obtained from the numerical subtangent analyses
usually exhibited excessive scatter, which complicated
the selection of c_u(Peak) and c_u(Ult.); and (2) peak
strengths computed via the Modified Prevost-Hoeg analytical
method were frequently too low due to curve fitting problems.
One must be very careful, however, in applying the P-Log
($\Delta V/V$) method to tests involving changes in expansion rate.

Figures 7-14 and 15 summarize c_u data obtained from
analyses that attempted to minimize adverse effects of im-
proper test procedures and that used methods of interpre-
tation believed most appropriate based on both theoretical
and practical considerations. Although the CAMKOMETER
tests in the upper more overconsolidated BBC give reasonable
c_u values from the elastic-plastic and derived methods of
analysis, the other results are far less satisfactory. This
is especially true in the deep "soft" clay were the derived
peak strengths are obviously much too large.   In fact,

all of the elastic-plastic c_u values and most of the derived c_u(Ult.) data plot above the SHANSEP peak c_u(V) and are therefore excessive.

The derived methods of analysis assume that the following conditions exist:

(1) The surrounding soil is homogeneous and saturated and has an unique stress-strain relationship unaffected by variations in strain rate.

(2) Expansion starts from the in situ σ_{ho} after self-boring which causes negligible disturbance to the soil.

(3) Expansion occurs at a sufficiently rapid rate to preclude any significant drainage within the soil mass.

(4) The length to diameter ratio of the measurement cell is large enough to satisfy the plane strain assumption.

In reality, the above conditions can never be completely satisfied and the writers unfortunately can offer little guidance as to which assumptions are most important.

On the positive side, the data in Figures 7-12 and 7-13 suggest that the SBPT can yield quite reasonable estimates of undrained shear modulus G_{50} for BBC. Jamiolkowski (1979) reached a similar conclusion from PAFSOR and CAMKOMETER tests at several other sites. If generally true, this finding has considerable practical significance since it is very difficult to estimate undrained modulus from laboratory tests.

8.6 PRINCIPAL CONCLUSIONS AND RECOMMENDATIONS

The CAMKOMETER and PAFSOR test programs performed in the medium to stiff, fairly sensitive Boston Blue clay having a decreasing overconsolidation ratio with depth showed that:

(1) The initial pressure P_o recorded after self-boring gives

188

a very poor (and frequently much too low) measure of the in situ total horizontal stress (σ_{ho}), even in tests with no obvious problems. The empirical inflection point and inverse volume techniques are also unreliable.

(2) The graphical iteration method proposed by Marsland and Randolph (1977) appears very promising as a reliable procedure for predicting the in situ σ_{ho}, especially in overconsolidated clay (Figure 8-1). This approach may be fairly insensitive to moderate disturbance during self-boring, but requires tests having a smooth expansion curve with a reasonably well defined "point of marked increase in curvature".

(3) Most of the tests appear to give quite reasonable esti- mates of undrained shear modulus, G_{50} (secant modulus at 50% of the peak strength).

(4) Values of undrained strength (c_u) obtained from elastic- plastic and various derived methods of analysis are very sensitive to the input data, often show consider- able scatter and generally exceed the in situ c_u appro- priate for bearing capacity and stability analyses. In particular, derived peak strengths in the deep "soft" clay are excessively high, often by a factor of two or more (Figures 7-14 and 7-15).

The reliability of the graphical iteration procedure for predicting σ_{ho} should be further evaluated via self- boring pressuremeter test programs in other clay deposits. Politecnico di Torino in Italy is currently doing this as part of its subcontract with MIT. If the results prove equally satisfactory, this will greatly enhance the prac- tical value of the self-boring pressuremeter test since prediction of in situ σ_{ho} is a very important and difficult task.

Whether or not the SBPT can ever yield reliable un- drained strength data remains uncertain since we have so

189

little understanding of the many factors that can potentially affect the results. Politecnico di Torino's test program may shed further light on this problem and thereby help indicate what experimental and theoretical research should be conducted in the future.

TABLE 8-1   EXPERIMENTAL PROGRAM

A.   SBPT EQUIPMENT AND PROCEDURES

   1.   CAMKOMETER (Mk3 Version)

      (a)   Measurement cell: diameter=6.35 cm; initial
            volume≈1200cc; covered by thin rubber membrane.

      (b)   Self-boring: cutting tool rotated by central
            drill rod driven by electric motor located at
            ground surface; rubber membrane held against
            thick walled tube via partial vacuum.

      (c)   Expansion: stress controlled by applying inter-
            nal gas pressure; transducer measures applied
            pressure; radial expansion measured via three
            internally averaged electric feelers located at
            center of cell.

   2.   PAFSOR   (PAF-72)

      (a)   Measurement cell: diameter=13.2cm; initial
            volume=3612cc; covered by thick rubber membrane
            with vertical metal strips.

      (b)   Self-boring: cutting tool rotated by hydraulic
            motor located above measurement cell; cell in-
            flated with water but actual volume during in-
            sertion was generally too small.

      (c)   Expansion: strain controlled by pumping metered
            water into cell; surface pressure gages measure
            applied pressure.

B.   SBPT PROGRAM

   1.   CAMKOMETER AT STA. 263 in 1973 (See Table 4-4)

      (a)   14 tests at El. -27 to -80.5, but 3 were "reload"
            tests.

   2.   PAFSOR At Sta. 246 in 1977 (see Table 4-2)

      (a)   15 tests at El. -19.7 to -101.7

      (b)   Initial volume too low by up to 215 cc in most
            tests

      (c)   Expansion rate increased from 6 to 20 to
            60cc/min during most tests.

Table 8-1 (continued)

3. PAFSOR AT STA. 263 in 1977 (see Table 4-3)

    (a) 5 tests at El.-54.3 to -79.3 run after embank-
         ment failure.

    (b) Initial volume too low by 165 to 215 cc.

    (c) Expansion rate increased from 6 to 60 cc/min.

C. OTHER TEST PROGRAMS

    1. Measurements of horizontal stress at Sta. 246 with
        three specially designed earth pressure cells at
        three elevations shown in Figure 3-6.

    2. Atterberg limits, incremental and constant rate of
        strain consolidation tests and unconfined compres-
        sion tests on BBC samples taken adjacent to PAFSOR
        tests.

TABLE 8-2. SCOPE OF ANALYSES OF SBPT DATA

| Parameter	Methods of Interpretation and/or Analysis	Reference	Comments*
A. In Situ Total Horizontal Stress (σ_{ho})	1. Initial pressure 2. Inflection point 3. Inverse volume 4. Graphical iteration	– Fig. 5-1 Fig. 5-2 Fig. 5-3	Applied to P " Applied to C Applied to P&C
B. Limit Pressure (P_1) (a) Conventional at $\Delta V/V_o = 1$ (b) Theoretical at $\Delta V/V = 1$	Extrapolation Using 1. P vs ΔV 2. Log P vs Log($\Delta V/V_o$) 3. P vs Log($\Delta V/V$) 4. P vs $1/\Delta V$	Fig. 6-1 Fig. 6-1 Fig. 6-1 Fig. 6-1	Not used " Also varied initial con- dition
C. Elastic-Plastic Undrained G and c_u	1. $G = V_o(\Delta P/\Delta V)$ 2. $c_u = (P_1 - P_o)/Np$	Section 7.2.1	Analysis varied P_o and P_1 $Np = [1 + \ln(G/c_u)]$
D. Derived Undrained G and Peak and Ultimate c_u	1. Numerical subtangent 2. Graphical P-Log($\Delta V/V$) 3. Analytical Modified Prevost-Hoeg	Section 7.2.2	See Table 7-3 for scope of analyses

* C=CAMKOMETER, P=PAFSOR

193
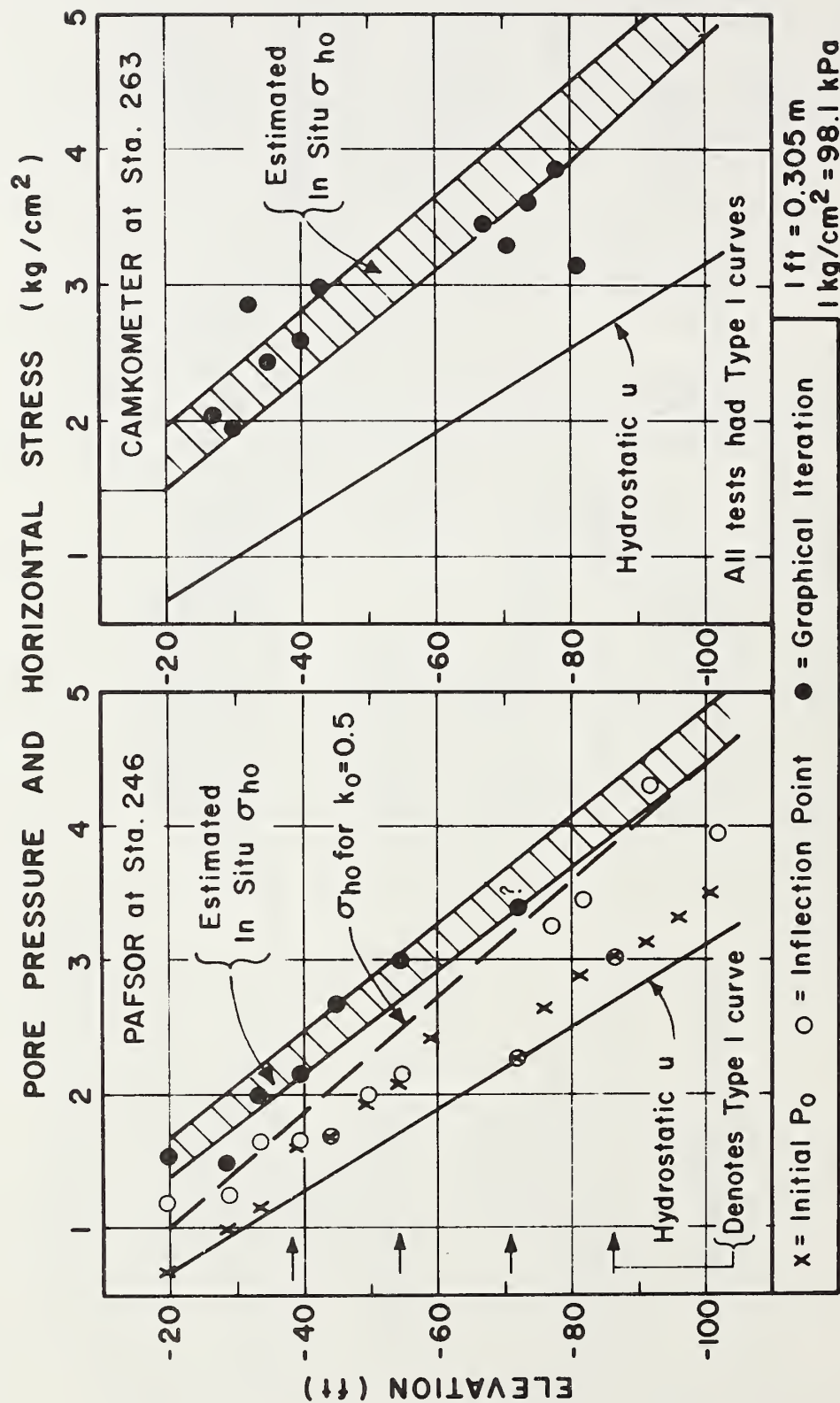
FIGURE 8-1 HORIZONTAL STRESS FROM STA. 246 PAFSOR AND STA. 263 CAMKOMETER
TESTS

194

9. REFERENCES

Note: ASCE   = American Society of Civil Engineers
         ASTM   = American Society for Testing and Materials
         JGED   = Journal of the Geotechnical Engineering
                   Division
         JSMFD   = Journal of the Soil Mechanics and Founda-
                   tions Division
         ICSMFE = International Conference on Soil Mechanics
                   and Foundation Engineering
         STP   = Special Technical Publication
         TRB   = Transportation Research Board

Arthur, J.R.F. and Roscoe, K.H. (1961), "An Earth Pressure
     Cell for the Measurement of Normal and Shear
     Stresses", Civil Engineering and Public Works Review,
     56:659, pp. 765-770.

Azzouz, A.S. (1977), "Three-Dimensional Analysis of Slopes",
     ScD Thesis, Dept. of Civil Engr., Mass. Inst. of
     Technology, Cambridge, MA 383p.

Baguelin, F., Jezequel, J.F., Le Mee, H. and Le Mehaute, A.
     (1972), "Expansion of Cylindrical Probes in Cohesive
     Soils," JSMFD, ASCE, Vol. 98, No. SM11, pp. 1129-1142.

Baguelin, F., Jezequel, J.F. and Le Mehaute, A. (1974),
     "Self-Boring Placement Method of Soil Characteristics
     Measurements," Proc. ASCE Spec. Conf. on Subsurface
     Exploration for Underground Excavation and Heavy
     Construction, Henniker, New Hampshire, pp. 312-332.

Baguelin, F., Jezequel,J.F. and Shields, D.H. (1978),
     The Pressuremeter and Foundation Engineering, Trans.
     Tech. Publ., Germany, 617 p.

Baligh, M.M. (1975), "Theory of Deep Site Static Cone
     Penetration Resistance," Res. Report R75-56, No. 517,
     Dept. of Civil Eng., Mass. Inst. of Technology,
     Cambridge, MA, 133p.

Brooker, E.W. and Ireland, H.O. (1965), "Earth Pressures
     at Rest Related to Stress History," Canadian Geo-
     technical Journal, Vol. 2, No. 1, pp. 1-15.

Gibson, R.E. and Anderson, W.F. (1961), "In Situ Measurement
     of Soil Properties with the Pressuremeter", Civil
     Engineering Public Works Review, Vol. 56, No. 658, pp.
     615-618.

Jamiolkowski, M. and Lancellotta, R. (1977), "Remarks on the Use of Self-Boring Pressuremeter in Three Italian Clays". Rivista Italiana di Geotechnica, Anno XI, No. 3, pp. 153-171.

Jamiolkowski, M. (1979), Istituto di Scienza delle Costruzioni, Politecnico di Torino, Private Communication.

Kenney, T.C. (1964), "Sea Level Movements and the Geologic Histories of the Post Glacial Marine Soils at Boston, Nicolet, Ottawa and Oslo", Geotechnique Vol. 14, No. 3, pp. 203-230.

Kinner, E.B. and Ladd, C.C. (1973), "Undrained Bearing Capacity of Footing on Clay", Proceedings, 8th International Conference on Soil Mechanics and Foundation Engineering, Moscow, Vol. 1.1, pp. 209-215.

Lacasse, S.M., Ladd, C.C. and Baligh, M.M. (1978), "Evaluation of Field Vane, Dutch Cone Penetrometer and Piezometer Probe Testing Devices", Res. Report R78-26, Dept. of Civil Eng., Mass. Inst. of Technology, Cambridge, 375p.

Ladanyi, B. (1972), "In Situ Determination of Undrained Stress-Strain Behavior of Sensitive Clays with the Pressuremeter," Canadian Geotechnical Journal, Vol. 9, No. 3, pp. 313-319.

Ladanyi, B. (1977), Discussion on "Undrained Stress-Strain-Time Behavior of Clays" by J.H. Prevost, JGED, ASCE, Vol. 103, GT8, pp. 933-934.

Ladd, C.C. (1975), "Predicted Performance of a Embankment on Boston Blue Clay I-95 Station 263", in M.I.T. (1975), Proc. of the Foundations Deformation Prediction Symposium, Vol. 2, Appendix B, 111p.

Ladd, C.C., Bovee, R.B., Edgers, L. and Rixner, J.J. (1971), "Consolidated-Undrained Plane Strain Shear Tests on Boston Blue Clay," Res. Report R71-13, No. 273, Dept. of Civil Eng., Mass Inst. of Technology, Cambridge, MA, 243 p.

Ladd, C.C. and Edgers, L. (1972), "Consolidated-Undrained Direct-Simple Shear Tests on Saturated Clays," Res. Report R72-82, No. 284, Dept. of Civil Eng., Mass. Inst. of Technology, Cambridge, MA, 354 p.

Ladd, C.C., Foott, R., Ishihara, K., Schlosser, F. and
    Poulos, H.G. (1977), "Stress-Deformation and Strength
    Characteristics", State-of-the-Art Report for Sesssion
    I, Proc. 9th ICSMFE, Tokyo, Vol. 2, pp. 421-494.

Ladd, R.S. (1965), "Use of Electrical Pressure Transducers
    to Measure Soil Pressure", Res. Report R65-48, Dept.
    of Civil Eng., Mass. Inst. of Technology, Cambridge,
    MA, 79 p.

Marr, W.A. (1974), "In Situ Measurement of Stresses in
    Soil," Ph.D. Thesis, Dept. of Civil Eng., Mass.
    Inst. of Technology, Cambridge, MA, 241 p.

Marsland, A. and Randolph, M.F. (1977), "Comparison of the
    Results from Pressuremeter Tests and Large In Situ
    Plate Tests in London Clay", Geotechnique, Vol. 27,
    No. 2, pp. 217-243.

M.I.T. (1975), "Proceedings of the Foundation Deforma-
    tion Prediction Symposium," US Dept. of Transportation,
    Federal Highway Administration, 2 Vol.

Massarsch, K.R. (1975), "New Method for Measurement of
    Lateral Earth Pressure in Cohesive Soils," Canadian
    Geotechnical Journal, Vol. 12, No. 1, pp. 142-145.

Massarsch, K.R., Holtz, R.D., Holm, B.G. and Fredriksson,
    A. (1975), "Measurement of Horizontal In Situ
    Stresses," Proc. ASCE Spec. Conf. on the In Situ
    Measurement of Soil Properties, Raleigh, Vol. I,
    pp. 266-286.

Menard, L. (1956), "An Apparatus for Measuring the Strength
    of Soils in Place," M.Sc. Thesis, Dept. of Civil
    Eng., Univ. of Illinois, Urbana.

Palmer, A.C. (1972), "Undrained Plane Strain Expansion
    of a Cylindrical Cavity in Clay: A Simple Inter-
    pretation of the Pressuremeter Test," Geotechnique,
    Vol. 22, No. 3, pp. 451-457.

Prevost, J.H. (1976), "Undrained Stress-Strain-Time
    Behavior of Clays," JGED, ASCE, Vol. 102, No. GT12,
    pp. 1245-1259.

Prevost, J.H. and Hoeg, K. (1975), "Analysis of Pressure-
meter in Strain-Softening Soil," JGED, ASCE, Vol.
101, No. GT8, pp. 717-732.

Schmertmann, J.H. (1975), "Measurement of In Situ Shear
Strength," State-of-the-Art Report, Proc. ASCE Spec.
Conference on In Situ Measurement of Soil Properties,
Raleigh, Vol. II, pp. 57-138.

Tavenas, F.A., Blanchette, G., Leroueil, S., Roy, M.,
and LaRochelle, P. (1975), "Difficulties in the
In Situ Determination of K_O in Soft Sensitive Clays",
Proc. ASCE. Spec. Conf. on In Situ Measurement of
Soil Properties, Raleigh, Vol. I, pp. 450-476.

Terzaghi, K. and Peck, R.B. (1967), Soil Mechanics in
Engineering Practice, John Wiley & Sons, 2nd ed.,
New York, 729 p.

VanWambeke, A. and d'Hemricourt, J. (1975), "Courbes
Pressiometriques Inverses: Methode D'Interpreta-
tion de L'essai Pressiometrique", Soils-Sols, No. 25,
pp. 15-25.

Vivatrat, V. (1978), "Cone Penetration in Soft Clays",
Sc.D. Thesis, Dept. of Civil Eng., Mass. Inst. of
Technology, Cambridge, MA, 427p.

Windle, D. and Wroth, C.P. (1977), "In Situ Measurement
of the Properties of Stiff Clays", Proc. 9th ICSMFE,
Tokyo, Vol. I, pp. 347-352.

Wissa, A.E.Z., Martin, R.T. and Garlanger, J.E. (1975),
"The Piezometer Probe", Proc. ASCE Spec. Conf.
on In Situ Measurement of Soil Properties, Raleigh,
Vol. I, pp. 536-545.

Wood, D.M. and Wroth, C.P. (1977), "Some Laboratory
Experiments Related to the Results of Pressuremeter
Tests", Geotechnique, Vol. 27, No. 2, pp. 181-201.

Wroth, C.P. (1975), "In Situ Measurement of Initial
Stresses and Deformation Characteristics," State-of-
the-Art Paper, Proc. ASCE Spec. Conf. on In Situ
Measurement of Soil Properties, Raleigh, Vol. II,
pp. 181-230.

Wroth, C.P. and Hughes, J.M.O. (1973), "An Instrument for the In Situ Measurement of the Properties of Soft Clays," Proc. 8th ICSMFE, Moscow, Vol. 1.2, pp. 487-494.

Wroth, C.P., and Hughes, J.M.O. (1974), "Development of a Special Instrument for the In Situ Measurement of the Strength and Stiffness of Soils," Proc. ASCE Spec. Conf. on Subsurface Exploration for Underground Excavation and Heavy Construction, Henniker, New Hampshire, pp. 295-311.

APPENDIX A. EARTH PRESSURE CELL TEST PROGRAM

A.1 DESCRIPTION OF EARTH PRESSURE CELLS

Figure A-1, A-2, A-3 and A-4 show the four types of devices used. All consist of an elongated flat plate, 9 mm in thickness, with a width to thickness ratio on the order of 13. The pressure cell itself is filled with fluid (water in the present test program) backpressured to approximately 2 kg/cm^2 (196 kPa) and is hydraulically connected to a Tyco pressure transducer (14 kg/cm^2 (1400 kPa) capacity). The difference between the four types of cells used lies in the tip geometry:

Figure	Tip Geometry
A-1	Symmetrical tip, with 20° tip angle
A-2	Asymmetrical tip, with 20° tip angle
A-3	Symmetrical tip, with 40° tip angle
A-4	Enlarged tip, with 20° tip angle

The blunt (40°) symmetrical tip design was in fact an alternation on the asymmetrical 20° tip after the latter design proved unable to withstand the stress imposed on the steel housing during penetration (the asymmetrical tip geometry caused formation of a crack in the top weld during insertion of the device and the flat plate was bent lengthwise at an angle of about 10°). The asymmetrical tip was therefore reshaped to a symmetrical tip with a 40° angle. Three holes were drilled in the plate to enable addition of enlarged tips with varying thickness ratios if desired.

The enlarged cell was designed with the aim of obtaining a lower bound value for σ_h (and K). However the results proved inconclusive as unrealistically low values of σ_h were measured with this device.

The enlarged cell was also equipped with a course porous stone connected to a transducer to measure pore pressures. If properly deaired, the stone and transducer setup can measure excess pore pressures generated during penetration and monitor their dessipation with time. In any case, the equilibrium (in situ) pore pressures can be measured.

Each device was equipped with a thermistor mounted in the vicinity of the pressure transducers to record temperature changes since the transducer zero can shift significantly with temperature. Figure A-5 presents the calibration of the transducer zero with temperature. These were obtained after assembly of the device in the MIT laboratory after the field test program.

The pressure transducers were calibrated piror to mounting in the earth pressure devices. After assembly, new calibration curves were obtained by pressurizing the cells in a tank filled with water. Table A-1 summarizes the pressure and thermistor calibrations. The change in slope of the transducer before and after assembly in the earth pressure devices (called rigidity factor in the table) reflects compliance in the volume (measuring system) between the cell filled with water and the transducer. This compliance is the combined effect of imperfect deairing of the water and deflexion of the cell membrane.

A.2 TEST PROCEDURES

The following summarizes the steps taken to measure the total horizontal stress at Sta. 246 in March 1978.

1. Device Insertion Procedure

   a) Cells and sensors were deaired, assembled in MIT Laboratory.

b) Cells were calibrated in water pressurized up to 4.6 kg/cm^2 (450 kPa)

c) In field, cells were placed in circulating drilling mud to allow temperature equilibration during hole preparation.

d) Test hole was augered down to clay elevation and 6 in. (15 cm) casing was driven to hold sand walls (down to El.-15).

e) Test hole was washed to specified depth, using drilling mud (mud density was measured several times).

f) Device was lowered* in hole to within one inch (2.5 cm) of bottom and temperature allowed to equilibrate (until constant thermistor and stress readings were obtained). This step is mandatory since electronic zero shifts with temperature changes.

g) Zero reading was checked with weight of mud above cell.

h) Orientation of cell was kept perpendicular to longitudinal axis of embankment.

2. Device Penetration

i) After equilibration, device was pushed a distance between 1.5 and 6 ft (0.5 to 1.8 m) below bottom of washed hole, either by hand or by small pressure from drilling rig. (see Table A-2 for actual penetration depths).

j) During entire operation, total horizontal pressure, (and pore pressure if applicable) was recorded continuously. Temperature was read at regular intervals.

---

* Symmetrical cell: AW drilling rod used
Asymmetrical cell: NW drilling rod used (added stability against buckling)
Enlarged cell: NW drilling rod used (larger diameter needed since larger electrical and polyethylene leads used).

k) Drill rods were retrieved in the case of the symmetrical and enlarged cells and replaced by PVC 2 and 4 in dia. (5 and 10 cm) casing (to prevent hole cave-in over cell and possible settlement of cell under weight of rods.

l) In the case of the asymmetrical cell, drill rod was left in hole, but a clamp was fixed to top of casing cap to prevent settlement of cell under weight of rod.

m) Holes were filled with mud and sealed (to protect against vandalism).

3. Data Recording

n) Measurements were made regularly for the first several hours after insertion, then daily, then every two days.

o) Data were reduced and plotted immediately to check functioning of sensors and length of time required for equilibration.

4. Retrieval of Device

p) Drill rods were lowered in hole and screwed on device.

q) Device was gently pulled up inside the hole.

r) Data were recorded during the operation

s) Cells were rezeroed and recalibrated in MIT laboratory.

A.3   Test Program

Nine measurements of total horizontal stress (σ_h) and three of in situ pore pressures (u) were scheduled at three different elevations (El. -30, -50, -80) at Sta. 246. Figure 3-6 has shown already the location of each test and Section 3.4 discussed the values of σ_h obtained with the

203

symmetrical 20° tip cell. Table A-2 summarizes the entire
test program.

A.4   TEST RESULTS

A.4.1   <u>Stresses During Penetration</u>

Figures A-6 to A-8 summarize the horizontal stresses
and pore pressure generated during penetration of the earth
pressure devices at the three elevations investigated. In
Figure A-6 (first push at El.-30), penetration was inter-
rupted a few times, and partial dissipation of σ_h occurred*.
However, in the two subsequent pushes, the devices were
inserted continuously at a constant rate. In Figure A-7,
the relative increase in pore pressure, (u), and total
horizontal stress, (σ_h), as measured by the enlarged cell,
indicates that the pore pressure lags behind the total
stress, perhaps due to an hydraulic short which allowed
water to flow upward above the earth pressure cell plate
into the washed borehole. This problem appears to atten-
uate after 1.75 ft (0.5 m) insertion distance. Figure A-8
seems to confirm this hypothesis as the increase in pore
pressure in much less than the increase in total horizontal
stress for the first 1.5 ft (0.5 m) insertion. After a
2 ft (0.6 m) insertion, the pore pressure becomes approxi-
mately equal to the total stress, indicating that the open-
ing behind (above) the cell closed up and that a steady
state condition was reached. Of particular interest though,
the sharp 20° symmetrical cell developed a higher initial
pressure than the blunt 40° cell at El.-80 (soft Boston
Blue clay), in disagreement with the behavior observed at
El.-50 (Figure A-7) in the medium Boston Blue clay.

---

*   Due to an electronic connection loss after insertion,
    the enlarged cell had to be pulled up and pushed in a
    second time, at a larger depth, which explains the two
    sets of readings for this cell.

A.4.2 Equilibration Curves

Figures A-9 to A-11 summarize the equilibration curves for σ_h and u as measured by the earth pressure cells at El. -30, -50 and -80 respectively. The data indicate the following:

(1) At El.-30, the much longer time required to reach equilibrium with the enlarged cell reflects the increased disturbance caused by insertion of the larger tip. The relatively small changes in σ_h observed after long periods of time may be due to zero shifts of the transducer, variations in the input voltage, moisture permeating the system and/or minor stress redistributions around the cells.

(2) At El.-50, the symmetrical 20° tip essentially equilibrated in 24 hours. The blunt tip (40°) took more than 100 hours to reach equilibrium, and the enlarged tip required about 250 hours. The soil disturbance was therefore very much a function of the tip geometry. The equilibration times also increased as the clay deposit became less precompressed, probably because of a increase in the coefficient of consolidation at the lower overconsolidation ratio.

(3) At El.-80, the two symmetrical tip cells reached equilibrium at essentially the same time (about 100-200 hr) and exhibited nearly indentical dissipation behavior. These results appear reasonable since previous studies (Massarsch, 1975; Massarsch et al., 1975; Tavenas et al., 1975) mention times on the order of 4 to 10 days required for equilibration in soft clays (they used earth pressure devices working on the same general principle as those used by MIT, but with different geometries, pressure recording systems and insertion procedures).

The long term behavior of the 40° symmetrical cell was exceptionally stable over the three month measurement period and the final reading remained unchanged upon recalibration of the cell after its removal from the ground. The 20° symmetrical cell, however, showed a consistent increase in stress over the same period, perhaps due to a slight zero shift in the measurement system. Moreover, recalibration after removal produced a very large decrease in σ_h (almost 1 kg/cm^2=98 kPa). The removal and disassembly of the cell and drying of the transducer may have caused a significant change in the "zero reading". Based on the experience with the 40° symmetrical cell and the enlarged cell (to be discussed), the writers conclude that the final reading in the ground is slightly too high, the recalibrated result is much too low and a value of τ_h=3.85 kg/cm^2 (378 kPa) appears reasonable.

The σ_h cell of the enlarged tip device certainly became defective. As shown in Figure A-11, σ_h decreased continuously with time after 100 hours and eventually recorded values much less than the in situ pore pressure. The cell may have developed a slight leak such that the original backpressure (about 2 kg/cm^2=196 kPa) and hence "zero reading" decreased with time. Recalibration after removal did indeed show a much lower "zero reading", though the calibration factor remained essentially unchanged. Moreover, the value of σ_h equal to 2.9 kg/cm^2 (285 kPa) based on the recalibration (after removal of the device from the ground) appears quite reasonable.

Finally, the pore pressure measurements remained very stable with little change upon recalibration.

Ground temperatures recorded during the entire testing program appeared uniform and averaged 10.5°C between El.-30 and -80. Measurements were very consistent, as shown below:

Date	El.	Ground Temperature(°C)		
		Sym. 20°	Asym. 20° Sym. 40°	Enl. 20°
April 1978	-30	10.9	10.8	10.2(El.-37)
May 1978	-50	10.7	11.2	9.9
June-Sept. 1978	-80	10.8	11.0	10.3

A.4.3 Predicted Stresses

Table A-3 gives an example of the computations made to predict values of σ_h and K at various elevations at Sta. 246. Figure 3-12 plots the range of predicted stress versus elevation and Figure 3-13 presents the predicted K values at Sta. 246 assuming no excess pore pressures at the 200 ft (60 m) offset after the 1967 loading and 1974 unloading (reasonable based on measured u data). The range presented reflects uncertainties in (1) maximum past pressures, (2) K_O vs OCR (Figure 3-10) and (3) stress increases due to embankment construction.

A.4.4 Comparison of Measured and Predicted In Situ Horizontal Stress, Pore Pressure and Coefficient of Horizontal Stress

Figure A-12 compares the measured and predicted total horizontal stress at Sta. 246. At. El.-30, the total horizontal stress measured by the symmetrical and asymmetrical 20° tip cells fell within the predicted σ_h range based on laboratory data, while the enlarged tip yielded a value much too low. At El.-50, both symmetrical tips resulted in equilibrium values within the range of

207

predicted σ_h, but the 40° tip gave a lower value than the 20° tip, perhaps due to increased disturbance. Again the enlarged tip gave results much too low. At El.-80, the sharp 20° symmetrical tip resulted in an equilibrium σ_h within the range predicted from laboratory data whereas the blunt 40° symmetrical tip fell below the predicted range. The difference between the two symmetrical cells is even more pronounced than at El.-50. The enlarged tip gave an extremely low value, even after making a correction for the possible zero shift.

The equilibrium pore pressure at El.-80 indicates an artesian head of 6.5 ft (2 m) in the till at El.-148 if the water table is taken at El. 0 (as observed in 1978). For a water table at El.+2.5 (as observed in 1977), the measured u_o at El.-80 falls slightly above hydrostatic conditions.

Figure 3-13 summarizes the values of K (equal to σ_h'/σ_v') obtained from the three series of measurements with the earth pressure cells. The results of the symmetrical 20° tip compare very well with the best estimate of K_o obtained from laboratory measurements and the stress history as previoulsy noted. The range in K_o primarily reflects possible variations in the laboratory K_o vs OCR and the maximum past pressure. The asymmetrical 20° tip at El.-30 also gave a K well within the predicted range whereas K from the symmetrical 40° tip fell at or below the lower limit of the predicted range. The enlarged tip always gave K values considered much too low.

208

TABLE A-1   CALIBRATIONS OF EARTH PRESSURE CELL TRANSDUCERS AND THERMISTORS

Tip Geometry	Transducer Number	Measurement	Calibration(Kg/cm²/mv/v) Before Assembly	After Assembly	Rigidity Factor	Thermistor Calibration Curve (C°)
Sym.20°	86846	σ_h	0.7058	0.7314	96.5%	$77.27-22.003/n(K\Omega)$
Asym.20° Sym.40°	86951	σ_h	0.7070	0.7298 0.7228	96.9% 97.8%	$74.45-22.003ln(K\Omega)$
Enl.20°	86964	σ_h	0.7039	0.7722	91.2%	$72.36-22.003ln(K\Omega)$
Enl. 20°	76529	u	0.7058	0.7725	91.4%	

1 kg/cm² = 98.1 kPa

209

TABLE A-2. EARTH PRESSURE CELL TEST PROGRAM IN SAUGUS
(March to September 1978)

Date	Hole No.	Sta.	Tip Geometry	El. bottom of hole (ft)	Penetration Depth (ft)	El. of ₵ of cell (ft)	El. of porous stone (ft)
1978							
3/30	EPC-1	245+70	Sym. 20°	-28.0	3.0	-30.3	—
4/1	EPC-2	245+95	Asym. 20°	-28.0	2.5	-29.8	—
3/30	EPC-3*	246+10	Enl. 20°	-28.0	3.0	-30.3	—
3/31	EPC-3	246+10	Enl. 20°	-34.5	3.5	-37.3	-37.3
5/13	EPC-3	246+10	Sym. 20°	-48.6	5.2	-53.1	—
5/14	EPC-1	245+70	Sym. 40°	-48.0	5.5	-52.8	—
5/13	EPC-2	245+95	Enl. 20°	-48.5	3.0	-50.8	-50.5
6/13	EPC-3	246+10	Sym. 20°	-74.5	5.0	-78.8	—
6/14	PEC-1	245+70	Sym. 40°	-74.5	5.75	-79.6	—
6/13	EPC-2	245+95	Enl. 20°	-74.5	6.0	-70.8	-79.6

1 ft=0.305 m
*Loss of electronic signal on 3/30/78. Cell was retrieved, repaired and reinstalled on next day.

TABLE A-3.   SAMPLE CALCULATION FOR HORIZONTAL STRESS
AT STA. 246 (El.-30)

I.   In Situ Stresses before construction

σ_{vo} = 1.90 kg/cm^2 (Figure 3-7)

u = 0.95 kg/cm^2 (measured in 1978)

σ'_{vo} = 0.95 kg/cm^2

σ'_{vm} = 3.10-4.0 kg/cm^2 (Figure 3-8)

OCR = 3.26-4.21

K_o = 0.81-1.02 (Figure 3-10)

II.   Horizontal Stress After Embankment Construction

Before construction

σ'_{vo} = 0.95 kg/cm^2

σ'_{ho} = K_o σ'_{vo} = 0.77-0.97 kg/cm^2

u = 0.95 kg/cm^2 (measured)

Construction

$\Delta\sigma_h$ = 0.04-0.15 kg/cm^2 ($\Delta\sigma_v \simeq$ 0.0 kg/cm^2)

σ_h = σ'_{ho} + u + $\Delta\sigma_h$ = 1.67-2.07 kg/cm^2

III.   Stresses in 1978

Assume no excess pore pressures due to embankment loading in 1967-1969 and unloading in 1974.

σ'_{vo} = 0.95 kg/cm^2

σ'_{ho} = σ'_{ho} (1967) + $\Delta\sigma$ = 0.81 - 1.12 kg/cm^2

IV.   Predicted "K_o" in 1978

$$K_o = \frac{\sigma'_{ho}\ (1978)}{\sigma'_{vo}\ (1978)} = \frac{0.81-1.12}{0.95} = 0.85-1.18$$

1 kg/cm^2 = 98.1 kPa

211

Transducer
Housing Pipe — Weld

1 Tyco 200 psi
transducer and
1 thermistor

—A-rod

44

42

0.9

1.3

4
3

SECTION A-A
(not to scale)

84

345

565

960

9

40

dimensions in mm

1 in.=25.4mm
1 psi=6.9kPa

25

20°

114.5
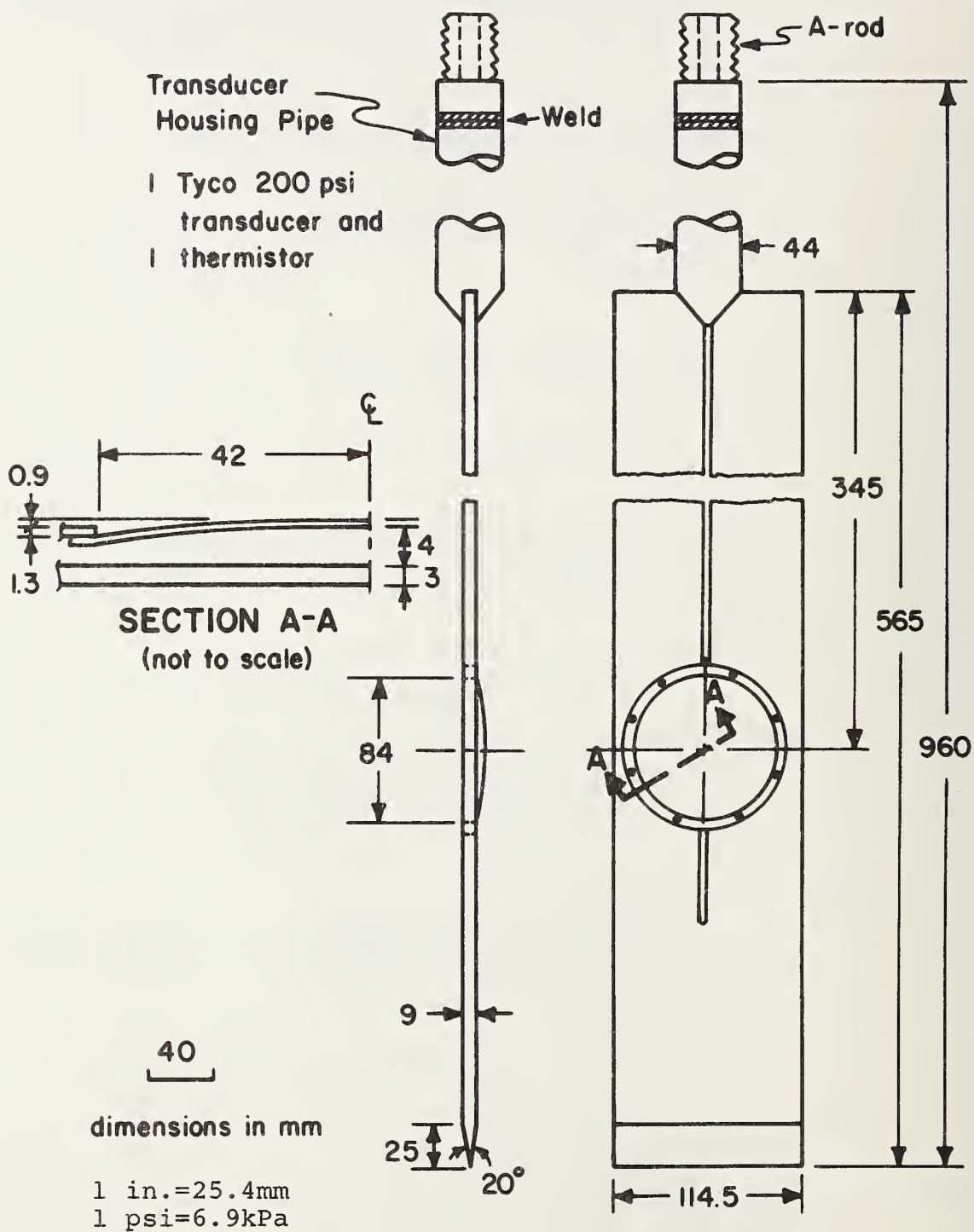
FIGURE A-1   SYMMETRICAL 20° TIP EARTH PRESSURE CELL

212

Transducer
Housing Pipe

1 Tyco 200 psi
  transducer &
1 thermistor

A-rod

Weld

44

42

1.2

.4

1.4

3

SECTION A-A
(not to scale)

243

958

563

84

40

dimensions in mm

1 in.=25.4mm
1 psi=6.9kPa

9

25   20°

114
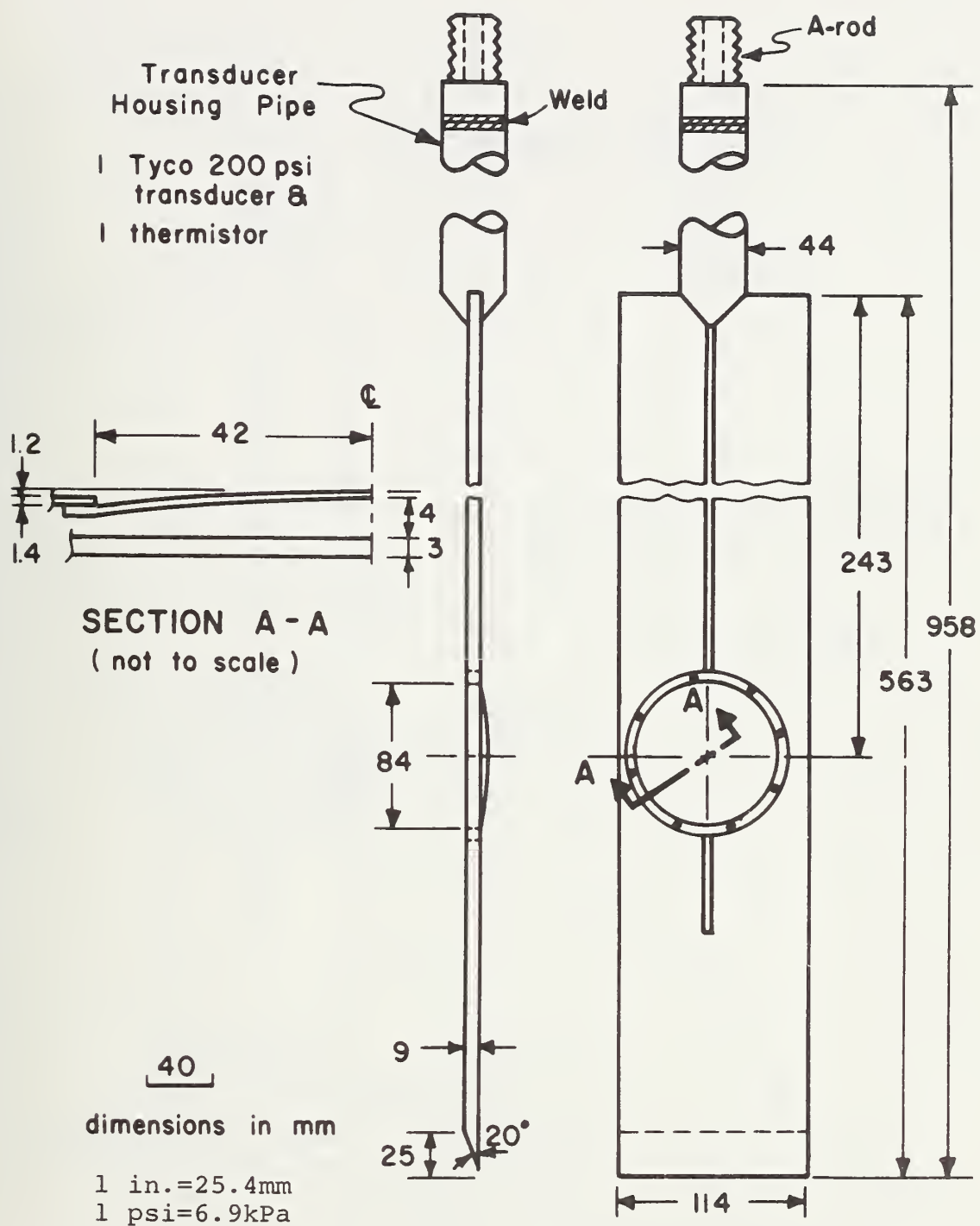
FIGURE A-2   ASYMMETRICAL 20° TIP EARTH PRESSURE CELL

213
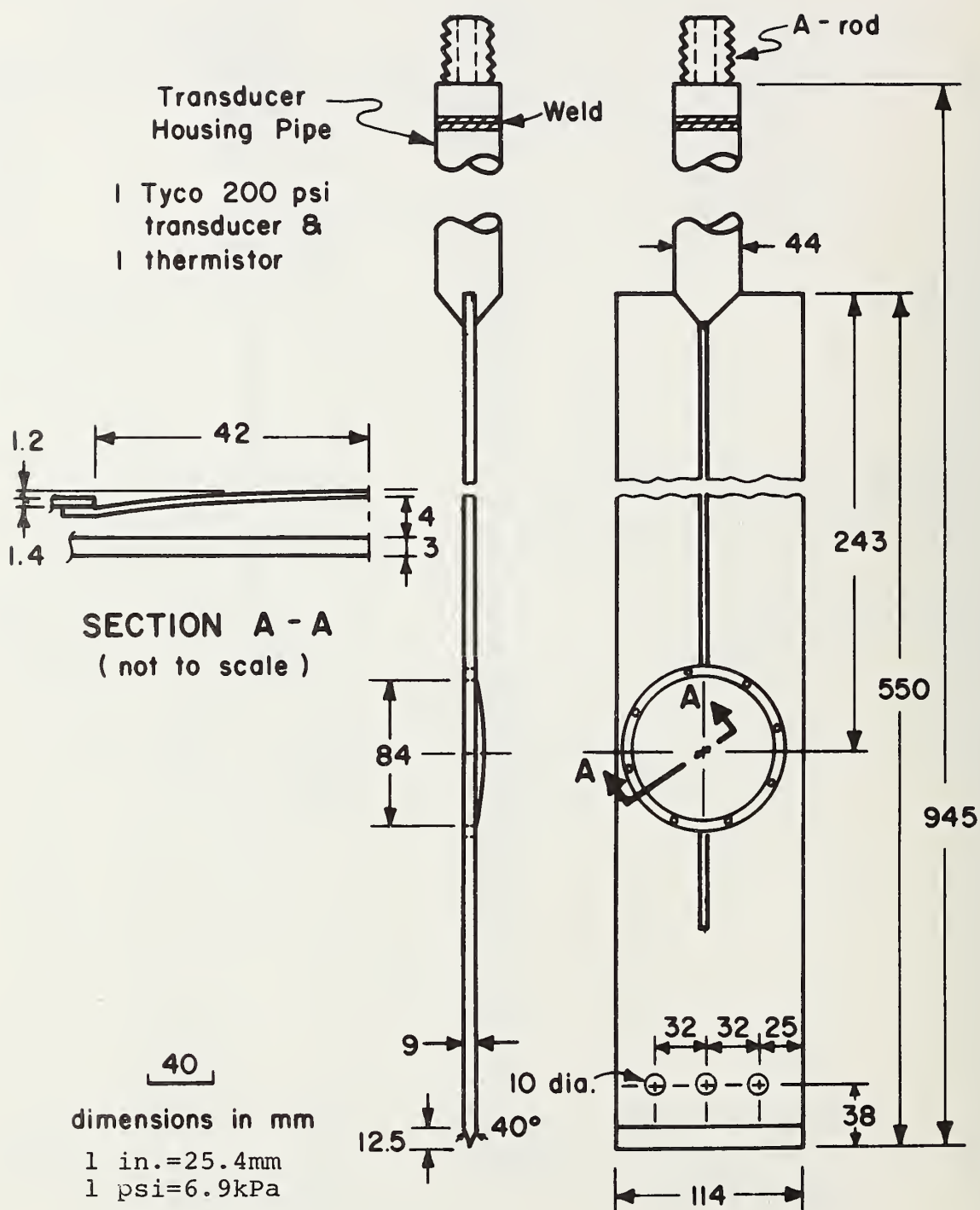
FIGURE A-3 SYMMETRICAL 40° TIP EARTH PRESSURE CELL
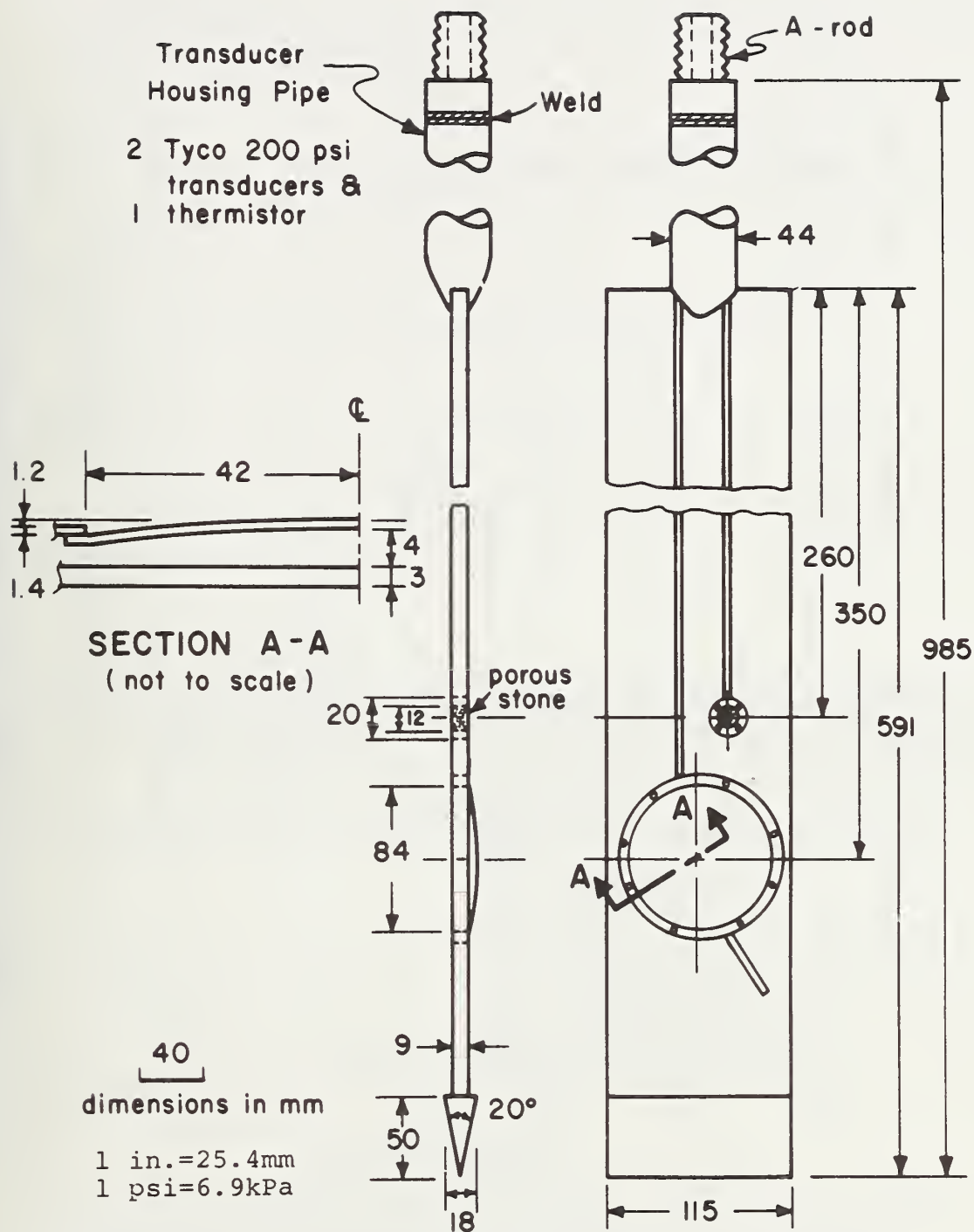
FIGURE A-4 ENLARGED 20° TIP EARTH PRESSURE CELL

215
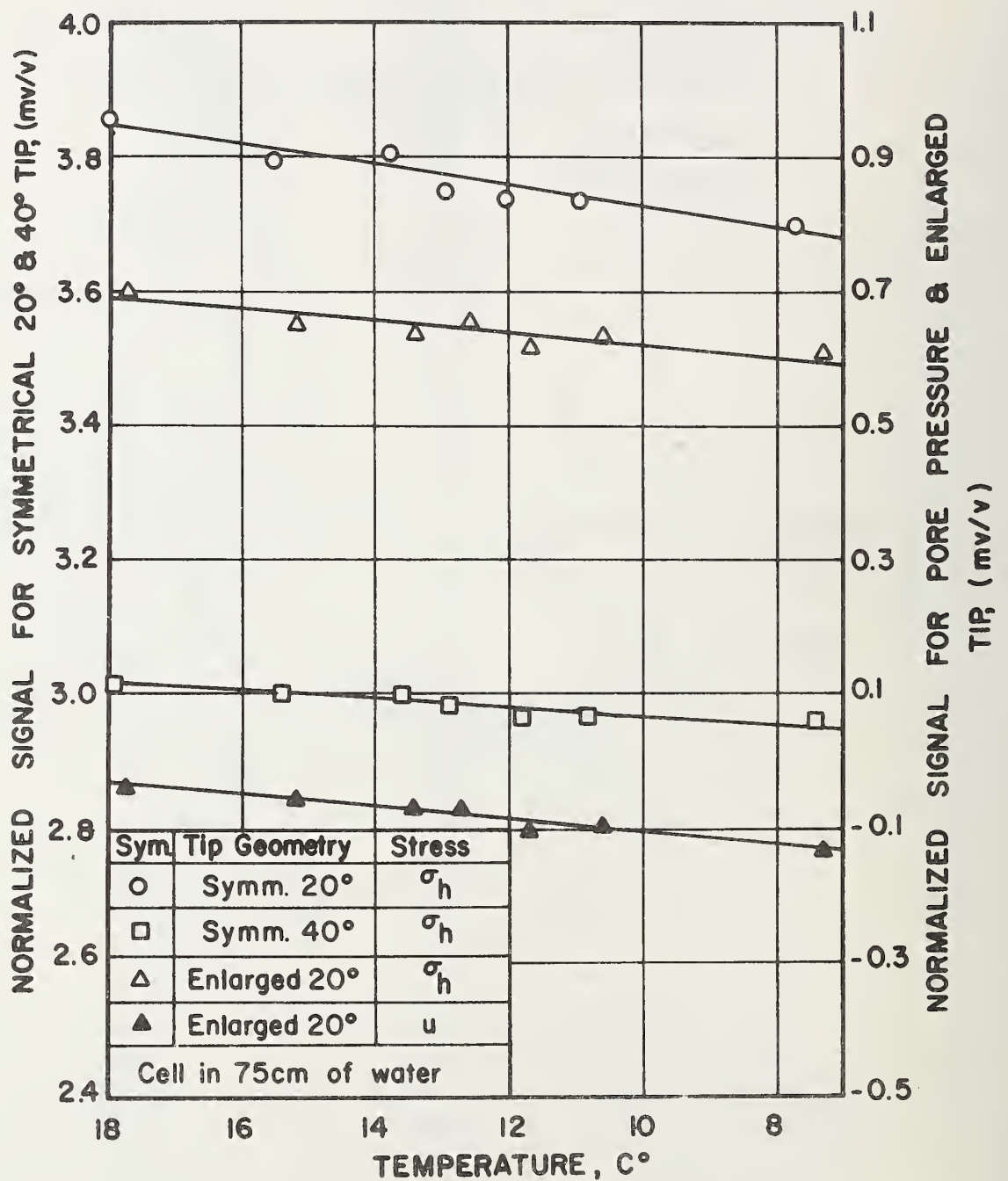
FIGURE A-5 TRANSDUCER ZERO SHIFT WITH TEMPERATURE
OF EARTH PRESSURE CELLS
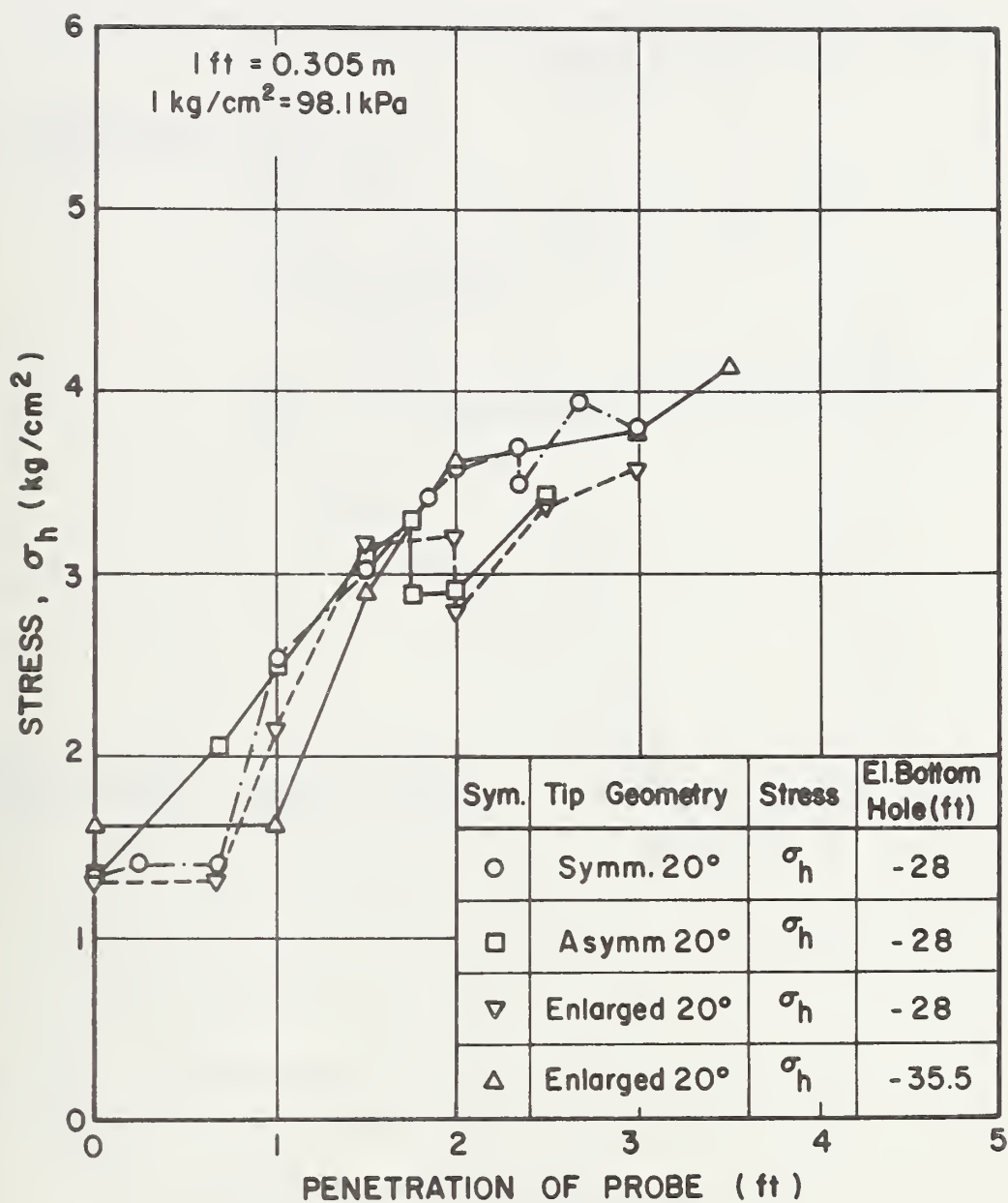
FIGURE A-6   STRESS INCREASE DURING EARTH PRESSURE CELL
                    PENETRATION AT EL.-30
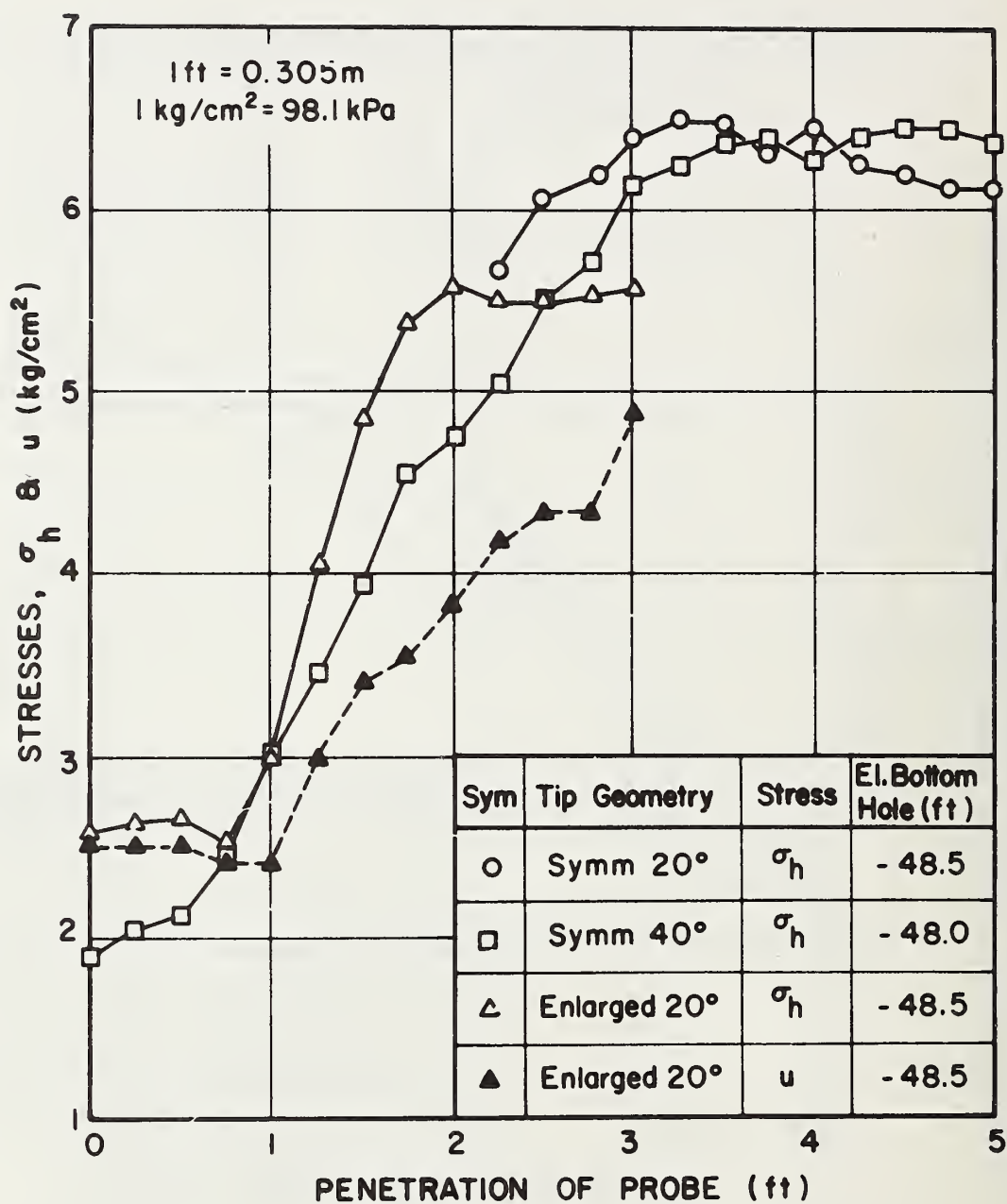
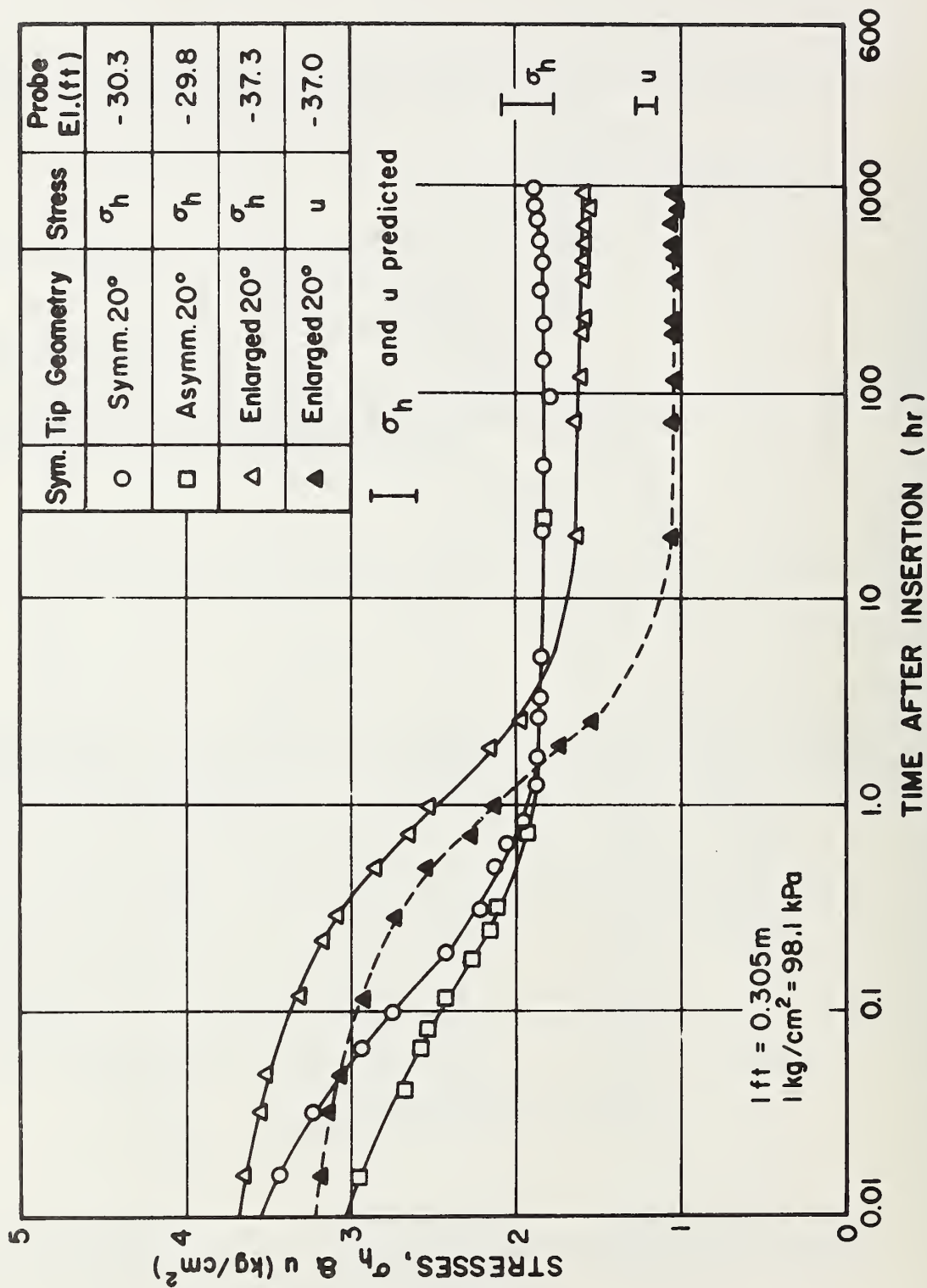FIGURE A-7   STRESS INCREASE DURING EARTH PRESSURE CELL
PENETRATION AT EL.-50

218
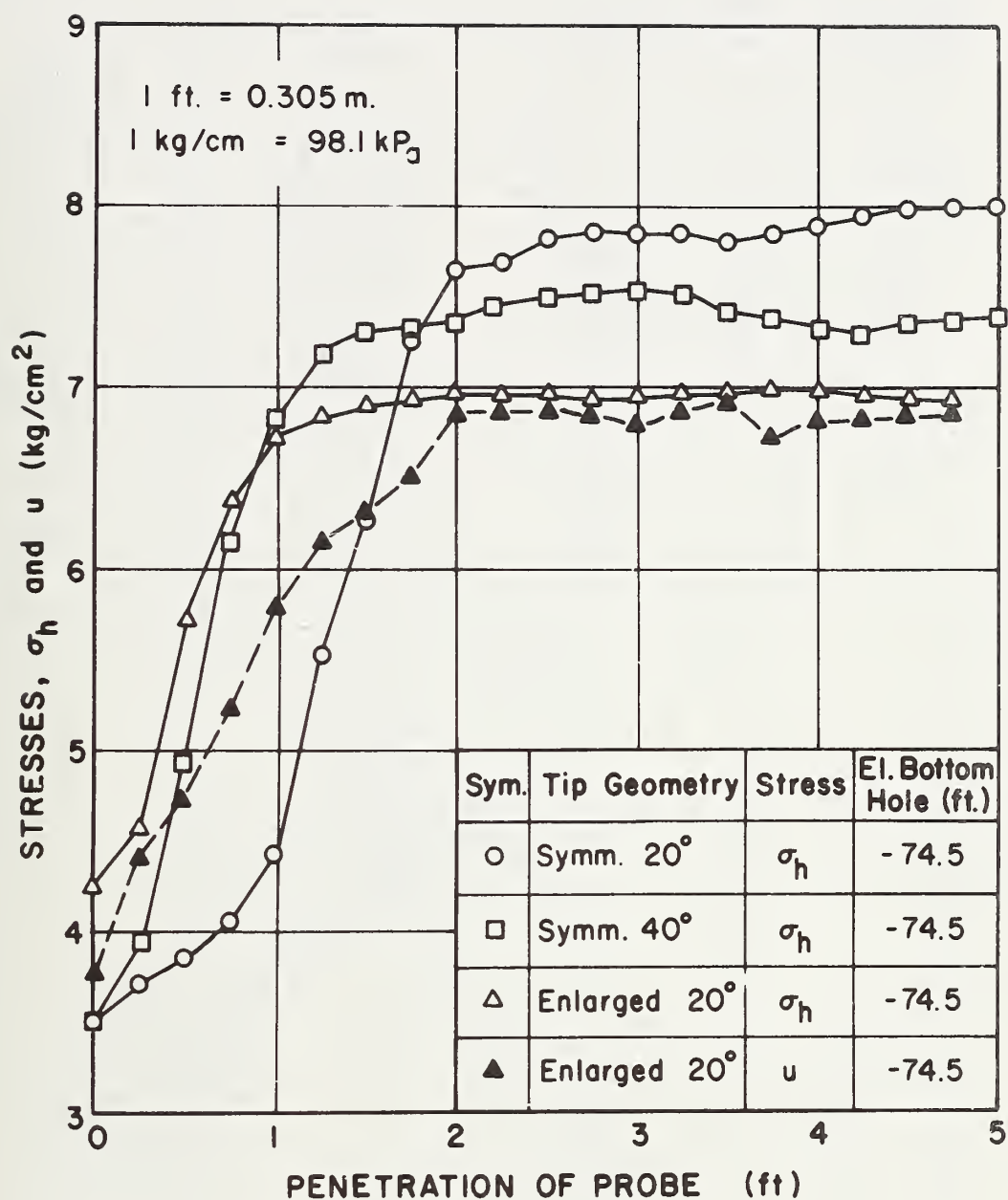
FIGURE A-8   STRESS INCREASE DURING EARTH PRESSURE CELL
PENETRATION AT EL.-80

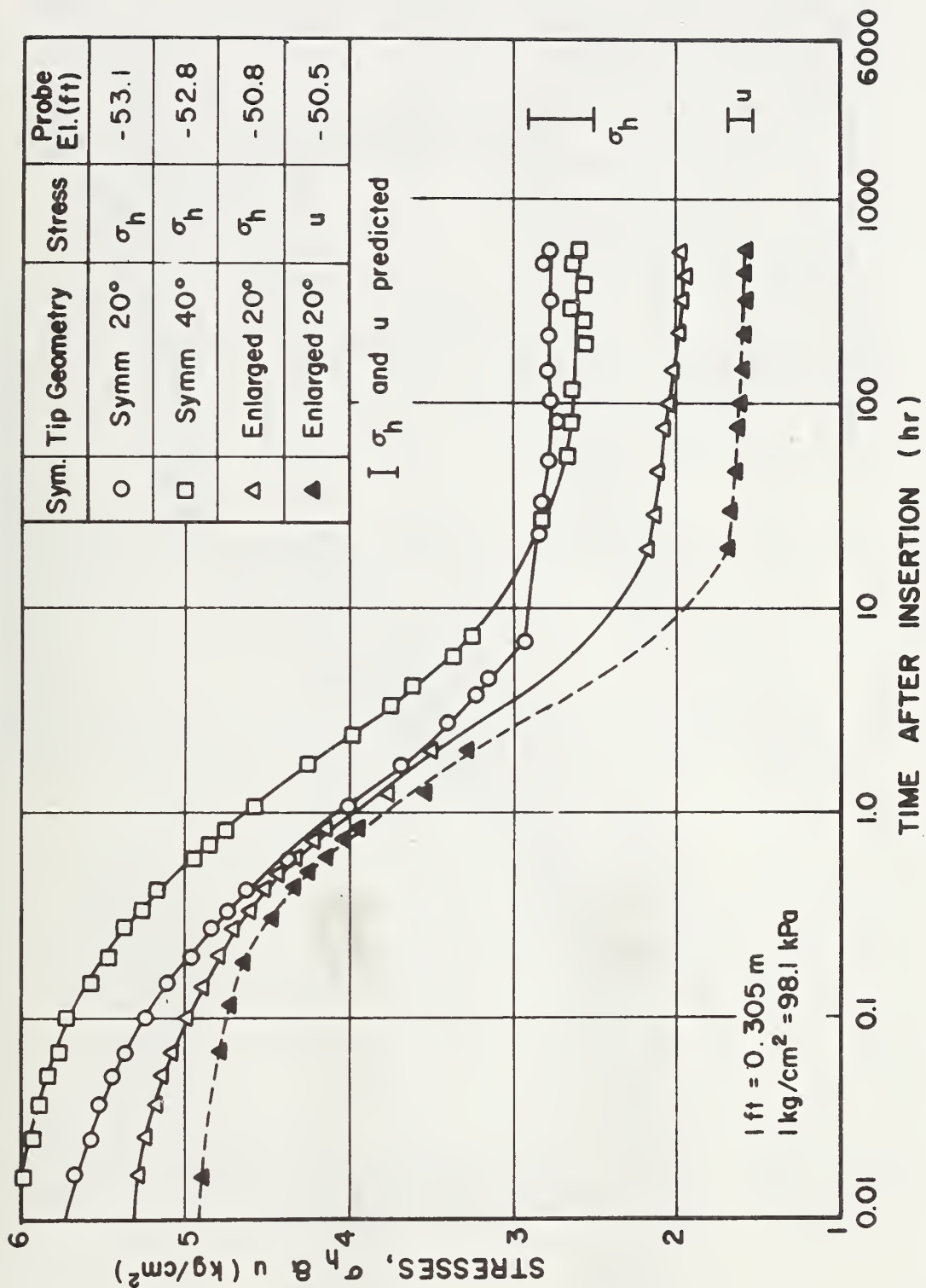FIGURE A-9   TOTAL HORIZONTAL STRESS AND PORE PRESSURE EQUILIBRATION AT El.-30

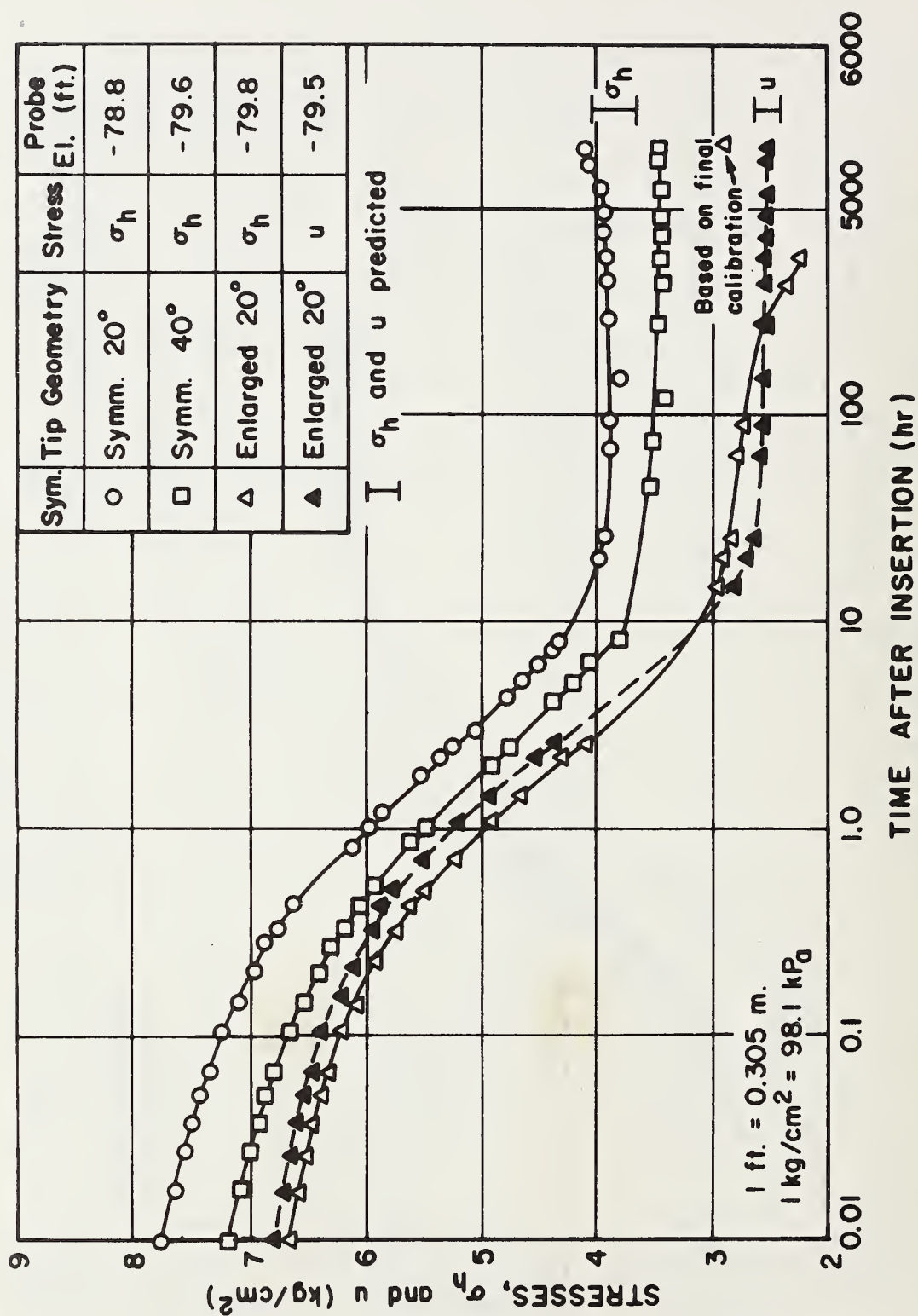FIGURE A-10   TOTAL HORIZONTAL STRESS AND PORE PRESSURE EQUILIBRATION AT EL.-50

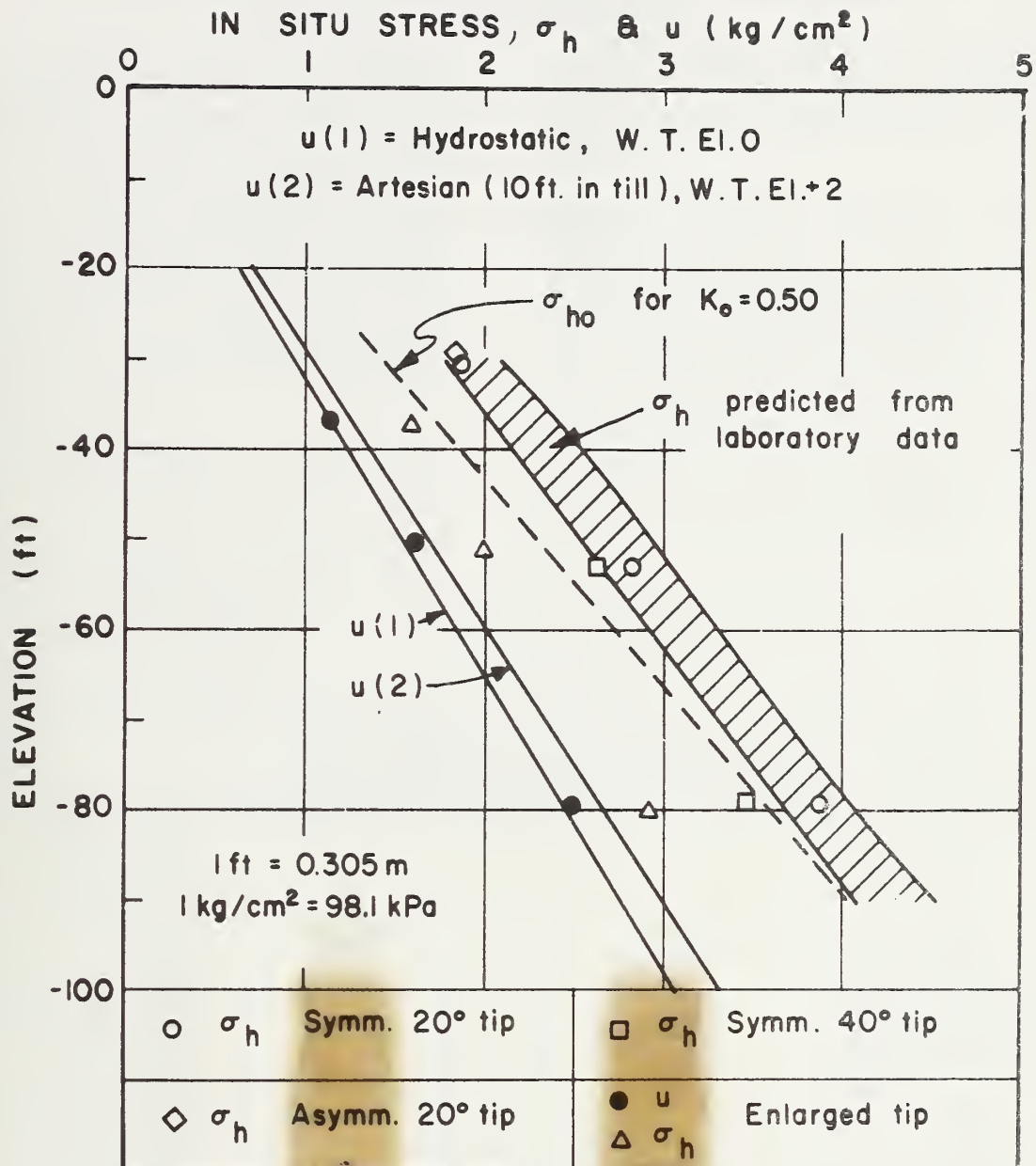FIGURE A-11   TOTAL HORIZONTAL STRESS AND PORE PRESSURE EQUILIBRATION AT EL.-80

FIGURE A-12   MEASURED AND PREDICTED STRESSES AT STA. 246

FEDERALLY COORDINATED PROGRAM (FCP) OF HIGHWAY RESEARCH AND DEVELOPMENT

The Offices of Research and Development (R&D) of the Federal Highway Administration (FHWA) are responsible for a broad program of staff and contract research and development and a Federal-aid program, conducted by or through the State highway transportation agencies, that includes the Highway Planning and Research (HP&R) program and the National Cooperative Highway Research Program (NCHRP) managed by the Transportation Research Board. The FCP is a carefully selected group of projects that uses research and development resources to obtain timely solutions to urgent national highway engineering problems.*

The diagonal double stripe on the cover of this report represents a highway and is color-coded to identify the FCP category that the report falls under. A red stripe is used for category 1, dark blue for category 2, light blue for category 3, brown for category 4, gray for category 5, green for categories 6 and 7, and an orange stripe identifies category 0.

FCP Category Descriptions

1. **Improved Highway Design and Operation for Safety**

   Safety R&D addresses problems associated with the responsibilities of the FHWA under the Highway Safety Act and includes investigation of appropriate design standards, roadside hardware, signing, and physical and scientific data for the formulation of improved safety regulations.

2. **Reduction of Traffic Congestion, and Improved Operational Efficiency**

   Traffic R&D is concerned with increasing the operational efficiency of existing highways by advancing technology, by improving designs for existing as well as new facilities, and by balancing the demand-capacity relationship through traffic management techniques such as bus and carpool preferential treatment, motorist information, and rerouting of traffic.

3. **Environmental Considerations in Highway Design, Location, Construction, and Operation**

   Environmental R&D is directed toward identifying and evaluating highway elements that affect the quality of the human environment. The goals are reduction of adverse highway and traffic impacts, and protection and enhancement of the environment.

4. **Improved Materials Utilization and Durability**

   Materials R&D is concerned with expanding the knowledge and technology of materials properties, using available natural materials, improving structural foundation materials, recycling highway materials, converting industrial wastes into useful highway products, developing extender or substitute materials for those in short supply, and developing more rapid and reliable testing procedures. The goals are lower highway construction costs and extended maintenance-free operation.

5. **Improved Design to Reduce Costs, Extend Life Expectancy, and Insure Structural Safety**

   Structural R&D is concerned with furthering the latest technological advances in structural and hydraulic designs, fabrication processes, and construction techniques to provide safe, efficient highways at reasonable costs.

6. **Improved Technology for Highway Construction**

   This category is concerned with the research, development, and implementation of highway construction technology to increase productivity, reduce energy consumption, conserve dwindling resources, and reduce costs while improving the quality and methods of construction.

7. **Improved Technology for Highway Maintenance**

   This category addresses problems in preserving the Nation's highways and includes activities in physical maintenance, traffic services, management, and equipment. The goal is to maximize operational efficiency and safety to the traveling public while conserving resources.

0. **Other New Studies**

   This category, not included in the seven-volume official statement of the FCP, is concerned with HP&R and NCHRP studies not specifically related to FCP projects. These studies involve R&D support of other FHWA program office research.